DOKUZ EYLUL UNIVERSITY
GRADUATE SCHOOL OF NATURAL AND APPLIED SCIENCES

APPLICATIONS OF GRINDING MODELLING FOR DIFFERENT ORE TYPES IN MINERAL PROCESSING

by
Ali Kemal EYÜBOĞLU

October, 2011
İZMİR

APPLICATIONS OF GRINDING MODELING FOR DIFFERENT ORE TYPES IN MINERAL PROCESSING

A Thesis Submitted to the
Graduate School of Natural and Applied Sciences of Dokuz Eylül University
In Partial Fulfillment of the Requirements for the Degree of Master of Science
in Mining Engineering, Mineral Processing Program

by
Ali Kemal EYÜBOĞLU

October, 2011
IZMIR

M.Sc THESIS EXAMINATION RESULT FORM

We have read the thesis entitled **"APPLICATIONS OF GRINDING MODELING FOR DIFFERENT ORE TYPES IN MINERAL PROCESSING"** completed by **ALI KEMAL EYÜBOĞLU** under the supervision of **PROF. DR. EROL KAYA** and we certify that in our opinion it is fully adequate, in scope and in quality, as a thesis for the degree of Master of Science.

PROF. DR. EROL KAYA

Supervisor

Prof. Dr. Ilkan Gürer

(Jury Member)

Prof. Dr. Ali Aydın GÖKTAŞ

(Jury Member)

Prof. Dr. Mustafa SABUNCU

Director

ACKNOWLEDGEMENTS

I would like to thank to my supervisor Prof.Dr.Erol Kaya, for his kind supervision, support, valuable comments, innumerable suggestions, and friendship through all stages of this work.

It is a pleasure to thank those who helped me with knowledge and research materials as M. Baran Tufan, V. Taylan Engin and Sezai Şen.

Lastly, I offer my regards and blessings to those who made this thesis possible by giving me the moral support such as my family and my best friends.

Ali Kemal EYÜBOĞLU

APPLICATIONS OF GRINDING MODELING FOR DIFFERENT ORE TYPES IN MINERAL PROCESSING

ABSTRACT

Mill grinding is an important in the processing of most minerals, in that it may be used to produce particles of the required size and shape, to liberate minerals from each other for concentration purposes, and to increase the powder surface area. Grinding of minerals is probably the most energy consuming task and optimization of this operation has vital importance in processing plant operations to achieve the lowest operating cost. Therefore, many scientific and technical problems are related to fine grinding operations and its associated problems. As mineral particles are reduced to finer product sizes, their surface become more important. Surface characteristics and properties affect any of the fine particle processing operations.

In this study, the grindability properties of three different mineral samples (perlite, pumice, and zeolite) are investigated with both Bond grindability test and batch grinding conditions based on a kinetic model. Firstly, four different mono-size fractions were prepared between (1,7mmx1,18mm ; 0,850mmx600mm ; 0,425mmx0,300mm ; 0,212mmx0,150mm) formed by a root 2 sieve series. Si and (Bi,j) values were determined from the size distributions at different grinding times (0,13 ; 1 ; 3 and 6 minute) and the model parameters (Si, aT, alpha, gama and phi) compared at different grinding conditions.

Keywords: Pumice, perlite, zeolite, grinding, kinetic modelling

CEVHER HAZIRLAMADA FARKLI CEVHERLERİ KULLANARAK ÖĞÜTME MODELLEMESİ UYGULAMALARI

ÖZ

Boyut küçültme birçok cevherin hazırlanmasında istenen boyut ve şekilde taneye ulaşmak, minerallerin serbestleşmesinde ve yüzey alanının artırılması amacıyla uygulanan çok önemli bir işlemdir. Enerji tüketimi çok yüksek seviyede olduğundan bu işlemin optimizasyonu ekonomi ve zaman açısından önem arz etmektedir. Bundan başka, boyut küçültme işlemlerinde hem bilimsel hem de teknik açılardan birçok problemle karşılaşılmaktadır.

Bu çalışmada üç farklı mineralin (perlit,pomza ve zeolit) öğütülebilirlik özellikleri Bond öğütülebilirlik testi ve kinetik model kullanılarak araştırılmıştır. İlk olarak kök 2 elek serisine gore 4 dar-tane boyu fraksiyon (1,7mmx1,18mm ; 0,850mmx600mm ; 0,425mmx0,300mm ; 0,212mmx0,150mm) hazırlanmıştır. Farklı öğütme zamanlarında (0,13 ; 1 ; 3 ve 6 dakika) Si ve Bi,j değerleri hesaplanıp ve model parametreleri (Si, aT, alfa, gama and phi) farklı öğütme koşullarında karşılaştırılmıştır.

Anahtar sözcükler : Ponza, perlit, zeolit, öğütme, kinetik modelleme

CONTENTS

Page

M. SC.THESIS EXAMINATION RESULTS FORM……...…….ii

ACKNOWLEDGEMENTS…….iii

ABSTRACT……...…iv

ÖZ…….v

CHAPTER ONE - INTRODUCTION……..1

1.1 History of Grinding…….……....1

1.2 Some Principles of Size Reduction…….3

1.2.1 Grindability…….…….3

1.2.2 Grindability Methods……...4

1.2.3 The Relationship between Energy and Size Reduction…….5

1.2.3.1 Kick's Law…….7

1.2.3.2 Rittinger's Law…….7

1.2.3.3 Bond's Law……9

CHAPTER TWO - DETERMINATION OF BREAKAGE PARAMETERS OF MINERALS……..11

2.1 Introduction …….11

2.2 Formulation of the Problem for Grinding Circuits…….12

2.3 Mill Conditions in Tumbling Ball Mills and Operation of Ball Mills……13

2.3.1 Critical Speed (N_c), Fractional Ball Filling (J_B), Fractional Powder Filling (f_c) and Fraction of Void Spaces in Ball Bed Filled with Powder (U) Values..14

2.4 Models of Size Reduction……15

2.4.1 Kinetic Model……...17

2.4.1.1 The Specific Rate of Breakage…….17

2.4.1.2 The Primary Breakage Distribution Function…….19

2.4.1.3 The Batch Grinding Equation……21

2.4.1.4 Methods for Estimation of Breakage Rate and Distribution……24

CHAPTER THREE - EXPERIMENTAL STUDIES……29

3.1 Test Materials……...29
3.2 Bond Work Index Estimation Studies……..29
3.2.1 Bond Ball Mill Standard Grindability Test……..…30
3.3 Determination of Breakage Parameters of Perlite, Pumice and Zeolite……...34

CHAPTER FOUR - EXPERIMENTAL RESULTS……36

4.1 Results and Discussion of Bond Work Index Estimation Studies……...36
4.2 Results and Discussion of Breakage Parameters of Samples……..39
4.2.1 Breakage Parameters of Perlite……39
4.2.1.1 The Specific Rates of Breakage (Si) and The Primary Breakage Distribution Functions ($B_{i,j}$) Values of Perlite at 38 mm Ball Size Charge..39
4.2.1.2 The Specific Rates of Breakage (Si) and The Primary Breakage Distribution Functions ($B_{i,j}$) Values of Perlite at 30 mm Ball Size Charge..41
4.2.1.3 The Specific Rates of Breakage (Si) and The Primary Breakage Distribution Functions ($B_{i,j}$) Values of Perlite at 30 – 25,4 – 19 mm Ball Size Charge……..43
4.2.2 Breakage Parameters of Pumice……...44
4.2.2.1 The Specific Rates of Breakage (Si) and The Primary Breakage Distribution Functions ($B_{i,j}$) Values of Pumice at 38mm Ball Size Charge.44
4.2.2.2 The Specific Rates of Breakage (Si) and The Primary Breakage Distribution Functions ($B_{i,j}$) Values of Pumice at 30mm Ball Size Charge.46
4.2.2.3 The Specific Rates of Breakage (Si) and The Primary Breakage Distribution Functions ($B_{i,j}$) Values of Pumice at 30 -25,4 -19,05 mm Ball Size Charge……..48
4.2.3 Breakage Parameters of Zeolite……50
4.2.3.1 The Specific Rates of Breakage (Si) and The Primary Breakage Distribution Functions ($B_{i,j}$) Values of Zeolite at 38 mm Ball Size Charge.50
4.2.3.2 The Specific Rates of Breakage (Si) and The Primary Breakage Distribution Functions ($B_{i,j}$) Values of Zeolite at 30 mm Ball Size Charge.51

4.2.3.3 The Specific Rates of Breakage (Si) and The Primary Breakage Distribution Functions ($B_{i,j}$) Values of Zeolite at 30- 25,4 19,05 mm Ball Size Charge……..53

CHAPTER FIVE - CONCLUSIONS AND DISCUSSIONS……56

CHAPTER SIX – RECOMMENDATIONS……..……..59

REFERENCES……61

APPENDICES……...62

Appendix A - Bond Work Index Test Result Tables of Perlite, Pumice and Zeolite……..62

Appendix B - Tables and Figures for Determination Breakage Parameters of Perlite…….……..68

Appendix C - Tables and Figures for Determination Breakage Parameters of Pumice…….137

Appendix D - Tables and Figures for Determination Breakage Parameters of Zeolite…….……206

Appendix E - Variations of The S_i Values of Perlite, Pumice and Zeolite with Particle Size for Different Ball Diameters at U=0,6 and U=1……..275

CHAPTER ONE
INTRODUCTION

1.1 History of Grinding

Grinding is the last stage in the process of comminution and is often said to be to key to good mineral processing. A detailed knowledge of the type, hardness and size of the different mineral particles, and their distribution throughout the ore, is vital when deciding how best to grind to ore. Under-grinding may not “liberate” all of valuable mineral grains from the enveloping rock, whilst over-grinding may produce mineral particles so fine that they cannot be economically recovered. Thus the grinding of ores and minerals has developed into an exacting science (Lynch, Alban J. , 1930).

For many hundreds of years the most commonly used machine for grinding ore were stamps. Stamps are mechanical pestles and mortars. In their simplest form the pestle takes the form of the heavy weight (the head) fastened to stem. Fixed to upper part of the stem is a ‘tappet’ this engages a ‘cam’ fixed to a horizontal shaft or ‘barrel’. As the barrel rotates the cam lifts the stem upward as the cam (disengages) the stem and head falls back to grind to ore placed beneath. The ore is held in the mortar, essentially the box with an opening at the back to receive the ore, and a perforated metal plate et the front. As the ore is ground a flow of water is directed through the mortar box washing the particles of ground ore out through the perforated screen – thus the ore is ground to a pulp with a maximum particle size. (Lynch, Alban J. , 1930).

Of all the machines tried only one type was to become successful. In 1880 Mitchell and Tregonning patented the tube mill. Their machine comprised of an iron cylinder partly filled with pieces of scrap iron, this was supported by hallow trunnions and rotated about the horizontal axis. As the ore pulp flowed through the mill (entering and discharging via the trunnions) it was ground by the tumbling scrap iron. This machine was the forerunner of all ball and tube mills. In modern mill,

grinding is achieved by tumbling the ore, either on its own (autogenous grinding) or with grinding media (hardened steel balls or rods) (Lynch, Alban J. , 1930).

The mill usually takes the form of a cylinder, sometimes with conical section, formed from steel plate. Mill varies in size from less than one meter, to over ten meters in diameter, with largest over nine meters in length and can grind from a few tones to many hundreds of tones of ore an hour (Lynch, Alban J. , 1930).

Between 1925 and 1937 many changes were made to the milling operation with additional re-grinding of concentrates and classifier underflow using small Hardinge ball mills and a Holman Grit mill (pan grinder). During 1937/8 the mill was upgraded to increase its capacity and improve recovery rates. The main change was to the grinding section. A new 7 ft.. x 3 ft. Hardinge conical ball mill was installed to replace the existing stamps. This worked in close circuit with three 18 mesh Hummer screens – the undersize from the screens feeding primary shaking tables. (Lynch, Alban J. , 1930).

The batch flotation circuit incorporated a tube mill. This 1,96 ft. x 5,97 ft. mill originally used steel rods (old drill steels) to grind the sulphides from the primary batch flotation cells. These rods were replaced by stell grinding balls in the mid 1970's (Austin, L,G., Klimpel, R,R., and Luckie, P,T, 1984).

The last major change to the grinding circuits at Geevor took place during 1979/80. A 2, 20x2, 25 meter Newell Dunford grate discharge rubber lined ball mill was installed as the primary grinding mill. This worked in closed circuit with Allis Chalmers screens. The output of this circuit fed the primary sand tables in New Table Plant. The original Hardinge 7 ft. mill, now over forty years old, was modified to work in open circuit as a regrind mill (Austin, L,G., Klimpel, R,R., and Luckie, P,T, 1984).

1.2 Some Principles of Size Reduction

1.2.1 Grindability

Grindability is the amount of product from a particular mill meeting a particular specification in a unit of grinding time e.g., tons per hour passing 200 mesh. The chief purpose of study of grindability is to evaluate the size and type of mill needed to produce a specified tonnage and the power requirement for grinding. So many variables affect grindability that is concept can be used only as a rough guide to mill sizing. It says nothing about product-size distribution or type or size of mill. If particular energy law is assumed, then the grinding behavior in various mills can be expressed as an energy coefficient or work index. This more precise concept is limited by the inadequacies of these laws but often provides the only available information (Lynch, Alban J. , 1930).

The technology based on grindability and energy considerations is being supplanted by computer simulation of milling circuits, in which the gross concept of grindability is replaced by the rate of breakage function (sometimes called the selection function), which is the grindability of each particle size referred to the fraction of that size present (Lynch, Alban J. , 1930)..

Factors of hardness, elasticity, toughness, and cleavage are important in determining grindability. Grindability is related to modulus of elasticity and speed of sound in the material (Dahlhoff, 1967).

The hardness of a mineral as measured by the Mohs scale is a criterion of its resistance to crushing. It is a fairly good indication of the abrasive character of the mineral, a factor that determines the wear on the grinding media. Arranged in increasing order or hardness, the Mohs scale is as follows: 1-talc, 2-gypsium, 3-calcite, 4-fluoride, 5-apatite, 6-feldspar, 7-quartz, 8-topaz, 9-corundum, and 10-diamond.

Materials of hardness 1 to 3 inclusive maybe classed as soft; 4 to 7 as intermediate; and the others as hard (Fahrenwald, 1934).

1.2.2 Grindability Methods

Laboratory experiments on single particles have been used to correlate grindability. In the past it has usually been assumed that the total energy is applied in a single blow or by repeated dropping of a weight on the sample. In fact, the results depend on the way in which the force is applied. In spite of this, the results of large mill tests can often be correlated within 25 to 50 percent by a simple test, such as the number of drops of a particular weight needed to reduce a given amount of feed to below a certain mesh size (Gross and Zimmerly, 1930; Axelson, 1949).

Two methods having particular application for coal are known as the ball-mill and Handgrove methods. In the ball-mill method, the relative amounts of energy necessary to pulverize different coals are determined by placing a weighed sample of coal in a ball mill of a specified size and counting the number of revolutions required to grind the sample so that 80 percent of it will pass through a No. 200 µm sieve. The grindability index in percent is equal to the quotient of 50,000 divided by average of the number of revolutions required by two tests (Gross and Zimmerly, 1930).

In the Handgrove method a prepared sample receives a definite amount of grinding energy in a miniature ball-ring pulvarizer. The unknown sample is compared with a coal chosen as having 100 grindability. The Handgrove grindability index = (13+6,93 W), where W is the weight of material passing the No. 200 sieve (Gross and Zimmerly, 1930).

Manufactures of various types of mill maintain laboratories in which grindability tests are made to determine the suitably of their machines. When grindability comparisons are made on small equipment of the manufactures' own class, there is basis for scale-up to commercial equipment. This is better than relying on a

grindability index obtained in a ball mill to estimate the size and capacity of different types such as hammer or jet mills (Gross and Zimmerly, 1930).

1.2.3 The Relationship between Energy and Size Reduction

Progress in size reduction machines has always depended on available sources of energy. First, it was necessary to supplement human muscle power as an energy, source and then to replace it entirely. Tools that used animals-horses and oxen-to drive grinding devices were developed. Next, water wheels and windmills were invented, followed by motor powered by steam. Finally steam-driven turbines-now a source of energy around the world were developed to the generate electricity. This largely eliminated the use of human energy to drive size-reduction tools and machinery (except in some developing countries, where grain is still ground by hand). Additionally, Figure 1.1 shows, effects of energy sources and materials on size reduction process (Forbes, 1955).

Today, grinding mills use about 2% of the electricity generated in the world and dry-grinding processes consume about 75% of this energy (Bond, 1961).

Size reduction machinery is generally described as mechanical breakage mechanisms capable of applying available power to break down material from a specified feed size to specified product size. The following key points summarize the types of energy used for size reduction as they developed over the years (Bond, 1961).

- The fuel for muscle power is the food eaten by humans and animals. Muscle powered machines work at about 0, 5 kW (0, 66 hp).
- The fuel for water power is from the flow of water that drives the water wheel. Water-powered machines work at about 5 kW (6, 6 hp).
- The fuel for steam power is the wood, coal or petroleum that, when combusted, provides the heat to convert water to steam. Steam-powered machines work at 50 kW (66 hp).

- Electrical energy is produced in electrical generators driven by water, steam or inertial combustion engines. Effectively, there is now no limit to the power that can be delivered by electric motors (Bond, 1961).

Size reduction is not only the most ancient technology; it is also the most widespread. It is used in every country and in every industry that involves solid particles. Here are some of the more important applications of technologies (Bond, 1961).

- Breaking wheat grains to separate endosperm from bran and grinding to endosperm to produce flour.
- Breaking rock masses into boulders and pebbles.
- Crushing and grinding ores to produce copper, iron, gold and other metals.
- Pulverizing coal to combust in power stations.
- Grinding limestone and clinker to make cement.
- Grinding industrial minerals to use as pigments and to manufacture fertilizers, glass, chemicals, pharmaceuticals and many other products (Bond, 1961).

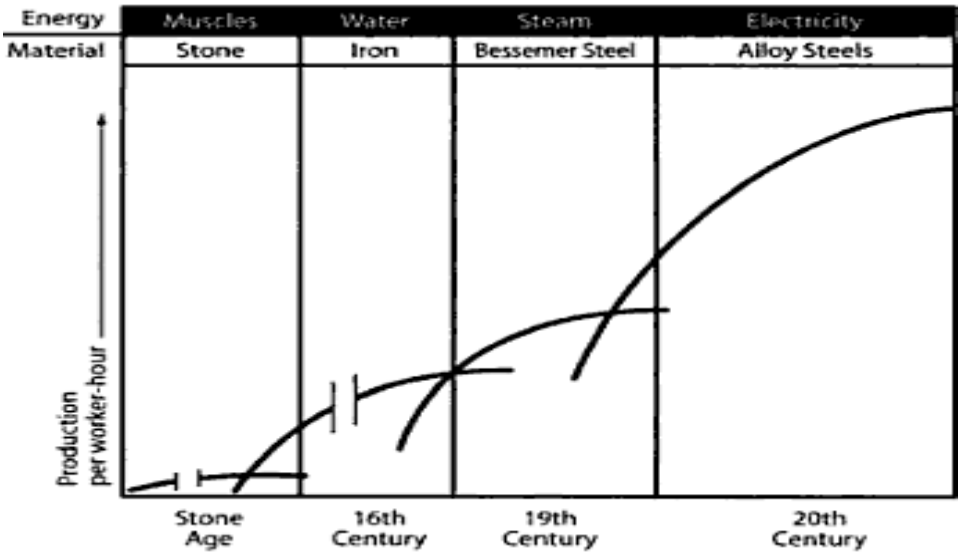

Figure 1.1 Effects of Energy Sources and Materials on Size Reduction Process (Forbes, 1955)

1.2.3.1 Kick's Law

Kick's concluded that the amount of the deformation is proportional to the energy applied and that "The pressure required for similar deformation of similar shaped bodies of similar material is proportional to the cross section area of those bodies." (Austin, 1973).

This work was extended to the breakage of stone, iron and glass spheres and cylinders, and then to rock breakage by blasting. The results of these studies was the energy size reduction hypothesis attributed to Kick "For any unit weight of ore particles the energy required to produce any given reduction ratio in the volumes is constant no matter what maybe the original size of the particles" (Richards and Locke 1940). Kick's hypothesis is defined by the equation (Austin, 1973);

$$E = Kk \ln \left(\frac{X1}{X2}\right) \tag{1.1}$$

Where;
E= Energy
Kk=Kick's constant
X1=Initial dimension
X2=Final dimension
(X1/X2=Reduction ratio)

Which states that the energy required to reduce the size of particles is proportion to the ratio of an initial dimension to the final dimension? Kick's law is best suited to coarse grinding where there is relatively little change in surface area (Austin, 1973).

1.2.3.2 Rittinger's Law

Rittinger earned a worldwide reputation as an outstanding scientist when he published a comprehensive textbook on mineral processing. The book described equipment and processes and was accompanied by two heavy volumes of beautiful

lithographic drawings of all the technical equipment that operated in mineral processing plans at the time. But his book went much farther than describing machines and processes. He recognized the importance of quantitatively explaining the principles involved in the processes, using equations to do so. Between his inventions and his outstanding textbook, it is not surprising that Rittinger is regarded as the man who laid the foundation for today's mineral processing technology. His achievements were of such stature that he was awarded civic as well as technical honors, including being enabled by the state (Austin, 1973).

In discussing size reduction in his textbook, Rittinger commented that "The throughput (of wet operated stamp mills) is proportional to the 0,4 power of the linear dimension of the openings of the discharge screen." This type of empirical relationship, which was unusual at the time, was similar to the later Bond equation. To clarify, he used an analogy of making estimates of the new surface produced by prepared breakage of particles into smaller particles. Although his original equation was correct, the analogy suffered the fate of many simplifications when other authors took it to be an actual hypothesis (Steiner 2002). Eventually energy-size reduction relationship attributed to Rittinger came to be stated in this ways: " The work done in crushing is proportional to the area of new surface produced" (i.e., proportional to the reduction in linear dimension; Richards and Locke 1940). The hypothesis attributed to Rittinger is defined by the equation (Austin, 1973);

$$E = k[\frac{1}{X2} - \frac{1}{X1}] \tag{1.2}$$

Where;
E= Energy
k= Constant
X1 and X2= The feed and product sizes

Which states that the energy required to reduce the size of particles is proportional to the change in surface of the particles (Austin, 1973).

Rittinger's law gives better results for fine grinding where there is a much greater change in surface area (Austin, 1973).

1.2.3.3 Bond's Law

Throughout the 20th century, grinding mills were selected based on the grindability of the material and the prediction of the power required per ton the grind material to a known product size. Before Bond's work this estimate was based on experience and judgment. Metallurgist and process engineers who worked with mill manufactures travelled extensively and gained wide exposure to plant data. Because it was generally accepted that they had a better knowledge of the relationship between grandability data and actual mill performance than the staff of mineral processing companies, whose experience was necessarily restricted to a few operations, engineers from mineral processing companies consulted with representatives of grinding mill manufacturers when mills and circuits were being selected for new mines and plant expansions (Austin, 1973).

To compute for the grinding mill business, manufacturers needed to increase their expertise in grinding technology, so they developed their own grindability tests and obtained operating data and corresponding ore samples from processing companies. From these, they could derive the relationship between grindability and mill performance. The early grindability tests were batch tests carried out in small-diameter ball or pebble mills, often called jar mills. The results were given in terms of revolutions of the test mill or time required to make the desired particle-size distributions and net weight of a specified mesh size produced per minute or per set number of revolution in the test mill (Austin, 1973).

Each business that developed grindability tests also developed its own testing procedures, which were kept confidential. Both wet and dry test procedures were developed, but dry grinding was found to give more reliable and reproducible data (Austin, 1973).

Bond concluded that a material could be characterized by the Work Index Wi defined by the following empirical equation (Austin, 1973);

$$W_i test = \frac{(1{,}10)x(44{,}5)}{\left\{\left(P_1{}^{0{,}25}\right)x(Gbp)^{0{,}82}x\left[\frac{10}{\sqrt{X_{QT}}}-\frac{10}{\sqrt{X_{GT}}}\right]\right\}}\ ,kWh/ton \tag{1.3}$$

Where P_1 is the opening of the classifying screen used in preparing the product and return to the mill in the Bond test, in micrometers; X_{QT} is the 80% passing size of the product in micrometers and X_{GT} the 80% size of the original feed (Austin, 1973).

Bond concluded that over some ranges the influence of the size of the feed and the size of the product on the grinding energy in closed circuit could be described by the relation;

$$E = Wi\left(\frac{10}{\sqrt{Xq}}-\frac{10}{\sqrt{Xg}}\right), kWh/t \tag{1.4}$$

Where E is specific grinding energy (based on shaft power, $E=m_p/Q$) and x_Q,x_G are 80% passing size of circuit product and circuit feed, respectively (Austin, 1973).

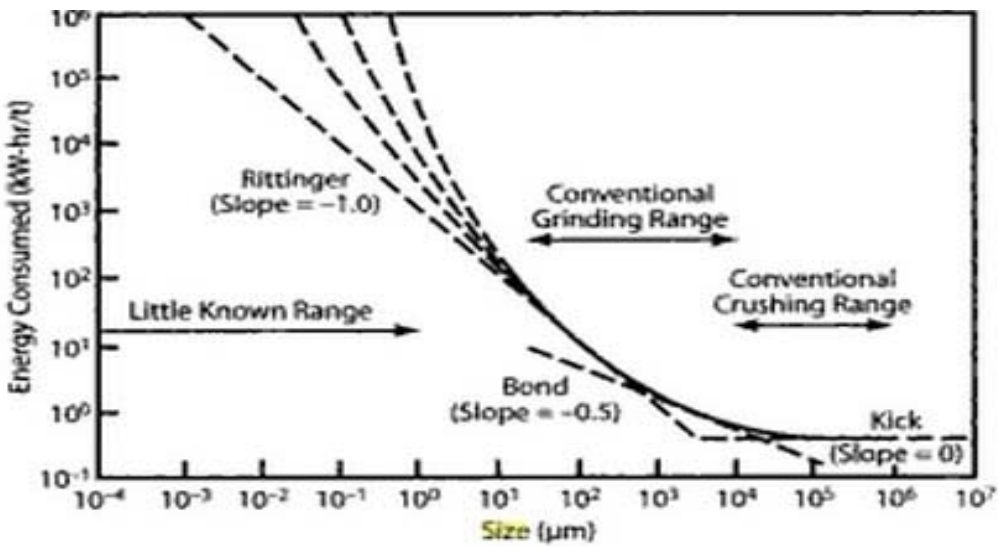

Figure 1.2 Relationship Between Energy and Particle Size in Breakage (Hukki, 1962)

CHAPTER TWO
DETERMINATION OF BREAKAGE PARAMETERS OF MINERALS

2.1 Introduction

Quantitative modeling and simulation of grinding circuits has been a major component of the research activity in mineral processing for the last several decades. Application of these models to practical engineering situations is not always easy, and information on suitable models must generally be searched for in the technical research literature. Modern simulators allow the user to combine models for many unit operations into a complete flow sheet and to calculate the expected performance. Simulation provides a useful tool that a mineral process engineers can use in variety of operational and design problems (Austin, L.G., Klimpel, R.R., Luckie, P.T., Rogers, R.S.C., 1982).

A simulation of a physical model is a mathematical model which behaves on computation in a manner identical to that of the real process. Generally, a simulation is only approximation to the real behavior, especially for a process as complicated as for a milling, and mathematical models can be more or less complex depending on how closely one wishes to simulate the real situation (Austin, L.G., Klimpel, R.R., Luckie, P.T., Rogers, R.S.C., 1982).

As the energy is the most critical cost factor in size reduction, comminution modeling was initially approached in terms of the energy size reduction relationships, which were concerned with the relationship between the energy consumed by a crusher or a grinding mill and the amount of size reduction that the consumption of this energy brought about. The energy approach, however, does not provide information on the transformation from feed the product size distribution and cannot accommodate the effects of the operating variables, such as feed rate, mill size and mill speed. The transformation relationship between the feed and product size distributions for a comminution machine is necessary for the optimum design and operation of a size reduction circuit and requires the formulation of mathematical

models based on recognition of physical events occurring in the size reduction. Such an approach to comminution modeling allows the prediction of product characteristics for known feed characteristics and values of the operating and design variables (Austin, L.G., Klimpel, R.R., Luckie, P.T., Rogers, R.S.C., 1982).

2.2 Formulation of the Problem for Grinding Circuits

Size reduction of solid and minerals by crushers and grinding mills is an important industrial operation involving many aspects of mineral, metallurgical, power and chemical industries. It is already known that machines for breakage of large lumps are called crushers and those for smaller sizes are called mills. Size reduction by crushers does not create problems due to having high energy consumption and capital cost per ton per hour; however, fine grinding by mills consumes a lot of energy and causes high abrasive wear. Therefore, many scientific and technical problems are related to fine grinding operations and its associated problems. As mineral particles are reduced to finer product sizes, their surfaces become more important. Surface characteristics and properties affect any of the fine particle processing operations (Austin, L.G., Klimpel, R.R, Luckie, P.T., 1984).

The aim in mill circuit design is to select a mill that will produce a desired tonnage per hour of required product from a specified feed; therefore, capital costs need to be minimized which are related to correct mill conditions including rotational speed, ball load and sizes. In general, the mill employed for grinding circuits should be operated efficiently in terms of high mill capacity and low energy consumption, subject to lifter wear, maintenance costs, product contamination that will cause problems in the beneficiation stage. Another problem is the oversize product from the mill, which needs to be recycled by devising several stages of grinding with a classifier that splits the product into coarser and finer sizes. The coarse particles are recycled back to mill feed to be reground as seen in Fig.2.1. In order to design the efficient mill circuits, the following factors need to be considered: mill type and size, mill power, efficient grinding conditions, recycle and classification efficiency, mill

circuit behavior under different conditions and economic constraints (Austin, L.G., Klimpel, R.R, Luckie, P.T., 1984).

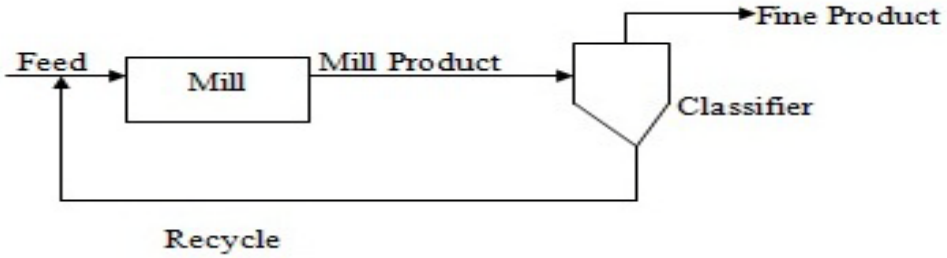

Figure 2.1 Mill circuit design with recycling of coarser particles
(Austin, L.G., Klimpel, R.R, Luckie, P.T., 1984).

2.3 Mill Conditions in Tumbling Ball Mills and Operation of Ball Mills

The tumbling ball mill is the most important type of industrial mill, and much of the work about grinding depends on it, so the terms describing mill conditions in ball mills are now defined. The tumbling ball mill contains a reservoir of powder being acted on by the breakage action and the fineness of grind depends on how long the material is retained, that is, the product becomes coarser as the feed rate increases. This type of machine is a retention device (Austin, L.G., Klimpel, R.R, Luckie, P.T., 1984).

Coarse feed particles enter one end of the mill, pass down the mill receiving breakage actions because of the heavy balls, and exit as an end product with a finer size distribution. Here, energy input is converted to mechanical breakage action to form the broken finer size particles. The key point in designing the mill circuit is to size a mill to produce a desired tonnage per hour of a required product from a specified feed (Austin, L.G., Klimpel, R.R, Luckie, P.T., 1984).

2.3.1 Critical Speed (N_c), Fractional Ball Filling (J_B), Fractional Powder Filling (f_c) and Fraction of Void Spaces in Ball Bed Filled with Powder (U) Values

The critical speed of the mill is defined as the rotational speed at which balls just start to centrifuge on the mill case and not tumble. By balancing the force of gravity

on a ball at the top of a mill against the radial centrifugal force for a ball on the case (Shoji, K., 1982):

$$critical\ speed, rpm = \frac{42{,}2}{\sqrt{D-d}}, (D\ and\ d\ in\ meter) \tag{2.1}$$

Where, *D* is the internal mill diameter and *d* the maximum ball diameter. It is reasonable to expect that the tumbling action in a mill will depend on the fraction of critical speed at which the mill is run, thus the rotational speed condition of the mill is normally specified by Φ_c, the fraction of critical speed (Shoji, K., 1982).

The tumbling action and the rates of breakage will clearly depend on how much of the mill volume is filled with balls. The most precise measure of this is the fractional volume filled by ball volume. However, in tests on large scale mills it is often not possible to determine the weight of balls in a mill and therefore not possible to determine their volme, but it is possible to stop the mill and measure the height from the ball bed to top of the mill (Shoji, K., 1982)..

Thus the fractional ball filling, *J*, is conventionally expressed as the fraction of the mill filled by the ball bed at rest. To convert the bed volume to mass of balls present, or vice versa, it is necessary to know the bulk density of the ball bed. The bed porosity varies slightly depending on the ball size mix, powder filling, etc., but it is conventional to define constant formal bed porosity for all calculations. Different industries and different manufactures use slightly different values of porosity. We will use a formal bed porosity of 0,4 which gives (Shoji, K., 1982):

$$J = \left(\frac{mass\ of\ balance\ \div ball\ density}{mill\ volume}\right) x \left(\frac{1{,}0}{0{,}6}\right) \tag{2.2}$$

since a true steel volume of 0,6 gives a steel-plus-porosity volume of 1. For normal, forged steel balls, a formal, porosity of 0,4 gives a bed bulk density of 4,70 t/m^3 (Shoji, K., 1982).

Similarly, the mill filling by powder is expressed as the fraction of mill volume filled by powder bed, f_c , again using a formal bed porosity of 0,4 (Shoji, K., 1982):

$$f_c = \left(\frac{mass\ of\ powder\ \div powder\ density}{mill\ volume}\right) x \left(\frac{1{,}0}{0{,}6}\right) \tag{2.3}$$

In order to relate the powder loading to the ball loading the formal bulk volume of powder is compared to the formal porosity of the ball bed (Shoji, K., 1982):

$$U = \left(\frac{f_c}{0{,}4\ x\ J}\right) \tag{2.4}$$

Thus U is the fraction of the spaces between balls at rest which is filled with powder; it is found empirically that U=0,6 to 1,1 is a good powder ball loading ratio to give efficient breakage in the mill (Shoji, K., 1982).

2.4 Models of Size Reduction

The phenomenological approach to the modeling of size reduction is based on a mechanistic description of the breakage process coupled with mass (or number) balance on each size interval. The feed-product size distribution transformation in a comminution machine is a consequence of a summation of numerous single breakage events which may operate simultaneously or consecutively or both. During the comminution process a certain proportion of each size is selected for breakage at any repetitive step and complete range of finer breakage product sizes is produced from the single breakage of just one specified particle size. Thus, the breakage event may be conveniently described by two fundamental concepts (Lynch, A.C., 1977):

- Probability of each size being selected for breakage
- Characteristic size distribution after breakage

As most comminution machines operate so that sequential breakage events occur while the particles are in the machines, the selection of the particles for breakage at each event is influenced by the type and operating characteristics of comminution machines and the extent of size reduction depends on the number of successive breakage events. Thus, observed that to describe the complete process in a machine requires the introduction of two more concepts (Lynch, A.C., 1977).

- Internal classification of particles prior to a breakage event within the process (e.g., preferential breakage of coarser particles)
- Residence time within the comminution machine

The phenomenological models of comminution based on the above concepts fall into two main groups defined by (Austin, L.G., Klimpel, R.R, Luckie, P.T., 1984).

- Matrix type models, and
- Kinetic type models

In the matrix model, comminution is considered as a succession of discrete breakage events (cycles or stages of breakage), the feed to each event being the product from the preceding event. The longer the period of size reduction, the greater is the number of events and the size reduction attained. Time is implicit the model (Austin, L.G., Klimpel, R.R, Luckie, P.T., 1984).

The matrix model is preferred for fixed residence time machines like jaw and cone crushers were internal material transport depends on the jaw-cone geometry and movement, being in dependent of feed rate. In the kinetic model, comminution is considered as a process continuous time. Time is explicit in the model; the longer the time of grinding, the greater is the size reduction attained. This type of model is commonly and generally used for tumbling grinding mills having strongly varying

residence time as a function of feed rate. There is a quite similarity between the two types of the models as they are based on common concepts. However, different symbols and names have been used to represent what are effectively the same parameters or concepts (Austin, L.G., Klimpel, R.R, Luckie, P.T., 1984).

2.4.1 Kinetic Model

In the kinetic approach, details are given by Austin et al., used mainly for the accurate formulation of tumbling ball mill grinding models, comminution is considered as a rate process continuous in time. Knowledge of rates at which particle of given sizes break (breakage kinetics) and in what sizes their products appear (breakage distribution) and the residence time of particles in the mill (material transport) are fundamental concepts required in the kinetic description of size reduction. The description of grinding of a given particle size as a rate process contains two part (Austin, L.G., Klimpel, R.R., Luckie, P.T., Rogers, R.S.C., 1982).

- The specific rate of breakage (or selection function) of that size.
- The size distribution of daughter particles produced by the fragmentation of each disappearing particle size (primary breakage distribution function or primary progeny distribution).

2.4.1.1 The Specific Rate of Breakage

The specific rate of breakage, s_i, of material within a size interval “i” can be defined as the mass of material of that size broken per unit time per unit mass of material of that size present in the mill. In other words, s_i gives the fraction of material in the size interval “i” which will be selected for breakage per unit time, and has units of time^{-1} (Austin, L.G., Klimpel, R.R., Luckie, P.T., Rogers, R.S.C., 1982).

The selection function, s_i, in the models simply describes the probability of breakage of particles of different sizes. If s_i describes the selection function (i.e., the fractional breakage) occurring in a single stage of breakage, Eq.(2.5), Δt being the

time in the single breakage stage (Austin, L.G., Klimpel, R.R., Luckie, P.T., Rogers, R.S.C., 1982).

$$s_i = \frac{S_i}{\Delta t} \tag{2.5}$$

Experimental work on the grinding of a geometric size interval of many homogeneous materials in a completely mixed dry ball mill has shown that the disappearance with time of the material in this finite size interval appears to follow a first-order law that is rate of disappearance of size j material in the mill (Austin, L.G., Klimpel, R.R., Luckie, P.T., Rogers, R.S.C., 1982).

Rate of breakage (or disappearance) of size “i” is

$$\frac{dm_i(t)}{dt} = s_i m_i(t) \tag{2.6}$$

Where m_i is the mass fraction of size i and t, the grind time.

It has been observed that the selection function size dependence frequently follows a power-law relationship (Herbst, J.A. & Fuerstenau, D.W., 1973):

$$S_i = S_1 \left[\frac{\sqrt{X_i X_{i+1}}}{X_1 X_2} \right]^{\alpha} \tag{2.7}$$

with a slope α approximately equal to the slope of the cumulative breakage function B_{ij} (on a log scale) versus size (on arithmetic scale) plot in the fine size range; s_1 is the experimentally determined rate parameter of the coarsest size interval, X_1 and X_2 being the upper size limits of the coarsest interval (Herbst, J.A. & Fuerstenau, D.W., 1973).

As far as the rates of production of fine material are concerned, the b values appear as:

Rate of production of size i from j= (fraction to i from j). (Rate of breakage of size j). = $b_{ij}S_jm_j(t)M$

And in the same way,

Rate of production of less-than-size i from breakage of larger size j=$B_{ij}S_jm_j(t)M$ (Herbst, J.A. & Fuerstenau, D.W., 1973).

2.4.1.2 The Primary Breakage Distribution Function

Grinding of a given feed produces a whole range of product sizes, down to near zero. After the first breakage occurs, these product size are mixed back into the mill charge and will continue to be broken with time again and again. If this distribution of fragments can be measured before any of the fragments are re-selected for further breakage, that is before any further breakage occurs, then the resulting distribution is the primary breakage distribution or primary progeny distribution (Austin, L.G., Klimpel, R.R., Luckie, P.T., Rogers, R.S.C., 1982).

The breakage distribution functions, b_{ij}, represent the fraction of material that is broken from size interval j and appears in size interval i after breakage where i<j.
In this sense, breakage is described as occurring only when the particles are broken out of their original size range throughout this study. Thus in a $\sqrt{2}$ size interval, the material must be broken below the top size interval to be considered as broken and hence the products of breakage are defined as appearing in sizes less than the lower limit of the top size interval. As an example, when a material of size interval 1 is broken in the weight fraction of the products which then occur in the size interval i is called $b_{i,1.}$ The set of numbers $b_{i,1}$, where i ranges from 2 to n, which, apparently describes the distribution of fragments produced from size 1 (Austin, L.G., Klimpel, R.R., Luckie, P.T., Rogers, R.S.C., 1982).

The second symbolism convenient for characterizing the primary breakage distribution is to accumulate the b_{ij} values from the finest interval, n, and let $B_{i,j}$ be the cumulative mass fraction of material broken from size j which appears in size intervals less than the upper size of size interval i (Austin, L.G., Klimpel, R.R., Luckie, P.T., Rogers, R.S.C., 1982)..

$$B_{i,j} = \sum_{\substack{k=i \\ i>j}}^{n} b_{k,j} \tag{2.8}$$

thus $b_{i,j}=B_{i,j} - B_{i+1,j}$

Unlike the breakage rate parameter, the breakage distribution function is accepted to be an essential property of the material and independent of the mill variables and the mode operation (wet or dry), in the normal operating range of milling conditions (Austin, L.G., Klimpel, R.R., Luckie, P.T., Rogers, R.S.C., 1982).

The cumulative weight fraction of material broken from size 1 into i is denoted by $B_{i,1}$. The matrix of $b_{i,j}$ and $B_{i,j}$ values are needed for a complete understanding of the size reduction process and breakage actions. The values of B can be obtained from one-size-fraction tests at short grinding times, where approximate corrections to allow for reselection for breakage of the primary fragments are reasonably valid. It is inherent in this technique the values of B do not vary with grinding time (Gardner, R.P., Austin, L.G., 1972).

It is a complicated task to measure the matrix of B values for all materials, under all milling conditions. However, it is often found that the B values are insensitive to precise mill conditions, at least in the normal operating range of milling conditions. It is often observed that the breakage distribution functions for homogenous materials can be normalized with respect to the feed size material; that is, the fraction of the starting size is independent of the starting size. A breakage distribution function can be normalized and it relates all other distribution function to the feed size distribution function by (Shoji, K., Lohrasb, S., Austin, L.G., 1980);

$$B_{i,j}=b_{i-j+1,1} \text{ or } B_{i,j}=B_{i-j+1,1} \quad \text{for } j=2,3,4,\ldots n; \text{ and } i=j, j+1,\ldots n$$

so that the number of $b_{i,j}$ parameters to be estimated is reduced from (n-1)(n-2)/2 to (n-2) number feed size parameters can be calculated by the above normalizing equation (Shoji, K., Lohrasb, S., Austin, L.G., 1980).

2.4.1.3 The Batch Grinding Equation

A simple batch test mill is a well mixed container where the amount of mass W held is constant and the size intervals are geometric mean series and the starting feed is all in the top size, that is $m_i(0)=1$ and the mill is run for a given time t_1. After time t_1, sample is removed from the mill and the fraction still remaining within the original size interval is determined by sieving and weighing methods to analyze the mill conditions. The remaining sample which still reports to original size fraction is returned to the mill and ground once more to give a total grinding time t_2, reanalyzed and so on, until the end (Luckie, P.T., Austin, L.G., 1972).

This analyzes results in a first order law of disappearance of size 1 and the rate of disappearance should be proportional to m_1 (t) and M.

$$-\left[\frac{dm_1(t)M}{dt}\right] \infty\ m_1(t)\ M \tag{2.9}$$

and since the total mass M is constant for a steady state circuit, this becomes;

$$-\left[\frac{dm_i(t)}{dt}\right] = -S_1 m_1(t) \tag{2.10}$$

where S_1 is a constant and called the specific rate of breakage, having units time-1. Then, if S does not differ with time,

$$m_1(t) = m_1(0)\ exp\ (-S_1 t) \tag{2.11}$$

then the equation may be written as;

$$log[m_1(t)] = log\ [m_1(0) - \frac{S_1 t}{2,3}] \tag{2.12}$$

giving a slope of value ($-S_1/2,3$) (Luckie, P.T., Austin, L.G., 1972).

When the breakage rate and distribution function parameters are independent of both the size distribution in the mill and time, as treated in the equation above, the equation expresses linear kinetics. However, such a linear plot does not prove that the finer material generated by breakage of the original size material will also break in a first order manner. The build-up of the fines does not affect the specific rate of breakage of the original size, until a reasonable amount of original material exists in the mill. The part of the material in any size interval in a batch mill disappears because of breakage, while other material enters the size interval as a result of breakage of particles in larger size intervals. Thus, using the rate process parameters s_i and b_{ij} for grinding, a complete size mass balance on the fully mixed batch grinding system can be formulated as a set of n differential equations (Austin, L.G., Klimpel, R.R., Luckie, P.T., Rogers, R.S.C., 1982):

$$\begin{pmatrix} \text{the net rate of} \\ \text{production} \\ \text{of the size} \\ \text{i material} \end{pmatrix} = \begin{pmatrix} \text{the rate of appearance} \\ \text{of size i} \\ \text{from breakage} \\ \text{of larger sizes} \end{pmatrix} - \begin{pmatrix} \text{the rate of} \\ \text{disapperance} \\ \text{of size i} \\ \text{by breakage} \end{pmatrix}$$

$$\frac{d[Hm_i(t)]}{dt} = -S_i Hm_i(t) + \sum_{\substack{j=1 \\ i>1}}^{i-1} b_{ij}\, s_j Hm_j(t) \qquad 1 \le i \le n \tag{2.13}$$

Where n is the number of size intervals and H is the total mass of material (hold-up) being ground. It is convenient to use geometric size intervals down to (n-1)-th interval and let the nth interval be a sink containing all finer material. Since material

cannot be broken out of the finest n-th interval k_n must always be zero; and $b_{nj} = B_{nj}$. For a batch mill H is constant and, therefore, can be dropped from the equation (Austin, L.G., Klimpel, R.R., Luckie, P.T., Rogers, R.S.C., 1982).

The equation may become non-linear if the breakage rate parameters are influenced by the size distribution in the batch mill which is itself a function of time. The rate parameters (and breakage distribution function parameters as well) may have explicit or implicit dependence on time. The explicit dependence on time implies that the operating conditions are changed as a function of time but the material breakage properties are time invariant. The implicit dependence on time implies that the material properties themselves are changing with time, but yet the process kinetics may be linear. Herbst et. al. (1973) assumed if s_i and b_{ij} do not vary with time, the batch grinding is described by a set of n linear differential equations with constant coefficients, which can be compactly represented by the matrix equation would be (Herbst, J.A., Grandy, G.A., Fuerstenau, D.W., 1973):

$$\frac{d}{dt}[m(t)] = -[I - b]s\, m(t) \tag{2.14}$$

where;

“m” is an nx1 matrix (vector) representing the mass fraction of particles in each size interval in the mill.

“s” is an nxn diagonal matrix giving the specific rates of breakage.

“b” is an nxn lower triangular matrix with diagonal and upper diagonal elements being all zeroes and the lower diagonal elements being the breakage distribution functions.

“I” is the nxn identity matrix (Herbst, J.A., Grandy, G.A., Fuerstenau, D.W., 1973).

In practice, the grinding of a √2 geometric size interval experimentally gives first-order breakage, but this does not mean that the first-order breakage concept can be

applied to a wider size interval or to a very narrow size interval (or a differential size interval in the limit when size is considered as a continuous variable like time). In fact, the crushing strength of an irregularly shaped particle depends on its size, and the magnitude and orientation of the applied force as well. Therefore, it is very unlikely that the strengths of a number of particles all of a certain differential size are the same (Austin, L.G., Klimpel, R.R, Luckie, P.T., 1984).

The time-independent breakage rate parameter, s_i, depends not only on the material properties but also on grinding mill variables such as the mill size, the filling ratio, the rotational speed, the ball size and the load, etc. The specific rates of breakage are lower for smaller particle sizes because smaller particles are inherently stronger and because it is more difficult to nip unit mass of small sizes between the balls. For a given ball size, specific breakage rate values increase up to a certain size, passing through a maximum, and then start to decrease for coarser particles because large particles are too strong to be broken in the mill (Lynch, A.C., 1977).

2.4.1.4 Methods for Estimation of Breakage Rate and Distribution

Batch grinding tests performed by with narrow size fractions (one-size fraction method) are found to be the most accurate method for obtaining s_i and b_{ij} values for grinding in laboratory scale mills because there are no effects of RTD or variation of hold-up to complicate the analysis, so long as the power input into the batch test mill remains constant (Herbst, J.A., Rajamani, R.K., 1982).

The one-size-fraction (single size-interval) consists of grinding a starting material which is predominantly of one size interval (e.g. a 2 sieve interval). Alternatively, a fresh original-size feed may be used for each grind time (Herbst, J.A., Rajamani, R.K., 1982) .

For the determination of s_i values, only the fraction left in the top size needs to be determined, however to determine b_{ij} values, however, very accurate complete size analysis at short grind times is necessary. A complete study on a given material

under a given set of conditions normally involves measuring si values for three or four starting sizes, getting the size distribution at short times to enable bij values to be calculated for each of these sizes, and determining the complete family of size distributions resulting from one or two of the starting sizes (Austin, L.G., Klimpel, R.R, Luckie, P.T., 1984).

If the kinetics of disappearance of the single size-interval feed follows the first-order grinding hypothesis, a plot of $m_i(t)$ on a log scale vs. t on a linear scale should give a straight line. It is not correct to force the line to pass through $m_1(0)=1$ at zero time as there may be an incomplete-sieving error with the original-size feed, which should be determined by a blank sieving test before grinding tests. The value of s_i is determined from the slope of the plot, as seen from Figure 2.1 (Austin, L.G., Klimpel, R.R, Luckie, P.T., 1984).

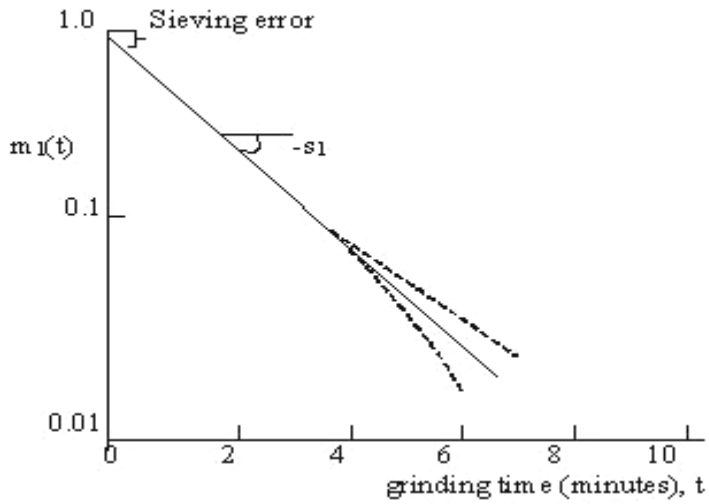

Figure 2.2 Determination of s_1 value (Austin, et al., 1984).

Non-first-order effects (abnormal breakage) may arise either due to change in properties of the material being ground or the change of grinding environment in the mill, such as cushioning action and altered mechanics of the mill action as fines increase in the mill. It is also likely that the starting material can contain abnormally weak particles due to flaws introduce during feed preparation. In this case, it has been suggested to precondition the sized feed in a ball mill for a very short grind time and re-sieve to eliminate the broken particles (Austin, et al., 1984).

The method proposed by Austin et. al. (1984) say that the best results for B values are obtained when 20 to 30% of the top size material is broken out of their original size. Assuming there is no re-breakage of fragments, then BI method is formulized as (Austin, et al., 1984):

$$B_{i,1} = \frac{P_i(t) - P_i(0)}{P_2(t) - P_2(0)} \tag{2.15}$$

where $P_i(t)$ is the product amount for size i at time t.

An alternative and a more precise method which uses the compensation condition to correct re-breakage of fragments, BII method based on the batch grinding equation (Austin, et al., 1984).

For the top size assuming that the compensation conditions applied approximately;

$$1 - P_i(t) \cong [1 - P_i(0)] \exp(-B_{i,1}\, s_1\, t), \qquad i > 1 \tag{2.16}$$

For the top size interval, first-order breakage gives;

$$1 - P_2(t) \cong [1 - P_2(0)] \exp(-s_1\, t), \quad \text{since } B_{2,1}=1 \tag{2.17}$$

Then ;

$$-s_1 t = \ln\left[\frac{(1 - P_2(t))}{(1 - P_2(0))}\right] \tag{2.18}$$

$$-B_{i,1} s_1 t \cong \ln\left[\frac{(1 - P_i(t))}{(1 - P_i(0))}\right] \tag{2.19}$$

$$B_{i,1} = \frac{\log\left[\frac{1-P_i(0)}{1-P_i(t)}\right]}{\log\left[\frac{1-P_2(0)}{1-P_2(t)}\right]} \quad i > 1 \; BII \; METHOD \tag{2.20}$$

Cumulative primary breakage distribution function Bi,j is also defined in an empirical form by;

$$B_{i,j} = \Phi_j \left(\frac{X_{i-1}}{X_j}\right)^{\gamma} + (1-\Phi_j)\left(\frac{X_{i-1}}{X_j}\right)^{\beta} \tag{2.21}$$

where xi is the top size and $B_{i,j}$ is the weight fraction of primary breakage products. The parameters Φ, γ and β define the size distribution of the material being ground. On plotting size versus Bi,j on the log scale, the slope of the lower portion of the curve gives the value of γ while the slope of the upper portion of the curve gives the value of β, and Φ is the intercept as shown in Fig. 2.3 (Austin, et al., 1984).

The primary characteristic of the $B_{i,j}$ curves is the final slope of each plot γ. The smaller the curve of γ, the higher the relative amounts of progeny fines that are produced from breakage. Conversely, materials having a large γ value give less relative amounts of fines and can therefore be expected to produce steeper size distributions when ground in a given machine. The β, and Φ values show how rapidly fractions close to feed size are reduced to a lower size. The Bi,j values are said to be normalisable if the fraction which appears at sizes less than the starting size is indepented of the starting size. In terms of plots, the curves should be super-imposed on each other if the $B_{i,j}$ values are normalisable. If the values of breakage distribution are dependent on starting feed size, that is, if they are normalisable, the Bi,j values are represented by the following equation (Austin et.al, 1984, Austin and Bagga, 1981, Austin and Luckie, 1971/1972):

$$\Phi_j = \Phi_1 \left[\frac{X_j}{X_1}\right]^{-\delta} \tag{2.23}$$

for normalized B values δ=0.

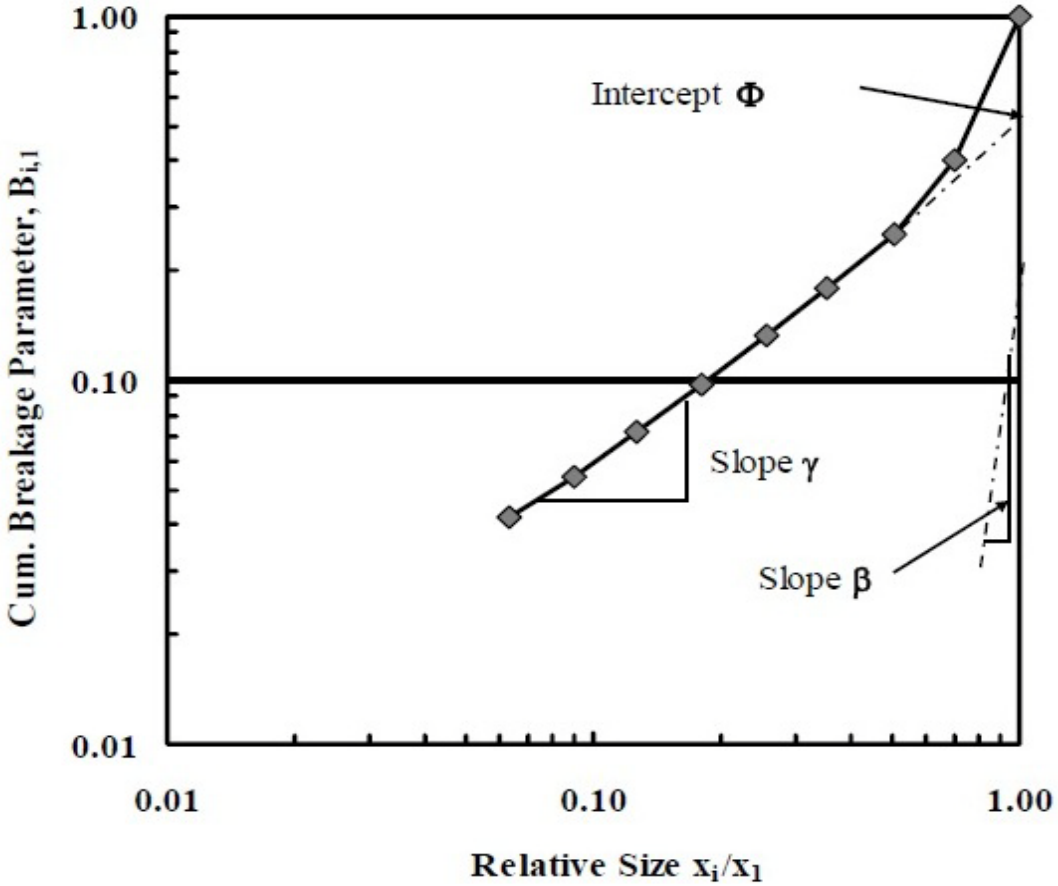

Figure 2.3 Obtaining primary breakage distribution function parameters for any single size fraction feed ground in the mill (Austin, et al., 1984).

CHAPTER THREE
EXPERIMENTAL STUDIES

3.1 Test Materials

In this study; pumice, perlite and zeolite samples were used as the experimental materials. They are taken from Aegean region of Turkey. The chemical compositions of the materials are presented in Table 3.1.

Table 3.1. Chemical composition of samples used in this study

Contents, %	Pumice	Perlite	Zeolite
SiO_2	80,50	79,73	78,48
Fe_2O_3	0,50	0,47	0,39
Al_2O_3	8,36	8,91	8,45
Na_2O	1,71	2,47	0,83
K_2O	4,22	3,75	3,52
MnO	0,003	0,004	0,001
MgO	0,21	0,18	0,46
CaO	0,52	0,50	1,54
($CaCO_3$)	–	–	–
Loss of ignition	4,04	3,95	6,29

3.2 Bond Work Index Estimation Studies

F.C. Bond developed the Bond ball mill standard grindability testing in the 1930s. He modified the testing procedure several times and the final version has existed unaltered since 1961.The Bond grindability testing procedure has been standardized in such a way that the same grindability values, i.e. Bond work index, can be measured for the same ore when tests are performed by different operators. This is achieved by ensuring that the material in the mill receives the same grinding energy

per mill revolution. This involves standardization of mill dimensions, charge weight, grinding media weight and size distribution, test screen size, screening time, speed of rotation and operating practice. For daily control purposes at the operations, a minor loss in the accuracy of the work index can be sacrificed. However, the best possible estimate of the work index is need for design purposes (Kaya et al., 2003).

The standard Bond grindability testing has changed over the years due to changes in ball size distributions and densities, test closure criteria, sample preparation, sample splitting, screening etc. There is often great confusion on the sensitivity of the Bond grindability testing (Kaya et al., 2003).

250% circulating load. The mill is 30,5 x 30,5 cm with rounded corners and a smooth lining, except Mosher and Tague (2001), Angove and Dunne (1997), Kaya (2001) and Kaya et al. (2003) presented excellent papers on the precision, repeatability and reproducibility of the Bond grindability testing. The differences up to 13% in the Bond indices were reported by different laboratories using the same ore with different operators and equipment (Kaya et al., 2003).

Tuzun (2001) and Deniz et al. (2003) have shown that the Bond work index values generally increase with decreasing test sieving size. On the other hand, Smith and Lee (1968) showed that the work index values for certain ores do not change and sometimes decrease with decreasing test sieve size. This study investigates the effect of different test screen sizes (Pi) on the Bond work index (Wi) for different materials of pumice, perlite, zeolite and limestone (Kaya et al., 2003).

3.2.1 Bond Ball Mill Standard Grindability Test

According to the standard Bond test (Bond, 1961) the feed is prepared by stage crushing to pass a 3,36 mm screen. It is screen analyzed and packed into a 700 cm^3 graduated cylinder, and the weight of 700 cm^3 is placed in the mill and ground dry at for a 10,2 x 20,3 cm hand-hole door for charging. It has revolution counter and runs at 70 rpm (about 85% of the critical speed). The grinding charge consists of 285 iron

balls weighing 20,125 g. It has a calculated surface area of 5,432 cm^2. Tests are performed different closing sieve sizes. The first grinding cycle is usually allowed to run for 100 revolutions. The product is dumped, the ball is screened out, the 700 cm^3 of material is screened on sieves of the mesh size tested, with a coarser protecting screen of 0,297 mm. The under size is weighed, and fresh feed is added to the oversize to bring its weight back to that of the original charge. Then, it is returned to the mill and ground for the number of revolutions calculated to produce a 250% circulating load, dumped and rescreened. The number of revolutions required is calculated from the results of the previous period to produce sieve undersize equal to 1/3,5 of the total charge in the mill. The locked-cycle grinding test continuous until the net grams of the sieve undersize produced per mill revolution reaches equilibrium and reverses its direction of increase or decrease. Then, the undersize product and circulating load are screen analyzed and the average of the last three net grams per revolution (Gbp) is the ball mill grindability. The ball mill work index, Wi (kWh/st) is calculated from this equation 3.1, (Bond, 1961):

$$W_i = \frac{44.5}{P_i^{0.23} x Gbp^{0.82} x \left(\frac{10}{\sqrt{P}} - \frac{10}{\sqrt{F}} \right)} \tag{3.1}$$

F and P are 80% passing cumulative passing sizes in the microns for feed a product respectively, P_i is the opening in microns of the screen size tested. In this study, the tests are at different closing sieve sizes of 75 µm, 106 µm, 150 µm and 212 µm (Bond, 1961).

The Bond mill grinding ball charge presented in Table 3.2 along with Bond's original ball size distribution. The slight differences of weights between two charges is due to changes in the in the specific gravities of steel since 1930s. Total ball weights of 20,125 and the number of balls of 285 were kept the same. The Bond standard ball mill custom made by the Aymas Machine Inc. (in İzmir, Turkey), was used in this study and also it presented Fig. 3.3.

Table 3.2 Bond mill charge distribution used in this study.

Bond's Original			This Study		
Ball size, mm	Number of balls	Weight, g	Ball size, mm	Number of balls	Weight, g
36.8	43	8,800	38.0	39	8,807
29.7	67	7,209	30.0	64	7,087
25.4	10	672	25.4	10	670
19.1	71	2,012	19.1	70	1,984
15.5	97	1,432	15.9	90	1,477
			12.7	12	100
	285	20,125		285	20,125

In this study, the samples were prepared with the same standard sampling procedure. All the samples were brought to below 3,36 mm size by the stage crushing with laboratory jaw and roll crushers, different sizes (gap) of jaw crushers were used for primary (Fig.3.3) and secondary crushers (Fig.3.4). The sieving set for the size analysis of the feed was, 3.350 mm, 2.360 mm, 1.700 mm, 1,18 mm, 0.850 mm, 0.600 mm, 0.425 mm, 0.300 mm, 0.212 mm and 0.150 mm (Fig. 3.4). The set for the product size analysis was, 0.150 mm, 0.125 mm, 0.106 mm, 0.075 mm, 0.053 mm and 0.045 mm.

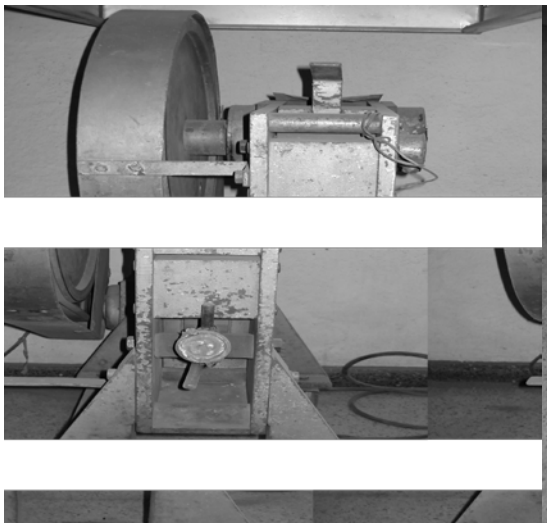

Fig. 3.1 The primary jaw crusher used in this study

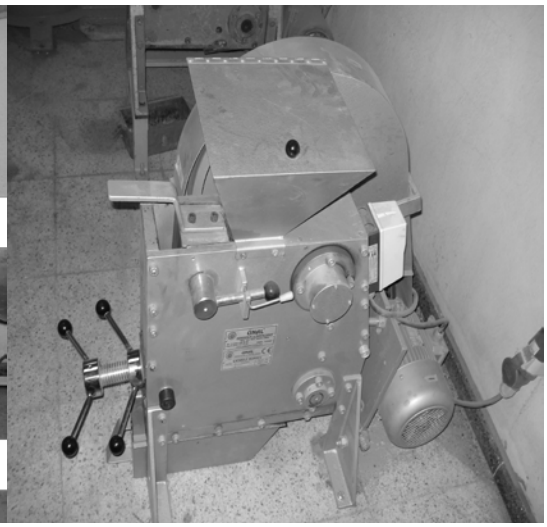

Fig. 3.2 The secondary laboratory type jaw crusher used in this study

Figure 3.3 The Bond mill and the ball charge used in this study

Figure 3.4 The sieving set and the vibratory sieving machine used in this study

3.3 Determination of Breakage Parameters of Perlite, Pumice and Zeolite

In this study, determining for breakage parameters of samples, 2 different grinding conditions were prepared. Perlite and Zeolite are in the same grinding conditions because of their densities are almost the same; otherwise pumice's density is different than perlite and zeolite. The grinding conditions for perlite, zeolite and pumice are shown in Table 3.3 and Table 3.4. The experimental studies were performed in a laboratory size ball mill (Fig. 3.5), whose characteristics and test conditions are described at Table 3.3 and Table 3.4. The breakage parameters were determined by using four mono-size feed fractions of (1,7mmx1,18mm ; 0,850mmx600mm ; 0,425mmx0,300mm ; 0,212mmx0,150mm) were prepared. The sieving schedules were established which gave complete sieving without excessive abrasion; usually, a sieving time of 10 min. on a sieving machine, with a sample of 50 g. taken from the ground product by cone and quartering method to be put on the top sieve for screen analysis. Considerable care was taken to accurate and reproducible sieve size distributions after each grinding tests. These conditions were chosen because it is known that both dry and wet grinding give normal first-order grinding kinetics under such conditions. After each grinding periods, the mill was left long enough to allow the particles to settle, the balls were cleaned and removed from the mill one by one, and the mixed powder was sampled for size analysis.

Figure 3.5 The laboratory type ball mill used in this study

Table 3.3 Grinding Conditions for Determining Breakage Parameters of Perlite and Zeolite

Mill	Diameter, cm	20	20	20	20	20	20
	Length, cm	30	30	30	30	30	30
	Volume, cm3	9420	9420	9420	9420	9420	9420
Mill Speed	Critical, Nc, rpm	103	105	103	103	105	103
	Operational (75%), rpm	77	79	77	77	79	77
Balls	**Diameter, mm**	**30**	**38**	**30 ; 25,4 ; 19,05**	**30**	**38**	**30 ; 25,4 ; 19,05**
	Number	53	26	36 ; 10 ; 44	53	26	36 ; 10 ; 44
	Average ball weight, g	111	226	111; 67 ; 28	111	226	111; 67 ; 28
	Specific gravity	7,8	7,9	7,8	7,8	7,9	7,8
	Quality	Aloy steel	Aloy steel	Aloy steel	Aloy steel	Aloy steel	Aloy steel
	Assumed bed porosity, %	40	40	40	40	40	40
	Fractional ball filling, JB	0,13	0,13	0,13	0,13	0,13	0,13
	Total ball weight, g	5869	5885	5903	5869	5885	5903
Material	Specific gravity	2,3	2,3	2,3	2,3	2,3	2,3
	Bulk density, g/cm3	1,38	1,38	1,38	1,38	1,38	1,38
	Weight, g (Hesaplandı)	413	412	416	689	687	693
	Fractional powder filling, fc	**0,032**	**0,032**	**0,032**	**0,053**	**0,053**	**0,053**
	Interstitial filling, U, %	**0,6**	**0,6**	**0,6**	**1**	**1**	**1**
Density	Zeolite, g/cm3	2,10-2,47	Loose bulk density = 0,8-0,9				
	Perlite	2,2-2,4	Bulk density = 30-150 kg/m3				
	Pumice	0,5-1					
Nc=42,3*((D-d)^(0,5)), (D and d in meter)			Grinding time, min	0,13 ; 1 ; 3 and 6			
J=[(Mass of balls/ball density)/(mill volume)]*(1/0,6)			Size Fractions	1700-1180 µm 850-600 µm ; 425-300 µm ; 212-150 µm			
fc=[(Mass of powder/powder density)/(mill volume)]*(1/0,6)			Sieving time ; min.	10			
U=fc/(0,4*J)			Sample desiccatio	1 hour at 105 C			
Volume of sphere=(4/3)*3,14*r^(3)			Mill	Ball mill			
Specific gravity=m/V							

Table 3.4 Grinding Conditions for Determining Breakage Parameters of Pumice

Mill	Diameter, cm	20	20	20	20	20	20
	Length, cm	30	30	30	30	30	30
	Volume, cm3	9420	9420	9420	9420	9420	9420
Mill Speed	Critical, Nc, rpm	103	105	103	103	105	103
	Operational (75%), rpm	77	79	77	77	79	77
Balls	**Diameter, mm**	**30**	**38**	**30 ; 25,4 ; 19,05**	**30**	**38**	**30 ; 25,4 ; 19,05**
	Number	53	26	36 ; 10 ; 44	53	26	36 ; 10 ; 44
	Average ball weight, g	111	226	111; 67 ; 28	111	226	111; 67 ; 28
	Specific gravity	7,8	7,9	7,8	7,8	7,9	7,8
	Quality	Aloy steel	Aloy steel	Aloy steel	Aloy steel	Aloy steel	Aloy steel
	Assumed bed porosity, %	40	40	40	40	40	40
	Fractional ball filling, JB	0,13	0,13	0,13	0,13	0,13	0,13
	Total ball weight, g	5869	5885	5903	5869	5885	5903
Material	Specific gravity	2,3	2,3	2,3	2,3	2,3	2,3
	Bulk density, g/cm3	1,38	1,38	1,38	1,38	1,38	1,38
	Weight, g (Hesaplandı)	413	412	416	689	687	693
	Fractional powder filling, fc	**0,032**	**0,032**	**0,032**	**0,053**	**0,053**	**0,053**
	Interstitial filling, U, %	**0,6**	**0,6**	**0,6**	**1**	**1**	**1**
Density	Zeolite, g/cm3	2,10-2,47	Loose bulk density = 0,8-0,9				
	Perlite	2,2-2,4	Bulk density = 30-150 kg/m3				
	Pumice	0,5-1					
Nc=42,3*((D-d)^(0,5)), (D and d in meter)			Grinding time, min	0,13 ; 1 ; 3 and 6			
J=[(Mass of balls/ball density)/(mill volume)]*(1/0,6)			Size Fractions	1700-1180 µm 850-600 µm ; 425-300 µm ; 212-150 µm			
fc=[(Mass of powder/powder density)/(mill volume)]*(1/0,6)			Sieving time ; min.	10			
U=fc/(0,4*J)			Sample desiccatio	1 hour at 105 C			
Volume of sphere=(4/3)*3,14*r^(3)			Mill	Ball mill			
Specific gravity=m/V							

CHAPTER FOUR
EXPERIMENTAL RESULTS

4.1 Results and Discussion of Bond Work Index Estimation Studies

The Bond work indices measured using four different materials and test closing sieve sizes are presented in Table 4.1 along with grind abilities (Gbp, g/rev.), P_{80} and F_{80} values and in Figure 4.1 and also all closing sizes test results tables were presented in Appendix A. The results of this investigation indicate that the measured Bond work indices for four different materials increase with decreasing test closing sieve sizes. This implies that the grinding energy increases with decreasing test sieve size. The slope of the line is the same with coarser sieve sizes but increases substantially at 75 micron test sieve size. The values for amorphous silica taken from the literature (Vedat et al. 2003) were added in Figure 4.1 for comparison purposes.

It is expected that the grinding energy would increase with decreasing particle size as seen from the measured Bond work indices that increased with decreased test sieve sizes. Similar results were obtained by Tuzun (2001) and Deniz et al. (2003), i.e increased work index values at decreasing test screen sizes. On the other hand, Smith and Lee (1968) reported that the work index values for certain ores may not change and also decrease with decreasing test sieve size as seen in Figure 4.2. For galena and limestone, the measured Bond indices stayed the same with changing closing sieve size. The measure Bond indices, however, decreased with decreasing test sieve size for taconite implying that the grinding energy decreases with decreasing particle size.

Table 4.1 Bond work indices (kWh/t) of four different materials measured at different test closing sieve sizes

Material	**P_i (µm)**	**Work Index W_i (kwh/t)**	**Grindability Gbp (g/rev.)**	**P_{80} (µm)**	**F_{80} (µm)**
Pumice	75	20,27	0,850	65,2	2136
	106	15,36	1,250	79,1	2136
	150	12,79	1,874	113,5	2136
	212	11,12	2,633	157,5	2137
Perlite	75	17,79	0,970	65,0	2611
	106	12,72	1,547	80,2	2611
	150	11,34	2,116	114,9	2611
	212	9,87	3,011	163,7	2614
Zeolite	75	15,39	1,123	61,0	2290
	106	13,31	1,510	81,7	2290
	150	11,80	1,963	107,9	2290
	212	9,46	2,925	143,5	2298
Limestone	75	11,80	1,646	62,6	1706
	106	9,02	2,624	85,9	1706
	150	8,82	3,400	128,7	1705

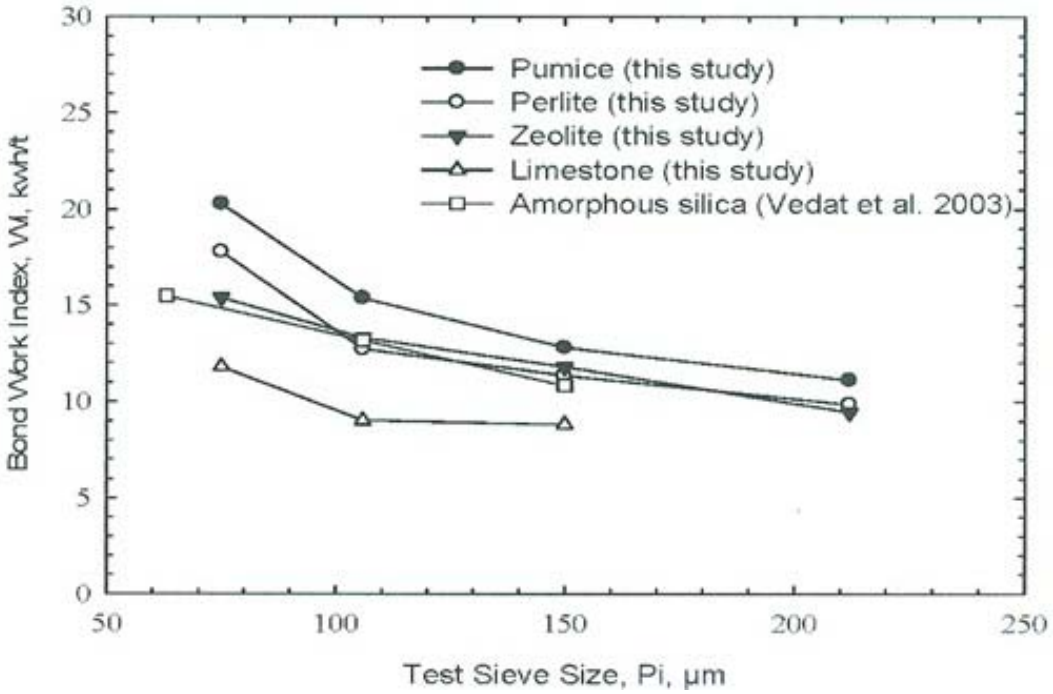

Figure 4.1 Variation of Bond Work Index with test screen size

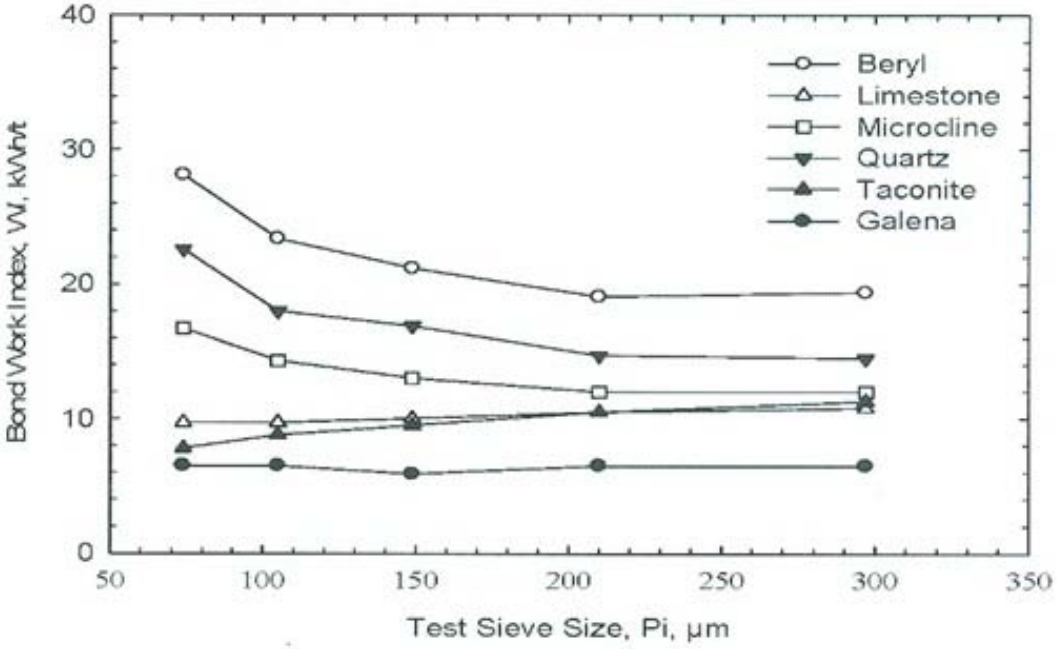

Figure 4.2 Variation of Bond Work Index with test screen size (Smith and Lee, 1968)

4.2 Results and Discussion of Breakage Parameters of Samples

In this study, effect of fraction of void spaces in ball bed filled with powder value (U) and ball sizes investigated on a perlite, pumice and zeolite samples received from the Aegean region of Turkey using dry batch grinding conditions. Four different mono-size fractions, between 1,7 and 0,150 mm, were prepared using √2 sieve series. The specific rates of breakage (S_i) and the primary breakage distribution ($B_{i,j}$) equations were determined from the size distributions at different grinding times (0,13 ; 1 ; 3 and 6 min.) and the model parameters were compared for the two different void spaces in ball bed filled with powder value (U= 0,6 and U=1) with three type (38mm), (30mm) and (30-25,4-19,05mm) ball size charge.

This presents the importance and usage of natural perlite, pumice and zeolite, which was recently recognized in the industry. Therefore, the grinding properties of natural perlite, pumice and zeolite were studied with the emphasis on a kinetic model study in a ball mill. The experimental mill employed was laboratory sized, it has also described with grinding conditions in Table 3.3 and Table 3.4.

4.2.1 Breakage Parameters of Perlite

4.2.1.1 The Specific Rates of Breakage (S_i) and The Primary Breakage Distribution Functions ($B_{i,j}$) Values of Perlite at 38 mm Ball Size Charge

Figure B.14 and Figure B.28, show the initial grinding results of perlite mineral plotted in first-order from for varying feed size fractions – 1700 + 1180, - 850 + 600, -425 + 300 and – 212 + 150 µm ground with a ball diameter of 38mm. Test results show specific rate of breakage values, Si, increased with increasing feed size.

According to figures the specific rates of breakage (S_i) value increase, as feed size fraction increases. The S_i values of -1700 + 1180, - 850 + 600, - 425 + 300 and – 212 + 150 µm feed fractions of perlite ground dry with a ball diameter of 38 mm were obtained to be 1.23, 0.81, 0.32 and 0.13 min.$^{-1}$ at U=0.6 respectively and the S_i values

of -1700 + 1180, - 850 + 600, - 425 + 300 and – 212 + 150 µm feed fractions of perlite ground dry with a ball diameter of 38 mm were obtained to be 0.88, 0.68, 0.27 and 0.11 $min.^{-1}$ at U=1 respectively.

The variations in specific rates of breakage, Si with interstitial filling U, were studied using -1700 + 1180, - 850 + 600, - 425 + 300 and – 212 + 150 µm feed size material. It was observed that the specific rate of breakage, Si, decreased with increasing interstitial powder filling.

The aT value indicates specific rate of breakage at x_0 = 1000 µm particle size. The aT value is 1.04 $min.^{-1}$ with α=1.01 at U=0.6 and the aT value is 0.83 $min.^{-1}$ with α=1.32 at U=1 for perlite ground dry with a ball diameter of 38 mm showed in Figure B.13 and B.27. Results show aT values, decreased with increasing interstitial powder filling.

Figures B.2; B.5; B.8 and B.11 at U=0.6 and Figures B.16; B.19; B.22 and B.25 at U=1 show the particle size distributions of dry grinding of the perlite at various grinding times (0.13; 1.0; 3.0 and 6;0 min.) for -1700 + 1180, - 850 + 600, - 425 + 300 and – 212 + 150 µm feed size the sieving data are given in Tables B.2; B.4; B.6 and B.8 at U=0.6 and Tables B.11; B.13; B.15 and B.17 at U=1.

The cumulative primary breakage distribution function results determined using the BII calculation method, the $B_{i,j}$ functions results showed for -1700 + 1180, - 850 + 600, - 425 + 300 and – 212 + 150 µm feed fractions of perlite ground dry with a ball diameter of 38 mm in Tables B.1; B.3; B.5 and B.7 at U=0.6 and Tables B.10; B.12; B.14 and B.16 at U=1, Figures B.1; B.4; B.7 and B.10 at U=0.6 and Figures B.15; B.18; B.21 and B.24 at U=1

The comparison of the breakage parameters of perlite in terms of the values of S, aT, α, γ and β are also presented in Table B.9 at U=0.6 and Table B.18 at U=1.

Φ value indicates how rapidly fractions close to feed size are reduced to a lower size. Test results show Φ values, decreased with increasing interstitial powder filling and increased with increasing feed size. The primary characteristic of the $B_{i,j}$ curves is the final slope of each plot γ. The smaller the curve of γ, the higher the relative amounts of progeny fines that are produced from breakage. Conversely, materials having a large γ value give less relative amounts of fines. Test results show γ values, increased with increasing interstitial powder filling and increased with decreasing feed size.

4.2.1.2 The Specific Rates of Breakage (S_i) and The Primary Breakage Distribution Functions ($B_{i,j}$) Values of Perlite at 30 mm Ball Size Charge

Figure B.42 and Figure B.56, show the initial grinding results of perlite mineral plotted in first-order from for varying feed size fractions – 1700 + 1180, - 850 + 600, -425 + 300 and – 212 + 150 µm ground with a ball diameter of 30mm. Test results show specific rate of breakage values, Si, increased with increasing feed size.

According to figures the specific rates of breakage (S_i) value increase, as feed size fraction increases. The S_i values of -1700 + 1180, - 850 + 600, - 425 + 300 and – 212 + 150 µm feed fractions of perlite ground dry with a ball diameter of 30 mm were obtained to be 1.09, 0.88, 0.48 and 0.27 $min.^{-1}$ at U=0.6 respectively and the S_i values of -1700 + 1180, - 850 + 600, - 425 + 300 and – 212 + 150 µm feed fractions of perlite ground dry with a ball diameter of 30 mm were obtained to be 0.91, 0.73, 0.31 and 0.13 $min.^{-1}$ at U=1 respectively. The S_i values at U=0.6 for perlite are higher than at U=1 by a factor of fractional powder filling (f_c).

The variations in specific rates of breakage, Si with interstitial filling U, were studied using -1700 + 1180, - 850 + 600, - 425 + 300 and – 212 + 150 µm feed size material. It was observed that the specific rate of breakage, Si, decreased with increasing interstitial powder filling.

The aT value indicates specific rate of breakage at x_0 = 1000 µm particle size. The aT value is 1.11 min.$^{-1}$ with α=0.91 at U=0.6 and the aT value is 0.87 min.$^{-1}$ with α=1.17 at U=1 for perlite ground dry with a ball diameter of 30 mm showed in Figure B.41 and B.55. Results show aT values, decreased with increasing interstitial powder filling.

Figures B.30; B.33; B.36 and B.39 at U=0.6 and Figures B.44; B.47; B.50 and B.53 at U=1 show the particle size distributions of dry grinding of the perlite at various grinding times (0.13; 1.0; 3.0 and 6;0 min.) for -1700 + 1180, - 850 + 600, - 425 + 300 and – 212 + 150 µm feed size the sieving data are given in Tables B.20; B.22; B.24 and B.26 at U=0.6 and Tables B.29; B.31; B.33 and B.35 at U=1.

The cumulative primary breakage distribution function results determined using the BII calculation method, the $B_{i,j}$ functions results showed for -1700 + 1180, - 850 + 600, - 425 + 300 and – 212 + 150 µm feed fractions of perlite ground dry with a ball diameter of 30 mm in Tables B.19; B.21; B.23 and B.25 at U=0.6 and Tables B.28; B.30; B.32 and B.34 at U=1, Figures B.29; B.32; B.35 and B.38 at U=0.6 and Figures B.43; B.46; B.49 and B.52 at U=1

The comparison of the breakage parameters of perlite in terms of the values of S, aT, α, γ and β are also presented in Table B.27 at U=0.6 and Table B.36 at U=1.

Φ value indicates how rapidly fractions close to feed size are reduced to a lower size. Test results show Φ values, decreased with increasing interstitial powder filling and increased with increasing feed size. The primary characteristic of the $B_{i,j}$ curves is the final slope of each plot γ. The smaller the curve of γ, the higher the relative amounts of progeny fines that are produced from breakage. Conversely, materials having a large γ value give less relative amounts of fines. Test results show γ values, increased with increasing interstitial powder filling and increased with decreasing feed size.

4.2.1.2 The Specific Rates of Breakage (S_i) and The Primary Breakage Distribution Functions ($B_{i,j}$) Values of Perlite at 30 – 25,4 – 19,05 mm Ball Size Charge

Figure B.70 and Figure B.83, show the initial grinding results of perlite mineral plotted in first-order from for varying feed size fractions – 1700 + 1180, - 850 + 600, -425 + 300 and – 212 + 150 µm ground with a ball diameter of 30 – 25,4 – 19,05 mm. Test results show specific rate of breakage values, Si, increased with increasing feed size.

According to figures the specific rates of breakage (S_i) value increase, as feed size fraction increases. The S_i values of -1700 + 1180, - 850 + 600, - 425 + 300 and – 212 + 150 µm feed fractions of perlite ground dry with a ball diameter of 30 – 25,4 – 19,05 mm were obtained to be 1.41, 1.16, 0.65 and 0.37 min.$^{-1}$ at U=0.6 respectively and the S_i values of -1700 + 1180, - 850 + 600, - 425 + 300 and – 212 + 150 µm feed fractions of perlite ground dry with a ball diameter of 30 -25,4 – 19,05 mm were obtained to be 0.98, 0.86, 0.46 and 0.23 min.$^{-1}$ at U=1 respectively. The S_i values at U=0.6 for perlite are higher than at U=1 by a factor of fractional powder filling (f_c).

The variations in specific rates of breakage, Si with interstitial filling U, were studied using -1700 + 1180, - 850 + 600, - 425 + 300 and – 212 + 150 µm feed size material. It was observed that the specific rate of breakage, Si, decreased with increasing interstitial powder filling.

The aT value indicates specific rate of breakage at x_0 = 1000 µm particle size. The aT value is 1.38 min.$^{-1}$ with α=0.74 at U=0.6 and the aT value is 1.28 min.$^{-1}$ with α=1.09 at U=1 for perlite ground dry with a ball diameter of 30 – 25,4 – 19,05 mm showed in Figure B.69 and B.83. Results show aT values, decreased with increasing interstitial powder filling.

Figures B.58; B.61; B.64 and B.67 at U=0.6 and Figures B.72; B.75; B.78 and B.81 at U=1 show the particle size distributions of dry grinding of the perlite at

various grinding times (0.13; 1.0; 3.0 and 6;0 min.) for -1700 + 1180, - 850 + 600, - 425 + 300 and – 212 + 150 µm feed size the sieving data are given in Tables B.38; B.40; B.42 and B.44 at U=0.6 and Tables B.47; B.49; B.51 and B.53 at U=1.

The cumulative primary breakage distribution function results determined using the BII calculation method, the $B_{i,j}$ functions results showed for -1700 + 1180, - 850 + 600, - 425 + 300 and – 212 + 150 µm feed fractions of perlite ground dry with a ball diameter of 30 – 25,4 – 19,05 mm in Tables B.37; B.39; B.41 and B.43 at U=0.6 and Tables B.46; B.48; B.50 and B.52 at U=1, Figures B.57; B.60; B.63 and B.66 at U=0.6 and Figures B.71; B.74; B.77 and B.80 at U=1

The comparison of the breakage parameters of perlite in terms of the values of S, aT, α, γ and β are also presented in Table B.45 at U=0.6 and Table B.54 at U=1.

Φ value indicates how rapidly fractions close to feed size are reduced to a lower size. Test results show Φ values, decreased with increasing interstitial powder filling and increased with increasing feed size. The primary characteristic of the $B_{i,j}$ curves is the final slope of each plot γ. The smaller the curve of γ, the higher the relative amounts of progeny fines that are produced from breakage. Conversely, materials having a large γ value give less relative amounts of fines. Test results show γ values, increased with increasing interstitial powder filling and increased with decreasing feed size.

4.2.2 Breakage Parameters of Pumice

4.2.2.1 The Specific Rates of Breakage (S_i) and The Primary Breakage Distribution Functions ($B_{i,j}$) Values of Perlite at 38 mm Ball Size Charge

Figure C.14 and Figure C.28, show the initial grinding results of pumice mineral plotted in first-order from for varying feed size fractions – 1700 + 1180, - 850 + 600,

-425 + 300 and – 212 + 150 µm ground with a ball diameter of 38mm. Test results show specific rate of breakage values, Si, increased with increasing feed size.

According to figures the specific rates of breakage (S_i) value increase, as feed size fraction increases. The S_i values of -1700 + 1180, - 850 + 600, - 425 + 300 and – 212 + 150 µm feed fractions of pumice ground dry with a ball diameter of 38 mm were obtained to be 1.65, 1.25, 0.5 and 0.17 min.$^{-1}$ at U=0.6 respectively and the S_i values of -1700 + 1180, - 850 + 600, - 425 + 300 and – 212 + 150 µm feed fractions of pumice ground dry with a ball diameter of 38 mm were obtained to be 0.97, 0.77, 0.33 and 0.13 min.$^{-1}$ at U=1 respectively.

The variations in specific rates of breakage, Si with interstitial filling U, were studied using -1700 + 1180, - 850 + 600, - 425 + 300 and – 212 + 150 µm feed size material. It was observed that the specific rate of breakage, Si, decreased with increasing interstitial powder filling.

The aT value indicates specific rate of breakage at x_0 = 1000 µm particle size. The aT value is 1.52 min.$^{-1}$ with α=1.14 at U=0.6 and the aT value is 0.94 min.$^{-1}$ with α=1.28 at U=1 for pumice ground dry with a ball diameter of 38 mm showed in Figure C.13 and C.27. Results show aT values, decreased with increasing interstitial powder filling.

Figures C.2; C.5; C.8 and C.11 at U=0.6 and Figures C.16; C.19; C.22 and C.25 at U=1 show the particle size distributions of dry grinding of the pumice at various grinding times (0.13; 1.0; 3.0 and 6;0 min.) for -1700 + 1180, - 850 + 600, - 425 + 300 and – 212 + 150 µm feed size the sieving data are given in Tables C.2; C.4; C.6 and C.8 at U=0.6 and Tables C.11; C.13; C.15 and C.17 at U=1.

The cumulative primary breakage distribution function results determined using the BII calculation method, the $B_{i,j}$ functions results showed for -1700 + 1180, - 850 + 600, - 425 + 300 and – 212 + 150 µm feed fractions of pumice ground dry with a ball diameter of 38 mm in Tables C.1; C.3; C.5 and C.7 at U=0.6 and Tables C.10;

C.12; C.14 and C.16 at U=1, Figures C.1; C.4; C.7 and C.10 at U=0.6 and Figures C.15; C.18; C.21 and C.24 at U=1

The comparison of the breakage parameters of perlite in terms of the values of S, aT, α, γ and β are also presented in Table C.9 at U=0.6 and Table C.18 at U=1.

Φ value indicates how rapidly fractions close to feed size are reduced to a lower size. Test results show Φ values, decreased with increasing interstitial powder filling and increased with increasing feed size. The primary characteristic of the $B_{i,j}$ curves is the final slope of each plot γ. The smaller the curve of γ, the higher the relative amounts of progeny fines that are produced from breakage. Conversely, materials having a large γ value give less relative amounts of fines. Test results show γ values, increased with increasing interstitial powder filling and increased with decreasing feed size.

4.2.2.2 The Specific Rates of Breakage (S_i) and The Primary Breakage Distribution Functions ($B_{i,j}$) Values of Pumice at 30 mm Ball Size Charge

Figure C.42 and Figure C.56, show the initial grinding results of pumice mineral plotted in first-order from for varying feed size fractions – 1700 + 1180, - 850 + 600, -425 + 300 and – 212 + 150 µm ground with a ball diameter of 30mm. Test results show specific rate of breakage values, Si, increased with increasing feed size.

According to figures the specific rates of breakage (S_i) value increase, as feed size fraction increases. The S_i values of -1700 + 1180, - 850 + 600, - 425 + 300 and – 212 + 150 µm feed fractions of pumice ground dry with a ball diameter of 30 mm were obtained to be 1.68, 1.36, 0.70 and 0.35 min.$^{-1}$ at U=0.6 respectively and the S_i values of -1700 + 1180, - 850 + 600, - 425 + 300 and – 212 + 150 µm feed fractions of pumice ground dry with a ball diameter of 30 mm were obtained to be 1.02, 0.80, 0.36 and 0.16 min.$^{-1}$ at U=1 respectively. The S_i values at U=0.6 for pumice are higher than at U=1 by a factor of fractional powder filling (f_c).

The variations in specific rates of breakage, Si with interstitial filling U, were studied using -1700 + 1180, - 850 + 600, - 425 + 300 and – 212 + 150 µm feed size material. It was observed that the specific rate of breakage, Si, decreased with increasing interstitial powder filling.

The aT value indicates specific rate of breakage at x_0 = 1000 µm particle size. The aT value is 1.61 $min.^{-1}$ with α=0.95 at U=0.6 and the aT value is 0.95 $min.^{-1}$ with α=1.06 at U=1 for pumice ground dry with a ball diameter of 30 mm showed in Figure C.41 and C.55. Results show aT values, decreased with increasing interstitial powder filling.

Figures C.30; C.33; C.36 and C.39 at U=0.6 and Figures C.44; C.47; C.50 and C.53 at U=1 show the particle size distributions of dry grinding of the pumice at various grinding times (0.13; 1.0; 3.0 and 6;0 min.) for -1700 + 1180, - 850 + 600, - 425 + 300 and – 212 + 150 µm feed size the sieving data are given in Tables C.20; C.22; C.24 and C.26 at U=0.6 and Tables C.29; C.31; C.33 and C.35 at U=1.

The cumulative primary breakage distribution function results determined using the BII calculation method, the $B_{i,j}$ functions results showed for -1700 + 1180, - 850 + 600, - 425 + 300 and – 212 + 150 µm feed fractions of pumice ground dry with a ball diameter of 30 mm in Tables C.19; C.21; C.23 and C.25 at U=0.6 and Tables C.28; C.30; C.32 and C.34 at U=1, Figures C.29; C.32; C.35 and C.38 at U=0.6 and Figures C.43; C.46; C.49 and C.52 at U=1

The comparison of the breakage parameters of pumice in terms of the values of S, aT, α, γ and β are also presented in Table C.27 at U=0.6 and Table C.36 at U=1.

Φ value indicates how rapidly fractions close to feed size are reduced to a lower size. Test results show Φ values, decreased with increasing interstitial powder filling and increased with increasing feed size. The primary characteristic of the $B_{i,j}$ curves is the final slope of each plot γ. The smaller the curve of γ, the higher the relative amounts of progeny fines that are produced from breakage. Conversely, materials

having a large γ value give less relative amounts of fines. Test results show γ values, increased with increasing interstitial powder filling and increased with decreasing feed size.

4.2.2.3 The Specific Rates of Breakage (S_i) and The Primary Breakage Distribution Functions ($B_{i,j}$) Values of Pumice at 30 – 25,4 – 19,05 mm Ball Size Charge

Figure C.70 and Figure C.83, show the initial grinding results of pumice mineral plotted in first-order from for varying feed size fractions – 1700 + 1180, - 850 + 600, -425 + 300 and – 212 + 150 µm ground with a ball diameter of 30 – 25,4 – 19,05 mm. Test results show specific rate of breakage values, Si, increased with increasing feed size.

According to figures the specific rates of breakage (S_i) value increase, as feed size fraction increases. The S_i values of -1700 + 1180, - 850 + 600, - 425 + 300 and – 212 + 150 µm feed fractions of pumice ground dry with a ball diameter of 30 – 25,4 – 19,05 mm were obtained to be 1.80, 1.57, 0.88 and 0.53 min.$^{-1}$ at U=0.6 respectively and the S_i values of -1700 + 1180, - 850 + 600, - 425 + 300 and – 212 + 150 µm feed fractions of pumice ground dry with a ball diameter of 30 -25,4 – 19,05 mm were obtained to be 1.27, 1.15, 0.63 and 0.37 min.$^{-1}$ at U=1 respectively. The S_i values at U=0.6 for pumice are higher than at U=1 by a factor of fractional powder filling (f_c).

The variations in specific rates of breakage, Si with interstitial filling U, were studied using -1700 + 1180, - 850 + 600, - 425 + 300 and – 212 + 150 µm feed size material. It was observed that the specific rate of breakage, Si, decreased with increasing interstitial powder filling.

The aT value indicates specific rate of breakage at x_0 = 1000 µm particle size. The aT value is 1.83 min.$^{-1}$ with α=0.81 at U=0.6 and the aT value is 1.32 min.$^{-1}$ with α=0.88 at U=1 for pumice ground dry with a ball diameter of 30 – 25,4 – 19,05 mm showed in Figure C.69 and C.83. Results show aT values, decreased with increasing

interstitial powder filling. Figures C.58; C.61; C.64 and C.67 at U=0.6 and Figures C.72; C.75; C.78 and C.81 at U=1 show the particle size distributions of dry grinding of the pumice at various grinding times (0.13; 1.0; 3.0 and 6;0 min.) for -1700 + 1180, - 850 + 600, - 425 + 300 and – 212 + 150 µm feed size the sieving data are given in Tables C.38; C.40; C.42 and C.44 at U=0.6 and Tables C.47; C.49; C.51 and C.53 at U=1.

The cumulative primary breakage distribution function results determined using the BII calculation method, the $B_{i,j}$ functions results showed for -1700 + 1180, - 850 + 600, - 425 + 300 and – 212 + 150 µm feed fractions of pumice ground dry with a ball diameter of 30 – 25,4 – 19,05 mm in Tables C.37; C.39; C.41 and C.43 at U=0.6 and Tables C.46; C.48; C.50 and C.52 at U=1, Figures C.57; C.60; C.63 and C.66 at U=0.6 and Figures C.71; C.74; C.77 and C.80 at U=1

The comparison of the breakage parameters of pumice in terms of the values of S, aT, α, γ and β are also presented in Table C.45 at U=0.6 and Table C.54 at U=1.

Φ value indicates how rapidly fractions close to feed size are reduced to a lower size. Test results show Φ values, decreased with increasing interstitial powder filling and increased with increasing feed size. The primary characteristic of the $B_{i,j}$ curves is the final slope of each plot γ. The smaller the curve of γ, the higher the relative amounts of progeny fines that are produced from breakage. Conversely, materials having a large γ value give less relative amounts of fines. Test results show γ values, increased with increasing interstitial powder filling and increased with decreasing feed size.

4.2.3 Breakage Parameters of Zeolite

4.2.3.1 The Specific Rates of Breakage (S_i) and The Primary Breakage Distribution Functions ($B_{i,j}$) Values of Zeolite at 38 mm Ball Size Charge

Figure D.14 and Figure D.28, show the initial grinding results of zeolite mineral plotted in first-order from for varying feed size fractions – 1700 + 1180, - 850 + 600, -425 + 300 and – 212 + 150 µm ground with a ball diameter of 38mm. Test results show specific rate of breakage values, Si, increased with increasing feed size.

According to figures the specific rates of breakage (S_i) value increase, as feed size fraction increases. The S_i values of -1700 + 1180, - 850 + 600, - 425 + 300 and – 212 + 150 µm feed fractions of zeolite ground dry with a ball diameter of 38 mm were obtained to be 0.81, 0.65, 0.27 and 0.10 min.$^{-1}$ at U=0.6 respectively and the S_i values of -1700 + 1180, - 850 + 600, - 425 + 300 and – 212 + 150 µm feed fractions of zeolite ground dry with a ball diameter of 38 mm were obtained to be 0.47, 0.40, 0.21 and 0.10 min.$^{-1}$ at U=1 respectively.

The variations in specific rates of breakage, Si with interstitial filling U, were studied using -1700 + 1180, - 850 + 600, - 425 + 300 and – 212 + 150 µm feed size material. It was observed that the specific rate of breakage, Si, decreased with increasing interstitial powder filling.

The aT value indicates specific rate of breakage at x_0 = 1000 µm particle size. The aT value is 0.89 min.$^{-1}$ with α=0.96 at U=0.6 and the aT value is 0.48 min.$^{-1}$ with α=1.04 at U=1 for zeolite ground dry with a ball diameter of 38 mm showed in Figure D.13 and D.27. Results show aT values, decreased with increasing interstitial powder filling.

Figures D.2; D.5; D.8 and D.11 at U=0.6 and Figures D.16; D.19; D.22 and D.25 at U=1 show the particle size distributions of dry grinding of the zeolite at various grinding times (0.13; 1.0; 3.0 and 6;0 min.) for -1700 + 1180, - 850 + 600, - 425 +

300 and – 212 + 150 µm feed size the sieving data are given in Tables D.2; D.4; D.6 and D.8 at U=0.6 and Tables D.11; D.13; D.15 and D.17 at U=1.

The cumulative primary breakage distribution function results determined using the BII calculation method, the $B_{i,j}$ functions results showed for -1700 + 1180, - 850 + 600, - 425 + 300 and – 212 + 150 µm feed fractions of zeolite ground dry with a ball diameter of 38 mm in Tables D.1; D.3; D.5 and D.7 at U=0.6 and Tables D.10; D.12; D.14 and D.16 at U=1, Figures D.1; D.4; D.7 and D.10 at U=0.6 and Figures D.15; D.18; D.21 and D.24 at U=1

The comparison of the breakage parameters of zeolite in terms of the values of S, aT, α, γ and β are also presented in Table D.9 at U=0.6 and Table D.18 at U=1.

Φ value indicates how rapidly fractions close to feed size are reduced to a lower size. Test results show Φ values, decreased with increasing interstitial powder filling and increased with increasing feed size. The primary characteristic of the $B_{i,j}$ curves is the final slope of each plot γ. The smaller the curve of γ, the higher the relative amounts of progeny fines that are produced from breakage. Conversely, materials having a large γ value give less relative amounts of fines. Test results show γ values, increased with increasing interstitial powder filling and increased with decreasing feed size.

4.2.3.2 The Specific Rates of Breakage (S_i) and The Primary Breakage Distribution Functions ($B_{i,j}$) Values of Pumice at 30 mm Ball Size Charge

Figure D.42 and Figure D.56, show the initial grinding results of zeolite mineral plotted in first-order from for varying feed size fractions – 1700 + 1180, - 850 + 600, -425 + 300 and – 212 + 150 µm ground with a ball diameter of 30mm. Test results show specific rate of breakage values, Si, increased with increasing feed size.

According to figures the specific rates of breakage (S_i) value increase, as feed size fraction increases. The S_i values of -1700 + 1180, - 850 + 600, - 425 + 300 and – 212

+ 150 µm feed fractions of zeolite ground dry with a ball diameter of 30 mm were obtained to be 0.92, 0.78, 0.41 and 0.22 min.$^{-1}$ at U=0.6 respectively and the S_i values of -1700 + 1180, - 850 + 600, - 425 + 300 and – 212 + 150 µm feed fractions of zeolite ground dry with a ball diameter of 30 mm were obtained to be 0.56, 0.46, 0.24 and 0.11 min.$^{-1}$ at U=1 respectively. The S_i values at U=0.6 for zeolite are higher than at U=1 by a factor of fractional powder filling (f_c).

The variations in specific rates of breakage, Si with interstitial filling U, were studied using -1700 + 1180, - 850 + 600, - 425 + 300 and – 212 + 150 µm feed size material. It was observed that the specific rate of breakage, Si, decreased with increasing interstitial powder filling.

The aT value indicates specific rate of breakage at x_0 = 1000 µm particle size. The aT value is 0.95 min.$^{-1}$ with α=0.91 at U=0.6 and the aT value is 0.58 min.$^{-1}$ with α=0.98 at U=1 for zeolite ground dry with a ball diameter of 30 mm showed in Figure D.41 and D.55. Results show aT values, decreased with increasing interstitial powder filling.

Figures D.30; D.33; D.36 and D.39 at U=0.6 and Figures D.44; D.47; D.50 and D.53 at U=1 show the particle size distributions of dry grinding of the zeolite at various grinding times (0.13; 1.0; 3.0 and 6;0 min.) for -1700 + 1180, - 850 + 600, - 425 + 300 and – 212 + 150 µm feed size the sieving data are given in Tables D.20; D.22; D.24 and D.26 at U=0.6 and Tables D.29; D.31; D.33 and D.35 at U=1.

The cumulative primary breakage distribution function results determined using the BII calculation method, the $B_{i,j}$ functions results showed for -1700 + 1180, - 850 + 600, - 425 + 300 and – 212 + 150 µm feed fractions of zeolite ground dry with a ball diameter of 30 mm in Tables D.19; D.21; D.23 and D.25 at U=0.6 and Tables D.28; D.30; D.32 and D.34 at U=1, Figures D.29; D.32; D.35 and D.38 at U=0.6 and Figures D.43; D.46; D.49 and D.52 at U=1

The comparison of the breakage parameters of zeolite in terms of the values of S, aT, α, γ and β are also presented in Table D.27 at U=0.6 and Table D.36 at U=1.

Φ value indicates how rapidly fractions close to feed size are reduced to a lower size. Test results show Φ values, decreased with increasing interstitial powder filling and increased with increasing feed size. The primary characteristic of the $B_{i,j}$ curves is the final slope of each plot γ. The smaller the curve of γ, the higher the relative amounts of progeny fines that are produced from breakage. Conversely, materials having a large γ value give less relative amounts of fines. Test results show γ values, increased with increasing interstitial powder filling and increased with decreasing feed size.

4.2.3.3 The Specific Rates of Breakage (S_i) and The Primary Breakage Distribution Functions ($B_{i,j}$) Values of Zeolite at 30 – 25,4 – 19,05 mm Ball Size Charge

Figure D.70 and Figure D.83, show the initial grinding results of zeolite mineral plotted in first-order from for varying feed size fractions – 1700 + 1180, - 850 + 600, -425 + 300 and – 212 + 150 µm ground with a ball diameter of 30 – 25,4 – 19,05 mm. Test results show specific rate of breakage values, Si, increased with increasing feed size.

According to figures the specific rates of breakage (S_i) value increase, as feed size fraction increases. The S_i values of -1700 + 1180, - 850 + 600, - 425 + 300 and – 212 + 150 µm feed fractions of zeolite ground dry with a ball diameter of 30 – 25,4 – 19,05 mm were obtained to be 1.06, 0.92, 0.49 and 0.28 min.$^{-1}$ at U=0.6 respectively and the S_i values of -1700 + 1180, - 850 + 600, - 425 + 300 and – 212 + 150 µm feed fractions of zeolite ground dry with a ball diameter of 30 -25,4 – 19,05 mm were obtained to be 0.79, 0.68, 0.36 and 0.19 min.$^{-1}$ at U=1 respectively. The S_i values at U=0.6 for pumice are higher than at U=1 by a factor of fractional powder filling (f_c).

The variations in specific rates of breakage, Si with interstitial filling U, were studied using -1700 + 1180, - 850 + 600, - 425 + 300 and – 212 + 150 µm feed size material. It was observed that the specific rate of breakage, Si, decreased with increasing interstitial powder filling.

The aT value indicates specific rate of breakage at x_0 = 1000 µm particle size. The aT value is 1.07 min.$^{-1}$ with α=0.89 at U=0.6 and the aT value is 0.77 min.$^{-1}$ with α=0.93 at U=1 for zeolite ground dry with a ball diameter of 30 – 25,4 – 19,05 mm showed in Figure D.69 and D.83. Results show aT values, decreased with increasing interstitial powder filling.

Figures D.58; D.61; D.64 and D.67 at U=0.6 and Figures D.72; D.75; D.78 and D.81 at U=1 show the particle size distributions of dry grinding of the zeolite at various grinding times (0.13; 1.0; 3.0 and 6;0 min.) for -1700 + 1180, - 850 + 600, - 425 + 300 and – 212 + 150 µm feed size the sieving data are given in Tables D.38; D.40; D.42 and D.44 at U=0.6 and Tables D.47; D.49; D.51 and D.53 at U=1.

The cumulative primary breakage distribution function results determined using the BII calculation method, the $B_{i,j}$ functions results showed for -1700 + 1180, - 850 + 600, - 425 + 300 and – 212 + 150 µm feed fractions of zeolite ground dry with a ball diameter of 30 – 25,4 – 19,05 mm in Tables D.37; D.39; D.41 and D.43 at U=0.6 and Tables D.46; D.48; D.50 and D.52 at U=1, Figures D.57; D.60; D.63 and D.66 at U=0.6 and Figures D.71; D.74; D.77 and D.80 at U=1

The comparison of the breakage parameters of zeolite in terms of the values of S, aT, α, γ and β are also presented in Table D.45 at U=0.6 and Table D.54 at U=1.

Φ value indicates how rapidly fractions close to feed size are reduced to a lower size. Test results show Φ values, decreased with increasing interstitial powder filling and increased with increasing feed size. The primary characteristic of the $B_{i,j}$ curves is the final slope of each plot γ. The smaller the curve of γ, the higher the relative amounts of progeny fines that are produced from breakage. Conversely, materials

having a large γ value give less relative amounts of fines. Test results show γ values, increased with increasing interstitial powder filling and increased with decreasing feed size.

CHAPTER FIVE
CONCLUSIONS AND DISCUSSIONS

Bond work index method has been using for many years about mill sizing. Bond method has a log experimental duration and also it is not enough suggestive about size distribution of material and etc., these reasons led to developing more efficient methods by researches. In recent years, some mathematical models and simulation techniques has been using for grinding technology.

Firstly, grindability of perlite, pumice and zeolite was investigated with Bond work index method. Following, kinetic model was used for investigate grindability of samples.

In this study, the effect of different sieve size s (Pi) on the bond work index (Wi) for different ores was investigated. The results indicate that the Bond work index grindability values measured for perlite, pumice, zeolite and limestone increase with decreasing test sieve sizes. Although the Bond work index values reported in the literature generally increase with decreasing sieve size, they, however, sometimes stay unchanged and also decrease with decreasing test sieve sizes as reported in the literature (Smith and Lee, 1968).

Dry grinding of four $\sqrt{2}$ screen size intervals at two different powder loading and three different type ball size charge conditions showed that the perlite, pumice and zeolite followed the first-order breakage law with constant normalized primary breakage distributions.

The S_i values and breakage parameters of -1700+1180, -850+600, -425+300 and -212+150 μm feed fractions of perlite, pumice and zeolite ground dry with a ball diameter of 38 mm, 30 mm and 30-25,4-19,05 mm and U= 0,6 – 1 were obtained respectively showed in Appendices B; C; and D.

S_i values of samples were compared to each other under similar experimental conditions in Figure E.1; E.2; E.3; E.4; E.5 and E.6. Figures show variations of the s_i values of perlite, pumice and zeolite with particle size for d=38; d=30 and d=30 - 25,4 - 19,05 mm ball size charge at U=0,6 and U=1. These figures indicate that the specific rates of breakage (S_i) value increase, as feed size fraction increases, due to the figures show that pumice is broken faster than perlite and perlite is broken faster than zeolite. The ball size charge, on the other hand, has an inverse effect on the S_i values, which means the smaller the ball size charge, the higher the S_i value. However, three different ball size charge (30 – 25,4 – 19,05 mm) is more effective about specific breakage rates of samples than single type ball size charges (30 and 38 mm). Secondhand, 30 mm single type ball size charge is more effective about specific breakage rates of samples than 38 mm single type ball size charge.

The aT value indicates specific rate of breakage at x_0 = 1000 µm particle size. Test results show, aT values decreased with increasing interstitial powder filling. Figures show variations of the aT values of perlite, pumice and zeolite with particle size for d=38; d=30 and d=30 - 25,4 - 19,05 mm ball size charge at U=0,6 and U=1. These figures indicate that the aT values increase with decreasing ball size charge. However, ball size charge has an inverse effect on the aT values, which means the smaller the ball size charge, the higher the aT values. The breakage parameters of samples were compared to each other under similar experimental conditions, i.e., it can be said that the pumice is broken faster than perlite and perlite is broken faster than zeolite in terms of the a_T values reported in figures previously.

Φ value indicates how rapidly fractions close to feed size are reduced to a lower size. Test results show Φ values, decreased with increasing interstitial powder filling and increased with increasing feed size. These figures indicate that the Φ value increases, as feed size fraction increases, due to the figures show that pumice is broken faster than perlite and perlite is broken faster than zeolite. The ball size charge, on the other hand, has an inverse effect on the Φ values, which means the smaller the ball size charge, the higher the Φ value.

The primary characteristic of the $B_{i,j}$ curves is the final slope of each plot γ. The smaller the curve of γ, the higher the relative amounts of progeny fines that are produced from breakage. Conversely, materials having a large γ value give less relative amounts of fines. Test results show γ values, increased with increasing interstitial powder filling and increased with decreasing feed size. The ball size charge has a directly proportional effect on the γ values, which means the smaller the ball size charge, the smaller the γ value. The smaller γ value means that more fines are produced in the grinding. Due to test results, by considering the γ value of B_{ij}, zeolite produces finer material than pumice and pumice produces finer material than perlite.

CHAPTER SIX
RECOMMENDATIONS

A grinding circuit should produce a desired quantity of product with quality specifications for specified feed material that is ground. The process engineer who designs the grinding circuits faces many choices such as mill type, size and power, selectivity (classification), the amount of coarse product to recycle, mode of operation, circuit configuration, the selection of efficient and stable operating conditions within reasonable cost limitations.

Particle breakage depends on a range of factors: particle size, mill diameter and size of grinding media. Breakage of one particle produces a complete range of finer breakage product sizes, known as a primary breakage distribution function. By knowing how fast each size is broken and how those broken sizes are distributed down to finer sizes gives rise to the concept of size–mass balance approach to characterize the breakage behavior. This method combines the concepts of specific rates of breakage, grinding time, primary breakage distribution function, and the relationship between volume of powder filling, mill conditions and ball sizes.

Studies show that just using the Bond work index method can be cause to wrong choices to mill sizing. For this reason, each kinetic model parameters of samples must be investigated. Besides all these, choosing optimum grinding conditions are more important as choosing optimum mill. However, interstitial powder filling volume, ball size charge, critical speed and etc., grinding conditions must be investigated very well.

In our country, many grinding facility is established without any experimental studies. As a result of this, cost of product increases depending on excessive energy consumption. So, it reduces the competitiveness of manufactured products.

The breakage parameters at two different powder filling volume and three different ball size charge of perlite, pumice and zeolite were presented in this study.

As a result, there is a correlation between breakage parameters of a material and grinding. Therefore, accurate prediction of plant-scale results from laboratory size milling requires detailed analysis using the breakage parameters of material approach. Obtaining the breakage parameters by laboratory studies helps us to better understand the breakage behavior of material and predict the process outputs in desired unit operations to solve complex grinding problems.

REFERENCES

Angove, J.E & Dunne, R.C. (1997). A review of standard physical ore property determinations. *Proceedings of World Gold'97 Conference, Singapore,* 139-144.

Austin, L.G. & Luckie, P.T. (1971/1972). Methods for determination of breakage distribution parameters, *Powder Tech., 5,* 215-221.

Austin, L.G. (1973). A commentary on the Kick, Bond and Rittinger laws of grinding. *Powder Tech., 7,* 315–317.

Austin, L.G. & Bagga, P. (1981). An analysis of fine dry grinding in ball mills, *Powder Tech., 28,* 836-90.

Austin, L.G. & Klimpel, R.R. & Luckie, P.T. & Rogers, R.S.C. (1982). "Simulation of Grinding Circuits for Design", In: Design and Installation of Comminution Circuits, *editors: A.L. Mular & J.V. Jergensen. SMEAIME, New York,* 301-324.

Austin, L,G. & Klimpel, R,R. & Luckie, P,T. (1984). Process Engineering of Size Reduction: Ball Milling, *AIME, New York, USA,* 306 -309.

Axelson (1949). Ph.D. thesis. *University of Minnesota, New York, USA,* 116 – 119.

Bond, F. C. & Maxon,W. I. (1939). Grindability and grinding characteristics of ores, *Trans. AIME, 134,* 296-323.

Bond, F. C. (1952). The third theory of comminution, *Trans. AIME, 193,* 484-494.

Bond, F. C. (1961). Crushing and grinding calculations, *British Chemical Engineering, 6,* 378-385 & 543-548.

Bond F.C. (1961). Crushing and grinding calculations Part I-II. *Br. Chem. Eng., 6*. 378 – 385, 543–54.

Deniz, V. & Sutcu, N. & Umucu, Y. (2003). The effect of circulating load and test sieve size on the Bond work index based on natural amorphous silica, *18th International Mining Congress and Exhibition of Turkey, IMCET*, 517-522.

Dahlhoff, (1967). Chem. Ing. Tech. 39(19), 1112 - 1116.

Fahrenwald, (1934). Trans. Am. Inst. Min. Metal. Pet. Eng. 112,88.

Forbes, J,R. (1955). Studies in the ancient technology VIII. 152–156, 213–246.

Gardner, R.P. & Austin, L.G. (1972). "Use of Radioactive Tracer Technique and a Computer in the Study of the Batch Grinding of Coals", *Journal of Institute of Fuel 35*, 174-177.

Gross & Zimmerly, (1930). Trans. Am. Inst. Min. Metal. Pet. Eng. 87,27,35.

Herbst, J.A. & Fuerstenau, D.W. (1973). "Mathematical Simulation of Dry Ball Mill Using Specific Power Information", *Trans.,254. SME Publications, Littleton, Colorado, USA*, 343– 348.

Herbst, J.A. & Grandy, G.A. & Fuerstenau, D.W. (1973). "Population Balance Models for the Design of Continuous Grinding Mills". *Proceedings of the 10th International Mineral Processing Congress*, 27– 37.

Herbst, J.A. & Fuerstenau, D.W. (1980). "Scale-Up Procedure for Continuous Grinding Mill Design Using Population Balance Models". *International Journal of Mineral Processing, 7*, 1-31.

Herbst, J.A. & Siddique, M. & Rajamani, K. & Sanchez, E. (1981). “Population Balance Approach to Ball Mill Scale-Up: Bench and Pilot Scale Investigations”, *Trans. SME/AIME 272,* 1945–1954.

Herbst, J.A. & Rajamani, R.K. & (1982). “Developing a Simulator for Ball Mill Scale-Up: A Case Study”, In: Design and Installation of Comminution Circuits, *Editors: Mular, A.L., Jergensen, G.V., AIME, New York,* 325 – 345.

Herbst, J.A. & Fuerstenau, D.W. (1973). Mathematical simulation of dry ball milling using specific power information. *SME/ AIME,* 254, 343-348.

HUKKI, R.T. (1962). Proposal for a solomonic settlement between the theories of von Rittinger, Kick, and Bond. *Trans. AIME 22,* 403–408.

Kaya, E. (2001). Evaluation of Bond grindability testing, *Third Internation SAG Conference Proceedings, Vancouver, Canada,* 1339-1347.

Kaya, E. & Fletcher, P. C. & Thompson, P. (2003). Reproducibility of Bond grindability word index, *Mineral and Metallurgical Processing, 20, No. 3,* 140-142.

Luckie, P.T. & Austin, L.G. (1972). “A Review Introduction to the Solution of the Grinding Equations by Digital Computation”. *Minerals Science Engineering, 4,* No.2, 26-32.

Lynch, A.C. (1977). “Mineral Crushing and Grinding Circuits”. *Elsevier Scientific Publishing Company, Amsterdam,* 86-93.

Mosher, J. B. & Tague, C. B. (2001). Conduct and precision of Bond grindability testing, *Minerals Engineering, 4, No. 10,* 1187-1197.

Rajamani, R.K. & Herbst, J.A. (1984). “Simultaneous Estimation of Selection and Breakage Functions from Batch and Continuous Grinding Data”. *Trans. Instn. Min. Metallurgy, Section C. 93*, C74- C85.

Shoji, K. (1982). Further studies of ball and powder filling effects in ball milling. *Powder Technology 31*, 121-126.

Shoji, K. & Lohrasb, S. & Austin, L.G. (1980). “The variation of Breakage Parameters with Ball and Powder Loading in Dry Ball Milling”. *Powder Technology, 25, Issue 1*, 109-114.

Smith, R. W. & Lee, K. H. (1968). A comparison of data from Bond type simulated closed-circuit and batch type grindability Tests. *Trans. SME-AIME, 241*, 99-101.

Tuzun, M. A. (2001). Technical note : Wet Bond mill test, *Mineral Engineering*, 369 – 373.

APPENDIX A
BOND WORK INDEX TEST RESULT TABLES OF PERLITE, PUMICE AND ZEOLITE

PERLITE

Table A.1 Perlite Bond work index test result table at 75 µm closing test sieve size

Size, US Stdt.		Feed				Product			
Feed	Prdct.	Weight	Percent Retained		% Passing	Weight	Percent Retained		% Passing
(µm)	(µm)	(grams)	Individual	Cum.	Cum.	(grams)	Individual	Cum.	Cum.
3.350		0,00	0,00	0,00	100,00				
2.360		55,59	29,36	29,36	70,64				
1.700		40,05	21,15	50,51	49,49				
1180		27,21	14,37	64,88	35,12				
850		14,31	7,56	72,43	27,57				
600		9,63	5,09	77,52	22,48				
425		9,21	4,86	82,38	17,62				
300		8,22	4,34	86,72	13,28				
212		7,19	3,80	90,52	9,48				
150		5,65	2,98	93,50	6,50				
106		4,09	2,16	95,66	4,34		0,00	0,00	100,00
75	75	2,82	1,49	97,15	2,85	0,00	0,00	0,00	100,00
Minus 75	53	5,39	2,85	100,00	0,00	140,78	49,10	49,10	50,90
	45		0,00	100,00	0,00	101,34	35,34	84,44	15,56
	Minus 45		0,00	100,00		44,63	15,56	100,00	
Totals		189,36	100,00			286,75	100,00		

Cir. Load Ratio	New Feed	Undersize in Feed	To be Produced	Mill Turns	Oversize In Product	Undersize In Product	Total Undersized Produced	Grams per Mill Rev.
0,82	1037,24	29,52	266,83	150	846,39	190,85	161,33	1,076
3,97	190,85	5,43	290,92	270	758,41	278,83	273,40	1,011
2,69	278,83	7,94	288,42	285	749,07	288,17	280,23	0,982
2,57	288,17	8,20	288,15	293	741,88	295,36	287,16	0,979
2,54	295,36	8,41	287,95	294	749,36	287,88	279,47	0,950

Table A.2 Perlite Bond work index test result table at 106 µm closing test sieve size

Size, US Stdt.		Feed				Product			
Feed	Prdct.	Weight	Percent Retained		% Passing	Weight	Percent Retained		% Passing
(µm)	(µm)	(grams)	Individual	Cum.	Cum.	(grams)	Individual	Cum.	Cum.
3.350		0,00	0,00	0,00	100,00				
2.360		55,59	29,36	29,36	70,64				
1.700		40,05	21,15	50,51	49,49				
1180		27,21	14,37	64,88	35,12				
850		14,31	7,56	72,43	27,57				
600		9,63	5,09	77,52	22,48				
425		9,21	4,86	82,38	17,62				
300		8,22	4,34	86,72	13,28				
212		7,19	3,80	90,52	9,48				
150		5,65	2,98	93,50	6,50				
106	106	4,09	2,16	95,66	4,34	0,00	0,00	0,00	100,00
Minus 106	75	8,21	4,34	97,84	2,16	113,94	38,37	38,37	61,63
	53		0,00	97,84	2,16	62,02	20,88	59,25	40,75
	45		0,00	97,84	2,16	23,16	7,80	67,05	32,95
	Minus 45		0,00	97,84		97,86	32,95	100,00	
Totals		189,36	100,00			296,98	100,00		

Cir. Load Ratio	New Feed	Undersize in Feed	To be Produced	Mill Turns	Oversize In Product	Undersize In Product	Total Undersized Produced	Grams per Mill Rev.
0,75	1040,44	45,11	252,16	150	784,89	255,55	210,44	1,403
2,84	255,55	11,08	286,19	204	726,11	314,33	303,25	1,487
2,33	314,33	13,63	283,64	191	730,92	309,52	295,89	1,551
2,40	309,52	13,42	283,85	183	744,19	296,25	282,83	1,545
2,51	296,25	12,84	284,42	184	743,08	297,36	284,52	1,546

Table A.3 Perlite Bond work index test result table at 150 µm closing test sieve size

Size, US Stdt.		Feed				Product			
Feed	Prdct.	Weight	Percent Retained		% Passing	Weight	Percent Retained		% Passing
(µm)	(µm)	(grams)	Individual	Cum.	Cum.	(grams)	Individual	Cum.	Cum.
3.350		0,00	0,00	0,00	100,00				
2.360		55,59	29,36	29,36	70,64				
1.700		40,05	21,15	50,51	49,49				
1180		27,21	14,37	64,88	35,12				
850		14,31	7,56	72,43	27,57				
600		9,63	5,09	77,52	22,48				
425		9,21	4,86	82,38	17,62				
300	150	8,22	4,34	86,72	13,28	0,00	0,00	0,00	100,00
212	125	7,19	3,80	90,52	9,48	66,14	22,46	22,46	77,54
150	106	5,65	2,98	93,50	6,50	47,59	16,16	38,62	61,38
Minus 150	75	12,30	6,50	100,00	0,00	53,48	18,16	56,77	43,23
	53		0,00	100,00	0,00	36,99	12,56	69,33	30,67
	45		0,00	100,00	0,00	15,32	5,20	74,53	25,47
	Minus 45		0,00	100,00		75,00	25,47	100,00	
Totals		189,36	100,00			294,52	100,00		

Cir. Load Ratio	New Feed	Undersize in Feed	To be Produced	Mill Turns	Oversize In Product	Undersize In Product	Total Undersized Produced	Grams per Mill Rev.
0,67	1039,36	67,51	229,45	150	697,16	342,20	274,69	1,831
2,09	342,20	22,23	274,73	150	715,11	324,25	302,02	2,013
2,25	324,25	21,06	275,90	137	729,94	309,42	288,36	2,104
2,39	309,42	20,10	276,86	132	739,25	300,11	280,01	2,128
2,48	300,11	19,49	277,47	130	744,21	295,15	275,66	2,114
2,52	295,15	19,17	277,79	131	743,33	296,03	276,86	2,107

Table A.4 Perlite Bond work index test result table at 212 µm closing test sieve size

Size, US Stdt.		Feed				Product			
Feed	Prdct.	Weight	Percent Retained		% Passing	Weight	Percent Retained		% Passing
(µm)	(µm)	(grams)	Individual	Cum.	Cum.	(grams)	Individual	Cum.	Cum.
			0,00	0,00	100,00				
3.350		0,00	0,00	0,00	100,00				
2.360		55,59	29,36	29,36	70,64				
1.700		40,05	21,15	50,51	49,49				
1.180		27,21	14,37	64,88	35,12				
850		14,31	7,56	72,43	27,57				
600		9,63	5,09	77,52	22,48				
425		9,21	4,86	82,38	17,62		0,00	0,00	100,00
300	212	8,22	4,34	86,72	13,28	0,00	0,00	0,00	100,00
212	150	7,19	3,80	90,52	9,48	108,61	37,02	37,02	62,98
Minus 212	106	17,95	9,48	100,00	0,00	68,33	23,29	60,31	39,69
	75					38,50	13,12	73,43	26,57
	53					26,58	9,06	82,49	17,51
	45					9,51	3,24	85,74	14,26
	Minus 45					41,85	14,26	100,00	
Totals		189,36	100,00			293,38	100,00		

Cir. Load Ratio	New Feed	Undersize in Feed	To be Produced	Mill Turns	Oversize In Product	Undersize In Product	Total Undersized Produced	Grams per Mill Rev.
0,55	1041,82	98,76	198,91	150	575,80	466,02	367,26	2,448
1,47	466,02	44,18	253,49	104	686,90	354,92	310,74	3,001
2,09	354,92	33,64	264,02	88	742,76	299,06	265,42	3,017
2,49	299,06	28,35	269,31	89	745,52	296,30	267,95	3,002
2,51	296,30	28,09	269,58	90	743,11	298,71	270,62	3,014

PUMICE

Table A.5 Pumice Bond work index test result table at 75 µm closing test sieve size

Size, US Stdt.		Feed				Product			
Feed	Prdct.	Weight	Percent Retained		% Passing	Weight	Percent Retained		% Passing
(µm)	(µm)	(grams)	Individual	Cum.	Cum.	(grams)	Individual	Cum.	Cum.
3.350		0,00	0,00	0,00	100,00				
2.360		33,20	16,70	16,70	83,30				
1.700		31,74	15,96	32,66	67,34				
1180		26,60	13,38	46,04	53,96				
850		19,31	9,71	55,75	44,25				
600		16,84	8,47	64,22	35,78				
425		14,15	7,12	71,34	28,66				
300		11,52	5,79	77,13	22,87				
212		9,95	5,00	82,14	17,86				
150		13,05	6,56	88,70	11,30				
106		3,36	1,69	90,39	9,61		0,00	0,00	100,00
75	75	5,54	2,79	93,18	6,82	0,00	0,00	0,00	100,00
Minus 75	53	13,57	6,82	100,00	0,00	144,92	57,78	57,78	42,22
	45		0,00	100,00	0,00	73,45	29,28	87,06	12,94
	Minus 45		0,00	100,00		32,45	12,94	100,00	
Totals		198,83	100,00			250,82	100,00		

Cir. Load Ratio	New Feed	Undersize in Feed	To be Produced	Mill Turns	Oversize In Product	Undersize In Product	Total Undersized Produced	Grams per Mill Rev.
0,78	927,81	63,32	201,77	150	721,54	206,27	142,95	0,953
3,32	206,27	14,08	251,01	263	684,48	243,33	229,25	0,870
2,75	243,33	16,61	248,48	285	669,11	258,70	242,09	0,848
2,56	258,70	17,66	247,43	292	662,88	264,93	247,27	0,847
2,51	264,93	18,08	247,01	291	664,25	263,56	245,48	0,842

Table A.6 Pumice Bond work index test result table at 106 µm closing test sieve size

Size, US Stdt.		Feed				Product			
Feed	Prdct.	Weight	Percent Retained		% Passing	Weight	Percent Retained		% Passing
(µm)	(µm)	(grams)	Individual	Cum.	Cum.	(grams)	Individual	Cum.	Cum.
3.350		0,00	0,00	0,00	100,00				
2.360		33,20	16,70	16,70	83,30				
1.700		31,74	15,96	32,66	67,34				
1180		26,60	13,38	46,04	53,96				
850		19,31	9,71	55,75	44,25				
600		16,84	8,47	64,22	35,78				
425		14,15	7,12	71,34	28,66				
300		11,52	5,79	77,14	22,86				
212		9,95	5,00	82,14	17,86				
150		13,05	6,56	88,70	11,30				
106	106	3,35	1,68	90,39	9,61	0,00	0,00	0,00	100,00
Minus 106	75	19,11	9,61	98,32	1,68	98,04	37,36	37,36	62,64
	53		0,00	98,32	1,68	46,60	17,76	55,11	44,89
	45		0,00	98,32	1,68	22,68	8,64	63,76	36,24
	Minus 45		0,00	98,32		95,12	36,24	100,00	
Totals		198,82	100,00			262,44	100,00		

Cir. Load Ratio	New Feed	Undersize in Feed	To be Produced	Mill Turns	Oversize In Product	Undersize In Product	Total Undersized Produced	Grams per Mill Rev.
0,71	927,81	89,18	175,91	150	659,51	268,30	179,12	1,194
2,44	268,30	25,79	239,30	200	653,64	274,17	248,38	1,239
2,38	274,17	26,35	238,74	193	651,66	276,15	249,80	1,297
2,41	276,15	26,54	238,55	184	664,36	263,45	236,91	1,288
2,51	263,45	25,32	239,77	186	662,19	265,62	240,30	1,291

Table A.7 Pumice Bond work index test result table at 150 µm closing test sieve size

Size, US Stdt.		Feed				Product			
Feed	Prdct.	Weight	Percent Retained		% Passing	Weight	Percent Retained		% Passing
(µm)	(µm)	(grams)	Individual	Cum.	Cum.	(grams)	Individual	Cum.	Cum.
3.350		0,00	0,00	0,00	100,00				
2.360		33,20	16,70	16,70	83,30				
1.700		31,74	15,96	32,66	67,34				
1180		26,60	13,38	46,04	53,96				
850		19,31	9,71	55,75	44,25				
600		16,84	8,47	64,22	35,78				
425		14,15	7,12	71,34	28,66				
300	150	11,52	5,79	77,14	22,86	0,00	0,00	0,00	100,00
212	125	9,95	5,00	82,14	17,86	47,03	20,03	20,03	79,97
150	106	13,05	6,56	88,70	11,30	35,25	15,02	35,05	64,95
Minus 150	75	22,46	11,30	100,00	0,00	46,26	19,71	54,75	45,25
	53		0,00	100,00	0,00	31,46	13,40	68,15	31,85
	45		0,00	100,00	0,00	9,71	4,14	72,29	27,71
	Minus 45		0,00	100,00		65,05	27,71	100,00	
Totals		198,82	100,00			234,76	100,00		

Cir. Load Ratio	New Feed	Undersize in Feed	To be Produced	Mill Turns	Oversize In Product	Undersize In Product	Total Undersized Produced	Grams per Mill Rev.
0,62	927,81	104,81	160,28	150	571,61	356,20	251,39	1,676
1,80	356,20	40,24	224,85	134	642,07	285,74	245,50	1,830
2,28	285,74	32,28	232,81	127	650,16	277,65	245,37	1,929
2,37	277,65	31,37	233,72	121	659,29	268,52	237,15	1,957
2,45	268,52	30,33	234,75	120	659,10	268,71	238,38	1,987
2,50	268,71	30,36	234,73	118	672,14	255,67	225,31	1,907

Table A.8 Pumice Bond work index test result table at 212 µm closing test sieve size

Size, US Stdt.		Feed				Product			
Feed	Prdct.	Weight	Percent Retained		% Passing	Weight	Percent Retained		% Passing
(µm)	(µm)	(grams)	Individual	Cum.	Cum.	(grams)	Individual	Cum.	Cum.
			0,00	0,00	100,00				
3.350		0,00	0,00	0,00	100,00				
2.360		33,20	16,63	16,63	83,37				
1.700		31,74	15,90	32,53	67,47				
1.180		26,60	13,33	45,86	54,14				
850		19,31	9,67	55,53	44,47				
600		16,84	8,44	63,97	36,03				
425		14,15	7,09	71,06	28,94		0,00	0,00	100,00
300	212	11,52	5,77	76,83	23,17	0,00	0,00	0,00	100,00
212	150	9,95	4,98	81,81	18,19	91,60	34,71	34,71	65,29
Minus 212	106	36,31	18,19	100,00	0,00	56,77	21,51	56,22	43,78
	75					33,89	12,84	69,06	30,94
	53					22,07	8,36	77,42	22,58
	45					8,43	3,19	80,62	19,38
	Minus 45					51,15	19,38	100,00	
Totals		199,62	100,00			263,91	100,00		

Cir. Load Ratio	New Feed	Undersize in Feed	To be Produced	Mill Turns	Oversize In Product	Undersize In Product	Total Undersized Produced	Grams per Mill Rev.
0,48	927,81	168,76	96,32	150	449,78	478,03	309,27	2,062
1,28	478,03	86,95	178,14	86	613,03	314,78	227,83	2,637
2,10	314,78	57,26	207,83	79	662,08	265,73	208,47	2,645
2,51	265,73	48,34	216,75	82	665,98	261,83	213,49	2,605
2,52	261,83	47,63	217,46	83	658,94	268,87	221,24	2,651

ZEOLITE

Table A.9 Zeolite Bond work index test result table at 75 µm closing test sieve size

Size, US Stdt.		Feed				Product			
Feed	Prdct.	Weight	Percent Retained		% Passing	Weight	Percent Retained		% Passing
(µm)	(µm)	(grams)	Individual	Cum.	Cum.	(grams)	Individual	Cum.	Cum.
3.350		0,34	0,17	0,17	99,83				
2.360		30,05	15,04	15,21	84,79				
1.700		32,15	16,09	31,29	68,71				
1180		24,22	12,12	43,41	56,59				
850		19,16	9,59	53,00	47,00				
600		16,75	8,38	61,38	38,62				
425		13,83	6,92	68,30	31,70				
300		11,15	5,58	73,88	26,12				
212		9,45	4,73	78,61	21,39				
150		7,96	3,98	82,59	17,41				
106		8,47	4,24	86,83	13,17		0,00	0,00	100,00
75	75	7,11	3,56	90,38	9,62	0,00	0,00	0,00	100,00
Minus 75	53	19,22	9,62	100,00	0,00	26,54	25,82	25,82	74,18
	45		0,00	100,00	0,00	21,89	21,30	47,12	52,88
	Minus 45		0,00	100,00		54,36	52,88	100,00	
Totals		199,86	100,00			102,79	100,00		

Cir. Load Ratio	New Feed	Undersize in Feed	To be Produced	Mill Turns	Oversize In Product	Undersize In Product	Total Undersized Produced	Grams per Mill Rev.
0,67	801,11	77,04	151,85	150	538,95	262,16	185,12	1,234
2,24	262,16	25,21	203,68	165	588,34	212,77	187,56	1,136
2,68	212,77	20,46	208,43	183	570,46	230,65	210,19	1,146
2,51	230,65	22,18	206,71	180	578,10	223,01	200,83	1,113
2,57	223,01	21,45	207,44	186	572,92	228,19	206,74	1,110

Table A.10 Zeolite Bond work index test result table at 106 µm closing test sieve size

Size, US Stdt.		Feed				Product			
Feed	Prdct.	Weight	Percent Retained		% Passing	Weight	Percent Retained		% Passing
(µm)	(µm)	(grams)	Individual	Cum.	Cum.	(grams)	Individual	Cum.	Cum.
3.350		0,00	0,00	0,00	100,00				
2.360		35,92	18,04	18,04	81,96				
1.700		30,54	15,34	33,38	66,62				
1180		25,45	12,78	46,16	53,84				
850		19,08	9,58	55,74	44,26				
600		16,07	8,07	63,81	36,19				
425		13,09	6,57	70,39	29,61				
300		10,28	5,16	75,55	24,45				
212		8,55	4,29	79,85	20,15				
150		8,46	4,25	84,09	15,91				
106	106	8,75	4,39	88,49	11,51	0,00	0,00	0,00	100,00
Minus 106	75	22,92	11,51	95,61	4,39	57,35	26,41	26,41	73,59
	53		0,00	95,61	4,39	60,89	28,04	54,45	45,55
	45		0,00	95,61	4,39	60,20	27,72	82,17	17,83
	Minus 45		0,00	95,61		38,72	17,83	100,00	
Totals		199,11	100,00			217,16	100,00		

Cir. Load Ratio	New Feed	Undersize in Feed	To be Produced	Mill Turns	Oversize In Product	Undersize In Product	Total Undersized Produced	Grams per Mill Rev.
0,61	786,98	90,59	134,26	150	481,72	305,26	214,67	1,431
1,81	305,26	35,14	189,71	133	551,98	235,00	199,86	1,508
2,39	235,00	27,05	197,80	131	561,23	225,75	198,70	1,515
2,49	225,75	25,99	198,86	131	563,13	223,85	197,86	1,507
2,51	223,85	25,77	199,08	132	561,97	225,01	199,24	1,508

Table A.11 Zeolite Bond work index test result table at 150 µm closing test sieve size

Size, US Stdt.		Feed				Product			
Feed (µm)	Prdct. (µm)	Weight (grams)	Percent Retained Individual	Percent Retained Cum.	% Passing Cum.	Weight (grams)	Percent Retained Individual	Percent Retained Cum.	% Passing Cum.
3.350		0,00	0,00	0,00	100,00				
2.360		27,27	13,64	13,64	86,36				
1.700		28,48	14,24	27,88	72,12				
1180		24,55	12,28	40,15	59,85				
850		19,39	9,70	49,85	50,15				
600		17,42	8,71	58,56	41,44				
425		14,97	7,49	66,04	33,96				
300	150	12,41	6,21	72,25	27,75	0,00	0,00	0,00	100,00
212	125	10,71	5,36	77,60	22,40	26,12	12,89	12,89	87,11
150	106	9,96	4,98	82,58	17,42	21,45	10,59	23,48	76,52
Minus 150	75	34,83	17,42	100,00	0,00	37,87	18,70	42,18	57,82
	53		0,00	100,00	0,00	31,43	15,52	57,70	42,30
	45		0,00	100,00	0,00	19,64	9,70	67,39	32,61
	Minus 45		0,00	100,00		66,05	32,61	100,00	
Totals		199,99	100,00			202,56	100,00		

Cir. Load Ratio	New Feed	Undersize in Feed	To be Produced	Mill Turns	Oversize In Product	Undersize In Product	Total Undersized Produced	Grams per Mill Rev.
0,51	793,49	138,19	88,52	150	408,20	385,29	247,10	1,647
1,40	385,29	67,10	159,61	97	540,47	253,02	185,92	1,919
2,21	253,02	44,07	182,65	95	560,05	233,44	189,37	1,990
2,43	233,44	40,66	186,06	94	566,84	226,65	185,99	1,989
2,53	226,65	39,47	187,24	94	574,02	219,47	180,00	1,912

Table A.12 Zeolite Bond work index test result table at 75 µm closing test sieve size

Size, US Stdt.		Feed				Product			
Feed (µm)	Prdct. (µm)	Weight (grams)	Percent Retained Individual	Percent Retained Cum.	% Passing Cum.	Weight (grams)	Percent Retained Individual	Percent Retained Cum.	% Passing Cum.
			0,00	0,00	100,00				
3.350		0,59	0,30	0,30	99,70				
2.360		36,52	18,27	18,56	81,44				
1.700		34,01	17,01	35,58	64,42				
1.180		26,17	13,09	48,67	51,33				
850		18,77	9,39	58,06	41,94				
600		15,78	7,89	65,95	34,05				
425		12,69	6,35	72,30	27,70		0,00	0,00	100,00
300	212	9,93	4,97	77,26	22,74	0,00	0,00	0,00	100,00
212	150	8,54	4,27	81,54	18,46	22,41	23,90	23,90	76,10
Minus 212	106	36,91	18,46	100,00	0,00	16,63	17,74	41,64	58,36
	75					12,54	13,37	55,01	44,99
	53					11,66	12,44	67,45	32,55
	45					8,41	8,97	76,42	23,58
	Minus 45					22,11	23,58	100,00	
Totals		199,91	100,00			93,76	100,00		

Cir. Load Ratio	New Feed	Undersize in Feed	To be Produced	Mill Turns	Oversize In Product	Undersize In Product	Total Undersized Produced	Grams per Mill Rev.
0,40	778,15	143,67	78,66	150	312,79	465,36	321,69	2,145
1,09	465,36	85,92	136,41	64	506,08	272,07	186,15	2,927
2,05	272,07	50,23	172,10	59	556,57	221,58	171,35	2,914
2,50	221,58	40,91	181,42	62	553,75	224,40	183,49	2,947
2,49	224,40	41,43	180,90	61	558,11	220,04	178,61	2,910

APPENDIX B
TABLES AND FIGURES FOR DETERMINATION BREAKAGE PARAMETERS OF PERLITE

38 mm ball size charge at U=0,6

1700 x 1180 micron

Table B.1 Determined B values of perlite for - 1700 + 1180 µm size interval ground with d = 38 mm ball diameter and U = 0,6.

INTERVAL NO,İ	SİZE (mesh)	Size (µm)	Xi/Xmax	B i,1	B VALUES
1	12x16	1700x1180	1,00	B1,1	1
2	16x20	1180x850	0,69	B2,1	1
3	20x30	850x600	0,50	B3,1	0,36281894
4	30x40	600x425	0,35	B4,1	0,200782173
5	40x50	425x300	0,25	B5,1	0,11947897
6	50x70	300x212	0,17	B6,1	0,06680259
7	70x100	212x150	0,12	B7,1	0,037327017
8	100x140	150x106	0,088	B8,1	0,020243477
9	140x200	106x75	0,062	B9,1	0,012454944
10	200x270	75x53	0,044	B10,1	0,00727693
11	270x400	53x38	0,031	B11,1	0,003987776
12	-400	-38	0,022	B12,1	0,002227627

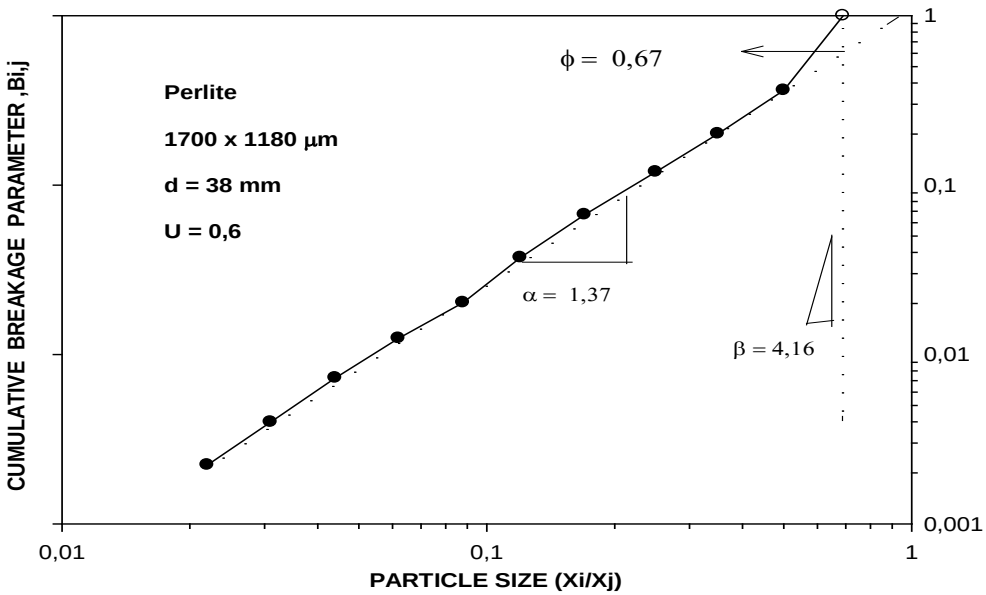

Figure B.1 Primary breakage distribution function of perlite for -1700 + 1180 µm feed size fraction ground with d = 38 mm ball diameter and U = 0,6.

Table B.2 Cumulative weight percent less than size values of perlite for 1700 x 1180 µm size interval ground with d = 38 mm ball diameter and U = 0,6.

SIZE	0 min.	0,133 min	1 min	3 min	6 min
1700	100,00	100,00	100,00	100,00	100,00
1180	1,56	35,75	76,94	98,26	99,96
850	0,22	14,53	59,07	97,15	98,54
600	0,00	8,21	39,25	91,02	98,06
425	0,00	4,97	26,94	73,86	97,01
300	0,00	2,81	18,12	51,34	82,59
212	0,00	1,58	11,21	33,45	54,28
150	0,00	0,86	6,84	20,64	33,57
106	0,00	0,53	4,02	12,85	20,16
75	0,00	0,31	1,93	7,02	11,89
53	0,00	0,17	1,06	4,08	7,41
38	0,00	0,10	0,59	2,27	3,97
%w.r.top size	98,44	64,25	23,06	1,74	0,05

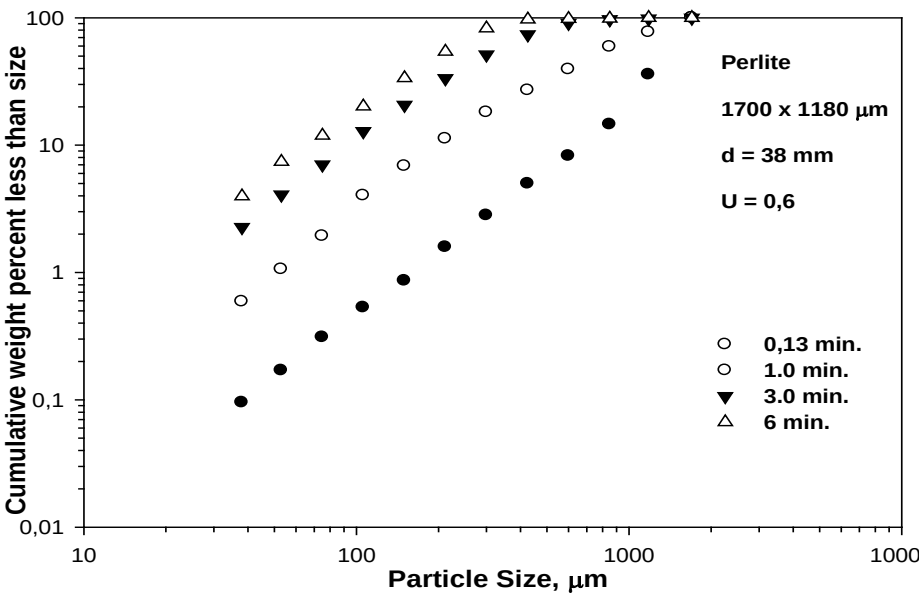

Figure B.2 Particle size distribution of perlite for -1700 + 1180 µm feed size fraction ground with d = 38 mm ball diameter and U = 0,6.

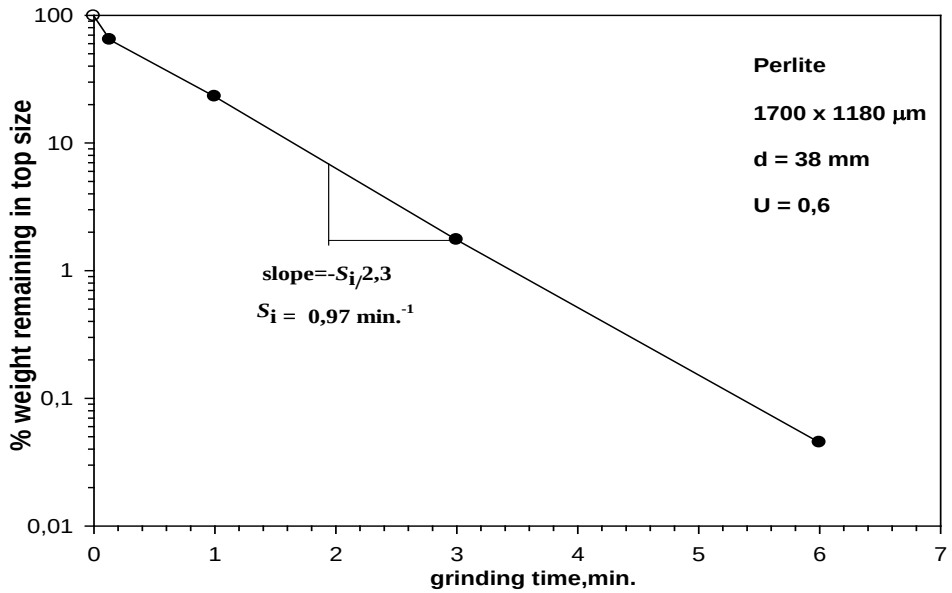

Figure B.3 First-order plot of breakage of - 1700 + 1180 µm feed of perlite ground with d = 38 mm ball diameter and U = 0,6.

850 x 600 micron

Table B.3 Determined B values of perlite for - 850 + 600 µm size interval ground with d = 38 mm ball diameter and U = 0,6.

INTERVAL NO,İ	SİZE (mesh)	Size (µm)	Xi/Xmax	B i,1	B VALUES
1	20x30	850x600	1,00	B3,1	1,0000
2	30x40	600x425	0,7	B4,1	1,0000
3	40x50	425x300	0,5	B5,1	0,3663
4	50x70	300x212	0,35	B6,1	0,2071
5	70x100	212x150	0,24	B7,1	0,1135
6	100x140	150x106	0,17	B8,1	0,0621
7	140x200	106x75	0,12	B9,1	0,0365
8	200x270	75x53	0,08	B10,1	0,0201
9	270x400	53x38	0,06	B11,1	0,0121
10	-400	-38	0,04	B12,1	0,0069

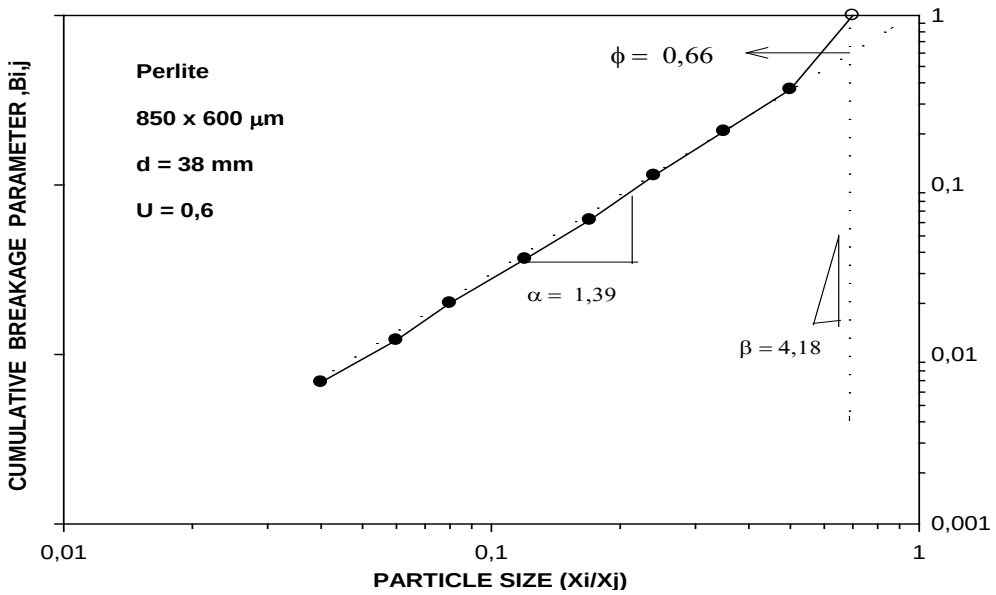

Figure B.4 Primary breakage distribution function of perlite for -850 + 600 µm feed size fraction ground with d = 38 mm ball diameter and U = 0,6.

Table B.4 Cumulative weight percent less than size values of perlite for - 850 + 600 µm size interval ground with d = 38 mm ball diameter and U = 0,6.

SIZE	0 min.	0,133 min	1 min	3 min	6 min
850	100,00	100,00	100,00	100,00	100,00
600	3,08	19,82	61,07	91,97	99,34
425	0,14	6,84	36,54	78,06	95,79
300	0,01	3,86	22,01	49,76	80,86
212	0,00	2,13	13,96	28,76	50,24
150	0,00	1,17	8,21	16,01	28,14
106	0,00	0,69	5,06	9,24	16,89
75	0,00	0,38	2,89	5,08	9,76
53	0,00	0,23	1,59	2,97	5,02
38	0,00	0,13	0,86	1,68	2,70
%w.r.top size	96,92	80,18	38,93	8,03	0,66

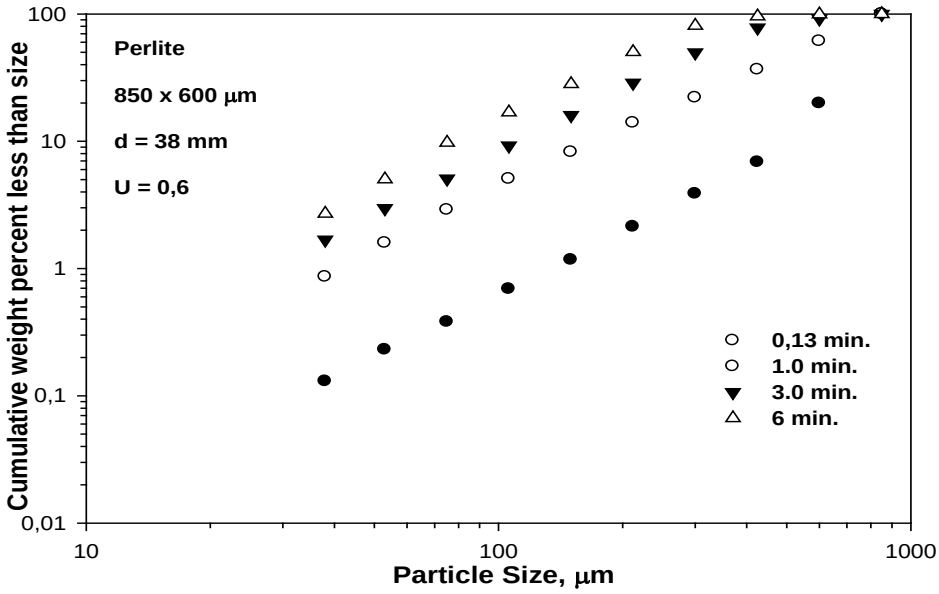

Figure B.5 Particle size distribution of perlite for -850 + 600 µm feed size fraction ground with d = 38 mm ball diameter and U = 0,6.

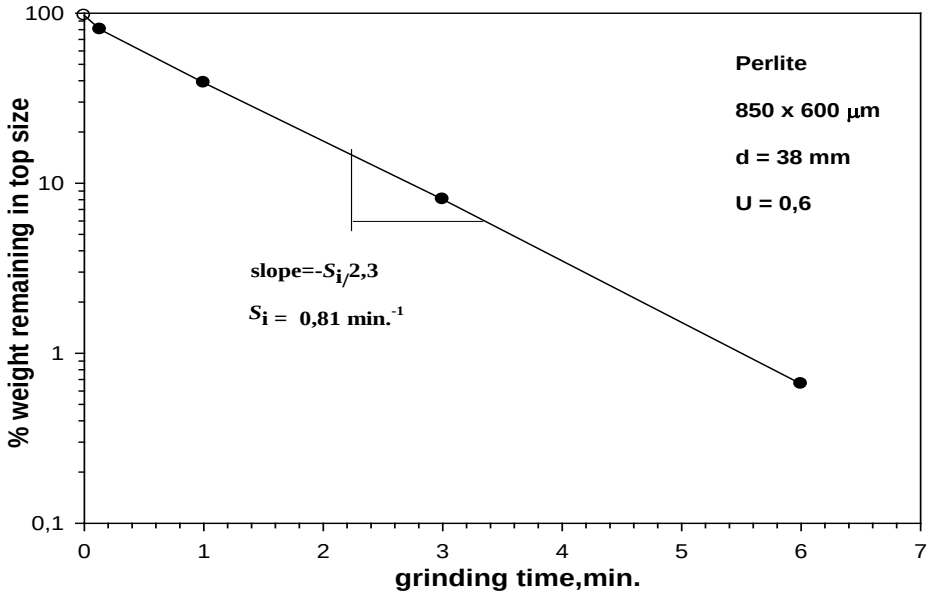

Figure B.6 First-order plot of breakage of - 850 + 600 µm feed of perlite ground with d = 38 mm ball diameter and U = 0,6.

425 x 300 micron

Table B.5 Determined B values of perlite for – 425 + 300 µm size interval ground with d = 38 mm ball diameter and U = 0,6.

INTERVAL NO,İ	SİZE (mesh)	Size (µm)	Xi/Xmax	B i,1	B VALUES
1	40x50	425x300	1,00	B1,1	1,0000
2	50x70	300x212	0,7	B2,1	1,0000
3	70x100	212x150	0,49	B3,1	0,3620
4	100x140	150x106	0,35	B4,1	0,2023
5	140x200	106x75	0,24	B5,1	0,1157
6	200x270	75x53	0,17	B6,1	0,0658
7	270x400	53x38	0,12	B7,1	0,0360
8	-400	-38	0,08	B8,1	0,0198

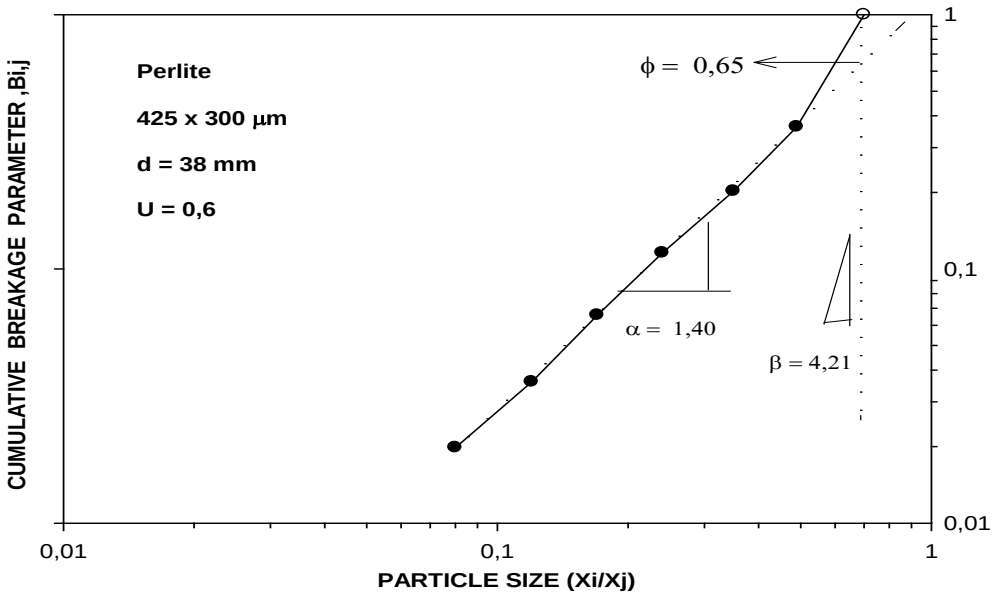

Figure B.7 Primary breakage distribution function of perlite for -425 + 300 µm feed size fraction ground with d = 38 mm ball diameter and U = 0,6.

Table B.6 Cumulative weight percent less than size values of perlite for - 425 + 300 µm size interval ground with d = 38 mm ball diameter and U = 0,6.

SIZE	0 min.	0,133 min	1 min	3 min	6 min
425	100,00	100,00	100,00	100,00	100,00
300	0,11	7,86	29,93	60,02	82,91
212	0,03	2,91	9,11	28,46	50,48
150	0,01	1,63	4,73	13,53	26,08
106	0,00	0,93	2,06	6,84	15,06
75	0,00	0,53	1,16	3,18	8,12
53	0,00	0,29	0,51	1,69	3,67
38	0,00	0,16	0,28	0,92	1,92
%w.r.top size	99,89	92,14	70,07	39,98	17,09

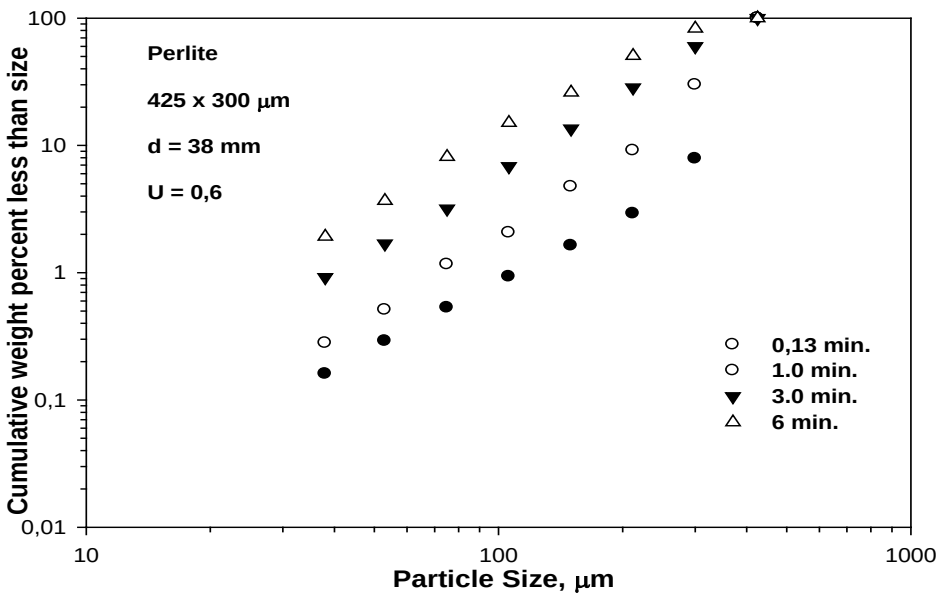

Figure B.8 Particle size distribution of perlite for -425 + 300 µm feed size fraction ground with d = 38 mm ball diameter and U = 0,6.

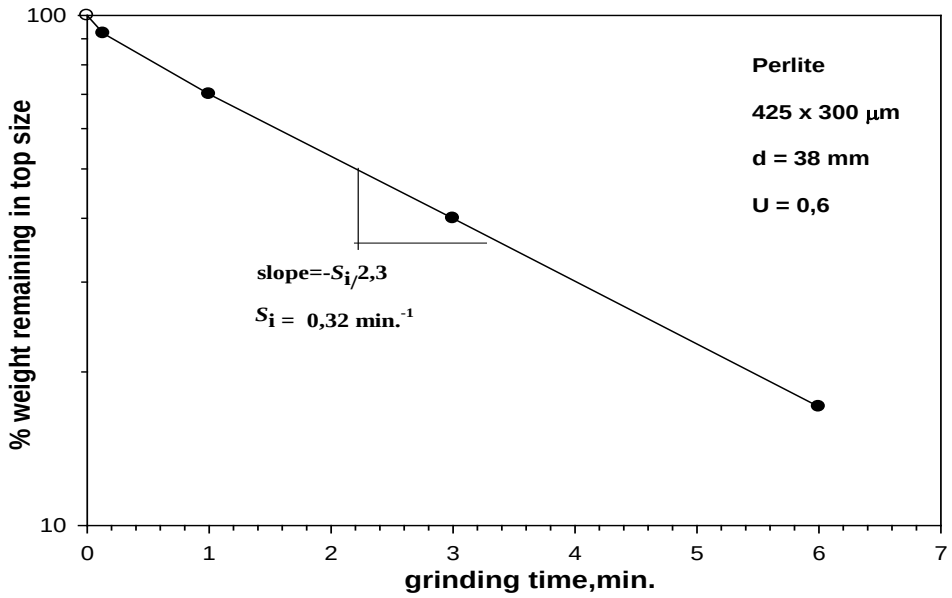

Figure B.9 First-order plot of breakage of - 425 + 300 µm feed of perlite ground with d = 38 mm ball diameter and U = 0,6.

212 x 150 micron

Table B.7 Determined B values of perlite for – 212 + 150 µm size interval ground with d = 38 mm ball diameter and U = 0,6.

INTERVAL NO,İ	SİZE (mesh)	Size (µm)	Xi/Xmax	B i,1	B VALUES
1	70x100	212x150	1,00	B1,1	1,0000
2	100x140	150x106	0,7	B2,1	1,0000
3	140x200	106x75	0,5	B3,1	0,3565
4	200x270	75x53	0,35	B4,1	0,2073
5	270x400	53x38	0,25	B5,1	0,1161
6	-400	-38	0,17	B6,1	0,0605

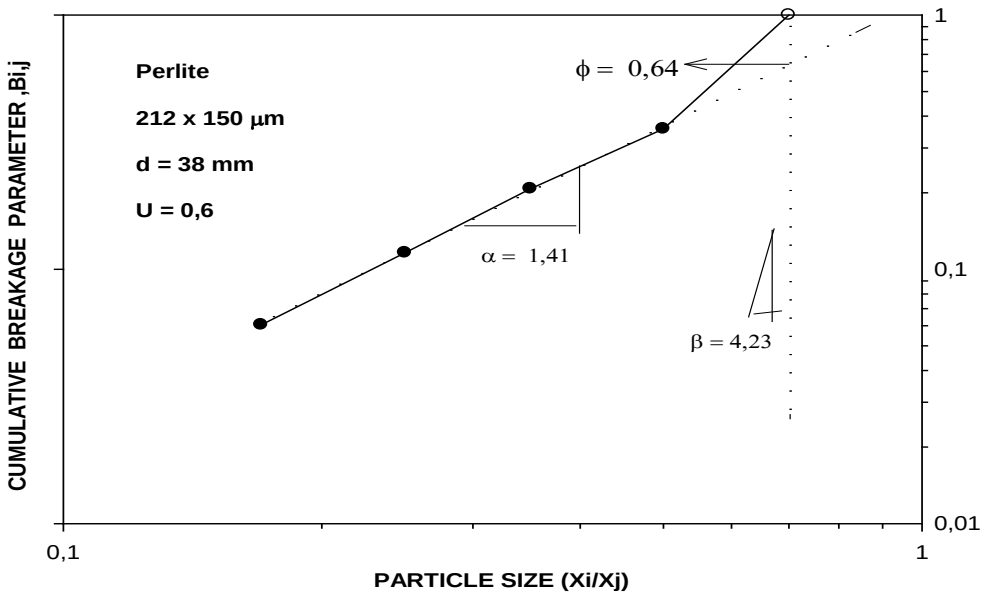

Figure B.10 Primary breakage distribution function of perlite for - 212 + 150 µm feed size fraction ground with d = 38 mm ball diameter and U = 0,6.

Table B.8 Cumulative weight percent less than size values of perlite for - 212 + 150 µm size interval ground with d = 38 mm ball diameter and U = 0,6.

SIZE	0 min.	0,133 min	1 min	3 min	6 min
212	100,00	100,00	100,00	100,00	100,00
150	1,12	4,97	12,87	31,93	49,76
106	0,41	1,81	8,16	17,12	25,19
75	0,01	0,83	3,86	9,51	13,46
53	0,00	0,46	1,92	4,96	7,58
38	0,00	0,24	1,03	2,68	4,33
%w.r.top size	98,88	95,03	87,13	68,07	50,24

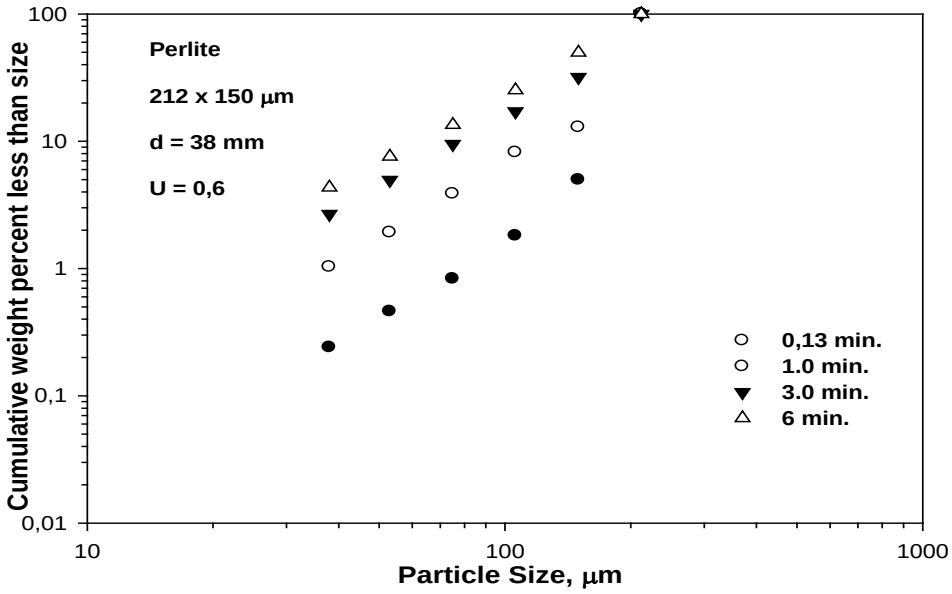

Figure B.11 Particle size distribution of perlite for -212 + 150 µm feed size fraction ground with d = 38 mm ball diameter and U = 0,6.

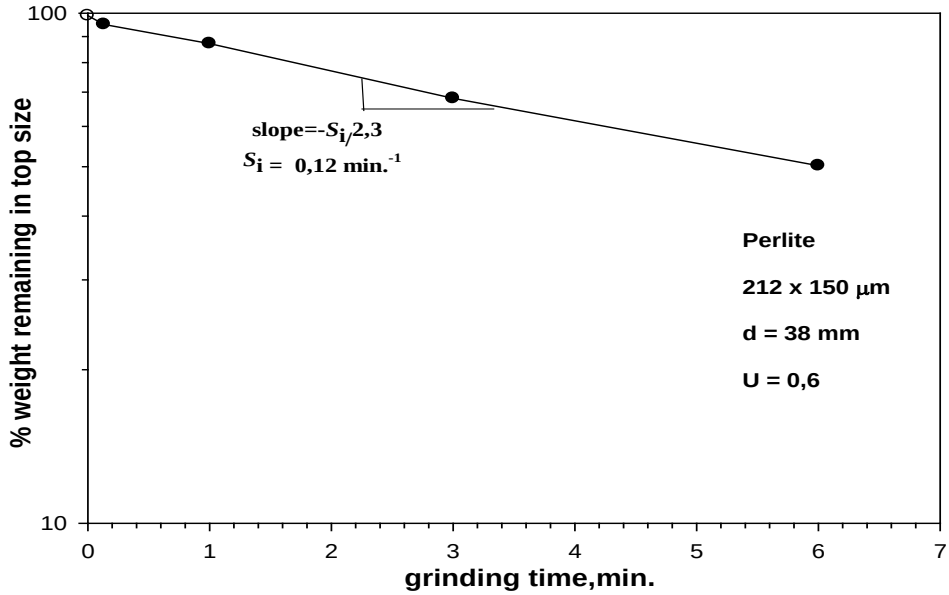

Figure B.12 First-order plot of breakage of - 212 + 150 µm feed of perlite ground with d = 38 mm ball diameter and U = 0,6.

Determination of aT value

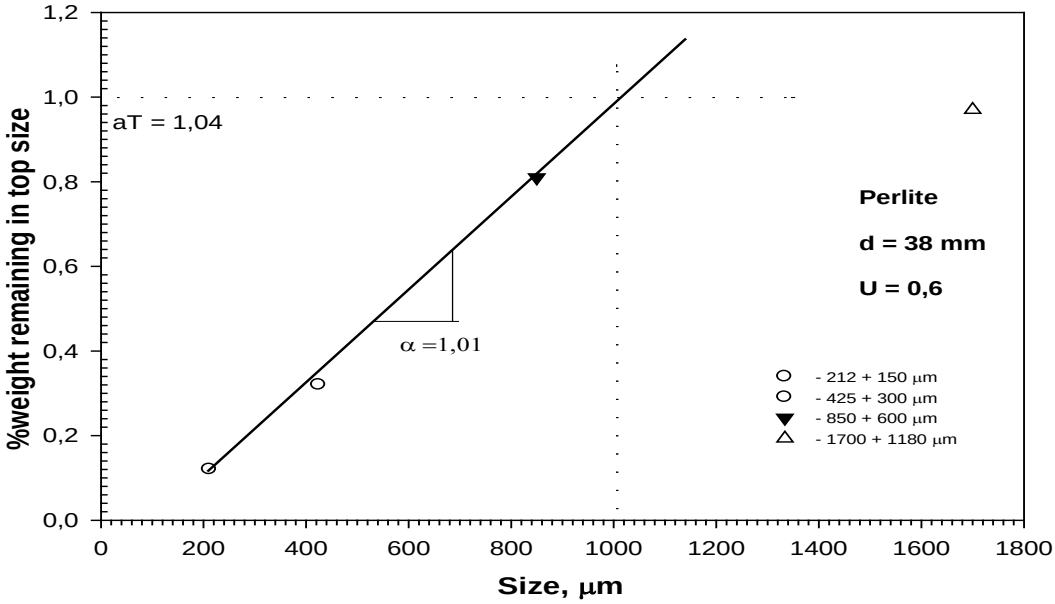

Figure B.13 Variation of first-order specific rates of breakage of perlite ground with d = 38 mm ball diameter and particle size: √2 intervals, plotted at upper size of interval at U=0,6.

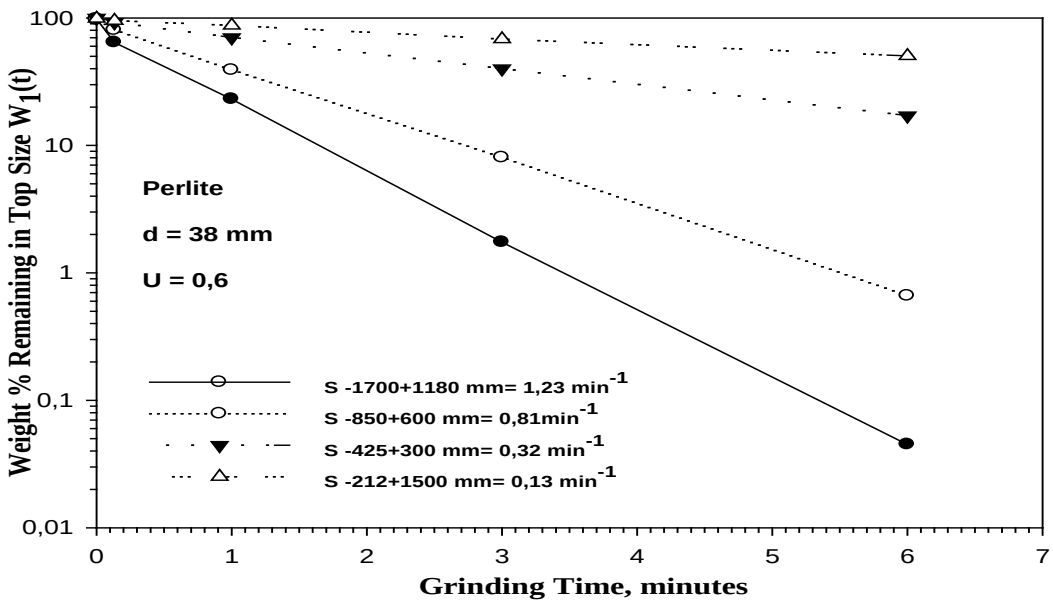

Figure B.14 First-order plots of breakage of -1700+1180, -850+600, -425+300, -212+150 μm feed size of perlite ground with d = 38 mm ball diameter and U=0,6.

Table B.9 Breakage parameters of perlite ground with d = 38 mm ball diameter at U=0,6.

1700x1180		**850x600**		**425x300**		**212x150**			
gama	1,37	**gama**	1,39	**gama**	1,40	**gama**	1,41		
beta	4,16	**beta**	4,18	**beta**	4,21	**beta**	4,23	**aT**	**α**
phi	0,67	**phi**	0,66	**phi**	0,65	**phi**	0,64	1,04	1,01
S value	0,970	**S value**	0,810	**S value**	0,320	**S value**	0,130		

38 mm ball size charge at U= 1

1700 x 1180 micron

Table B.10 Determined B values of perlite for - 1700 + 1180 µm size interval ground with d = 38 mm ball diameter and U = 1.

INTERVAL NO,İ	SİZE (mesh)	Size (µm)	Xi/Xmax	B i,1	B VALUES
1	12x16	1700x1180	1,00	B1,1	1
2	16x20	1180x850	0,69	B2,1	1
3	20x30	850x600	0,50	B3,1	0,386237721
4	30x40	600x425	0,35	B4,1	0,257836068
5	40x50	425x300	0,25	B5,1	0,175805644
6	50x70	300x212	0,17	B6,1	0,116877571
7	70x100	212x150	0,12	B7,1	0,076159691
8	100x140	150x106	0,088	B8,1	0,052549052
9	140x200	106x75	0,062	B9,1	0,035036936
10	200x270	75x53	0,044	B10,1	0,022899493
11	270x400	53x38	0,031	B11,1	0,015144138
12	-400	-38	0,022	B12,1	0,010500272

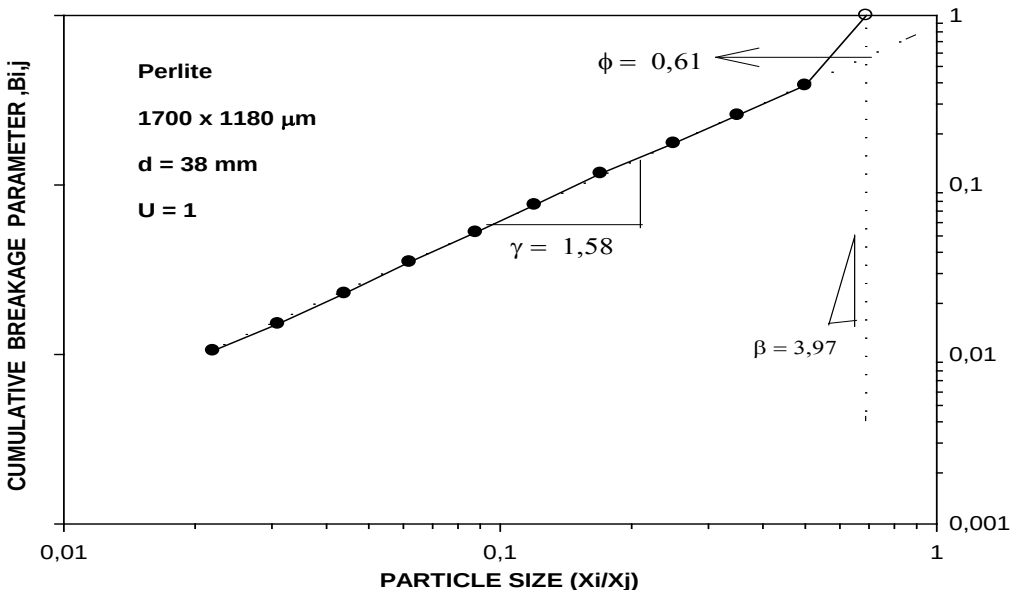

Figure B.15 Primary breakage distribution function of perlite for -1700 + 1180 µm feed size fraction ground with d = 38 mm ball diameter and U = 0,6.

Table B.11 Cumulative weight percent less than size values of perlite for 1700 x 1180 µm size interval ground with d = 38 mm ball diameter and U = 1.

SIZE	0 min.	0,133 min	1 min	3 min	6 min
1700	100,00	100,00	100,00	100,00	100,00
1180	2,24	29,32	69,38	95,79	99,77
850	0,72	12,41	55,18	94,36	97,91
600	0,16	8,17	35,47	88,16	93,68
425	0,05	5,59	22,19	63,28	85,07
300	0,00	3,72	12,03	42,69	74,19
212	0,00	2,44	7,24	26,42	47,63
150	0,00	1,69	4,58	14,83	26,71
106	0,00	1,13	3,07	8,17	15,24
75	0,00	0,74	1,83	4,93	8,79
53	0,00	0,49	1,19	2,78	4,82
38	0,00	0,34	0,71	1,56	2,98
%w.r.top size	97,76	70,68	30,62	4,21	0,23

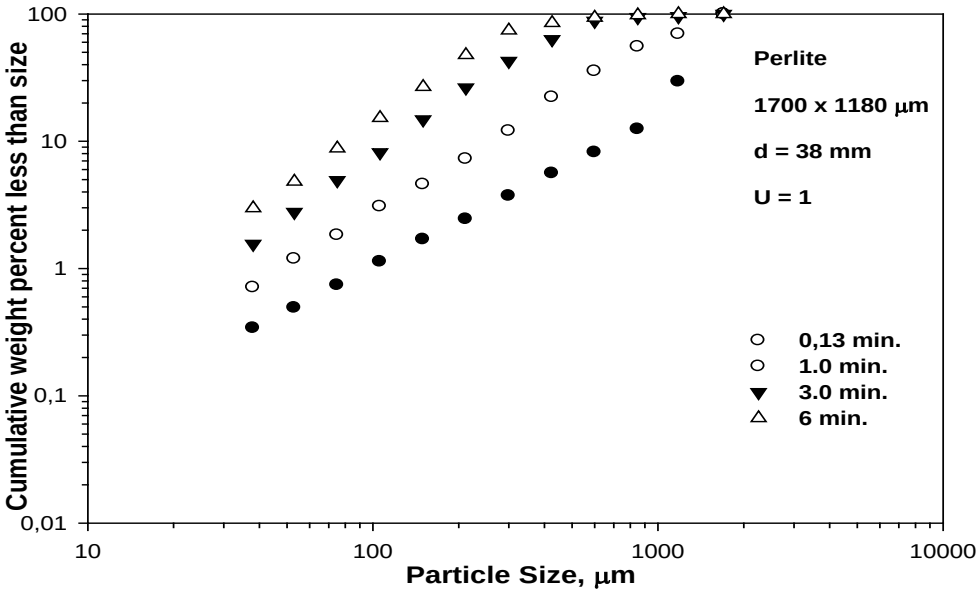

Figure B.16 Particle size distribution of perlite for -1700 + 1180 μm feed size fraction ground with d = 38 mm ball diameter and U = 1.

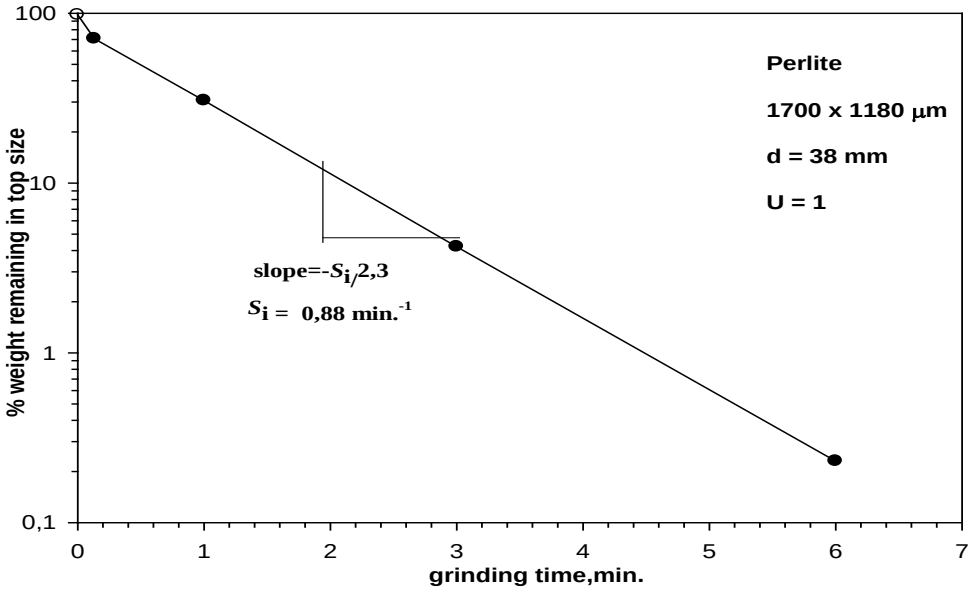

Figure B.17 First-order plot of breakage of - 1700 + 1180 μm feed of perlite ground with d = 38 mm ball diameter and U = 1.

850 x 600 micron

Table B.12 Determined B values of perlite for - 850 + 600 µm size interval ground with d = 38 mm ball diameter and U = 1.

INTERVAL NO,İ	SİZE (mesh)	Size (µm)	Xi/Xmax	B i,1	B VALUES
1	20x30	850x600	1,00	B3,1	1,0000
2	30x40	600x425	0,7	B4,1	1,0000
3	40x50	425x300	0,5	B5,1	0,3849
4	50x70	300x212	0,35	B6,1	0,2556
5	70x100	212x150	0,24	B7,1	0,1740
6	100x140	150x106	0,17	B8,1	0,1153
7	140x200	106x75	0,12	B9,1	0,0760
8	200x270	75x53	0,08	B10,1	0,0496
9	270x400	53x38	0,06	B11,1	0,0349
10	-400	-38	0,04	B12,1	0,0214

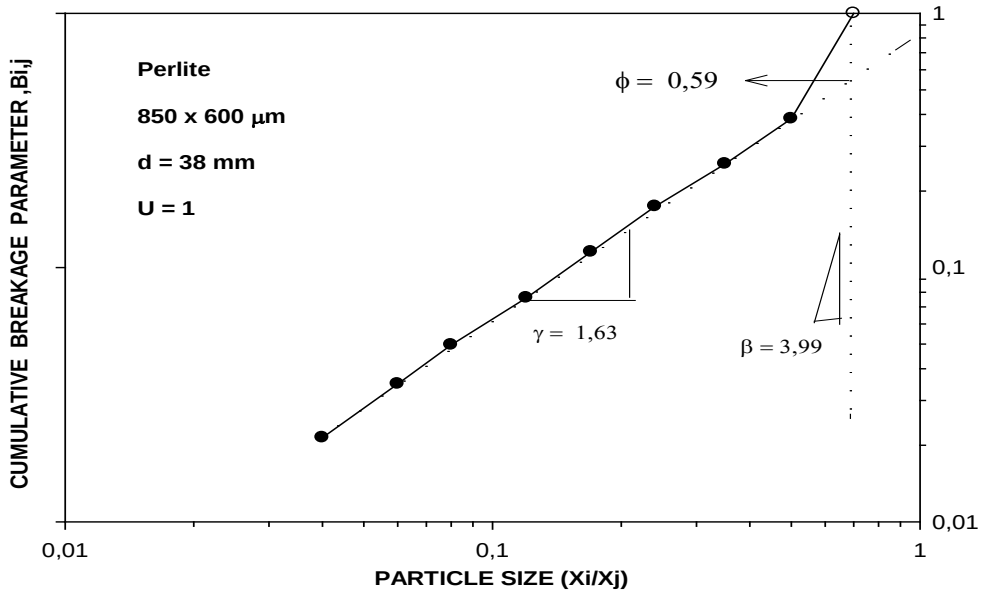

Figure B.18 Primary breakage distribution function of perlite for -850 + 600 µm feed size fraction ground with d = 38 mm ball diameter and U = 0,6.

Table B.13 Cumulative weight percent less than size values of perlite for - 850 + 600 µm size interval ground with d = 38 mm ball diameter and U = 1.

SIZE	0 min.	0,133 min	1 min	3 min	6 min
850	100,00	100,00	100,00	100,00	100,00
600	2,48	16,03	56,71	89,64	98,85
425	0,63	6,19	27,59	70,00	95,13
300	0,06	3,81	14,02	42,00	75,41
212	0,00	2,57	7,93	23,00	46,39
150	0,00	1,71	4,06	12,00	24,81
106	0,00	1,13	2,53	6,70	13,95
75	0,00	0,74	1,56	3,90	7,94
53	0,00	0,52	0,93	2,30	4,26
38	0,00	0,32	0,58	1,30	2,34
%w.r.top size	97,52	83,97	43,29	10,36	1,15

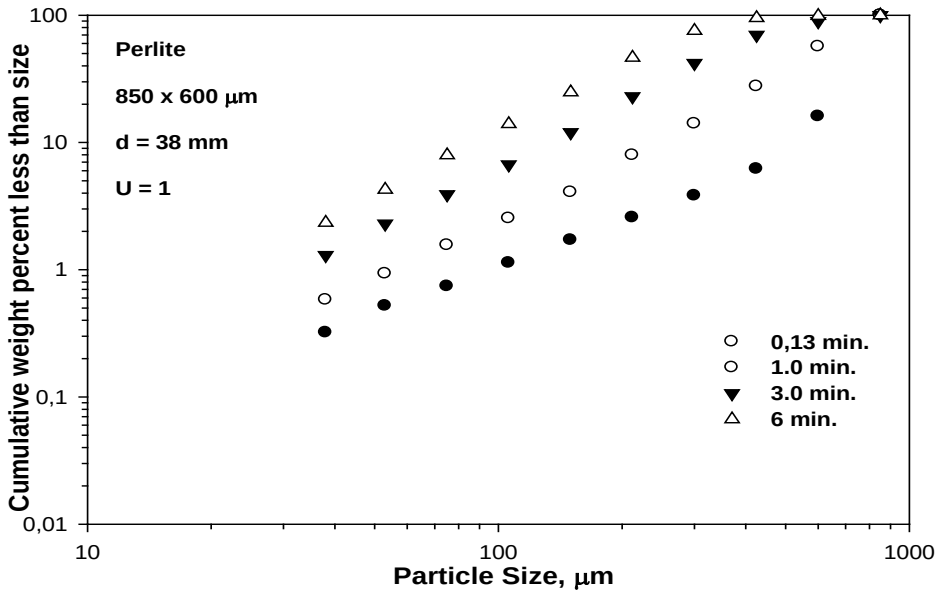

Figure B.19 Particle size distribution of perlite for -850 + 600 µm feed size fraction ground with d = 38 mm ball diameter and U = 1.

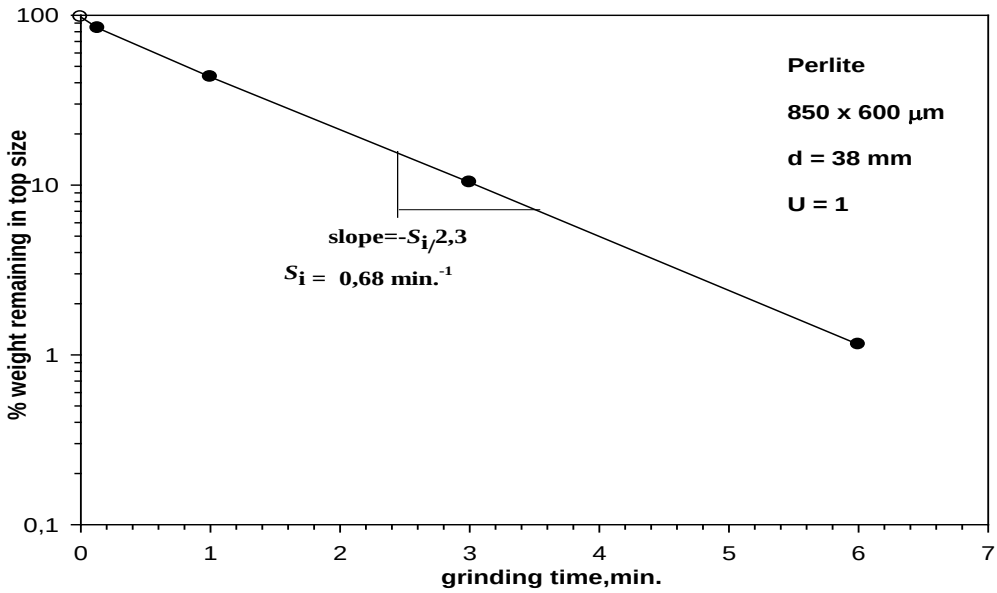

Figure B.20 First-order plot of breakage of - 850 + 600 µm feed of perlite ground with d = 38 mm ball diameter and U = 1.

425 x 300 micron

Table B.14 Determined B values of perlite for – 425 + 300 µm size interval ground with d = 38 mm ball diameter and U = 1.

INTERVAL NO,İ	SİZE (mesh)	Size (µm)	Xi/Xmax	B i,1	B VALUES
1	40x50	425x300	1,00	B1,1	1,0000
2	50x70	300x212	0,7	B2,1	1,0000
3	70x100	212x150	0,49	B3,1	0,3777
4	100x140	150x106	0,35	B4,1	0,2521
5	140x200	106x75	0,24	B5,1	0,1695
6	200x270	75x53	0,17	B6,1	0,1133
7	270x400	53x38	0,12	B7,1	0,0761
8	-400	-38	0,08	B8,1	0,0506

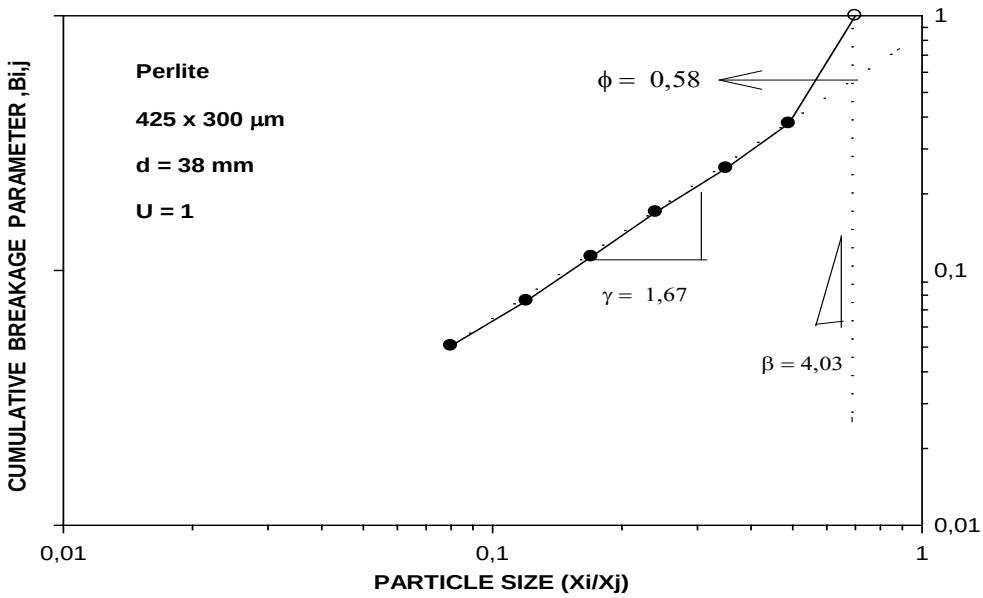

Figure B.21 Primary breakage distribution function of perlite for -425 + 300 µm feed size fraction ground with d = 38 mm ball diameter and U = 1.

Table B.15 Cumulative weight percent less than size values of perlite for - 425 + 300 µm size interval ground with d = 38 mm ball diameter and U = 1.

SIZE	0 min.	0,133 min	1 min	3 min	6 min
425	100	100,00	100,00	100,00	100,00
300	0,34	10,09	33,71	63,82	85,40
212	0,11	3,92	7,89	17,00	45,37
150	0,07	2,63	4,62	10,00	17,93
106	0,01	1,74	3,04	6,00	9,86
75	0,00	1,16	1,93	4,00	6,02
53	0,00	0,78	1,19	2,50	3,82
38	0,00	0,52	0,78	1,50	2,47
%w.r.top size	99,66	89,91	66,29	36,18	14,60

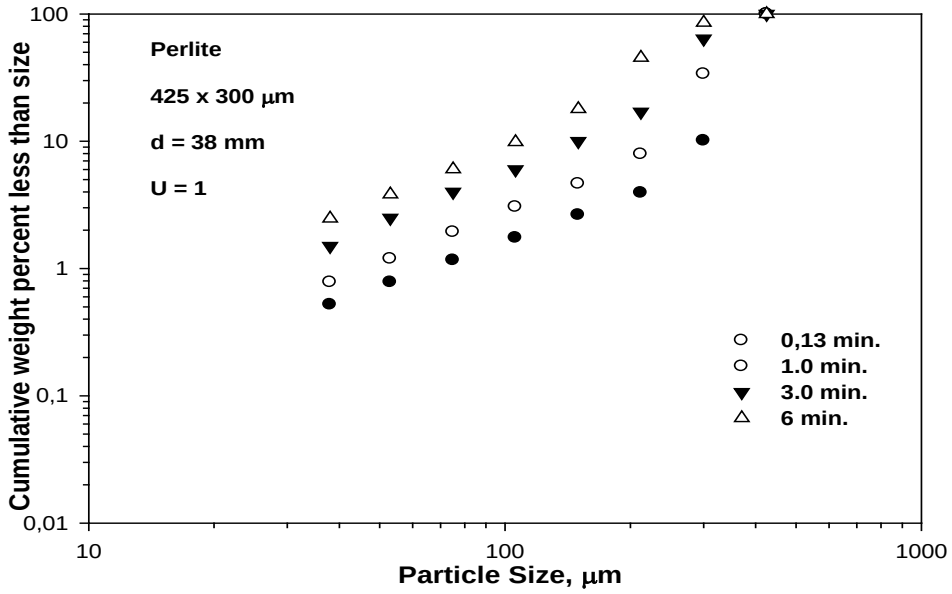

Figure B.22 Particle size distribution of perlite for -425 + 300 μm feed size fraction ground with d = 38 mm ball diameter and U = 1.

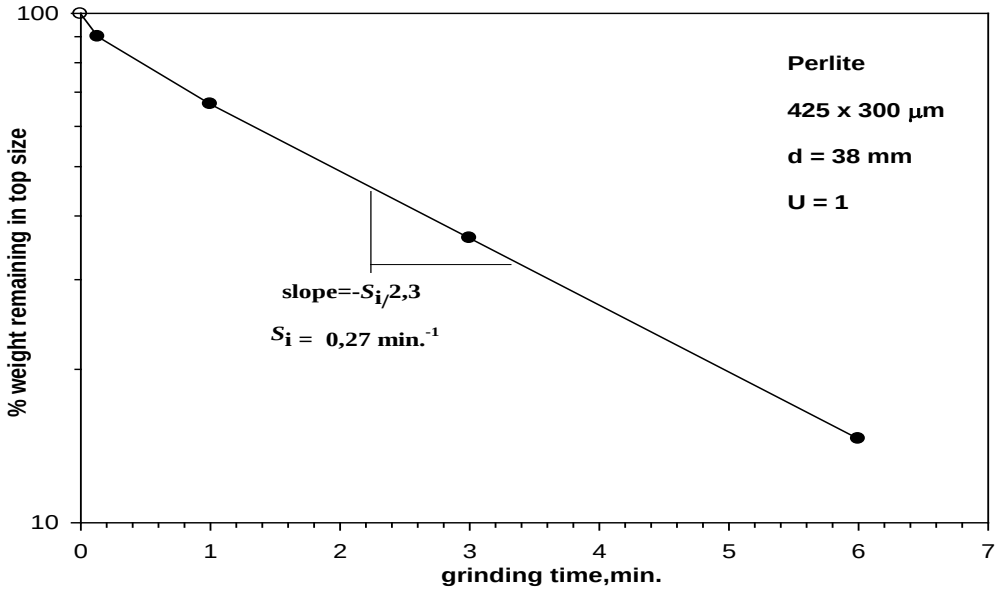

Figure B.23 First-order plot of breakage of - 425 + 300 μm feed of perlite ground with d = 38 mm ball diameter and U = 1.

212 x 150 micron

Table B.16 Determined B values of perlite for – 212 + 150 µm size interval ground with d = 38 mm ball diameter and U = 1.

INTERVAL NO,İ	SİZE (mesh)	Size (µm)	Xi/Xmax	B i,1	B VALUES
1	70x100	212x150	1,00	B1,1	1,0000
2	100x140	150x106	0,7	B2,1	1,0000
3	140x200	106x75	0,5	B3,1	0,3793
4	200x270	75x53	0,35	B4,1	0,2510
5	270x400	53x38	0,25	B5,1	0,1689
6	-400	-38	0,17	B6,1	0,1012

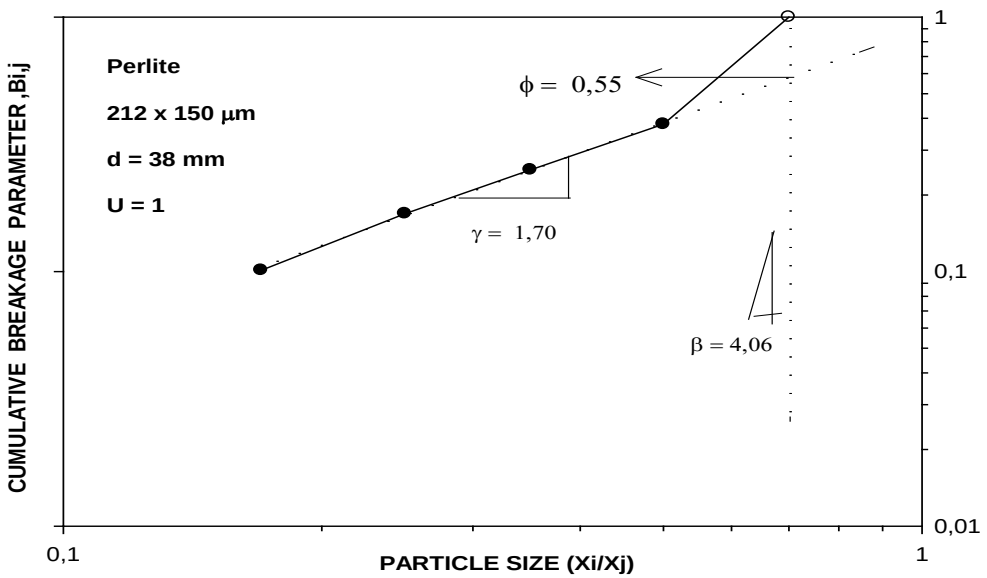

Figure B.24 Primary breakage distribution function of perlite for - 212 + 150 µm feed size fraction ground with d = 38 mm ball diameter and U = 1.

Table B.17 Cumulative weight percent less than size values of perlite for - 212 + 150 µm size interval ground with d = 38 mm ball diameter and U = 1.

SIZE	0 min.	0,133 min	1 min	3 min	6 min
212	100,00	100,00	100,00	100,00	100,00
150	1,72	5,16	17,61	36,92	59,88
106	0,93	2,26	4,97	15,14	30,79
75	0,02	0,91	2,59	8,05	16,28
53	0,00	0,60	1,38	4,51	8,82
38	0,00	0,36	0,76	2,16	4,51
%w.r.top size	98,28	94,84	82,39	63,08	40,12

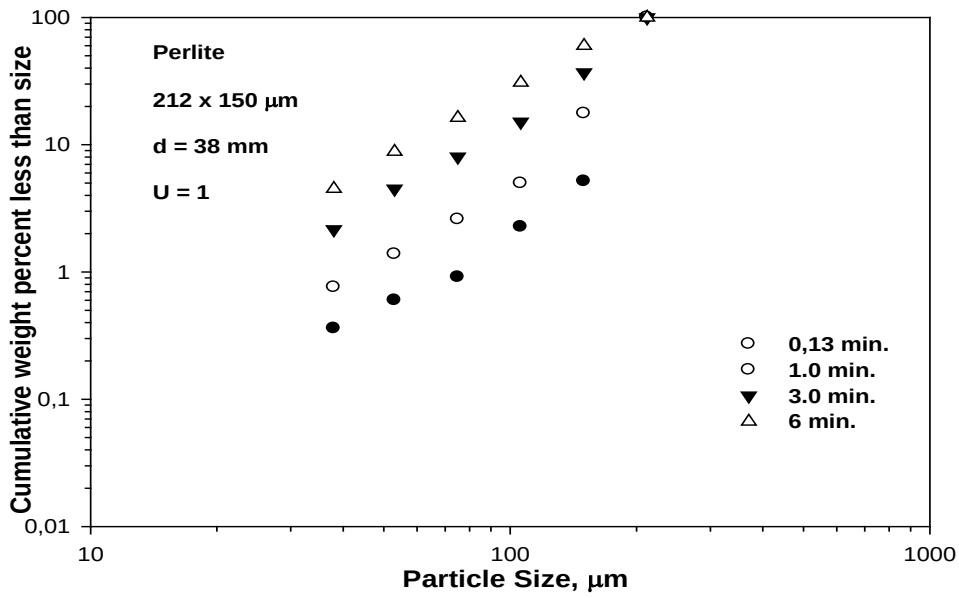

Figure B.25 Particle size distribution of perlite for -212 + 150 µm feed size fraction ground with d = 38 mm ball diameter and U = 1.

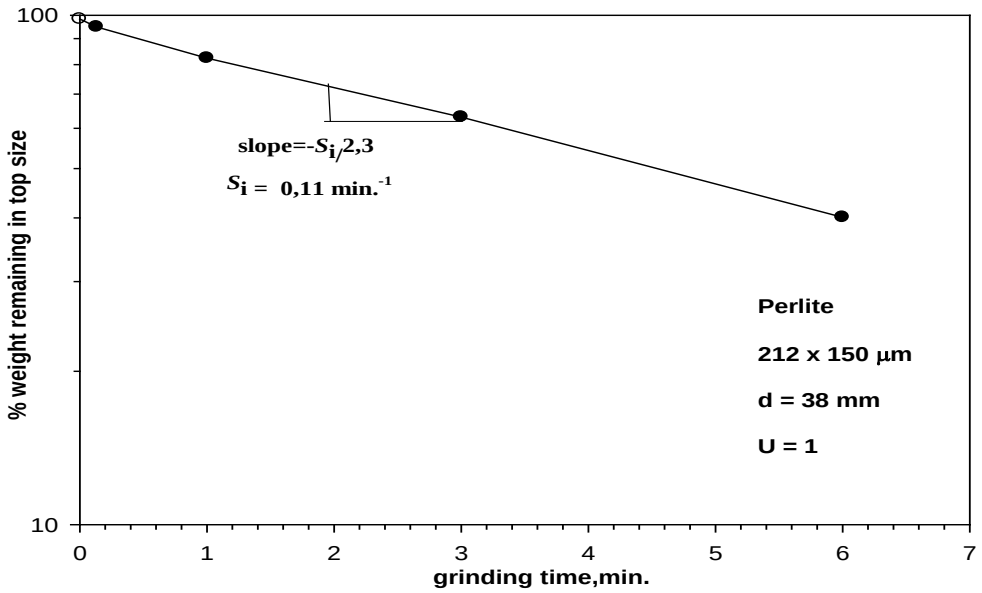

Figure B.26 First-order plot of breakage of - 212 + 150 μm feed of perlite ground with d = 38 mm ball diameter and U = 1.

Determination of aT value

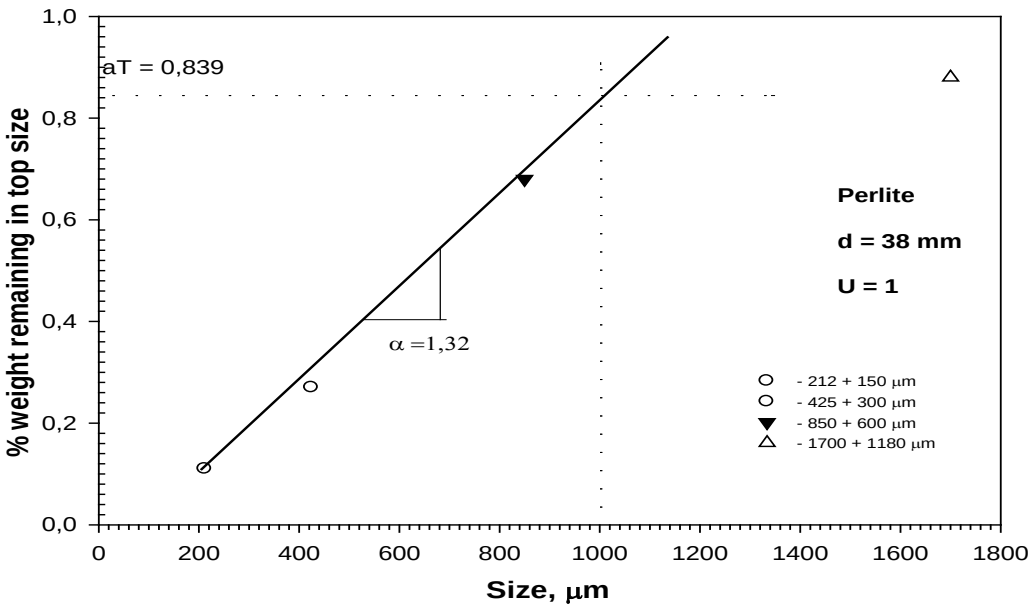

Figure B.27 Variation of first-order specific rates of breakage of perlite ground with d = 38 mm ball diameter and particle size: √2 intervals, plotted at upper size of interval at U=1.

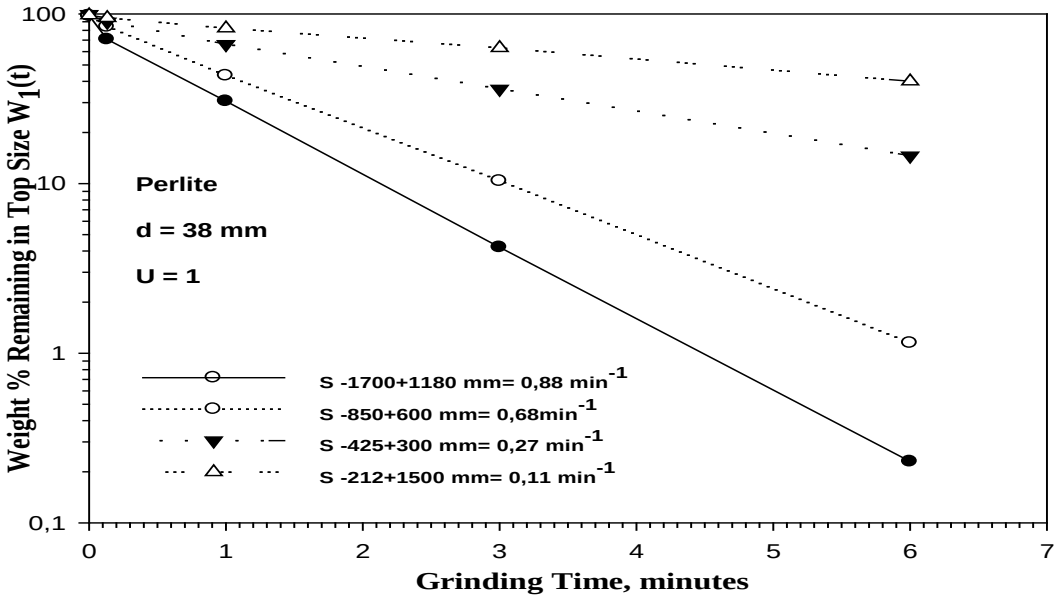

Figure B.28 First-order plots of breakage of -1700+1180, -850+600, -425+300, -212+150 μm feed size of perlite ground with d = 38 mm ball diameter and U=1.

Table B.18 Breakage parameters of perlite ground with d = 38 mm ball diameter at U=1.

1700x1180		**850x600**		**425x300**		**212x150**			
gama	1,58	**gama**	1,63	**gama**	1,67	**gama**	1,70		
beta	3,97	**beta**	3,99	**beta**	4,03	**beta**	4,06	**aT**	**α**
phi	0,61	**phi**	0,59	**phi**	0,58	**phi**	0,55	0,83	1,32
S value	0,880	**S value**	0,680	**S value**	0,270	**S value**	0,110		

30 mm ball size charge at U=0,6

1700 x 1180 micron

Table B.19 Determined B values of perlite for - 1700 + 1180 µm size interval ground with d = 30 mm ball diameter and U = 0,6.

INTERVAL NO,İ	SİZE (mesh)	Size (µm)	Xi/Xmax	B i,1	B VALUES
1	12x16	1700x1180	1,00	B1,1	1
2	16x20	1180x850	0,69	B2,1	1
3	20x30	850x600	0,50	B3,1	0,35752823
4	30x40	600x425	0,35	B4,1	0,198726243
5	40x50	425x300	0,25	B5,1	0,111048439
6	50x70	300x212	0,17	B6,1	0,057796581
7	70x100	212x150	0,12	B7,1	0,038571008
8	100x140	150x106	0,088	B8,1	0,020823155
9	140x200	106x75	0,062	B9,1	0,010658171
10	200x270	75x53	0,044	B10,1	0,00692295
11	270x400	53x38	0,031	B11,1	0,00399181
12	-400	-38	0,022	B12,1	0,002128219

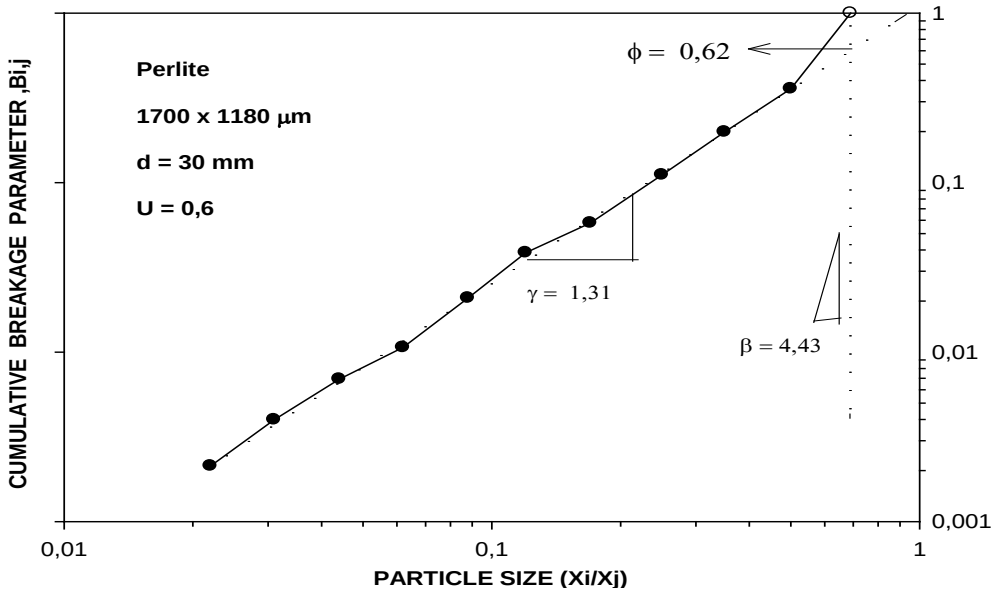

Figure B.29 Primary breakage distribution function of perlite for -1700 + 1180 µm feed size fraction ground with d = 30 mm ball diameter and U = 0,6.

Table B.20 Cumulative weight percent less than size values of perlite for 1700 x 1180 µm size interval ground with d = 30 mm ball diameter and U = 0,6.

SIZE	0 min.	0,133 min	1 min	3 min	6 min
1700	100,00	100,00	100,00	100,00	100,00
1180	1,34	32,26	74,87	98,21	99,97
850	0,32	12,86	57,65	97,03	98,51
600	0,01	7,21	37,79	90,56	98,03
425	0,00	4,09	25,88	74,12	96,94
300	0,00	2,15	17,27	50,33	83,32
212	0,00	1,44	10,87	34,02	54,00
150	0,00	0,78	6,51	19,94	32,49
106	0,00	0,40	3,79	11,02	19,53
75	0,00	0,26	1,84	6,79	11,26
53	0,00	0,15	0,93	3,72	7,02
38	0,00	0,08	0,49	2,09	3,97
%w.r.top size	98,66	67,74	25,13	1,79	0,03

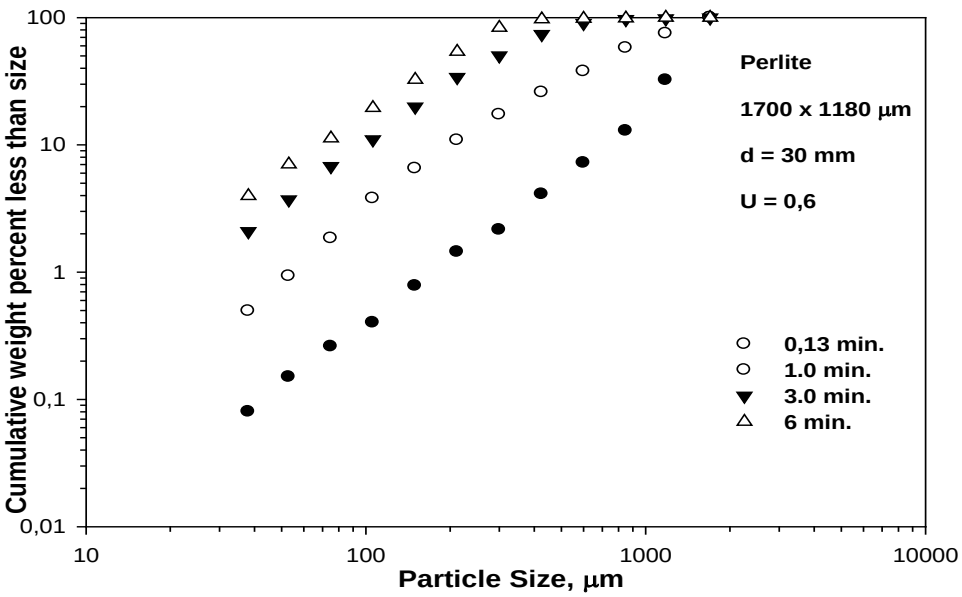

Figure B.30 Particle size distribution of perlite for -1700 + 1180 µm feed size fraction ground with d = 30 mm ball diameter and U = 0,6.

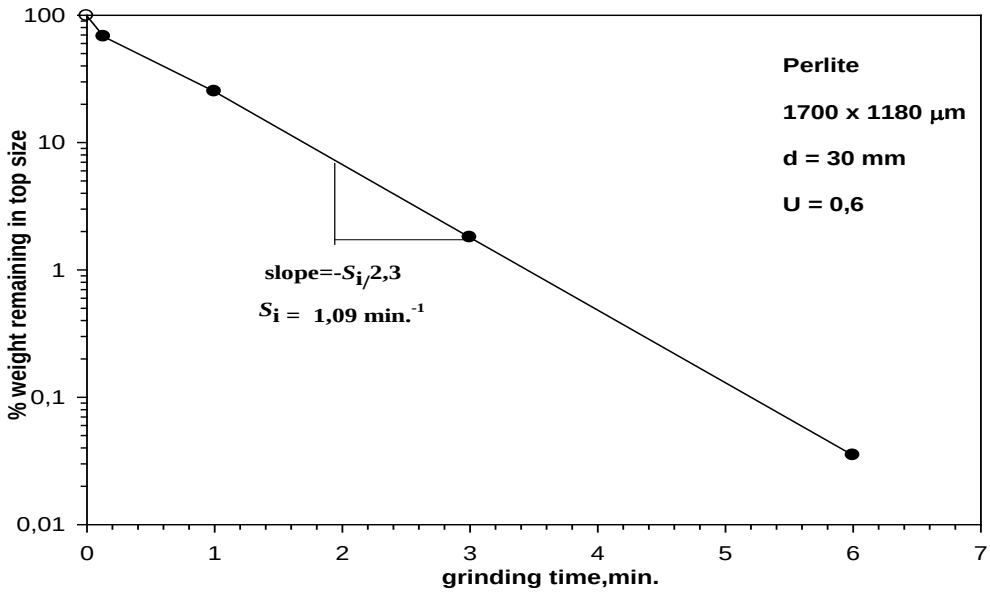

Figure B.31 First-order plot of breakage of - 1700 + 1180 µm feed of perlite ground with d = 30 mm ball diameter and U = 0,6.

850 x 600 micron

Table B.21 Determined B values of perlite for - 850 + 600 µm size interval ground with d = 30 mm ball diameter and U = 0,6.

INTERVAL NO,İ	SİZE (mesh)	Size (µm)	Xi/Xmax	B i,1	B VALUES
1	20x30	850x600	1,00	B3,1	1,0000
2	30x40	600x425	0,7	B4,1	1,0000
3	40x50	425x300	0,5	B5,1	0,3541
4	50x70	300x212	0,35	B6,1	0,1938
5	70x100	212x150	0,24	B7,1	0,1119
6	100x140	150x106	0,17	B8,1	0,0563
7	140x200	106x75	0,12	B9,1	0,0353
8	200x270	75x53	0,08	B10,1	0,0191
9	270x400	53x38	0,06	B11,1	0,0107
10	-400	-38	0,04	B12,1	0,0058

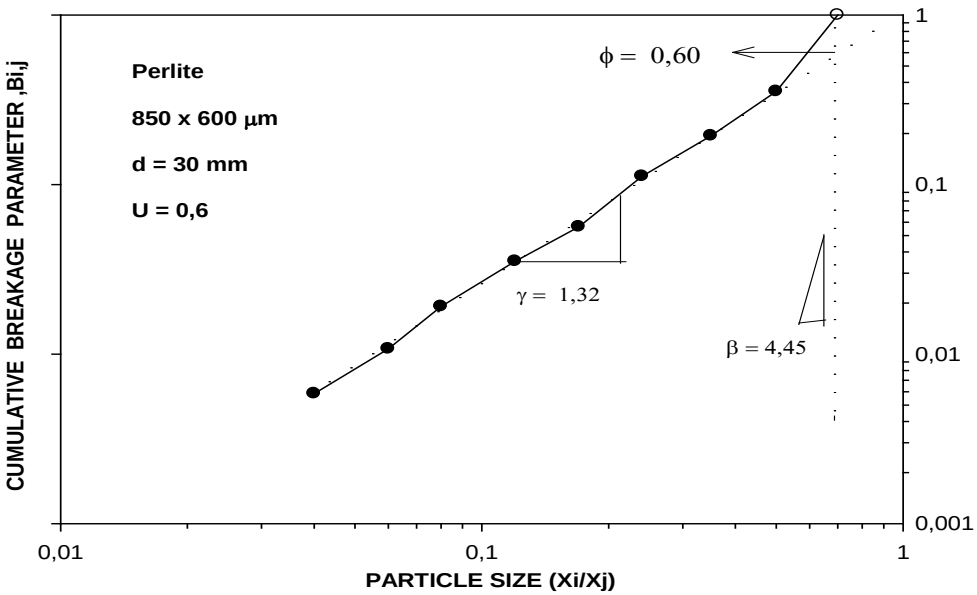

Figure B.32 Primary breakage distribution function of perlite for -850 + 600 µm feed size fraction ground with d = 30 mm ball diameter and U = 0,6.

Table B.22 Cumulative weight percent less than size values of perlite for - 850 + 600 µm size interval ground with d = 30 mm ball diameter and U = 0,6.

SIZE	0 min.	0,133 min	1 min	3 min	6 min
850	100,00	100,00	100,00	100,00	100,00
600	3,12	18,09	60,77	93,00	99,55
425	0,16	5,92	35,64	78,93	96,34
300	0,00	3,20	21,73	50,15	81,32
212	0,00	1,86	13,02	29,54	51,96
150	0,00	0,94	7,49	16,12	29,02
106	0,00	0,59	4,44	9,84	17,24
75	0,00	0,32	2,53	5,33	10,03
53	0,00	0,18	1,27	3,08	5,18
38	0,00	0,10	0,51	1,74	2,81
%w.r.top size	96,88	81,91	39,23	7,00	0,45

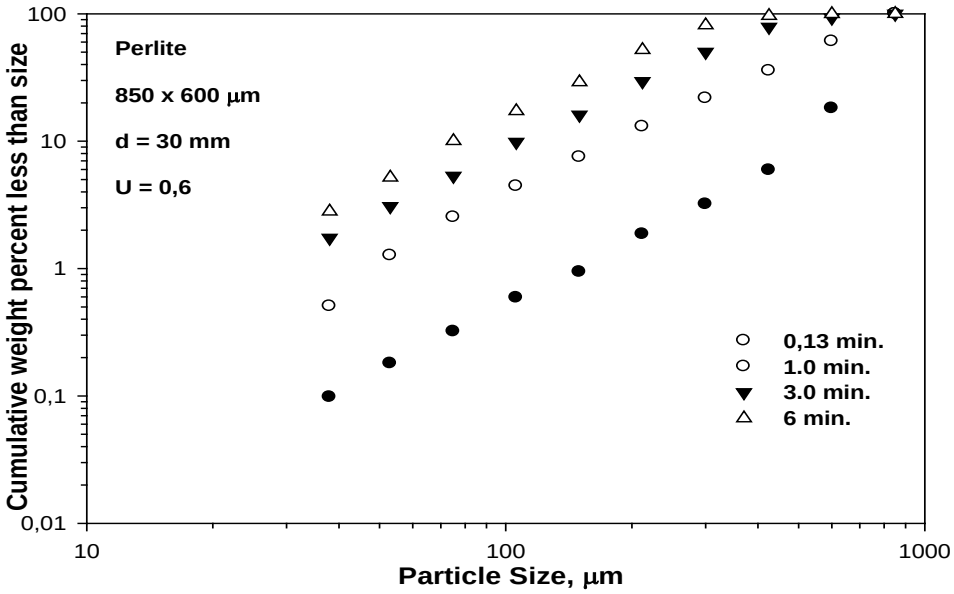

Figure B.33 Particle size distribution of perlite for -850 + 600 µm feed size fraction ground with d = 30 mm ball diameter and U = 0,6.

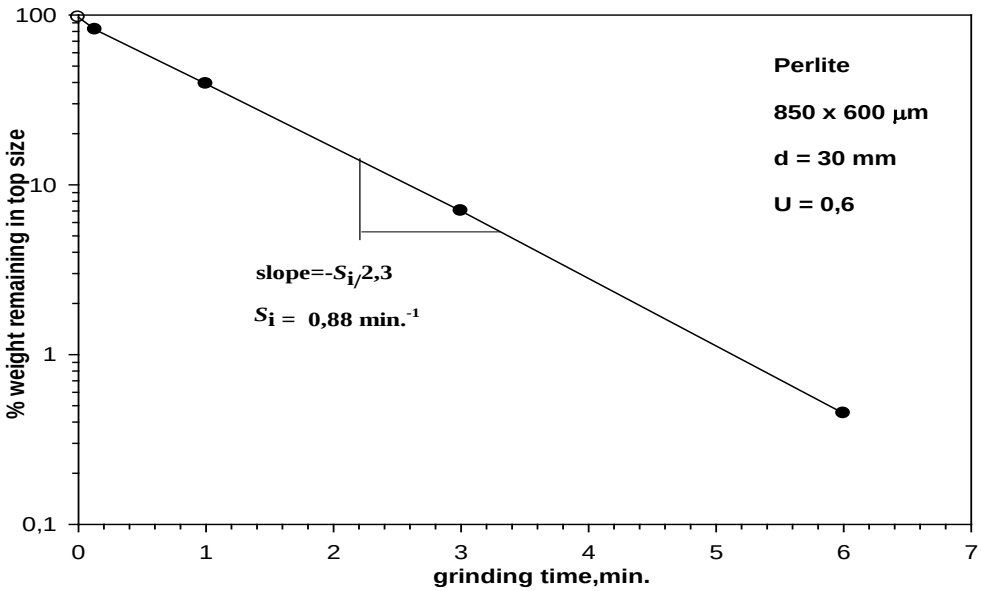

Figure B.34 First-order plot of breakage of - 850 + 600 µm feed of perlite ground with d = 30 mm ball diameter and U = 0,6.

425 x 300 micron

Table B.23 Determined B values of perlite for – 425 + 300 µm size interval ground with d = 30 mm ball diameter and U = 0,6.

INTERVAL NO,İ	SİZE (mesh)	Size (µm)	Xi/Xmax	B i,1	B VALUES
1	40x50	425x300	1,00	B1,1	1,0000
2	50x70	300x212	0,7	B2,1	1,0000
3	70x100	212x150	0,49	B3,1	0,3529
4	100x140	150x106	0,35	B4,1	0,2033
5	140x200	106x75	0,24	B5,1	0,1098
6	200x270	75x53	0,17	B6,1	0,0576
7	270x400	53x38	0,12	B7,1	0,0356
8	-400	-38	0,08	B8,1	0,0205

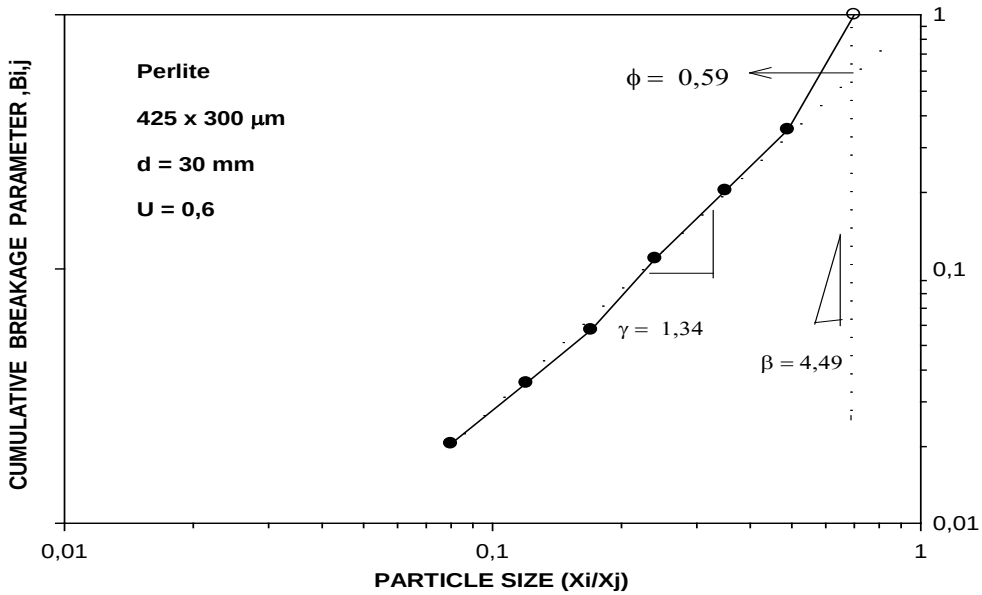

Figure B.35 Primary breakage distribution function of perlite for -425 + 300 µm feed size fraction ground with d = 30 mm ball diameter and U = 0,6.

Table B.24 Cumulative weight percent less than size values of perlite for - 425 + 300 µm size interval ground with d = 30 mm ball diameter and U = 0,6.

SIZE	0 min.	0,133 min	1 min	3 min	6 min
425	100,00	100,00	100,00	100,00	100,00
300	0,16	7,20	30,97	62,27	85,42
212	0,04	2,59	9,43	30,01	53,38
150	0,00	1,48	5,06	15,31	28,19
106	0,00	0,80	2,77	8,74	17,36
75	0,00	0,42	1,48	4,71	10,02
53	0,00	0,26	0,74	2,83	5,39
38	0,00	0,15	0,35	1,58	3,01
%w.r.top size	99,84	92,80	69,04	37,73	14,58

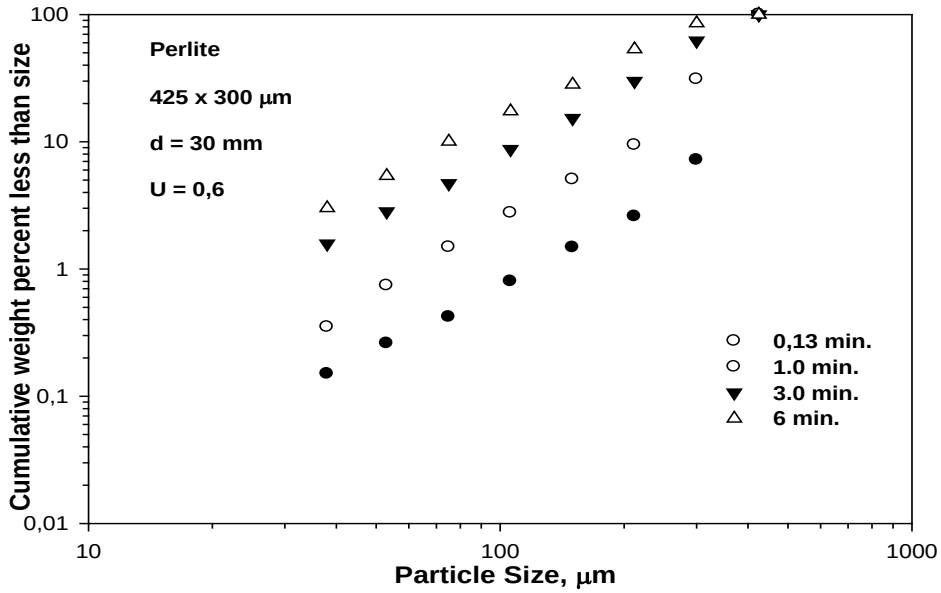

Figure B.36 Particle size distribution of perlite for -425 + 300 µm feed size fraction ground with d = 30 mm ball diameter and U = 0,6.

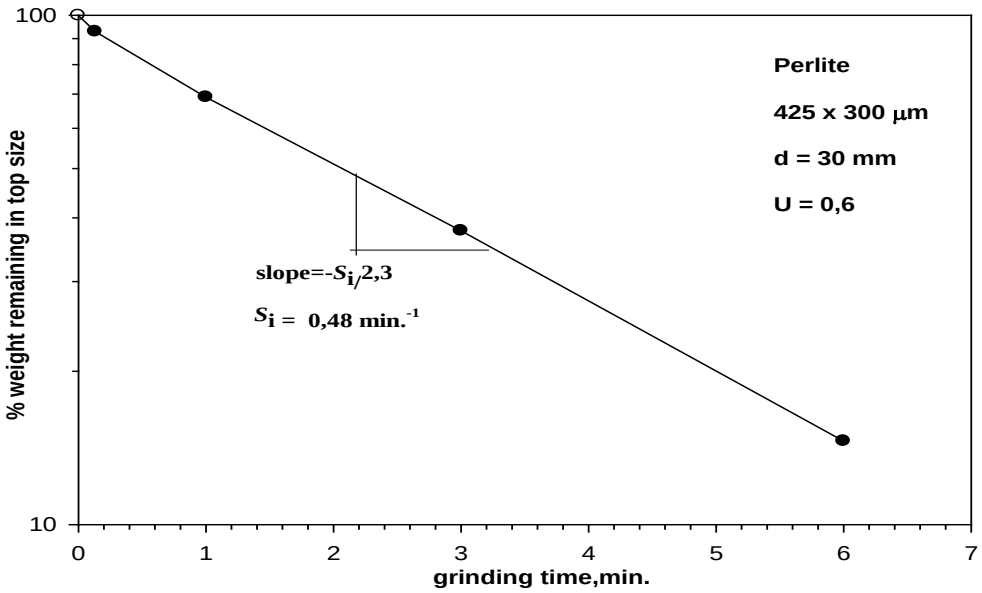

Figure B.37 First-order plot of breakage of - 425 + 300 µm feed of perlite ground with d = 30 mm ball diameter and U = 0,6.

212 x 150 micron

Table B.25 Determined B values of perlite for – 212 + 150 µm size interval ground with d = 30 mm ball diameter and U = 0,6.

INTERVAL NO,İ	SİZE (mesh)	Size (µm)	Xi/Xmax	B i,1	B VALUES
1	70x100	212x150	1,00	B1,1	1,0000
2	100x140	150x106	0,7	B2,1	1,0000
3	140x200	106x75	0,5	B3,1	0,3285
4	200x270	75x53	0,35	B4,1	0,1725
5	270x400	53x38	0,25	B5,1	0,0981
6	-400	-38	0,17	B6,1	0,0454

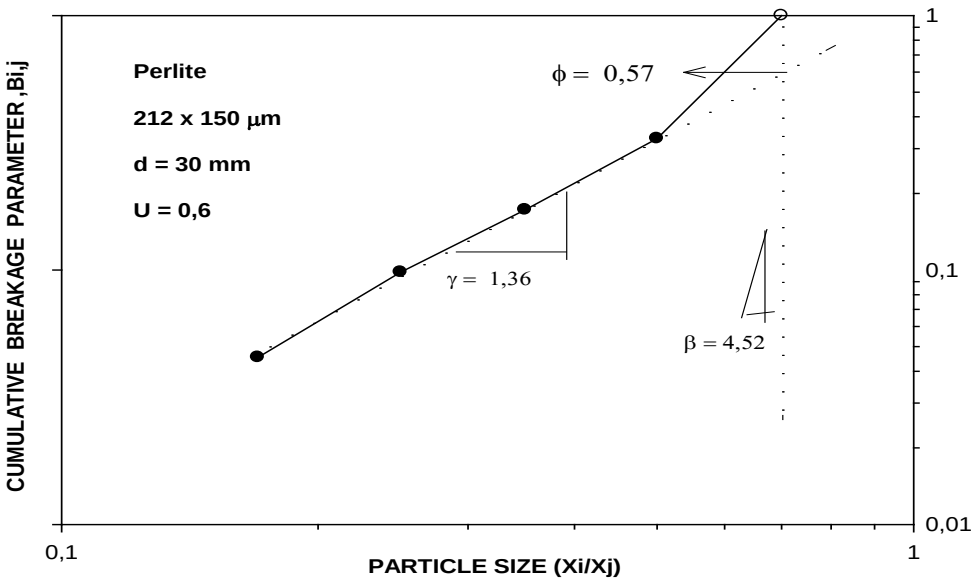

Figure B.38 Primary breakage distribution function of perlite for - 212 + 150 µm feed size fraction ground with d = 30 mm ball diameter and U = 0,6.

Table B.26 Cumulative weight percent less than size values of perlite for - 212 + 150 µm size interval ground with d = 30 mm ball diameter and U = 0,6.

SIZE	0 min.	0,133 min	1 min	3 min	6 min
212	100	100,00	100,00	100,00	100,00
150	1,06	5,12	14,23	33,16	57,14
106	0,52	1,88	8,37	19,02	32,06
75	0,00	0,72	5,06	11,14	19,73
53	0,00	0,41	2,65	7,09	12,14
38	0,00	0,19	1,54	4,32	7,49
%w.r.top size	98,94	94,88	85,77	66,84	42,87

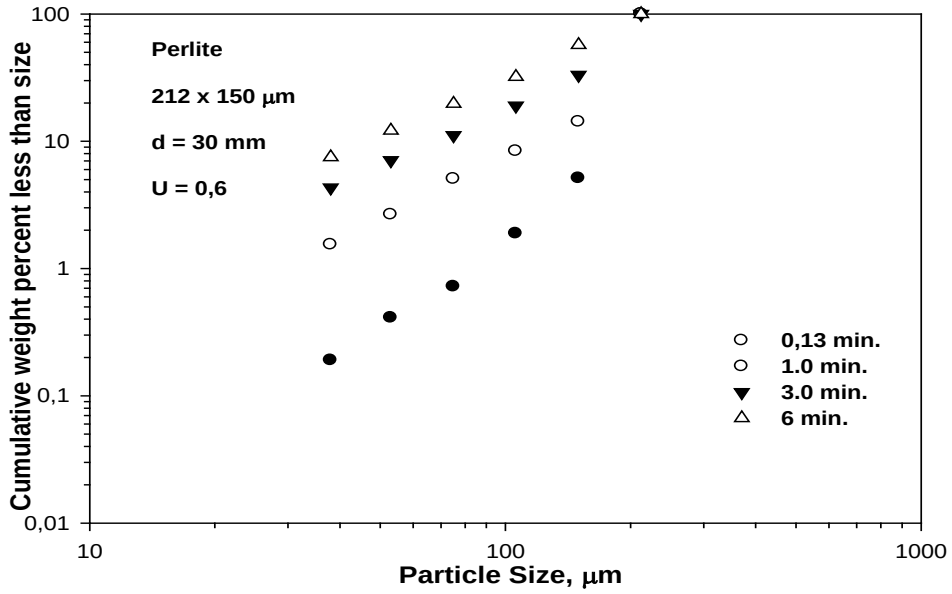

Figure B.39 Particle size distribution of perlite for -212 + 150 µm feed size fraction ground with d = 30 mm ball diameter and U = 0,6.

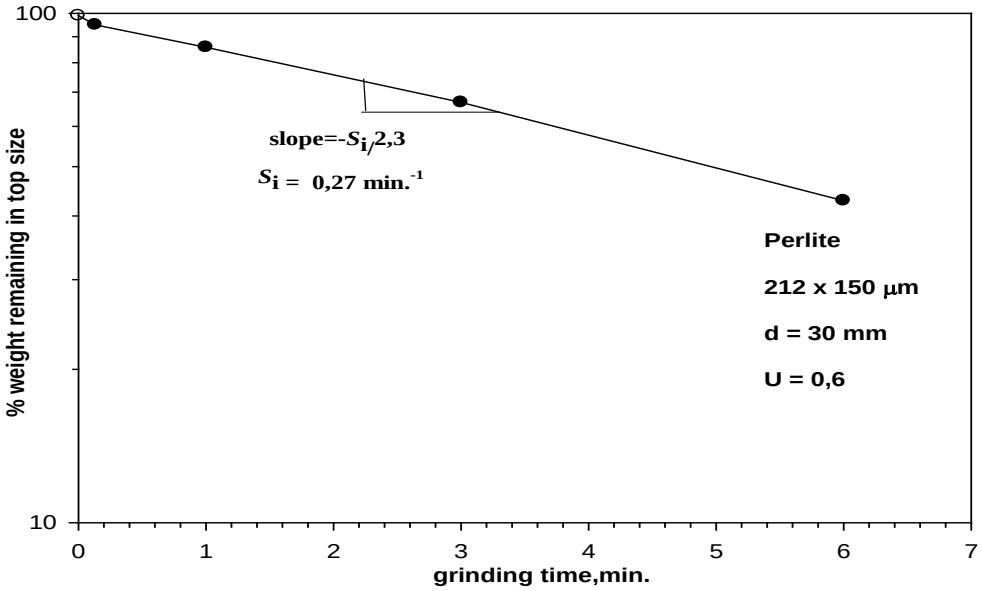

Figure B.40 First-order plot of breakage of - 212 + 150 µm feed of perlite ground with d = 30 mm ball diameter and U = 0,6.

Determination of aT value

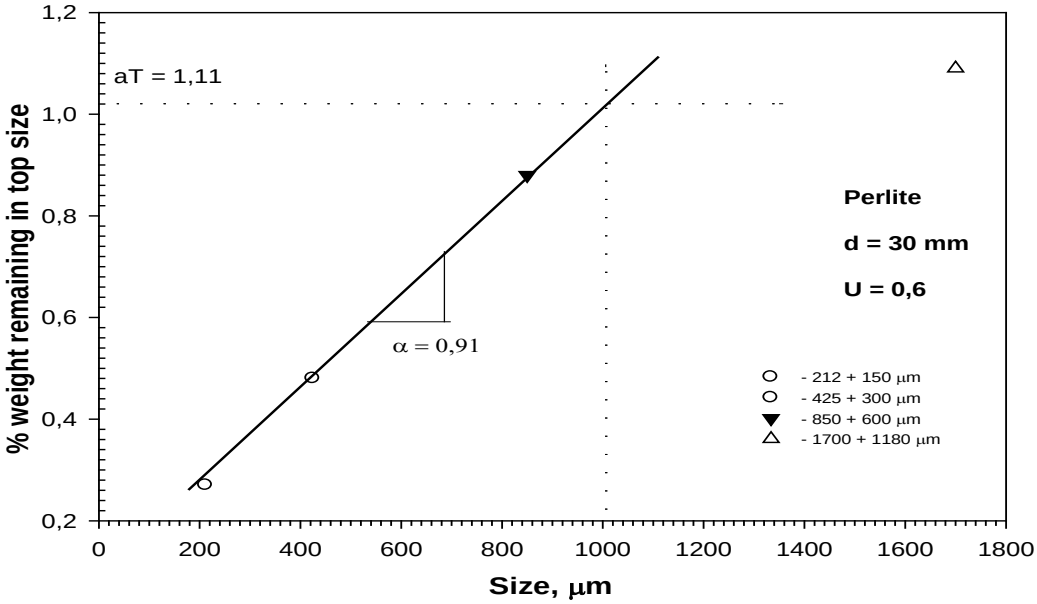

Figure B.41 Variation of first-order specific rates of breakage of perlite ground with d = 30 mm ball diameter and particle size: √2 intervals, plotted at upper size of interval at U=0,6.

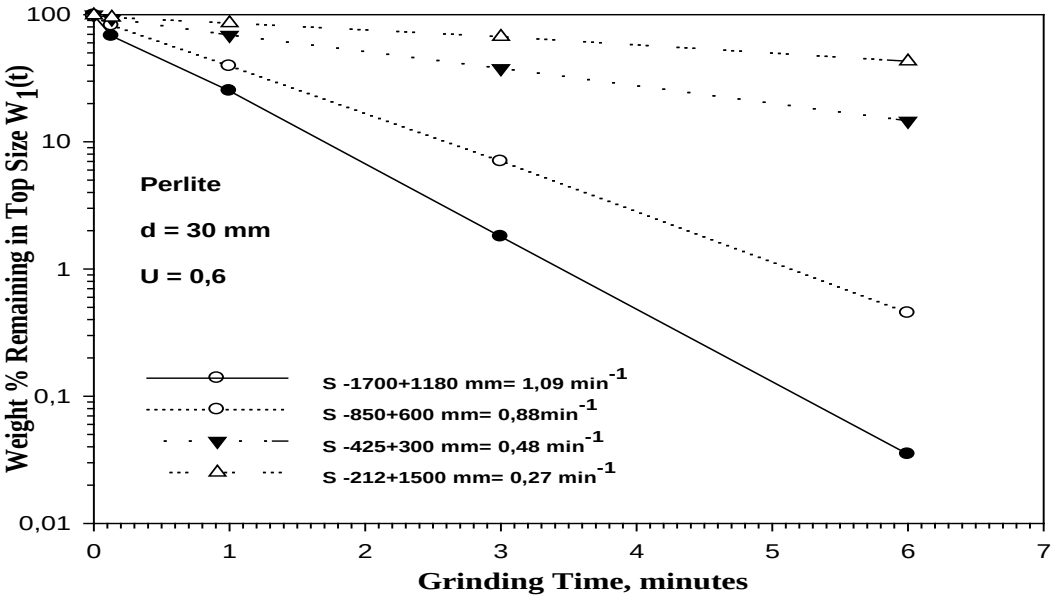

Figure B.42 First-order plots of breakage of -1700+1180, -850+600, -425+300, -212+150 μm feed size of perlite ground with d = 30 mm ball diameter and U=0,6.

Table B.27 Breakage parameters of perlite ground with d = 30 mm ball diameter at U=0,6.

1700x1180		**850x600**		**425x300**		**212x150**			
gama	1,31	**gama**	1,32	**gama**	1,34	**gama**	1,36		
beta	4,43	**beta**	4,45	**beta**	4,49	**beta**	4,52	**aT**	**α**
phi	0,62	**phi**	0,6	**phi**	0,59	**phi**	0,57	1,11	0,91
S value	1,090	**S value**	0,880	**S value**	0,480	**S value**	0,270		

30 mm ball size charge at U= 1

1700 x 1180 micron

Table B.28 Determined B values of perlite for - 1700 + 1180 µm size interval ground with d = 30 mm ball diameter and U = 1.

INTERVAL NO,İ	SİZE (mesh)	Size (µm)	Xi/Xmax	B i,1	B VALUES
1	12x16	1700x1180	1,00	B1,1	1
2	16x20	1180x850	0,69	B2,1	1
3	20x30	850x600	0,50	B3,1	0,43773206
4	30x40	600x425	0,35	B4,1	0,294906878
5	40x50	425x300	0,25	B5,1	0,195301288
6	50x70	300x212	0,17	B6,1	0,124501589
7	70x100	212x150	0,12	B7,1	0,083340331
8	100x140	150x106	0,088	B8,1	0,0581331
9	140x200	106x75	0,062	B9,1	0,037959985
10	200x270	75x53	0,044	B10,1	0,024967437
11	270x400	53x38	0,031	B11,1	0,016807439
12	-400	-38	0,022	B12,1	0,010913323

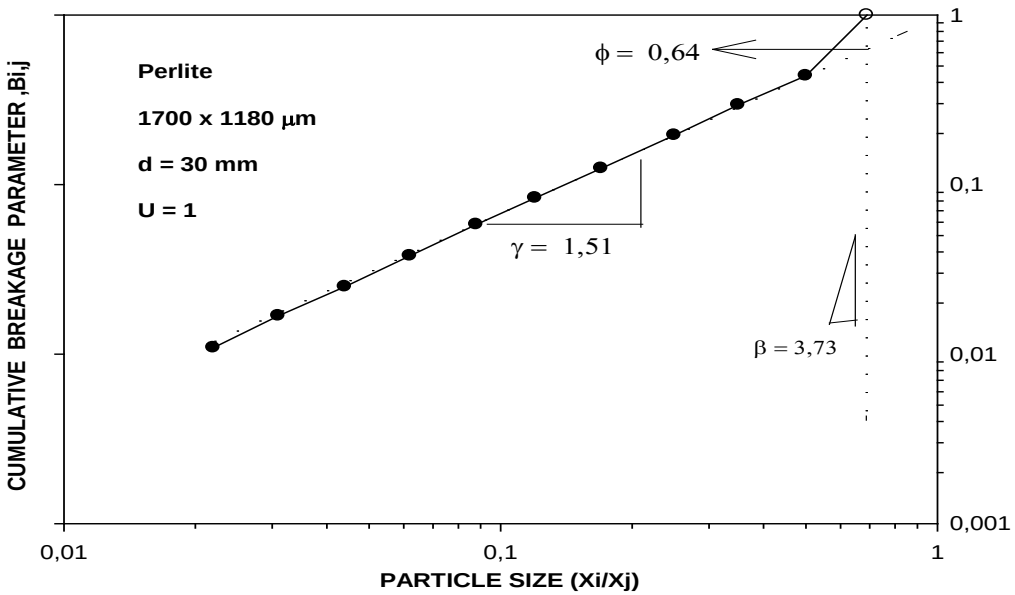

Figure B.43 Primary breakage distribution function of perlite for -1700 + 1180 µm feed size fraction ground with d = 30 mm ball diameter and U = 0,6.

Table B.29 Cumulative weight percent less than size values of perlite for 1700 x 1180 µm size interval ground with d = 30 mm ball diameter and U = 1.

SIZE	0 min.	0,133 min	1 min	3 min	6 min
1700	100,00	100,00	100,00	100,00	100,00
1180	1,95	31,46	71,74	96,41	99,83
850	0,53	14,96	59,22	96,42	98,02
600	0,21	10,21	38,33	90,13	95,24
425	0,06	6,81	25,57	68,17	88,71
300	0,00	4,36	18,31	46,73	76,93
212	0,00	2,94	11,64	28,16	51,12
150	0,00	2,06	8,26	17,68	28,78
106	0,00	1,35	4,91	10,05	17,28
75	0,00	0,89	2,86	5,72	10,02
53	0,00	0,60	1,62	3,58	5,92
38	0,00	0,39	0,93	1,97	3,47
%w.r.top size	98,05	68,54	28,26	3,59	0,17

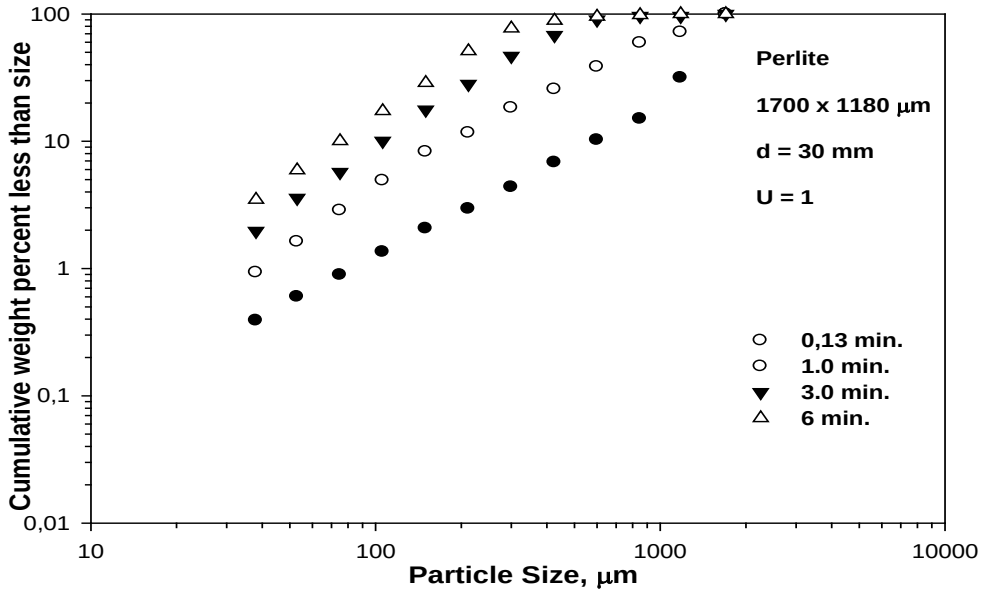

Figure B.44 Particle size distribution of perlite for -1700 + 1180 μm feed size fraction ground with d = 30 mm ball diameter and U = 1.

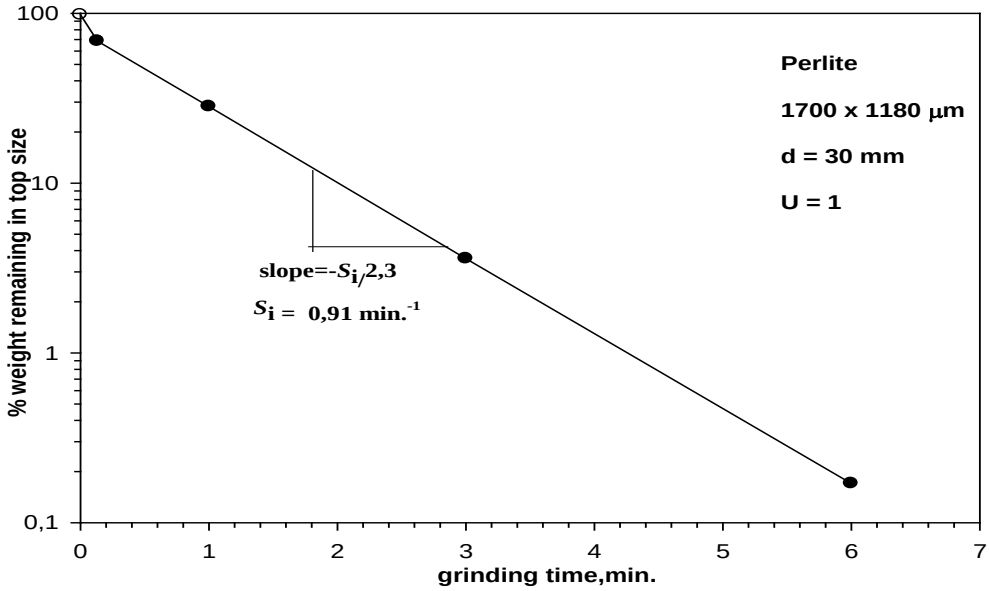

Figure B.45 First-order plot of breakage of - 1700 + 1180 μm feed of perlite ground with d = 30 mm ball diameter and U = 1.

850 x 600 micron

Table B.30 Determined B values of perlite for - 850 + 600 µm size interval ground with d = 30 mm ball diameter and U = 1.

INTERVAL NO,İ	SİZE (mesh)	Size (µm)	Xi/Xmax	B i,1	B VALUES
1	20x30	850x600	1,00	B3,1	1,0000
2	30x40	600x425	0,7	B4,1	1,0000
3	40x50	425x300	0,5	B5,1	0,4375
4	50x70	300x212	0,35	B6,1	0,2933
5	70x100	212x150	0,24	B7,1	0,1958
6	100x140	150x106	0,17	B8,1	0,1253
7	140x200	106x75	0,12	B9,1	0,0839
8	200x270	75x53	0,08	B10,1	0,0517
9	270x400	53x38	0,06	B11,1	0,0363
10	-400	-38	0,04	B12,1	0,0214

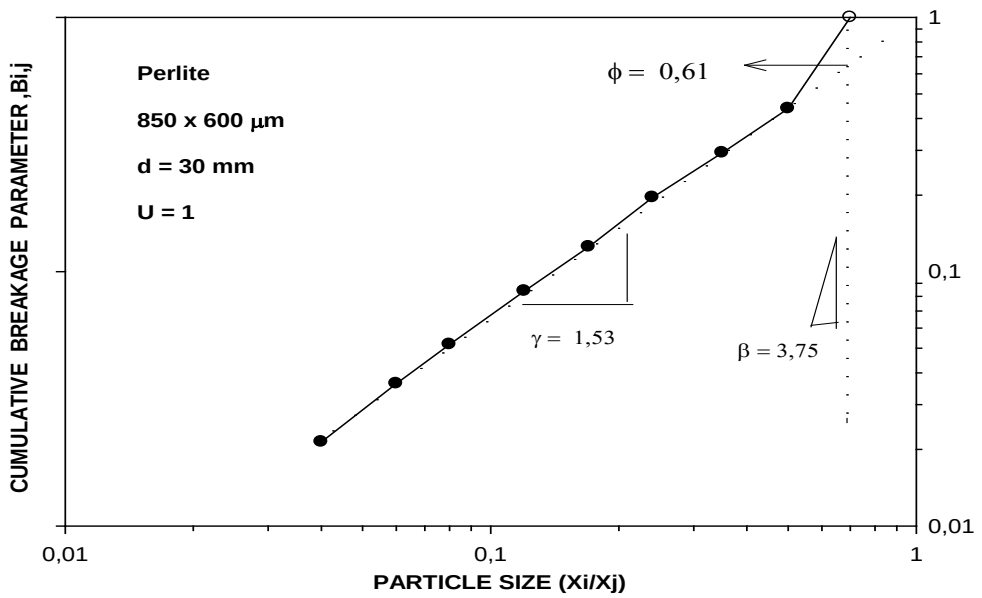

Figure B.46 Primary breakage distribution function of perlite for -850 + 600 µm feed size fraction ground with d = 30 mm ball diameter and U = 0,6.

Table B.31 Cumulative weight percent less than size values of perlite for - 850 + 600 µm size interval ground with d = 30 mm ball diameter and U = 1.

SIZE	0 min.	0,133 min	1 min	3 min	6 min
850	100,00	100,00	100,00	100,00	100,00
600	2,17	18,49	61,76	91,74	99,26
425	0,58	8,21	31,58	75,49	96,08
300	0,05	5,26	17,21	47,51	78,82
212	0,01	3,52	10,06	26,35	50,13
150	0,00	2,26	5,12	15,12	27,46
106	0,00	1,52	3,18	8,68	15,98
75	0,00	0,94	1,97	5,14	8,64
53	0,00	0,66	1,16	3,11	5,29
38	0,00	0,39	0,71	1,95	3,23
%w.r.top size	97,83	81,51	38,24	8,26	0,74

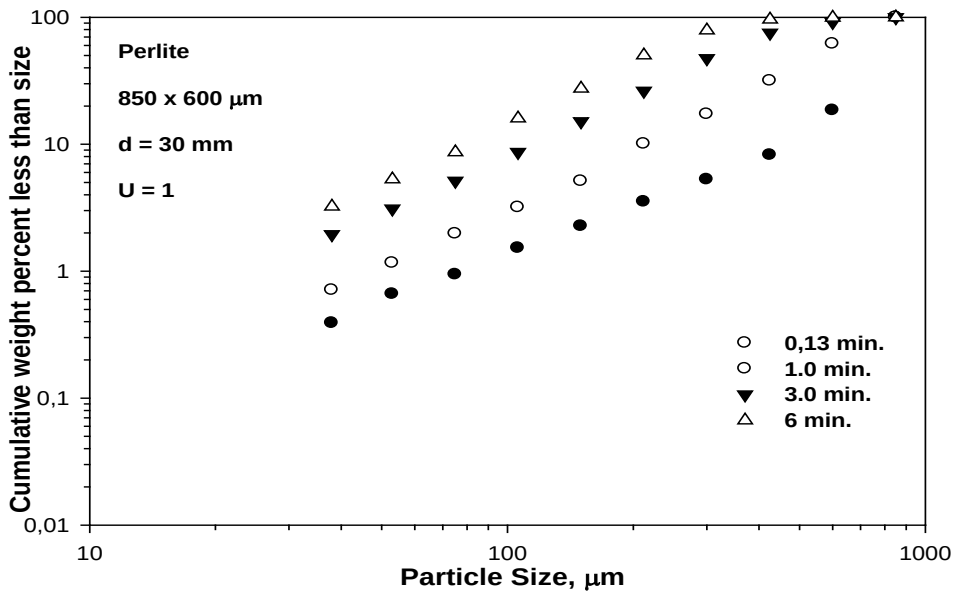

Figure B.47 Particle size distribution of perlite for -850 + 600 µm feed size fraction ground with d = 30 mm ball diameter and U = 1.

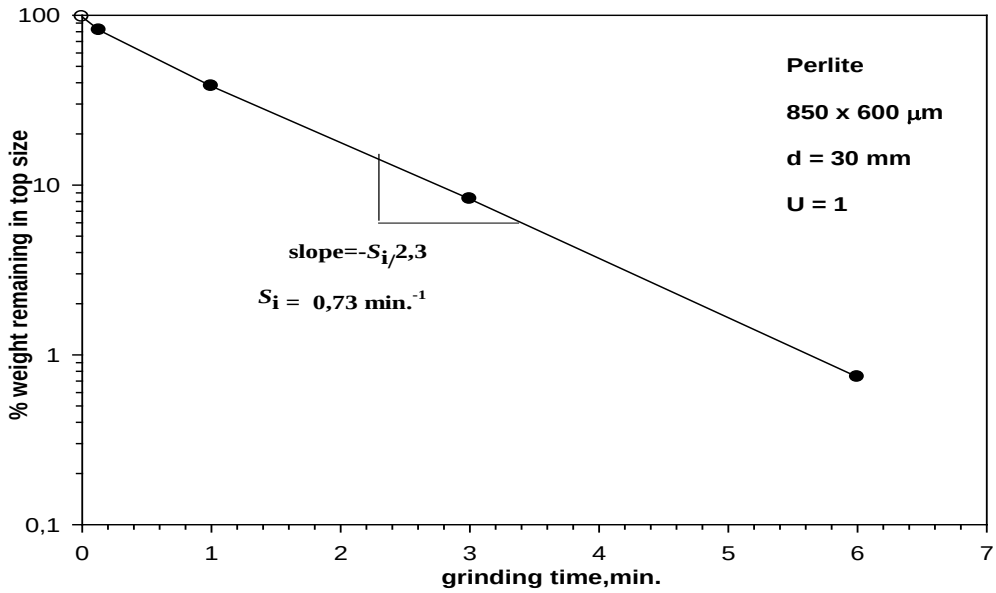

Figure B.48 First-order plot of breakage of - 850 + 600 µm feed of perlite ground with d = 30 mm ball diameter and U = 1.

425 x 300 micron

Table B.32 Determined B values of perlite for – 425 + 300 µm size interval ground with d = 30 mm ball diameter and U = 1.

INTERVAL NO,İ	SİZE (mesh)	Size (µm)	Xi/Xmax	B i,1	B VALUES
1	40x50	425x300	1,00	B1,1	1,0000
2	50x70	300x212	0,7	B2,1	1,0000
3	70x100	212x150	0,49	B3,1	0,4274
4	100x140	150x106	0,35	B4,1	0,2918
5	140x200	106x75	0,24	B5,1	0,1912
6	200x270	75x53	0,17	B6,1	0,1256
7	270x400	53x38	0,12	B7,1	0,0878
8	-400	-38	0,08	B8,1	0,0557

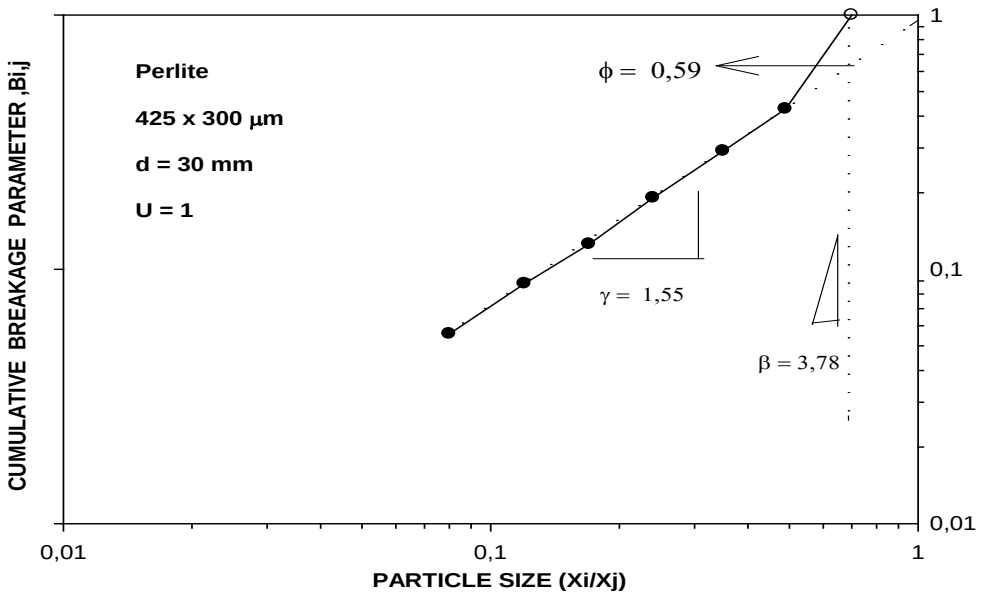

Figure B.49 Primary breakage distribution function of perlite for -425 + 300 µm feed size fraction ground with d = 30 mm ball diameter and U = 1.

Table B.33 Cumulative weight percent less than size values of perlite for - 425 + 300 µm size interval ground with d = 30 mm ball diameter and U = 1.

SIZE	0 min.	0,133 min	1 min	3 min	6 min
425	100,00	100,00	100,00	100,00	100,00
300	0,25	12,06	42,91	78,86	94,97
212	0,06	5,30	9,95	24,93	51,12
150	0,01	3,62	6,23	13,12	25,14
106	0,00	2,38	3,98	7,98	13,08
75	0,00	1,57	2,65	4,93	8,12
53	0,00	1,10	1,79	3,08	4,85
38	0,00	0,70	1,14	2,01	3,12
%w.r.top size	99,75	87,94	57,09	21,14	5,03

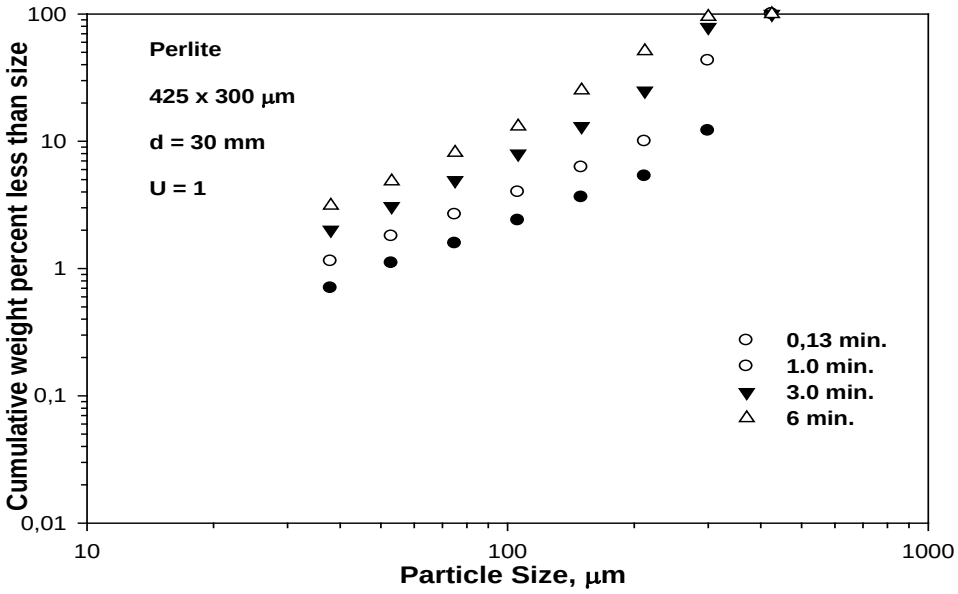

Figure B.50 Particle size distribution of perlite for -425 + 300 µm feed size fraction ground with d = 30 mm ball diameter and U = 1.

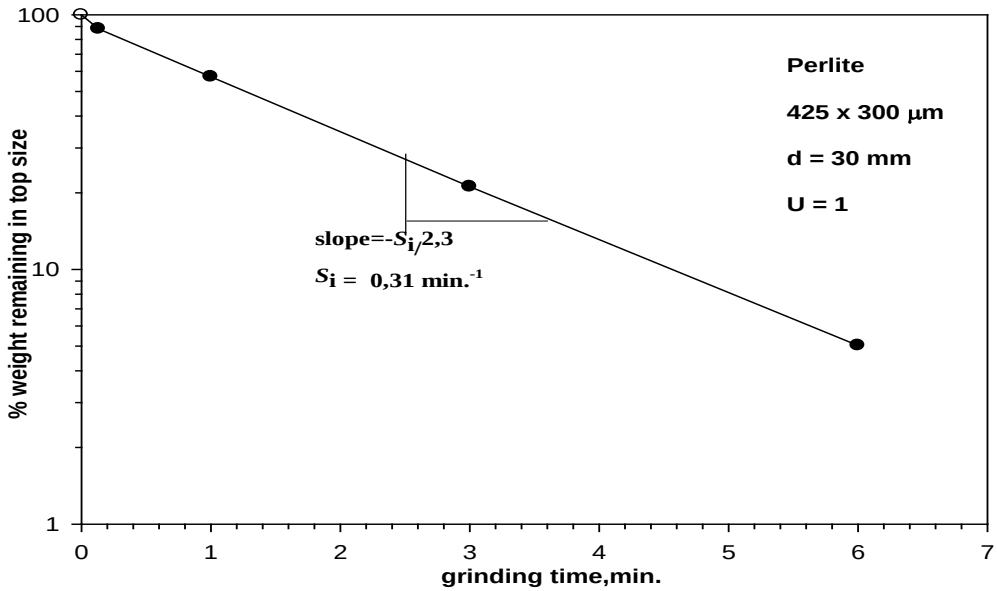

Figure B.51 First-order plot of breakage of - 425 + 300 µm feed of perlite ground with d = 30 mm ball diameter and U = 1.

212 x 150 micron

Table B.34 Determined B values of perlite for – 212 + 150 µm size interval ground with d = 30 mm ball diameter and U = 1.

INTERVAL NO,İ	SİZE (mesh)	Size (µm)	Xi/Xmax	B i,1	B VALUES
1	70x100	212x150	1,00	B1,1	1,0000
2	100x140	150x106	0,7	B2,1	1,0000
3	140x200	106x75	0,5	B3,1	0,4317
4	200x270	75x53	0,35	B4,1	0,2942
5	270x400	53x38	0,25	B5,1	0,1933
6	-400	-38	0,17	B6,1	0,1231

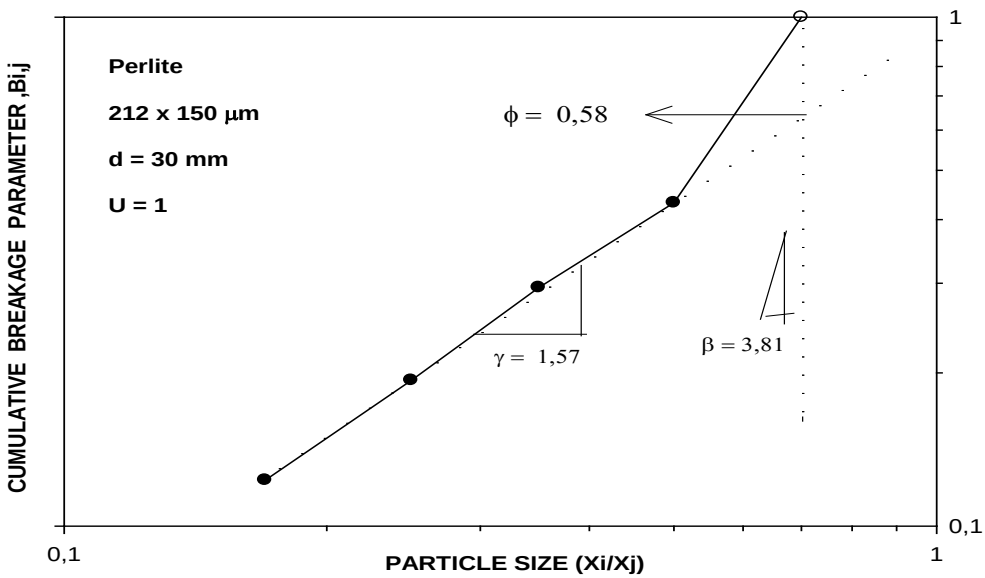

Figure B.52 Primary breakage distribution function of perlite for - 212 + 150 µm feed size fraction ground with d = 30 mm ball diameter and U = 1.

Table B.35 Cumulative weight percent less than size values of perlite for - 212 + 150 µm size interval ground with d = 30 mm ball diameter and U = 1.

SIZE	0 min.	0,133 min	1 min	3 min	6 min
212	100,00	100,00	100,00	100,00	100,00
150	1,14	6,93	25,84	57,71	80,99
106	0,06	2,63	7,52	21,44	46,93
75	0,00	1,76	4,36	11,34	22,86
53	0,00	1,16	2,29	6,68	12,85
38	0,00	0,74	1,37	4,06	7,35
%w.r.top size	98,86	93,07	74,16	42,29	19,01

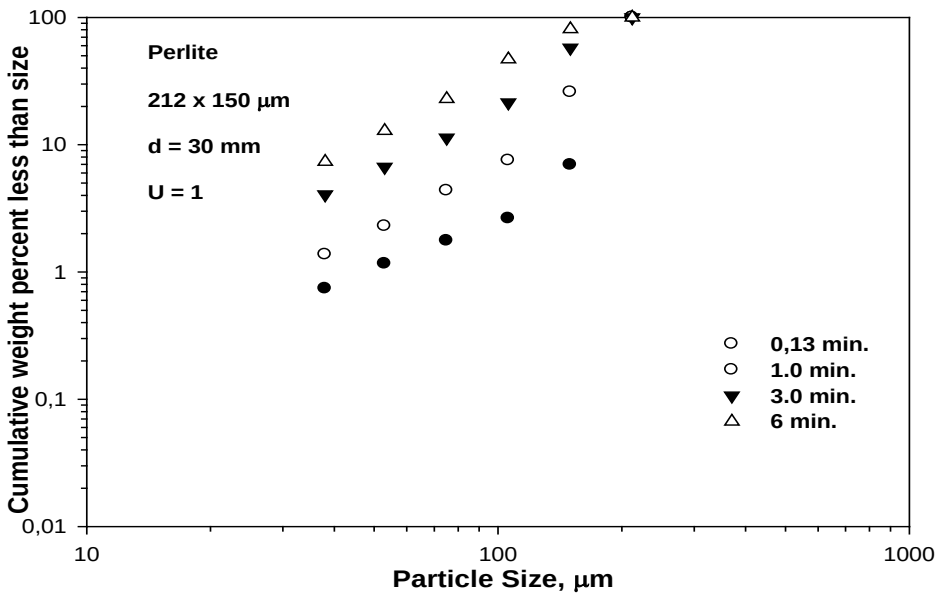

Figure B.53 Particle size distribution of perlite for -212 + 150 µm feed size fraction ground with d = 30 mm ball diameter and U = 1.

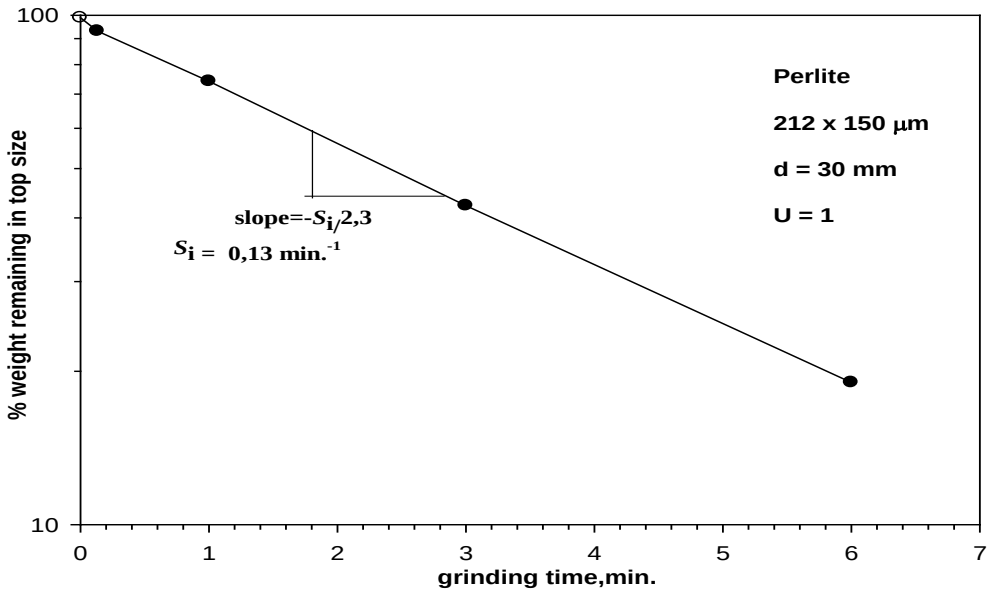

Figure B.54 First-order plot of breakage of - 212 + 150 μm feed of perlite ground with d = 30 mm ball diameter and U = 1.

Determination of aT value

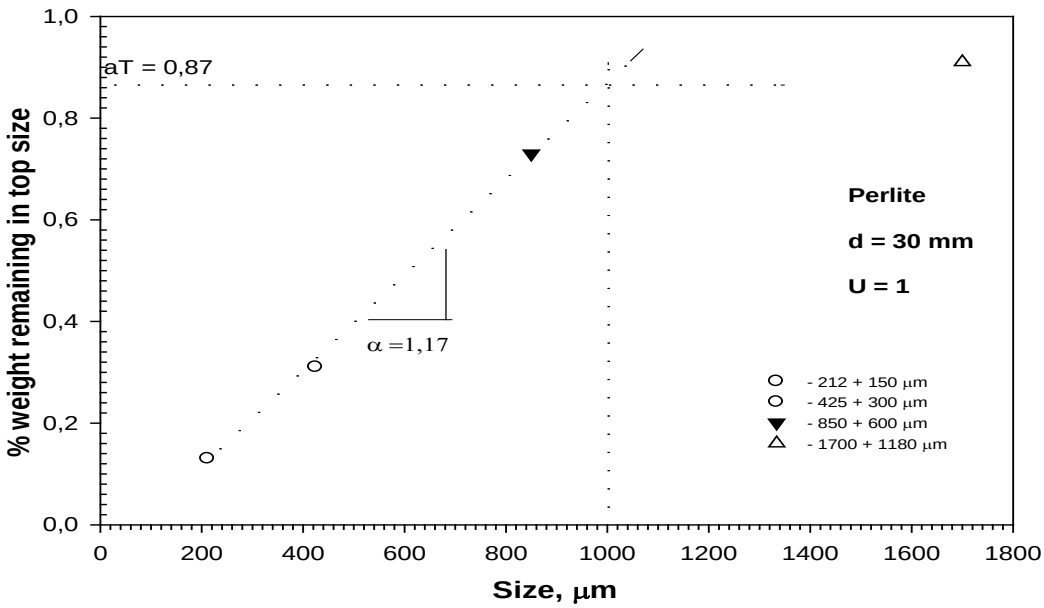

Figure B.55 Variation of first-order specific rates of breakage of perlite ground with d = 30 mm ball diameter and particle size: √2 intervals, plotted at upper size of interval at U=1.

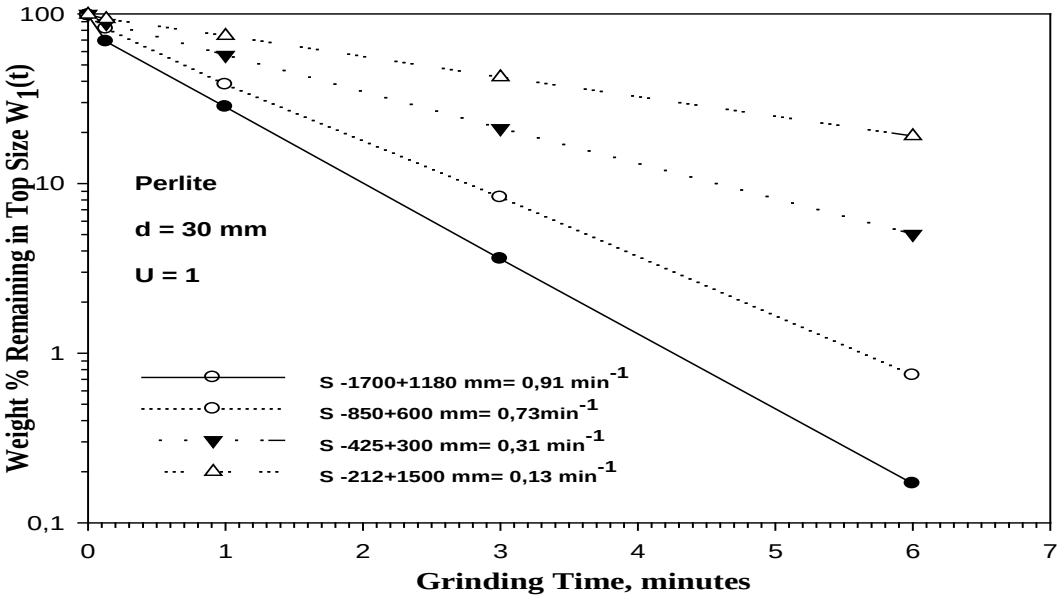

Figure B.56 First-order plots of breakage of -1700+1180, -850+600, -425+300, -212+150 μm feed size of perlite ground with d = 30 mm ball diameter and U=1.

Table B.36 Breakage parameters of perlite ground with d = 30 mm ball diameter at U=1.

1700x1180		**850x600**		**425x300**		**212x150**			
gama	1,51	**gama**	1,53	**gama**	1,55	**gama**	1,57		
beta	3,73	**beta**	3,75	**beta**	3,78	**beta**	3,81	**aT**	**α**
phi	0,64	**phi**	0,61	**phi**	0,59	**phi**	0,58	0,87	1,17
S value	0,910	**S value**	0,730	**S value**	0,310	**S value**	0,130		

30 – 25,4 – 19,05 mm ball size charge at U=0,6

1700 x 1180 micron

Table B.37 Determined B values of perlite for - 1700 + 1180 µm size interval ground with d = 30 – 25,4 – 19,05 mm ball diameter and U = 0,6.

INTERVAL NO,İ	SİZE (mesh)	Size (µm)	Xi/Xmax	B i,1	B VALUES
1	12x16	1700x1180	1,00	B1,1	1
2	16x20	1180x850	0,69	B2,1	1
3	20x30	850x600	0,50	B3,1	0,424377213
4	30x40	600x425	0,35	B4,1	0,245489367
5	40x50	425x300	0,25	B5,1	0,145930627
6	50x70	300x212	0,17	B6,1	0,073468365
7	70x100	212x150	0,12	B7,1	0,040685224
8	100x140	150x106	0,088	B8,1	0,024307371
9	140x200	106x75	0,062	B9,1	0,013079966
10	200x270	75x53	0,044	B10,1	0,007105969
11	270x400	53x38	0,031	B11,1	0,004029885
12	-400	-38	0,022	B12,1	0,002109835

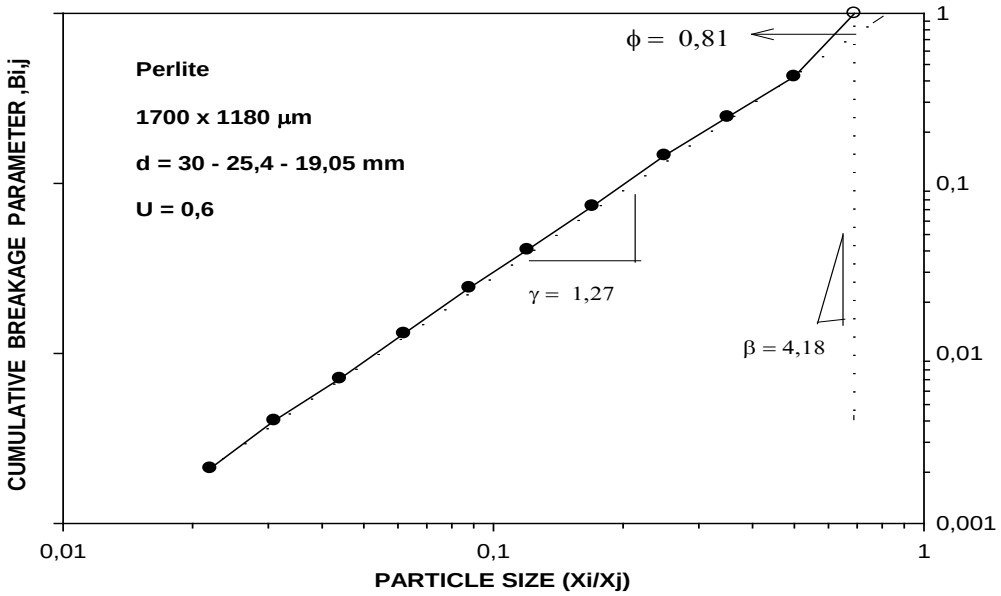

Figure B.57 Primary breakage distribution function of perlite for -1700 + 1180 µm feed size fraction ground with d = 30 – 25,4 – 19,05 mm ball diameter and U = 0,6.

Table B.38 Cumulative weight percent less than size values of perlite for 1700 x 1180 µm size interval ground with d = 30 – 25,4 – 19,05 mm ball diameter and U = 0,6.

SIZE	0 min.	0,133 min	1 min	3 min	6 min
1700	100,00	100,00	100,00	100,00	100,00
1180	3,11	42,49	86,09	99,38	99,99
850	1,02	20,68	65,08	97,79	99,91
600	0,00	12,02	46,55	92,92	99,73
425	0,00	7,33	33,12	76,00	98,35
300	0,00	3,76	23,28	54,70	85,17
212	0,00	2,10	15,15	35,78	57,63
150	0,00	1,26	9,53	22,42	36,50
106	0,00	0,68	5,79	13,78	22,98
75	0,00	0,37	3,63	8,40	14,69
53	0,00	0,21	1,96	5,20	8,78
38	0,00	0,11	1,21	3,36	5,40
%w.r.top size	96,89	57,51	13,91	0,62	0,01

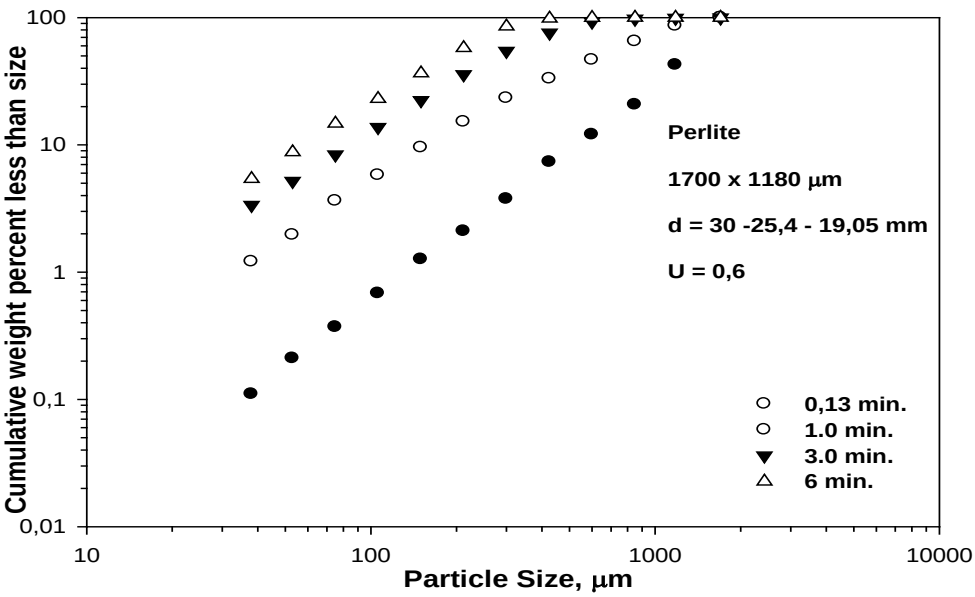

Figure B.58 Particle size distribution of perlite for -1700 + 1180 µm feed size fraction ground with d = 30 – 25,4 – 19,05 mm ball diameter and U = 0,6.

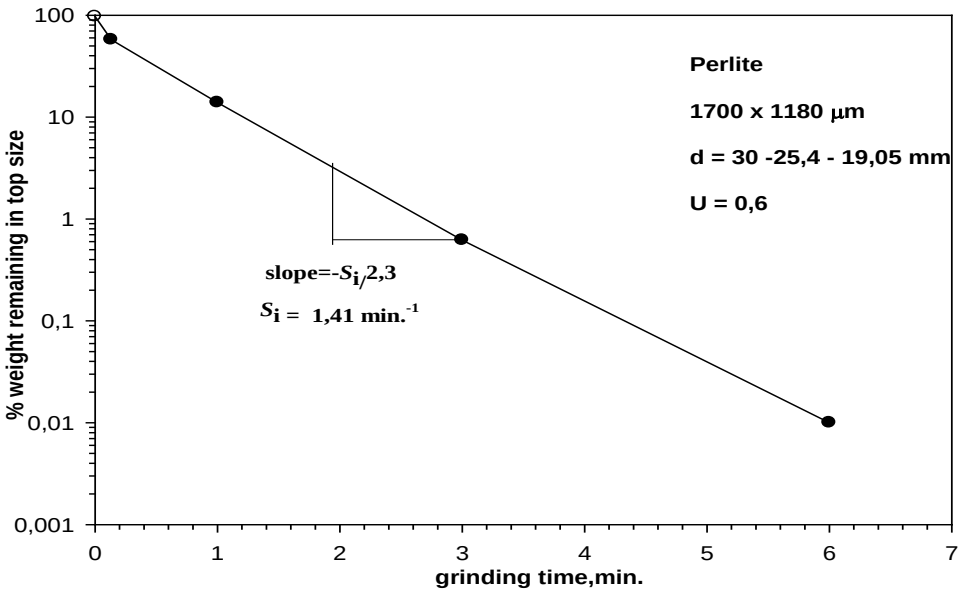

Figure B.59 First-order plot of breakage of - 1700 + 1180 µm feed of perlite ground with d = 30 – 25,4 – 19,05 mm ball diameter and U = 0,6.

850 x 600 micron

Table B.39 Determined B values of perlite for - 850 + 600 µm size interval ground with d = 30 – 25,4 – 19,05 mm ball diameter and U = 0,6.

INTERVAL NO,İ	SİZE (mesh)	Size (µm)	Xi/Xmax	B i,1	B VALUES
1	20x30	850x600	1,00	B3,1	1,0000
2	30x40	600x425	0,7	B4,1	1,0000
3	40x50	425x300	0,5	B5,1	0,4245
4	50x70	300x212	0,35	B6,1	0,2385
5	70x100	212x150	0,24	B7,1	0,1329
6	100x140	150x106	0,17	B8,1	0,0727
7	140x200	106x75	0,12	B9,1	0,0410
8	200x270	75x53	0,08	B10,1	0,0205
9	270x400	53x38	0,06	B11,1	0,0130
10	-400	-38	0,04	B12,1	0,0067

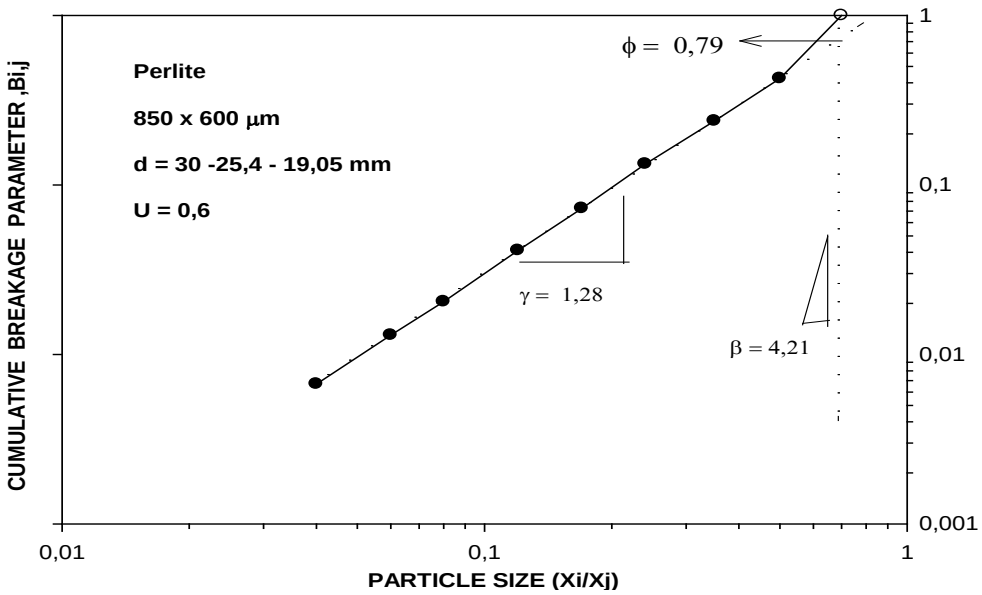

Figure B.60 Primary breakage distribution function of perlite for -850 + 600 µm feed size fraction ground with d = 30 – 25,4 – 19,05 mm ball diameter and U = 0,6.

Table B.40 Cumulative weight percent less than size values of perlite for - 850 + 600 µm size interval ground with d = 30 – 25,4 – 19,05 mm ball diameter and U = 0,6.

SIZE	0 min.	0,133 min	1 min	3 min	6 min
850	100,00	100,00	100,00	100,00	100,00
600	4,76	27,26	70,73	97,23	99,91
425	0,43	11,20	37,43	81,58	98,79
300	0,13	6,35	22,33	53,93	84,09
212	0,00	3,52	13,08	32,96	54,49
150	0,00	1,94	7,57	19,81	32,94
106	0,00	1,10	4,44	12,10	20,19
75	0,00	0,55	2,80	7,63	12,84
53	0,00	0,35	1,80	4,63	7,74
38	0,00	0,18	1,23	3,08	4,48
%w.r.top size	95,24	72,74	29,27	2,77	0,09

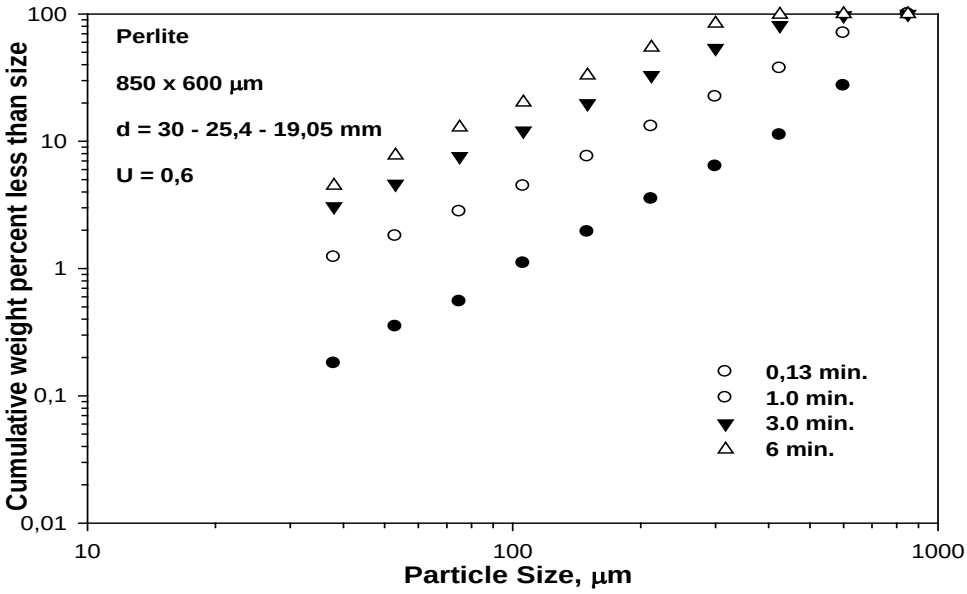

Figure B.61 Particle size distribution of perlite for -850 + 600 µm feed size fraction ground with d = 30 – 25,4 – 19,05 mm ball diameter and U = 0,6.

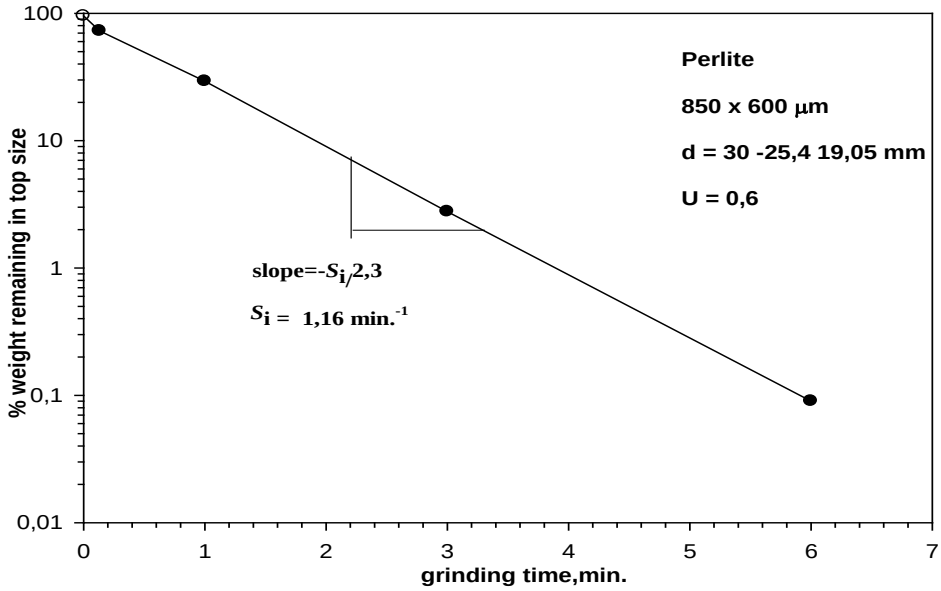

Figure B.62 First-order plot of breakage of - 850 + 600 µm feed of perlite ground with d = 30 – 25,4 – 19,05 mm ball diameter and U = 0,6.

425 x 300 micron

Table B.41 Determined B values of perlite for – 425 + 300 µm size interval ground with d = 30 – 25,4 – 19,05 mm ball diameter and U = 0,6.

INTERVAL NO,İ	SİZE (mesh)	Size (µm)	Xi/Xmax	B i,1	B VALUES
1	40x50	425x300	1,00	B1,1	1,0000
2	50x70	300x212	0,7	B2,1	1,0000
3	70x100	212x150	0,49	B3,1	0,4207
4	100x140	150x106	0,35	B4,1	0,2413
5	140x200	106x75	0,24	B5,1	0,1368
6	200x270	75x53	0,17	B6,1	0,0747
7	270x400	53x38	0,12	B7,1	0,0444
8	-400	-38	0,08	B8,1	0,0241

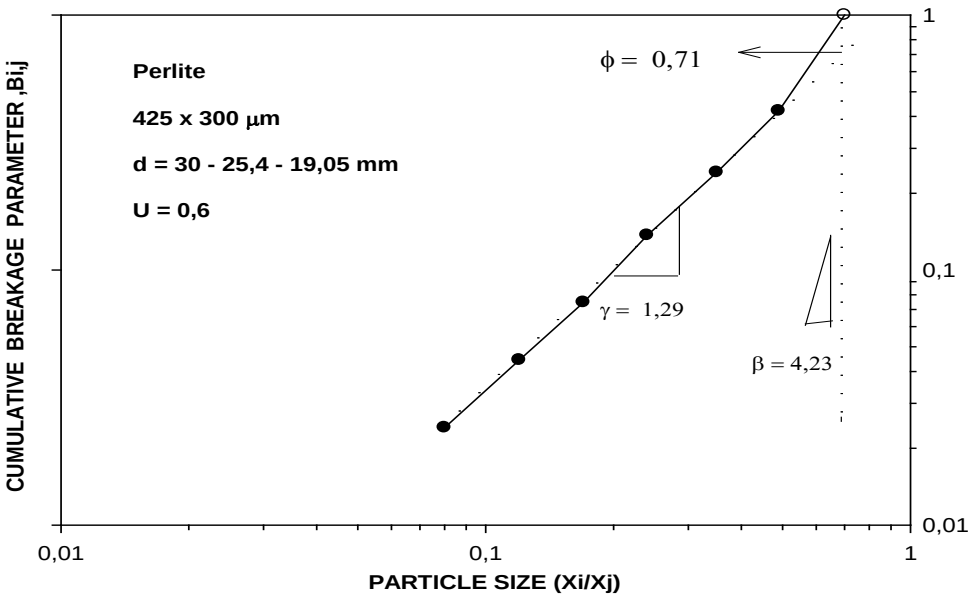

Figure B.63 Primary breakage distribution function of perlite for -425 + 300 µm feed size fraction ground with d = 30 – 25,4 – 19,05 mm ball diameter and U = 0,6.

Table B.42 Cumulative weight percent less than size values of perlite for - 425 + 300 µm size interval ground with d = 30 – 25,4 – 19,05 mm ball diameter and U = 0,6.

SIZE	0 min.	0,133 min	1 min	3 min	6 min
425	100,00	100,00	100,00	100,00	100,00
300	0,21	18,61	40,29	70,56	90,76
212	0,09	8,30	16,16	34,74	56,69
150	0,00	4,80	8,53	19,14	32,55
106	0,00	2,75	4,88	11,34	19,43
75	0,00	1,51	2,93	7,05	12,25
53	0,00	0,90	1,77	4,22	7,52
38	0,00	0,49	1,18	2,70	4,95
%w.r.top size	99,79	81,39	59,71	29,44	9,24

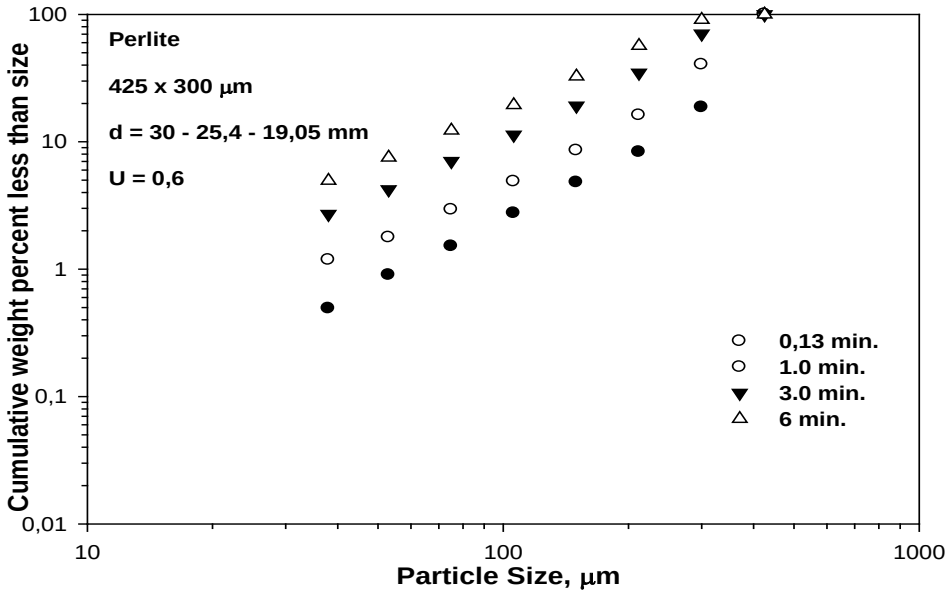

Figure B.64 Particle size distribution of perlite for -425 + 300 µm feed size fraction ground with d = 30 – 25,4 – 19,05 mm ball diameter and U = 0,6.

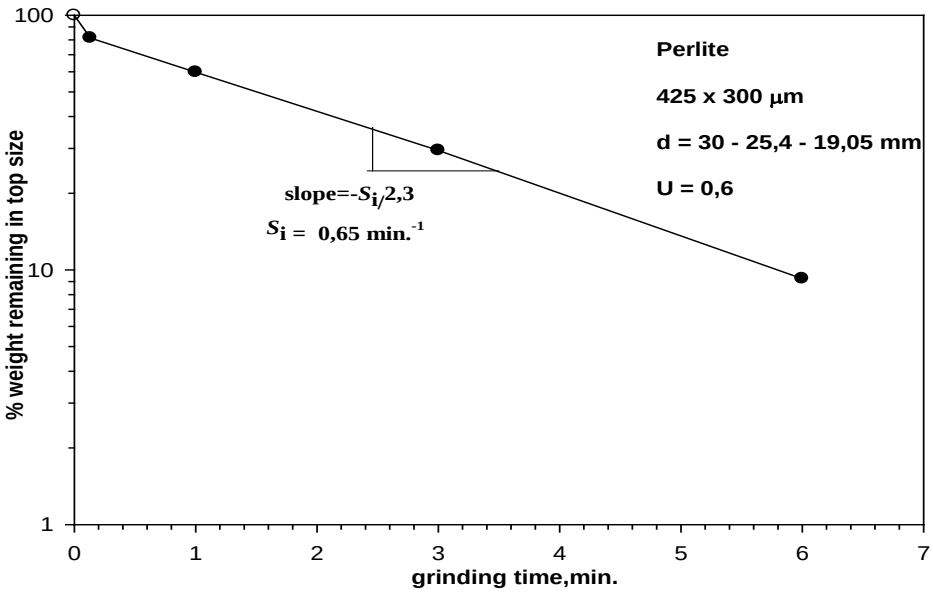

Figure B.65 First-order plot of breakage of - 425 + 300 µm feed of perlite ground with d = 30 – 25,4 – 19,05 mm ball diameter and U = 0,6.

212 x 150 micron

Table B.43 Determined B values of perlite for – 212 + 150 µm size interval ground with d = 30 – 25,4 – 19,05 mm ball diameter and U = 0,6.

INTERVAL NO,İ	SİZE (mesh)	Size (µm)	Xi/Xmax	B i,1	B VALUES
1	70x100	212x150	1,00	B1,1	1,0000
2	100x140	150x106	0,7	B2,1	1,0000
3	140x200	106x75	0,5	B3,1	0,4209
4	200x270	75x53	0,35	B4,1	0,2485
5	270x400	53x38	0,25	B5,1	0,1408
6	-400	-38	0,17	B6,1	0,0753

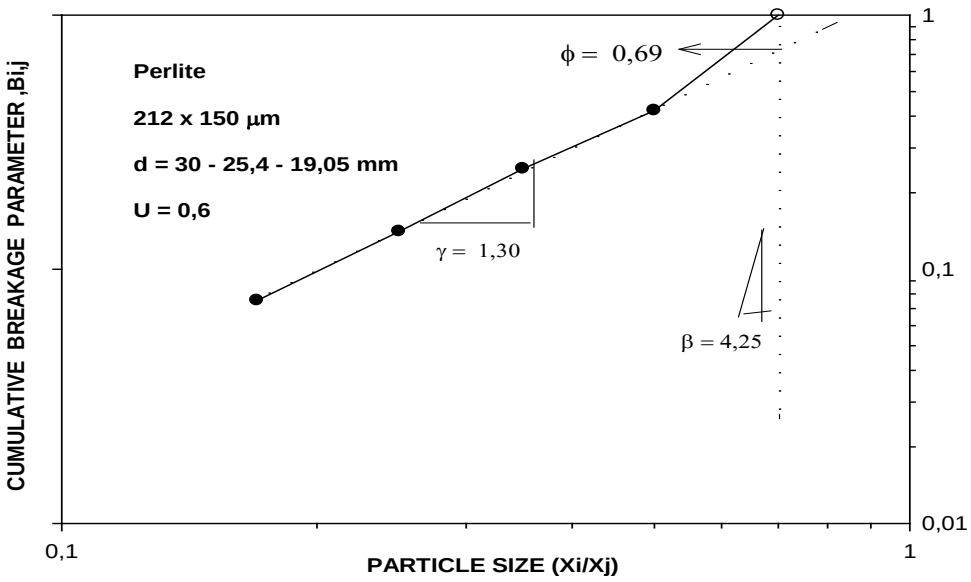

Figure B.66 Primary breakage distribution function of perlite for - 212 + 150 µm feed size fraction ground with d = 30 – 25,4 – 19,05 mm ball diameter and U = 0,6.

Table B.44 Cumulative weight percent less than size values of perlite for - 212 + 150 µm size interval ground with d = 30 – 25,4 – 19,05 mm ball diameter and U = 0,6.

SIZE	0 min.	0,133 min	1 min	3 min	6 min
212	100,00	100,00	100,00	100,00	100,00
150	1,17	11,99	29,97	49,84	69,91
106	0,32	5,07	12,74	30,06	50,74
75	0,06	2,90	7,48	18,22	31,76
53	0,00	1,62	4,43	11,20	20,83
38	0,00	0,87	2,84	6,27	12,09
%w.r.top size	98,83	88,01	70,03	50,16	30,09

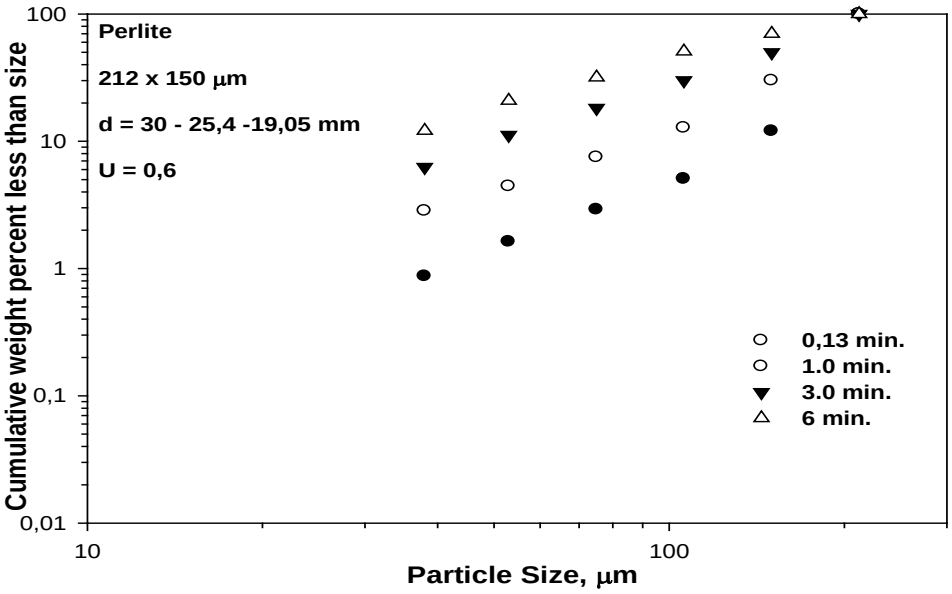

Figure B.67 Particle size distribution of perlite for -212 + 150 µm feed size fraction ground with d = 30 – 25,4 – 19,05 mm ball diameter and U = 0,6.

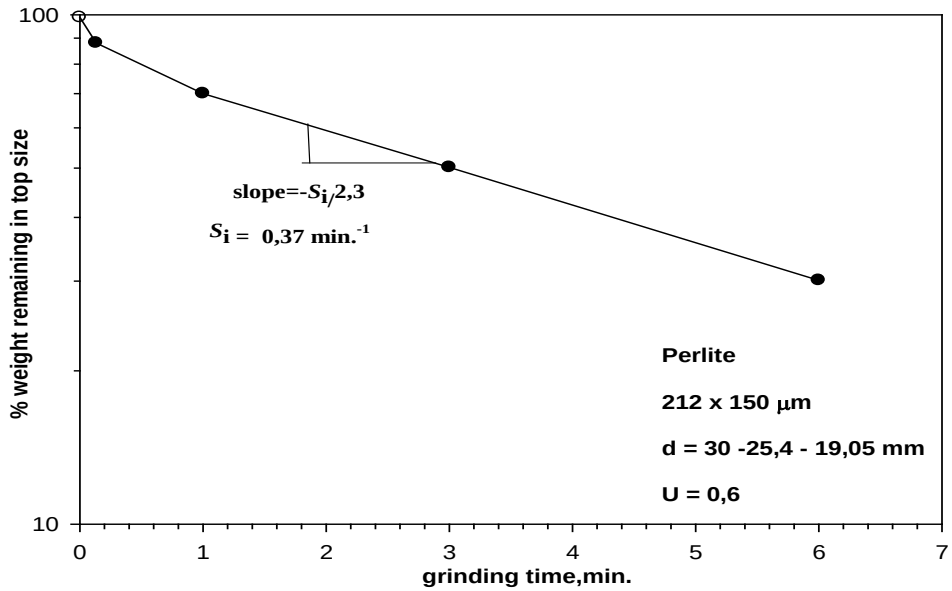

Figure B.68 First-order plot of breakage of - 212 + 150 µm feed of perlite ground with d = 30 – 25,4 – 19,05 mm ball diameter and U = 0,6.

Determination of aT value

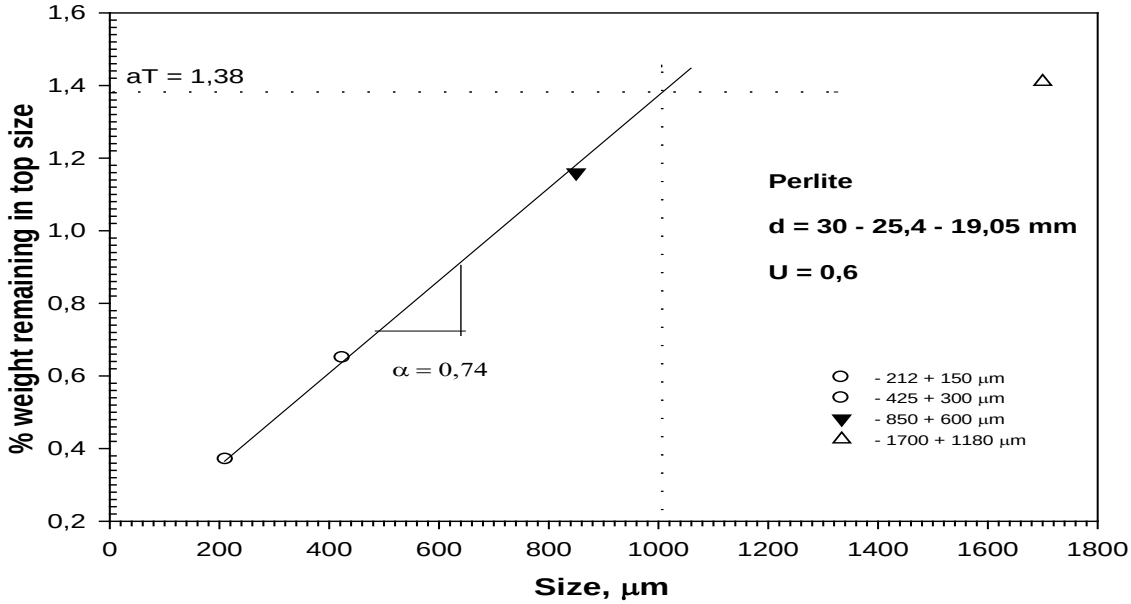

Figure B.69 Variation of first-order specific rates of breakage of perlite ground with d = 30 – 25,4 - 19,05 mm ball diameter and particle size: √2 intervals, plotted at upper size of interval at U=0,6.

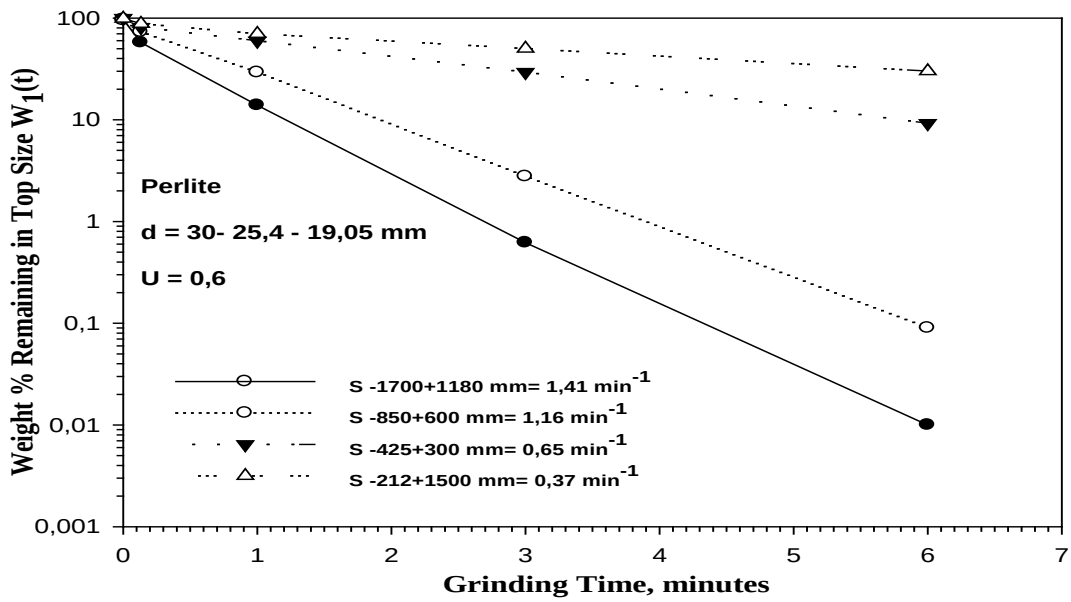

Figure B.70 First-order plots of breakage of -1700+1180, -850+600, -425+300, -212+150 μm feed size of perlite ground with d = 30 – 25,4 – 19,05 mm ball diameter and U=0,6.

Table B.45 Breakage parameters of perlite ground with d = 30 – 25,4 – 19,05 mm ball diameter at U=0,6.

1700x1180		**850x600**		**425x300**		**212x150**			
gama	1,27	**gama**	1,28	**gama**	1,29	**gama**	1,30		
beta	4,18	**beta**	4,21	**beta**	4,23	**beta**	4,25	**aT**	**α**
phi	0,81	**phi**	0,79	**phi**	0,71	**phi**	0,69	1,38	0,74
S value	1,410	**S value**	1,160	**S value**	0,650	**S value**	0,370		

30 -25,4 – 19,05 mm ball size charge at U= 1

1700 x 1180 micron

Table B.46 Determined B values of perlite for - 1700 + 1180 µm size interval ground with d = 30 – 25,4 – 19,05 mm ball diameter and U = 1.

INTERVAL NO,İ	SİZE (mesh)	Size (µm)	Xi/Xmax	B i,1	B VALUES
1	12x16	1700x1180	1,00	B1,1	1
2	16x20	1180x850	0,69	B2,1	1
3	20x30	850x600	0,50	B3,1	0,505041197
4	30x40	600x425	0,35	B4,1	0,336161444
5	40x50	425x300	0,25	B5,1	0,220931711
6	50x70	300x212	0,17	B6,1	0,136583807
7	70x100	212x150	0,12	B7,1	0,097874834
8	100x140	150x106	0,088	B8,1	0,064476189
9	140x200	106x75	0,062	B9,1	0,043037208
10	200x270	75x53	0,044	B10,1	0,027874414
11	270x400	53x38	0,031	B11,1	0,01959966
12	-400	-38	0,022	B12,1	0,012321928

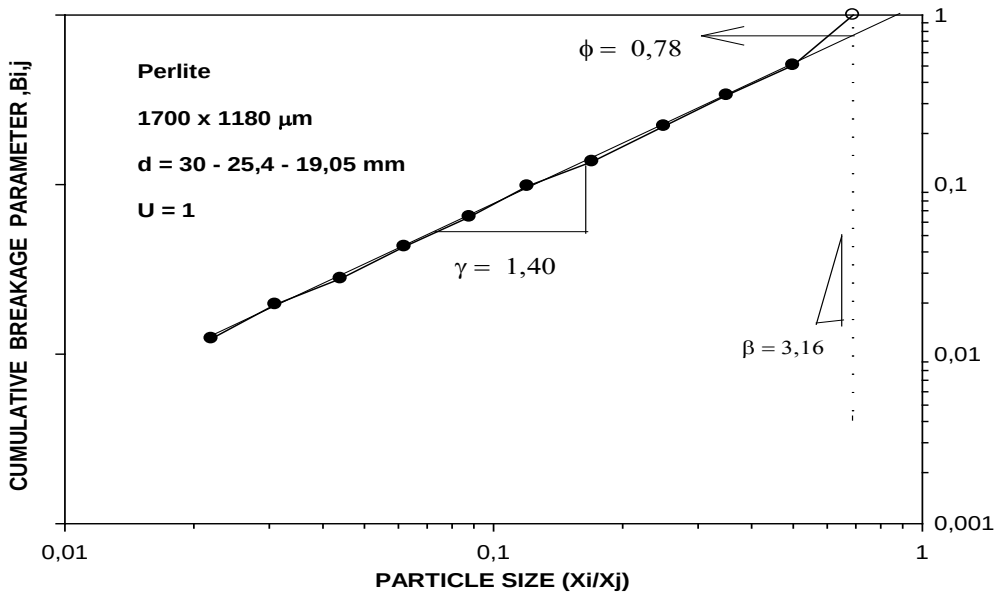

Figure B.71 Primary breakage distribution function of perlite for -1700 + 1180 µm feed size fraction ground with d = 30 – 25,4 – 19,05 mm ball diameter and U = 1.

Table B.47 Cumulative weight percent less than size values of perlite for 1700 x 1180 µm size interval ground with d = 30 – 25,4 – 19,05 mm ball diameter and U = 1.

SIZE	0 min.	0,133 min	1 min	3 min	6 min
1700	100,00	100,00	100,00	100,00	100,00
1180	2,06	35,32	77,86	97,83	99,94
850	0,67	19,45	61,74	97,21	98,63
600	0,00	13,02	43,92	91,30	96,24
425	0,00	8,76	31,68	72,49	91,36
300	0,00	5,51	22,40	51,40	82,18
212	0,00	3,98	15,05	32,90	54,03
150	0,00	2,64	9,19	20,11	32,00
106	0,00	1,77	5,33	11,97	19,90
75	0,00	1,15	3,06	6,99	12,38
53	0,00	0,81	1,70	4,42	7,49
38	0,00	0,51	1,00	2,81	4,82
%w.r.top size	97,94	64,68	22,14	2,17	0,06

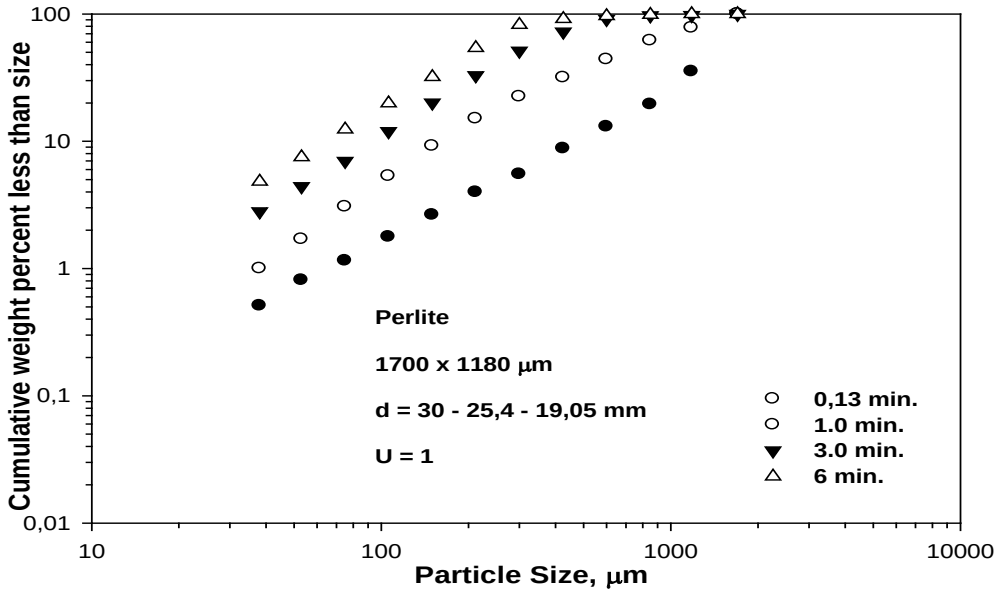

Figure B.72 Particle size distribution of perlite for -1700 + 1180 µm feed size fraction ground with d = 30 – 25,4 – 19,05 mm ball diameter and U = 1.

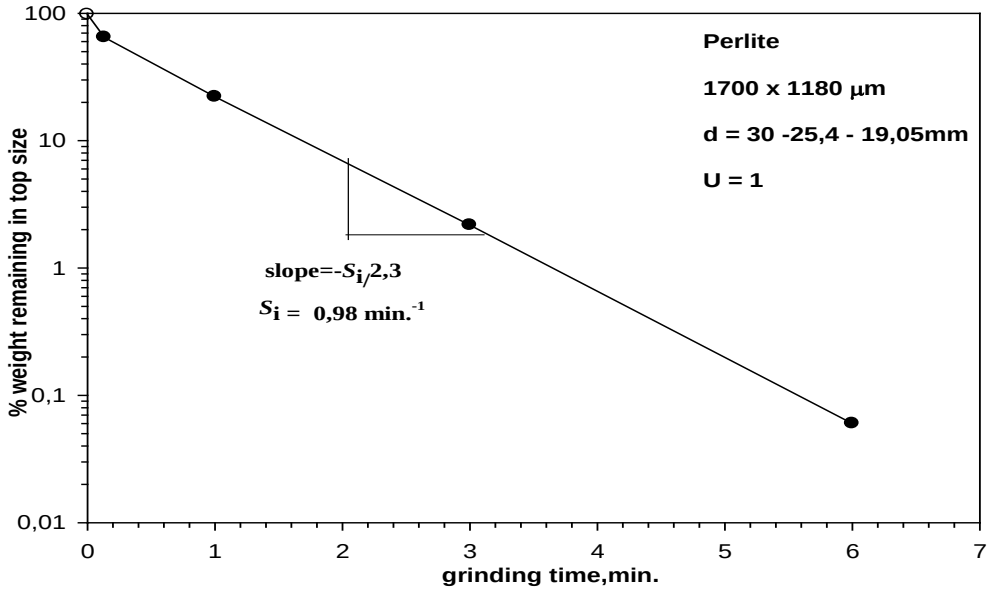

Figure B.73 First-order plot of breakage of - 1700 + 1180 µm feed of perlite ground with d = 30 – 25,4 – 19,05 mm ball diameter and U = 1.

850 x 600 micron

Table B.48 Determined B values of perlite for - 850 + 600 µm size interval ground with d = 30 – 25,4 – 19,05 mm ball diameter and U = 1.

INTERVAL NO,İ	SİZE (mesh)	Size (µm)	Xi/Xmax	B i,1	B VALUES
1	20x30	850x600	1,00	B3,1	1,0000
2	30x40	600x425	0,7	B4,1	1,0000
3	40x50	425x300	0,5	B5,1	0,5052
4	50x70	300x212	0,35	B6,1	0,3329
5	70x100	212x150	0,24	B7,1	0,2206
6	100x140	150x106	0,17	B8,1	0,1354
7	140x200	106x75	0,12	B9,1	0,0931
8	200x270	75x53	0,08	B10,1	0,0609
9	270x400	53x38	0,06	B11,1	0,0400
10	-400	-38	0,04	B12,1	0,0239

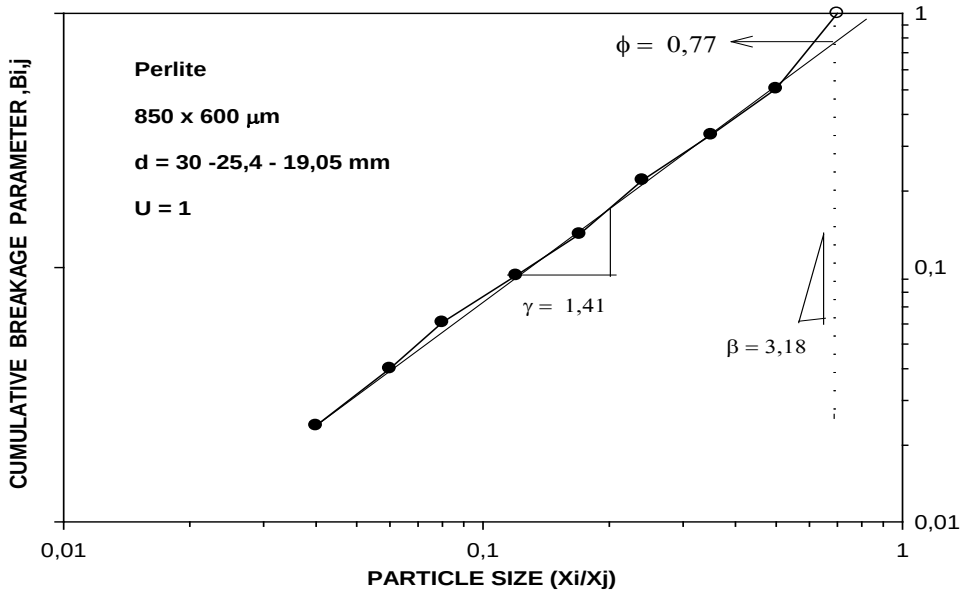

Figure B.74 Primary breakage distribution function of perlite for -850 + 600 µm feed size fraction ground with d = 30 – 25,4 – 19,05 mm ball diameter and U = 1.

Table B.49 Cumulative weight percent less than size values of perlite for - 850 + 600 µm size interval ground with d = 30 – 25,4 – 19,05 mm ball diameter and U = 1.

SIZE	0 min.	0,133 min	1 min	3 min	6 min
850	100,00	100,00	100,00	100,00	100,00
600	3,28	22,24	66,81	95,80	99,76
425	0,26	10,67	36,07	79,21	97,06
300	0,08	7,08	20,91	51,14	81,49
212	0,00	4,70	12,16	30,86	52,21
150	0,00	2,91	6,31	17,35	30,16
106	0,00	2,01	4,00	10,93	18,93
75	0,00	1,32	2,50	6,48	10,89
53	0,00	0,87	1,60	3,90	6,81
38	0,00	0,52	0,90	2,39	4,19
%w.r.top size	96,72	77,76	33,19	4,20	0,24

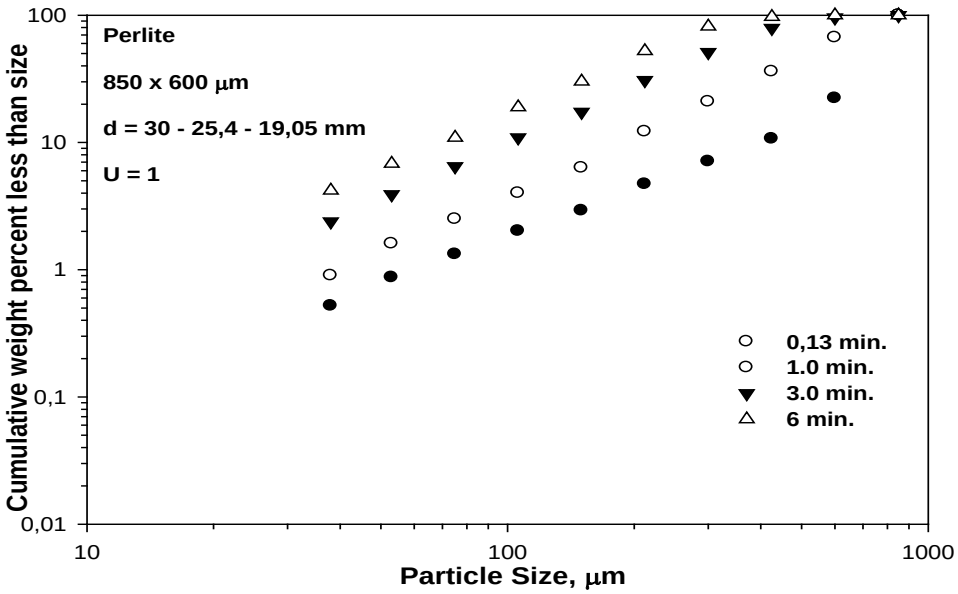

Figure B.75 Particle size distribution of perlite for -850 + 600 µm feed size fraction ground with d = 30 – 25,4 – 19,05 mm ball diameter and U = 1.

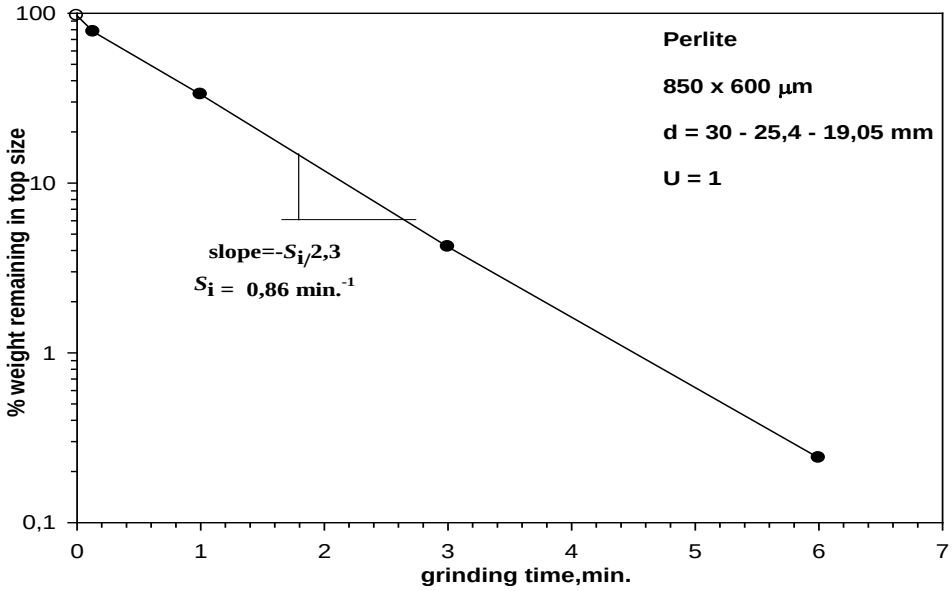

Figure B.76 First-order plot of breakage of - 850 + 600 µm feed of perlite ground with d = 30 – 25,4 – 19,05 mm ball diameter and U = 1.

425 x 300 micron

Table B.50 Determined B values of perlite for – 425 + 300 µm size interval ground with d = 30 – 25,4 – 19,05 mm ball diameter and U = 1.

INTERVAL NO,İ	SİZE (mesh)	Size (µm)	Xi/Xmax	B i,1	B VALUES
1	40x50	425x300	1,00	B1,1	1,0000
2	50x70	300x212	0,7	B2,1	1,0000
3	70x100	212x150	0,49	B3,1	0,5058
4	100x140	150x106	0,35	B4,1	0,3353
5	140x200	106x75	0,24	B5,1	0,2223
6	200x270	75x53	0,17	B6,1	0,1510
7	270x400	53x38	0,12	B7,1	0,1027
8	-400	-38	0,08	B8,1	0,0683

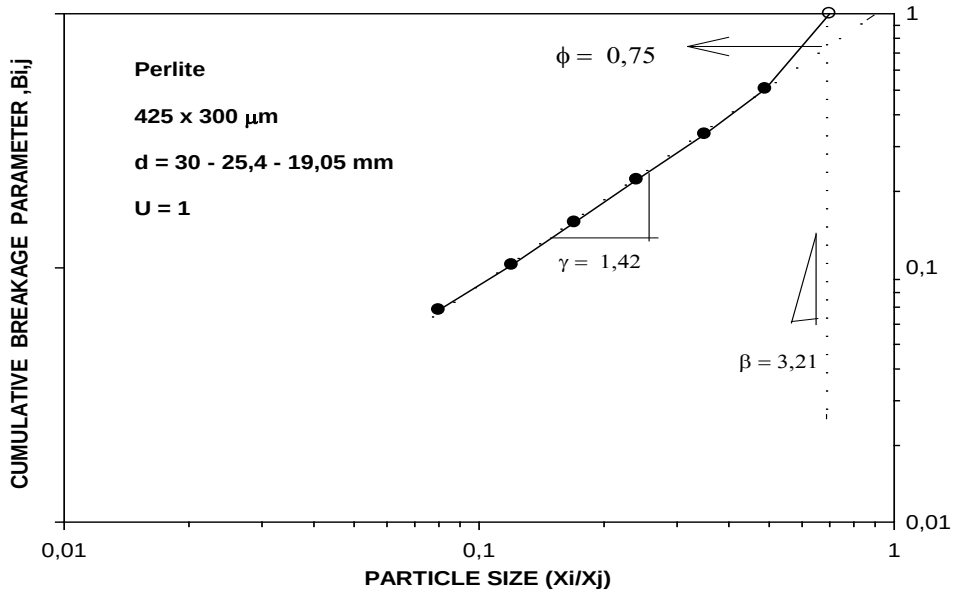

Figure B.77 Primary breakage distribution function of perlite for -425 + 300 µm feed size fraction ground with d = 30 – 25,4 – 19,05 mm ball diameter and U = 1.

Table B.51 Cumulative weight percent less than size values of perlite for - 425 + 300 µm size interval ground with d = 30 – 25,4 – 19,05 mm ball diameter and U = 1.

SIZE	0 min.	0,133 min	1 min	3 min	6 min
425	100,00	100,00	100,00	100,00	100,00
300	0,16	14,59	51,28	87,45	98,19
212	0,03	7,62	12,06	30,41	54,09
150	0,00	5,10	7,12	17,26	30,80
106	0,00	3,41	4,64	10,02	17,36
75	0,00	2,33	3,06	6,31	11,05
53	0,00	1,59	2,00	4,02	7,01
38	0,00	1,06	1,41	2,36	4,21
%w.r.top size	99,84	85,41	48,72	12,55	1,81

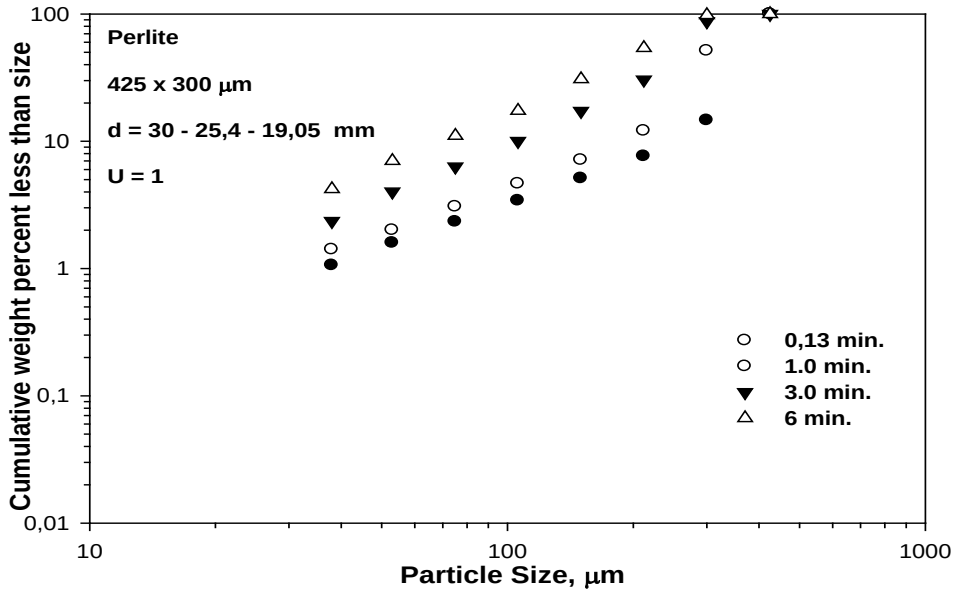

Figure B.78 Particle size distribution of perlite for -425 + 300 µm feed size fraction ground with d = 30 – 25,4 – 19,05 mm ball diameter and U = 1.

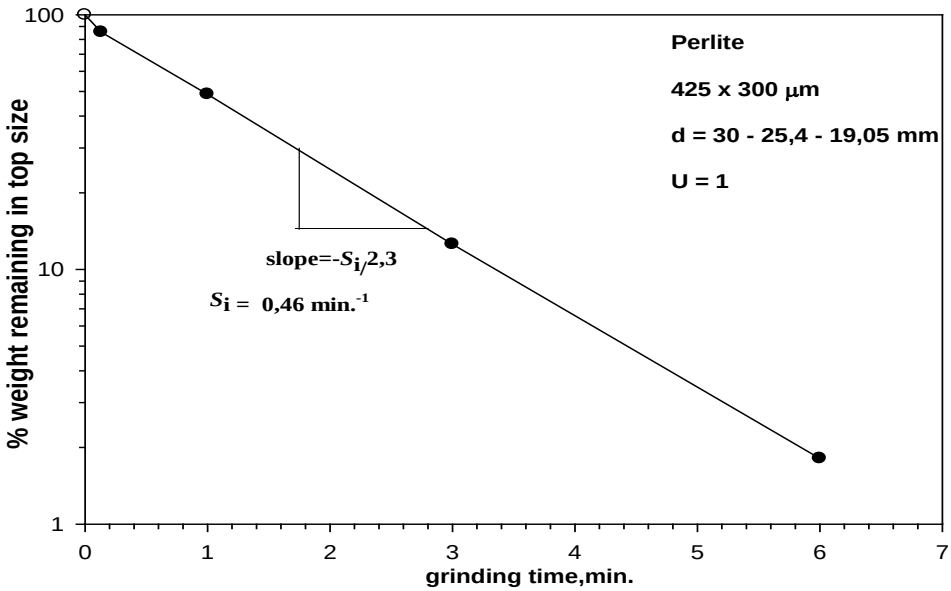

Figure B.79 First-order plot of breakage of - 425 + 300 µm feed of perlite ground with d = 30 – 25,4 – 19,05 mm ball diameter and U = 1.

212 x 150 micron

Table B.52 Determined B values of perlite for – 212 + 150 µm size interval ground with d = 30 – 25,4 – 19,05 mm ball diameter and U = 1.

INTERVAL NO,İ	SİZE (mesh)	Size (µm)	Xi/Xmax	B i,1	B VALUES
1	70x100	212x150	1,00	B1,1	1,0000
2	100x140	150x106	0,7	B2,1	1,0000
3	140x200	106x75	0,5	B3,1	0,5020
4	200x270	75x53	0,35	B4,1	0,3331
5	270x400	53x38	0,25	B5,1	0,2238
6	-400	-38	0,17	B6,1	0,1368

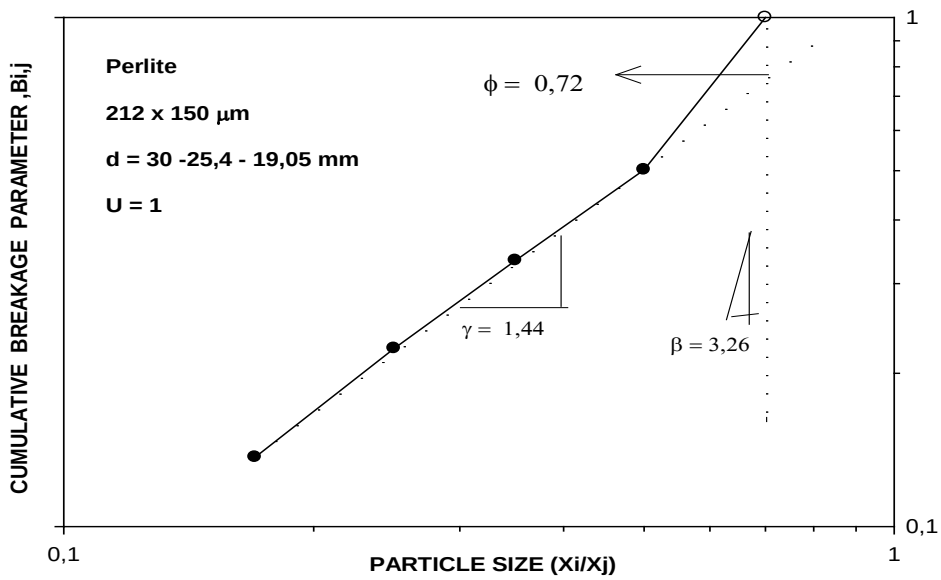

Figure B.80 Primary breakage distribution function of perlite for - 212 + 150 µm feed size fraction ground with d = 30 – 25,4 – 19,05 mm ball diameter and U = 1.

Table B.53 Cumulative weight percent less than size values of perlite for - 212 + 150 µm size interval ground with d = 30 – 25,4 – 19,05 mm ball diameter and U = 1.

SIZE	0 min.	0,133 min	1 min	3 min	6 min
212	100,00	100,00	100,00	100,00	100,00
150	0,90	9,00	35,02	71,56	91,50
106	0,01	4,20	10,68	25,13	51,16
75	0,00	2,80	7,06	15,95	28,37
53	0,00	1,89	4,00	10,42	17,23
38	0,00	1,16	2,26	6,09	11,14
%w.r.top size	99,10	91,00	64,98	28,44	8,50

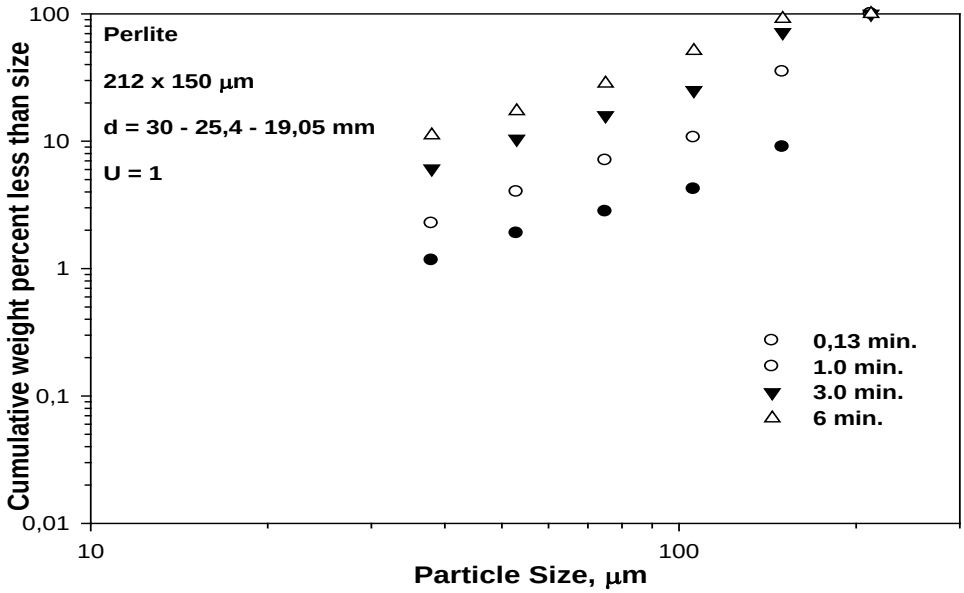

Figure B.81 Particle size distribution of perlite for -212 + 150 µm feed size fraction ground with d = 30 – 25,4 – 19,05 mm ball diameter and U = 1.

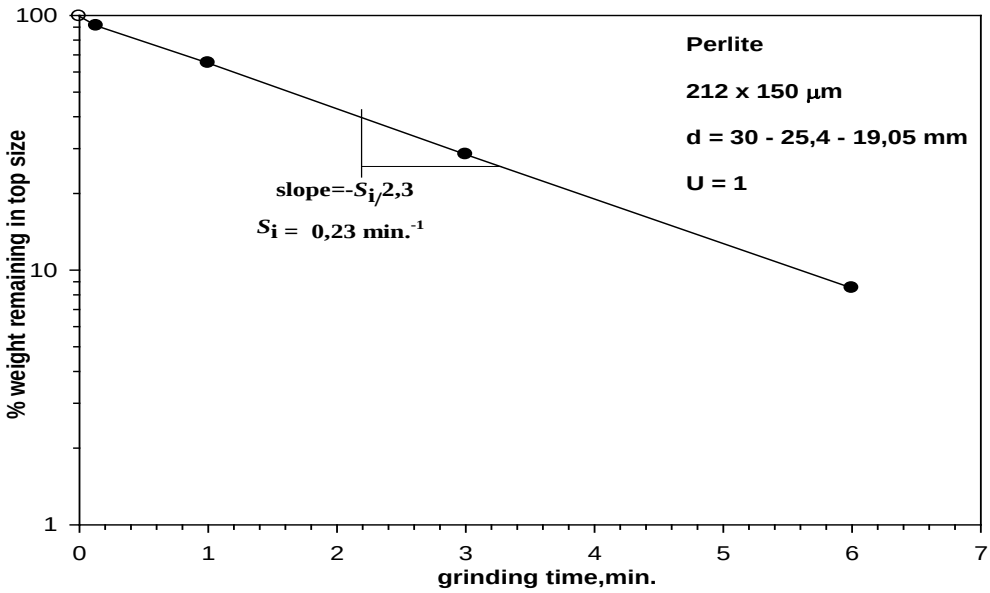

Figure B.82 First-order plot of breakage of - 212 + 150 μm feed of perlite ground with d = 30 – 25,4 – 19,05 mm ball diameter and U = 1.

Determination of aT value

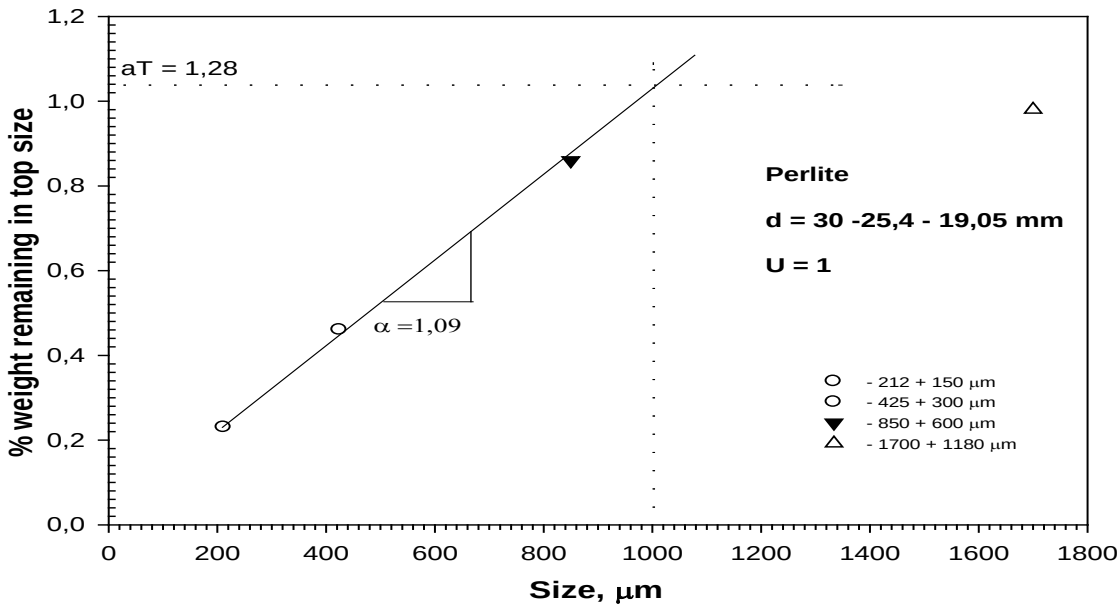

Figure B.83 Variation of first-order specific rates of breakage of perlite ground with d = 30 – 25,4 – 19,05 mm ball diameter and particle size: √2 intervals, plotted at upper size of interval at U=1.

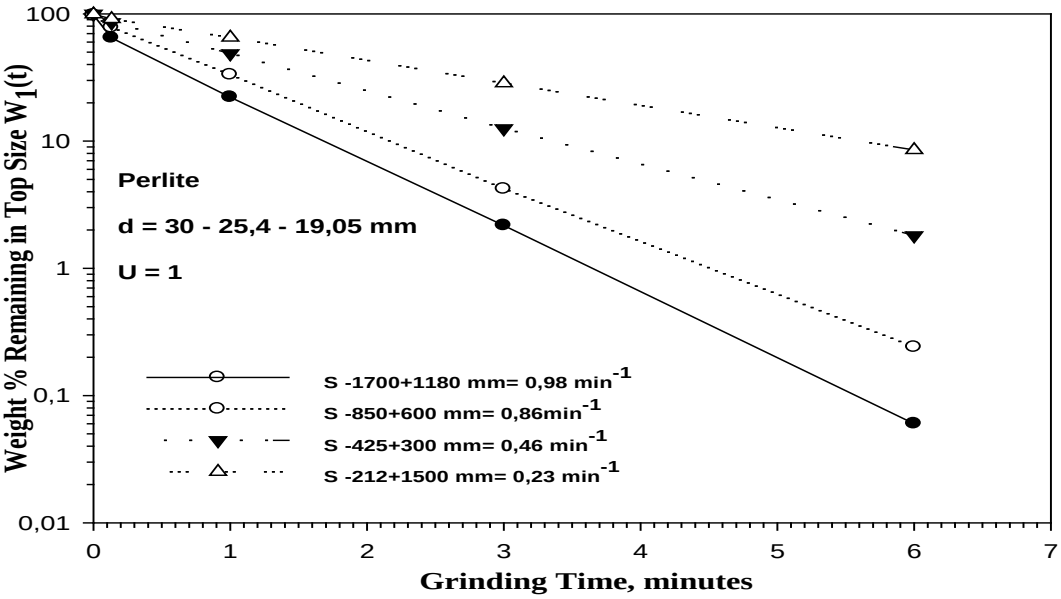

Figure B.84 First-order plots of breakage of -1700+1180, -850+600, -425+300, -212+150 µm feed size of perlite ground with d = 30 – 25,4 – 19,05 mm ball diameter and U=1.

Table B.54 Breakage parameters of perlite ground with d = 30 – 25,4 – 19,05 mm ball diameter at U=1.

1700x1180		**850x600**		**425x300**		**212x150**			
gama	1,40	**gama**	1,41	**gama**	1,42	**gama**	1,44		
beta	3,16	**beta**	3,18	**beta**	3,21	**beta**	3,26	**aT**	**α**
phi	0,78	**phi**	0,77	**phi**	0,75	**phi**	0,72	1,28	1,09
S value	0,980	**S value**	0,860	**S value**	0,460	**S value**	0,230		

APPENDIX C
TABLES AND FIGURES FOR DETERMINATION BREAKAGE PARAMETERS OF PUMICE

38 mm ball size charge at U=0,6

1700 x 1180 micron

Table C.1 Determined B values of pumice for - 1700 + 1180 µm size interval ground with d = 38 mm ball diameter and U = 0,6.

INTERVAL NO,İ	SİZE (mesh)	Size (µm)	Xi/Xmax	B i,1	B VALUES
1	12x16	1700x1180	1,00	B1,1	1,0000
2	16x20	1180x850	0,69	B2,1	1,0000
3	20x30	850x600	0,50	B3,1	0,5033
4	30x40	600x425	0,35	B4,1	0,3154
5	40x50	425x300	0,25	B5,1	0,2029
6	50x70	300x212	0,17	B6,1	0,1200
7	70x100	212x150	0,12	B7,1	0,0802
8	100x140	150x106	0,088	B8,1	0,0519
9	140x200	106x75	0,062	B9,1	0,0334
10	200x270	75x53	0,044	B10,1	0,0214
11	270x400	53x38	0,031	B11,1	0,0139
12	-400	-38	0,022	B12,1	0,0088

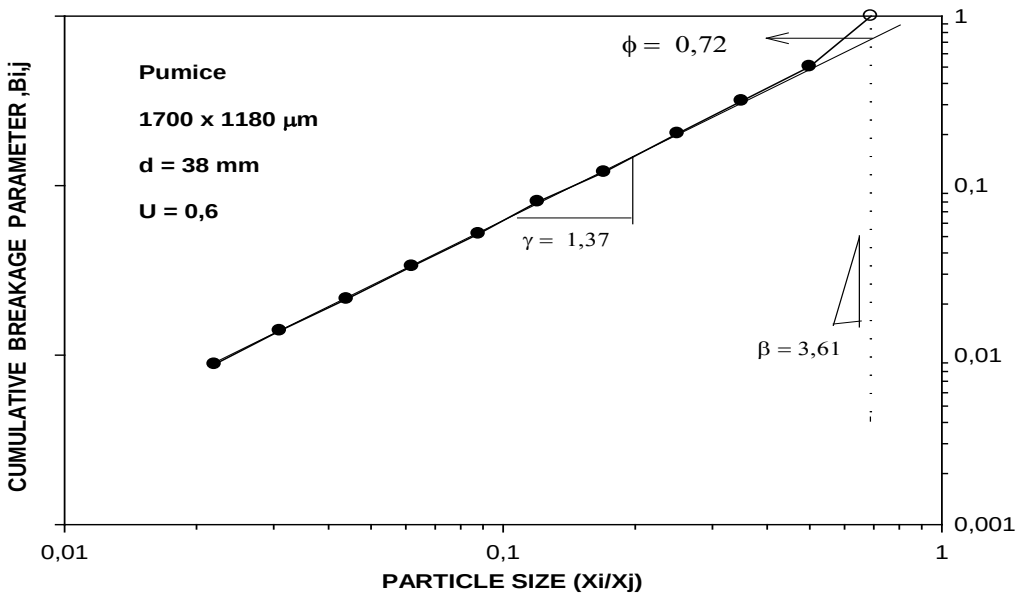

Figure C.1 Primary breakage distribution function of pumice for -1700 + 1180 µm feed size fraction ground with d = 38 mm ball diameter and U = 0,6.

Table C.2 Cumulative weight percent less than size values of pumice for 1700 x 1180 µm size interval ground with d = 38 mm ball diameter and U = 0,6.

SIZE	0 min.	0,133 min	1 min	3 min	6 min
1700	100,00	100,00	100,00	100,00	100,00
1180	1,21	26,45	82,26	99,56	100,00
850	0,30	14,06	71,03	99,24	99,74
600	0,06	8,94	49,16	98,02	99,08
425	0,01	5,82	33,78	89,18	98,92
300	0,00	3,48	23,41	68,73	98,51
212	0,00	2,34	16,79	46,12	90,42
150	0,00	1,52	10,42	26,03	63,14
106	0,00	0,98	6,09	15,41	40,81
75	0,00	0,63	3,74	8,27	26,18
53	0,00	0,41	1,98	4,64	16,02
38	0,00	0,26	1,03	2,19	10,28
%w.r.top size	98,79	73,55	17,74	0,44	0,00

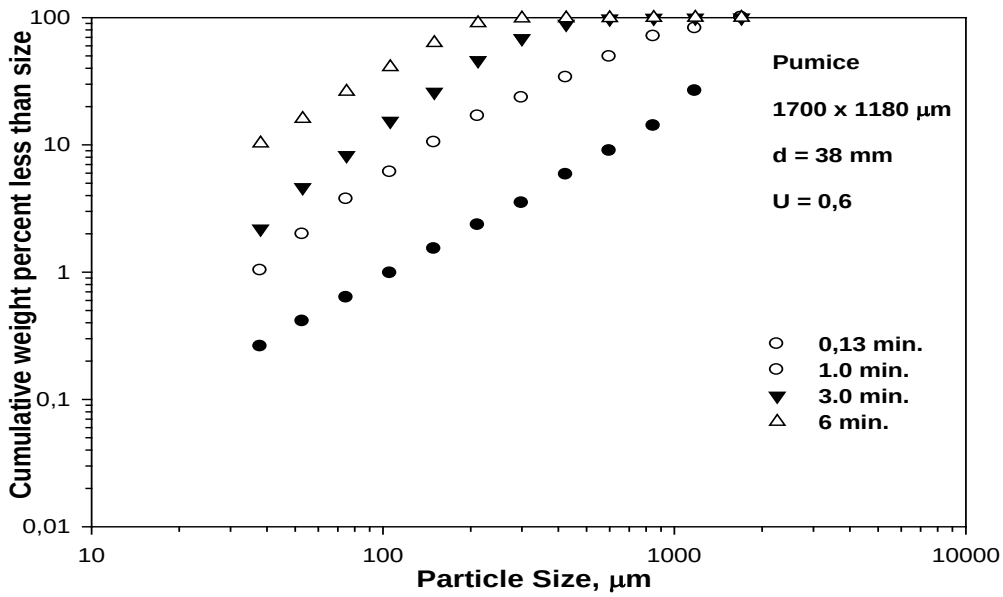

Figure C.2 Particle size distribution of pumice for -1700 + 1180 µm feed size fraction ground with d = 38 mm ball diameter and U = 0,6.

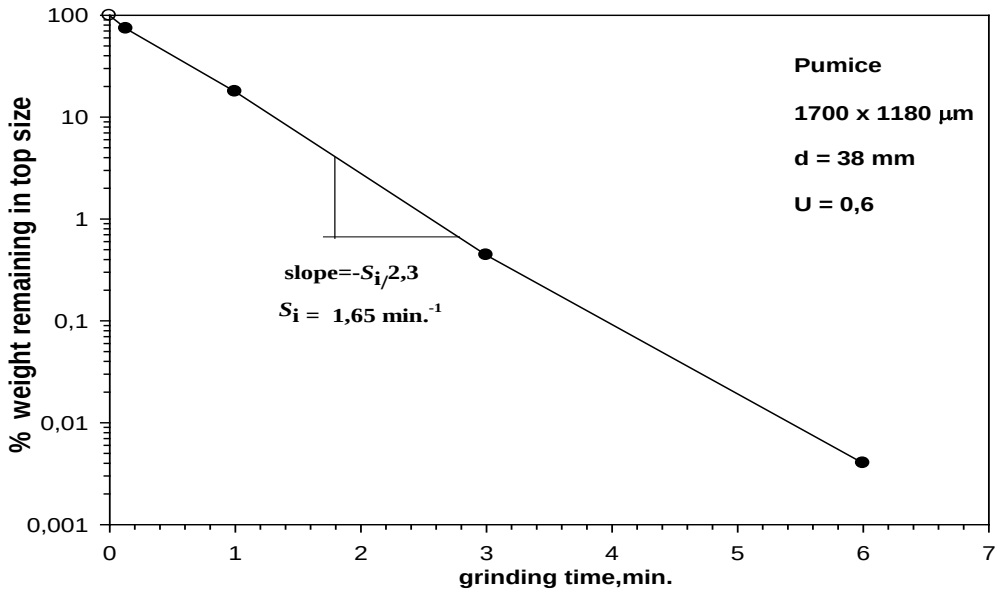

Figure C.3 First-order plot of breakage of - 1700 + 1180 µm feed of pumice ground with d = 38 mm ball diameter and U = 0,6.

850 x 600 micron

Table C.3 Determined B values of pumice for - 850 + 600 µm size interval ground with d = 38 mm ball diameter and U = 0,6.

INTERVAL NO,İ	SİZE (mesh)	Size (µm)	Xi/Xmax	B i,1	B VALUES
1	20x30	850x600	1,00	B3,1	1,0000
2	30x40	600x425	0,7	B4,1	1,0000
3	40x50	425x300	0,5	B5,1	0,5043
4	50x70	300x212	0,35	B6,1	0,3118
5	70x100	212x150	0,24	B7,1	0,2026
6	100x140	150x106	0,17	B8,1	0,1228
7	140x200	106x75	0,12	B9,1	0,0805
8	200x270	75x53	0,08	B10,1	0,0502
9	270x400	53x38	0,06	B11,1	0,0334
10	-400	-38	0,04	B12,1	0,0197

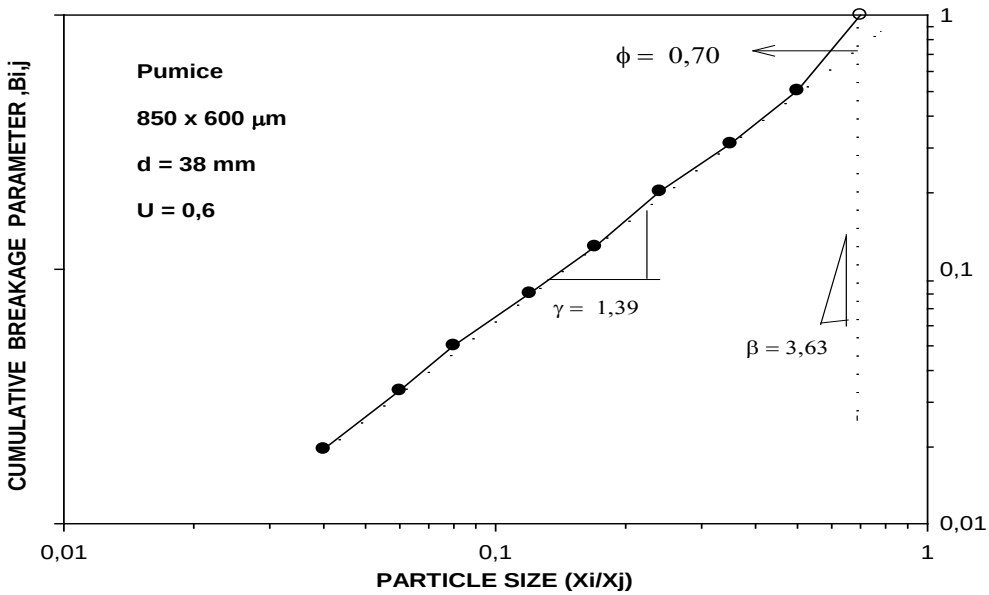

Figure C.4 Primary breakage distribution function of pumice for -850 + 600 µm feed size fraction ground with d = 38 mm ball diameter and U = 0,6.

Table C.4 Cumulative weight percent less than size values of pumice for - 850 + 600 µm size interval ground with d = 38 mm ball diameter and U = 0,6.

SIZE	0 min.	0,133 min	1 min	3 min	6 min
850	100,00	100,00	100,00	100,00	100,00
600	3,25	23,48	73,42	98,04	99,95
425	1,68	12,65	43,16	96,08	98,93
300	0,19	7,23	27,24	80,11	97,99
212	0,04	4,68	17,02	53,46	91,06
150	0,00	2,84	10,41	31,54	61,19
106	0,00	1,87	5,94	20,57	37,54
75	0,00	1,17	3,86	13,59	22,96
53	0,00	0,78	2,16	9,06	14,22
38	0,00	0,46	1,28	5,05	8,03
%w.r.top size	96,75	76,52	26,58	1,96	0,05

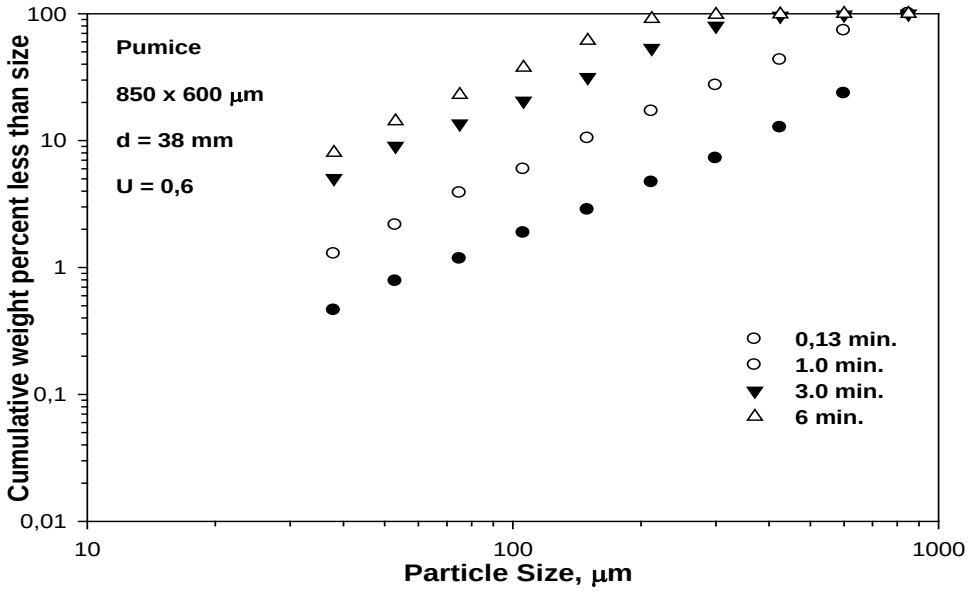

Figure C.5 Particle size distribution of pumice for -850 + 600 µm feed size fraction ground with d = 38 mm ball diameter and U = 0,6.

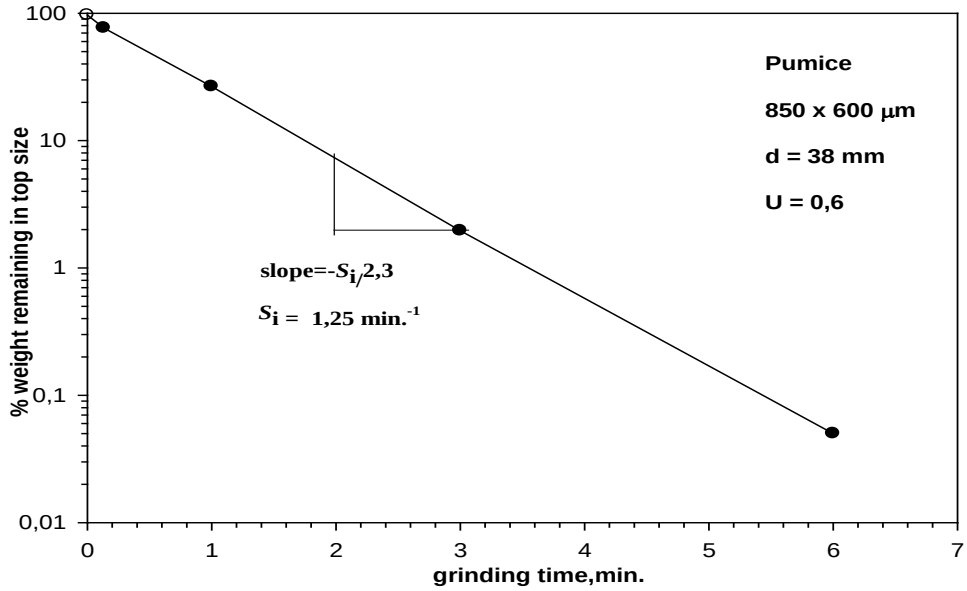

Figure C.6 First-order plot of breakage of - 850 + 600 µm feed of pumice ground with d = 38 mm ball diameter and U = 0,6.

425 x 300 micron

Table C.5 Determined B values of pumice for – 425 + 300 µm size interval ground with d = 38 mm ball diameter and U = 0,6.

INTERVAL NO,İ	SİZE (mesh)	Size (µm)	Xi/Xmax	B i,1	B VALUES
1	40x50	425x300	1,00	B1,1	1,0000
2	50x70	300x212	0,7	B2,1	1,0000
3	70x100	212x150	0,49	B3,1	0,5027
4	100x140	150x106	0,35	B4,1	0,3109
5	140x200	106x75	0,24	B5,1	0,2010
6	200x270	75x53	0,17	B6,1	0,1247
7	270x400	53x38	0,12	B7,1	0,0806
8	-400	-38	0,08	B8,1	0,0489

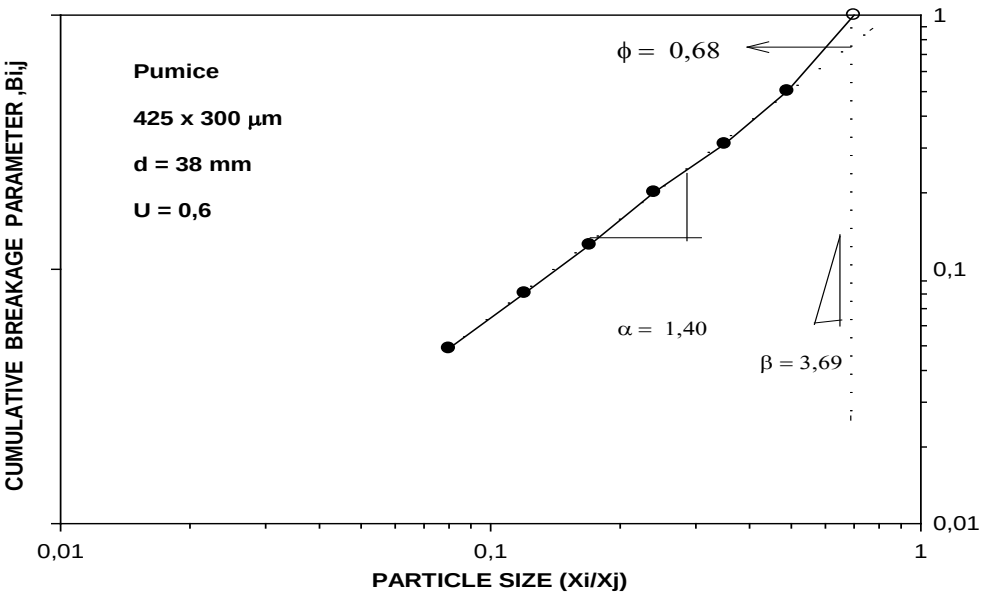

Figure C.7 Primary breakage distribution function of pumice for -425 + 300 µm feed size fraction ground with d = 38 mm ball diameter and U = 0,6.

Table C.6 Cumulative weight percent less than size values of pumice for - 425 + 300 µm size interval ground with d = 38 mm ball diameter and U = 0,6.

SIZE	0 min.	0,133 min	1 min	3 min	6 min
425	100,00	100,00	100,00	100,00	100,00
300	0,31	20,02	50,11	81,94	95,39
212	0,03	10,51	26,04	62,19	92,16
150	0,00	6,62	12,03	31,15	61,39
106	0,00	4,33	6,23	16,44	35,72
75	0,00	2,71	3,79	8,53	19,62
53	0,00	1,76	2,46	5,01	9,94
38	0,00	1,07	1,58	2,86	5,23
%w.r.top size	99,69	79,98	49,89	18,06	4,61

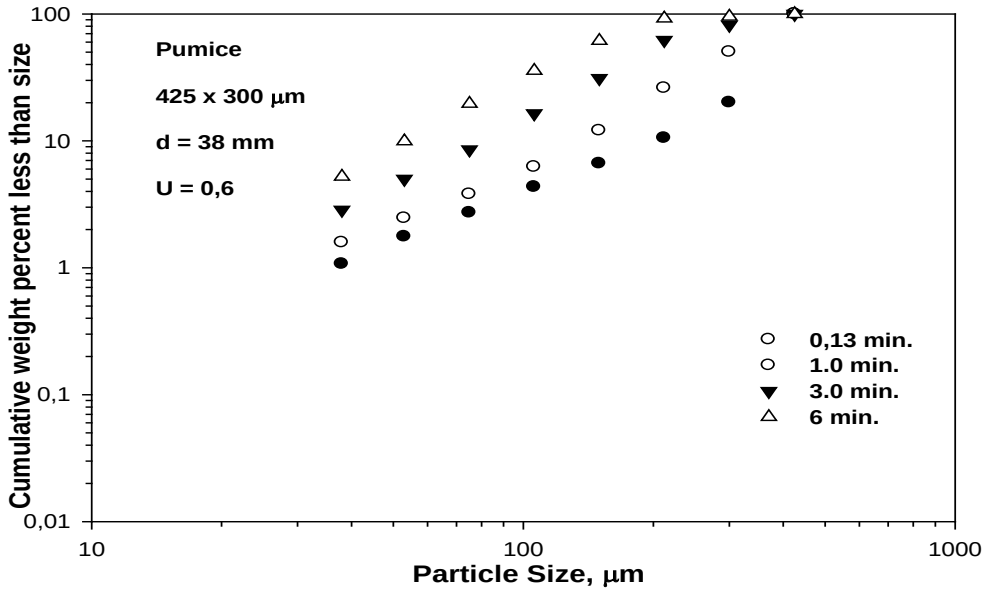

Figure C.8 Particle size distribution of pumice for -425 + 300 µm feed size fraction ground with d = 38 mm ball diameter and U = 0,6.

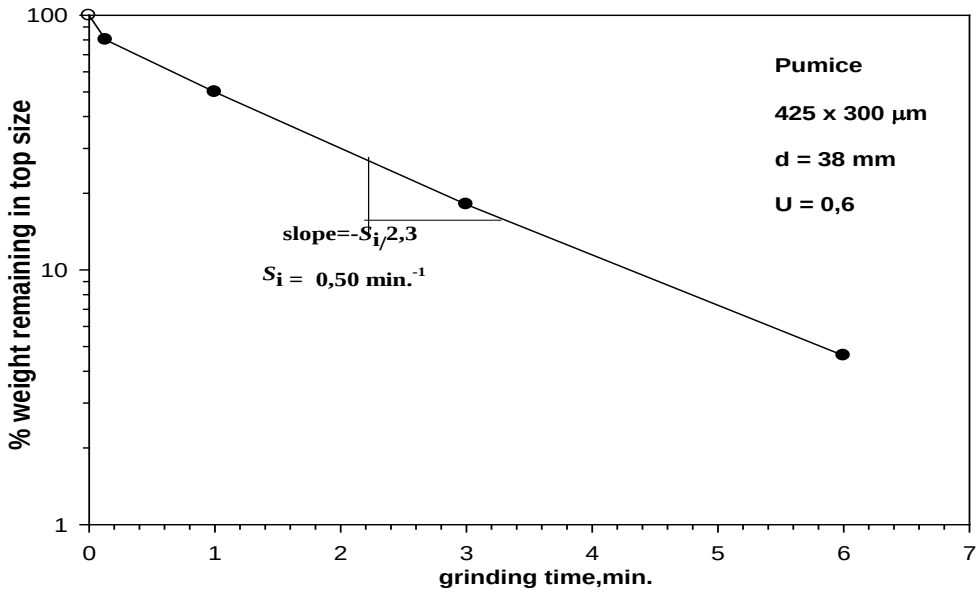

Figure C.9 First-order plot of breakage of - 425 + 300 µm feed of pumice ground with d = 38 mm ball diameter and U = 0,6.

212 x 150 micron

Table C.7 Determined B values of pumice for – 212 + 150 µm size interval ground with d = 38 mm ball diameter and U = 0,6.

INTERVAL NO,İ	SİZE (mesh)	Size (µm)	Xi/Xmax	B i,1	B VALUES
1	70x100	212x150	1,00	B1,1	1,0000
2	100x140	150x106	0,7	B2,1	1,0000
3	140x200	106x75	0,5	B3,1	0,4363
4	200x270	75x53	0,35	B4,1	0,2657
5	270x400	53x38	0,25	B5,1	0,1688
6	-400	-38	0,17	B6,1	0,1006

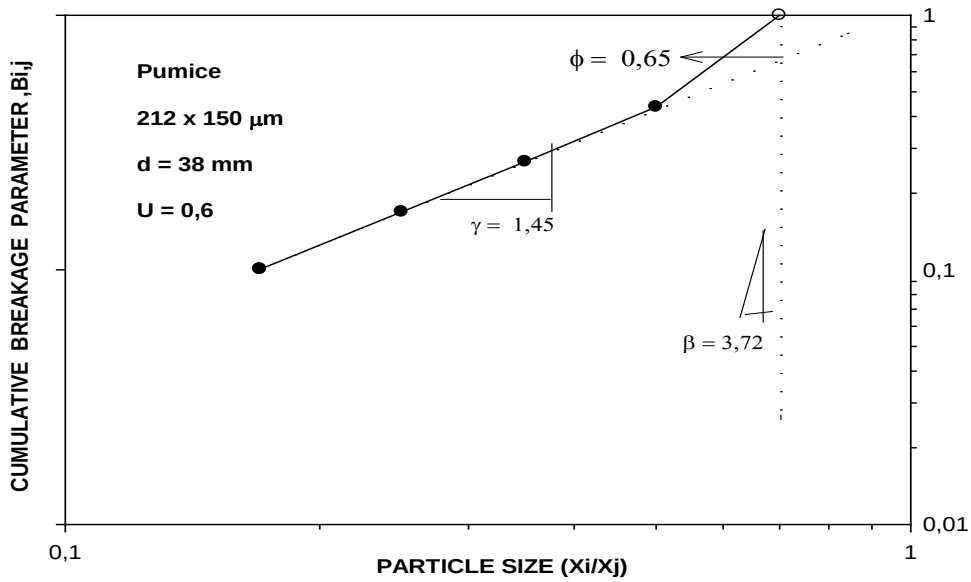

Figure C.10 Primary breakage distribution function of pumice for - 212 + 150 µm feed size fraction ground with d = 38 mm ball diameter and U = 0,6.

Table C.8 Cumulative weight percent less than size values of pumice for - 212 + 150 µm size interval ground with d = 38 mm ball diameter and U = 0,6.

SIZE	0 min.	0,133 min	1 min	3 min	6 min
212	100,00	100,00	100,00	100,00	100,00
150	4,19	13,91	29,96	50,03	68,99
106	0,23	5,43	11,04	21,42	32,59
75	0,07	3,38	4,96	10,34	16,26
53	0,00	2,13	3,02	5,16	8,37
38	0,00	1,26	2,16	2,98	4,52
%w.r.top size	95,81	86,09	70,04	49,97	31,01

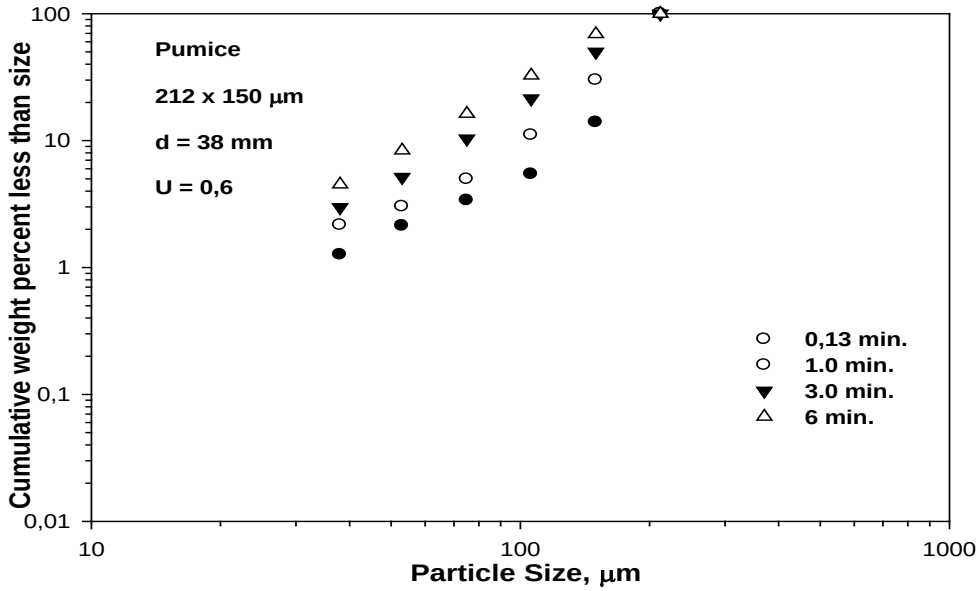

Figure C.11 Particle size distribution of pumice for -212 + 150 µm feed size fraction ground with d = 38 mm ball diameter and U = 0,6.

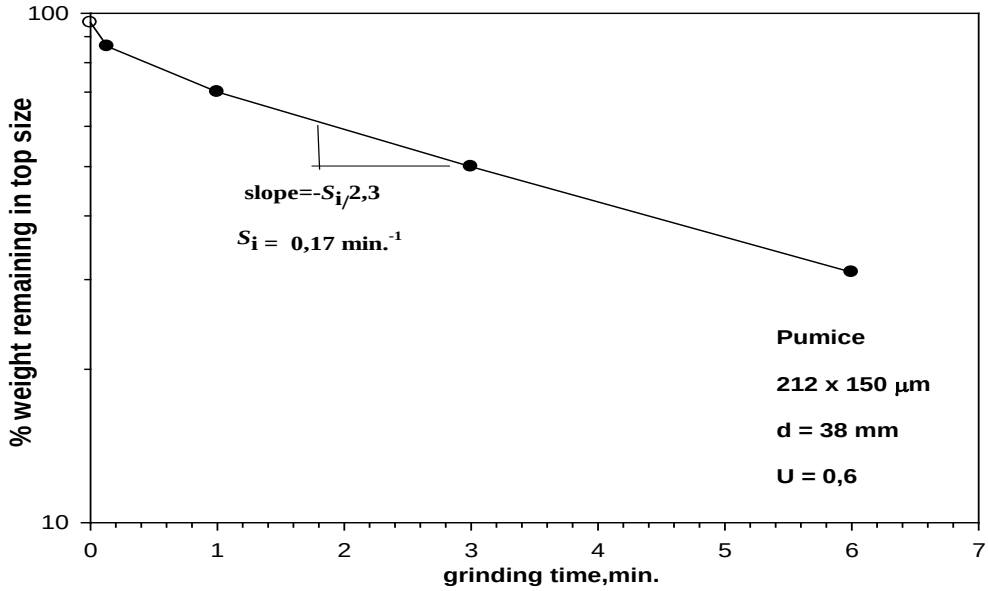

Figure C.12 First-order plot of breakage of - 212 + 150 µm feed of pumice ground with d = 38 mm ball diameter and U = 0,6.

Determination of aT value

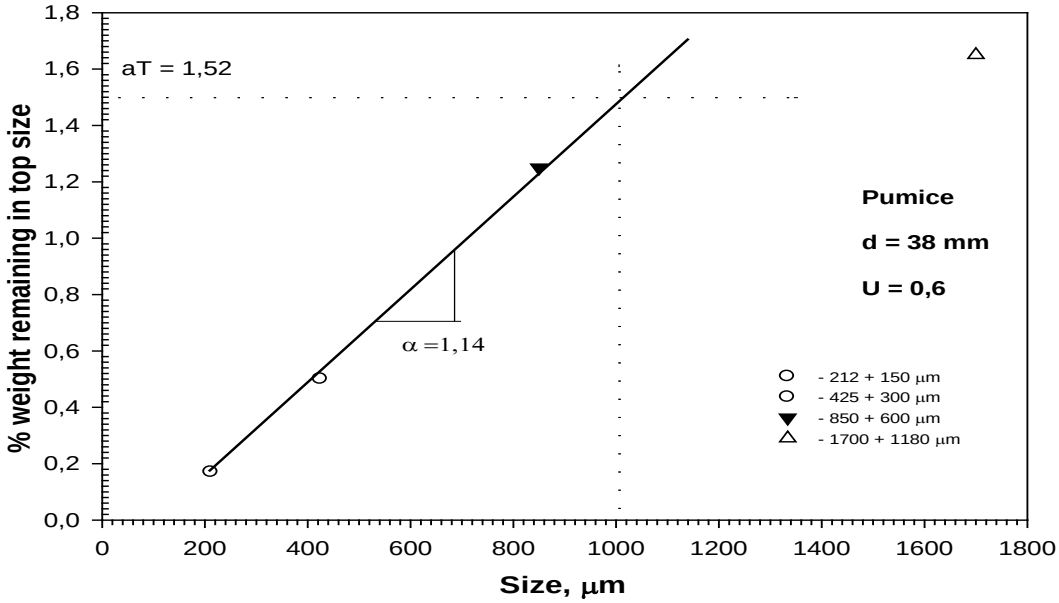

Figure C.13 Variation of first-order specific rates of breakage of pumice ground with d = 38 mm ball diameter and particle size: √2 intervals, plotted at upper size of interval at U=0,6.

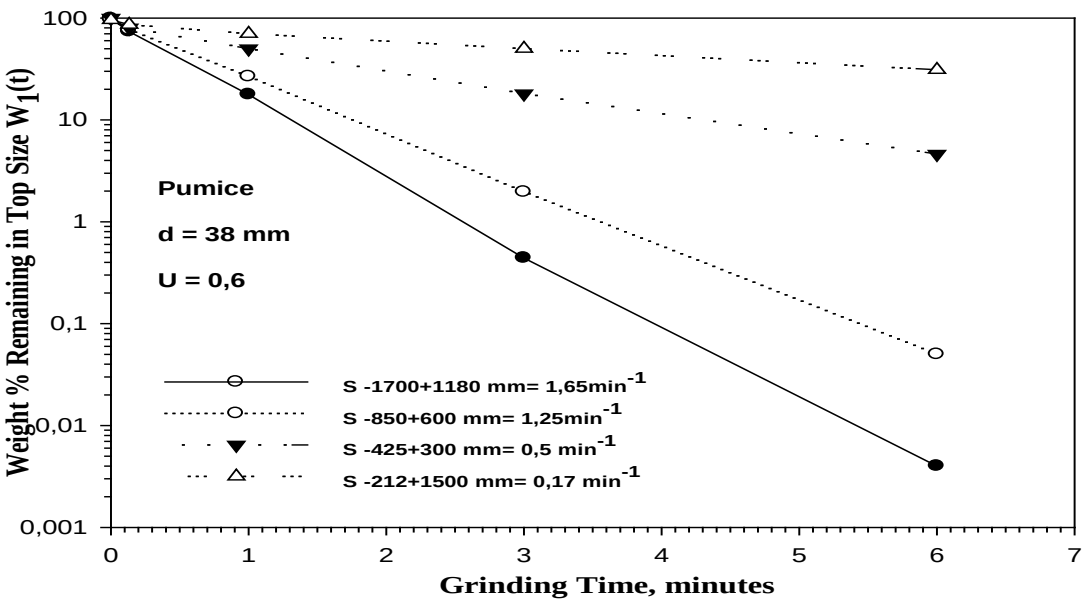

Figure C.14 First-order plots of breakage of -1700+1180, -850+600, -425+300, -212+150 μm feed size of pumice ground with d = 38 mm ball diameter and U=0,6.

Table C.9 Breakage parameters of pumice ground with d = 38 mm ball diameter at U=0,6.

1700x1180		**850x600**		**425x300**		**212x150**			
gama	1,14	**gama**	1,16	**gama**	1,18	**gama**	1,19		
beta	4,06	**beta**	4,08	**beta**	4,09	**beta**	4,11	**aT**	**α**
phi	0,81	**phi**	0,56	**phi**	0,53	**phi**	0,52	0,89	0,96
S value	0,810	**S value**	0,650	**S value**	0,27	**S value**	0,100		

38 mm ball size charge at U= 1

1700 x 1180 micron

Table C.10 Determined B values of pumice for - 1700 + 1180 µm size interval ground with d = 38 mm ball diameter and U = 1.

INTERVAL NO,İ	SİZE (mesh)	Size (µm)	Xi/Xmax	B i,1	B VALUES
1	12x16	1700x1180	1,00	B1,1	1,0000
2	16x20	1180x850	0,69	B2,1	1,0000
3	20x30	850x600	0,50	B3,1	0,2086
4	30x40	600x425	0,35	B4,1	0,1396
5	40x50	425x300	0,25	B5,1	0,0951
6	50x70	300x212	0,17	B6,1	0,0651
7	70x100	212x150	0,12	B7,1	0,0425
8	100x140	150x106	0,088	B8,1	0,0300
9	140x200	106x75	0,062	B9,1	0,0196
10	200x270	75x53	0,044	B10,1	0,0138
11	270x400	53x38	0,031	B11,1	0,0096
12	-400	-38	0,022	B12,1	0,0065

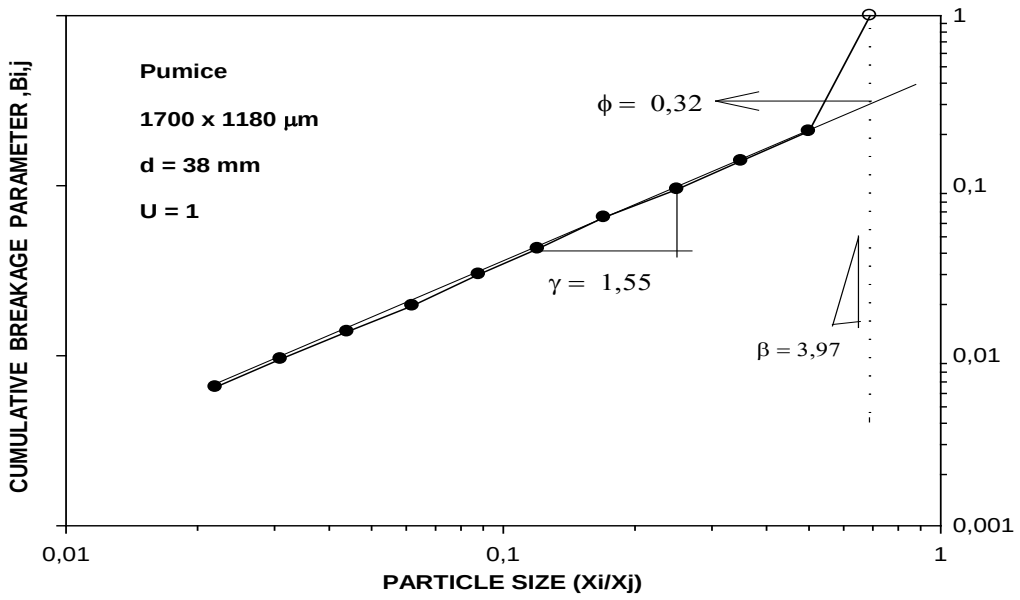

Figure C.15 Primary breakage distribution function of pumice for -1700 + 1180 µm feed size fraction ground with d = 38 mm ball diameter and U = 0,6.

Table C.11 Cumulative weight percent less than size values of pumice for 1700 x 1180 µm size interval ground with d = 38 mm ball diameter and U = 1.

SIZE	0 min.	0,133 min	1 min	3 min	6 min
1700	100,00	100,00	100,00	100,00	100,00
1180	1,93	34,17	69,91	94,76	99,64
850	0,09	8,06	53,71	94,27	95,73
600	0,03	5,44	36,21	91,35	92,17
425	0,00	3,72	20,04	80,52	90,41
300	0,00	2,56	11,78	61,79	88,23
212	0,00	1,68	7,13	40,16	77,98
150	0,00	1,19	4,68	24,93	57,33
106	0,00	0,78	2,78	15,12	34,65
75	0,00	0,55	1,63	9,04	19,07
53	0,00	0,38	1,08	5,61	9,94
38	0,00	0,26	0,73	3,29	5,83
%w.r.top size	98,07	65,83	30,09	5,24	0,36

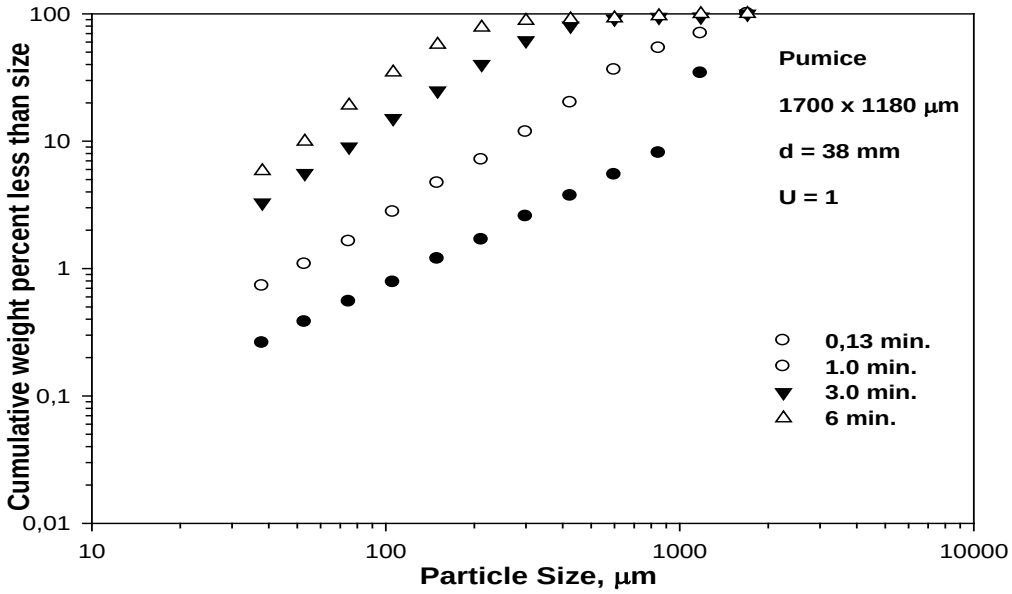

Figure C.16 Particle size distribution of pumice for -1700 + 1180 μm feed size fraction ground with d = 38 mm ball diameter and U = 1.

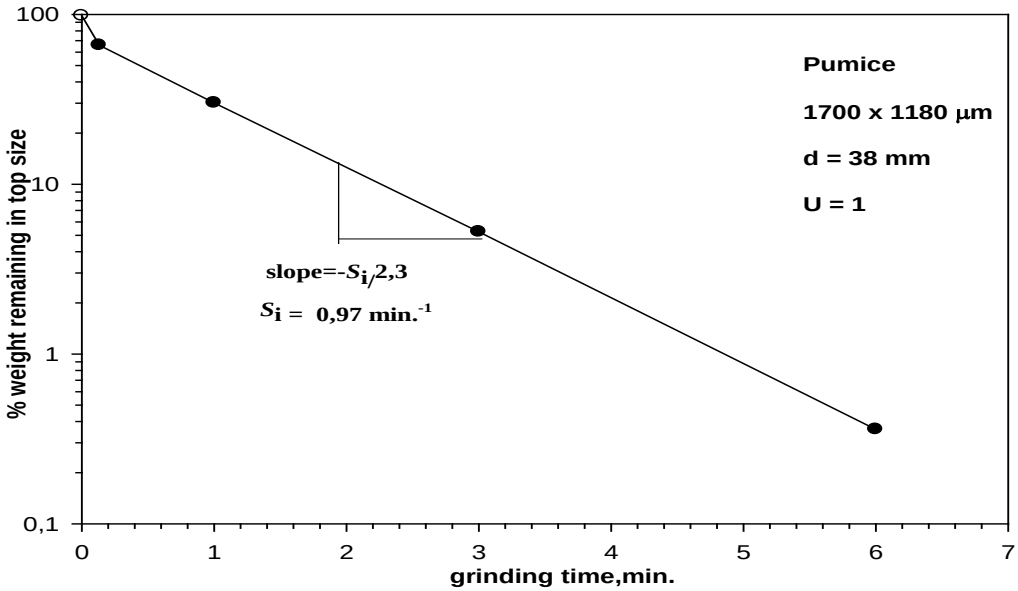

Figure C.17 First-order plot of breakage of - 1700 + 1180 μm feed of pumice ground with d = 38 mm ball diameter and U = 1.

850 x 600 micron

Table C.12 Determined B values of pumice for - 850 + 600 µm size interval ground with d = 38 mm ball diameter and U = 1.

INTERVAL NO,İ	SİZE (mesh)	Size (µm)	Xi/Xmax	B i,1	B VALUES
1	20x30	850x600	1,00	B3,1	1,0000
2	30x40	600x425	0,7	B4,1	1,0000
3	40x50	425x300	0,5	B5,1	0,2066
4	50x70	300x212	0,35	B6,1	0,1366
5	70x100	212x150	0,24	B7,1	0,0946
6	100x140	150x106	0,17	B8,1	0,0644
7	140x200	106x75	0,12	B9,1	0,0415
8	200x270	75x53	0,08	B10,1	0,0275
9	270x400	53x38	0,06	B11,1	0,0198
10	-400	-38	0,04	B12,1	0,0132

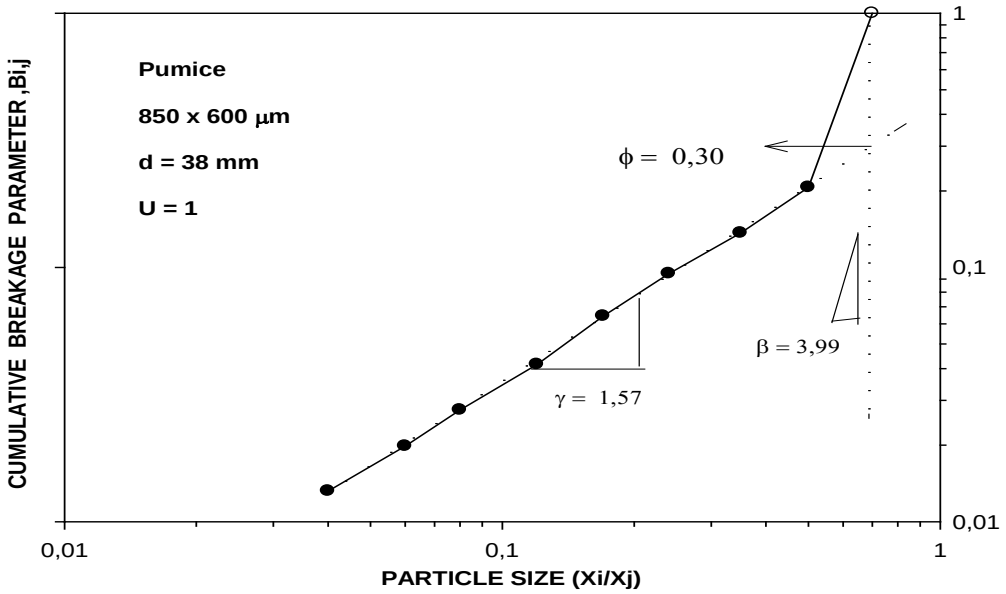

Figure C.18 Primary breakage distribution function of pumice for -850 + 600 µm feed size fraction ground with d = 38 mm ball diameter and U = 0,6.

Table C.13 Cumulative weight percent less than size values of pumice for - 850 + 600 µm size interval ground with d = 38 mm ball diameter and U = 1.

SIZE	0 min.	0,133 min	1 min	3 min	6 min
850	100,00	100,00	100,00	100,00	100,00
600	1,72	26,34	59,83	89,48	98,60
425	0,41	6,17	33,78	83,14	95,92
300	0,05	3,91	18,04	67,91	93,04
212	0,00	2,69	11,28	46,32	84,75
150	0,00	1,84	6,94	25,53	56,18
106	0,00	1,19	4,06	14,47	34,02
75	0,00	0,79	2,69	7,96	18,96
53	0,00	0,57	1,73	4,88	11,07
38	0,00	0,38	1,12	2,91	6,47
%w.r.top size	98,28	73,66	40,17	10,52	1,40

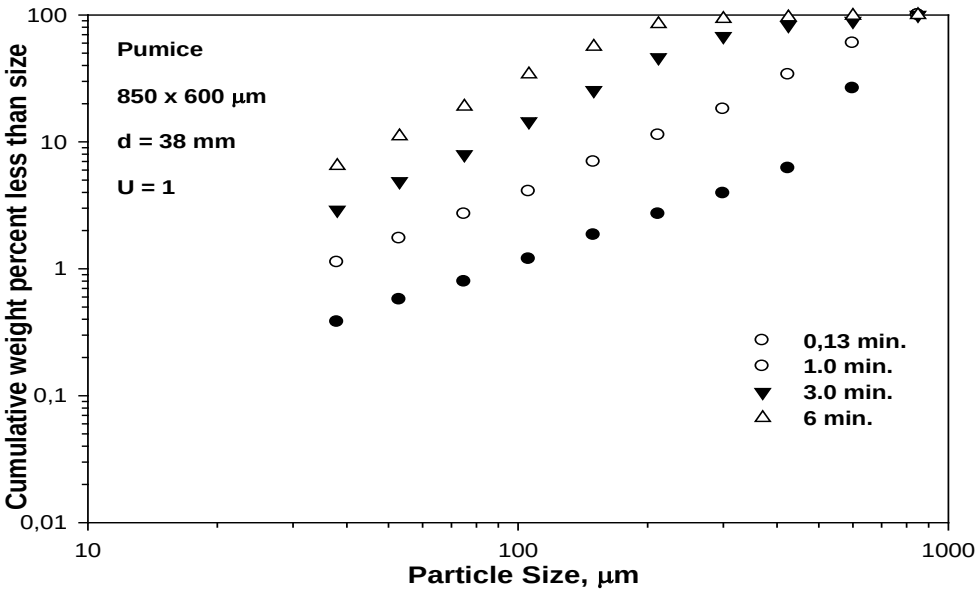

Figure C.19 Particle size distribution of pumice for -850 + 600 µm feed size fraction ground with d = 38 mm ball diameter and U = 1.

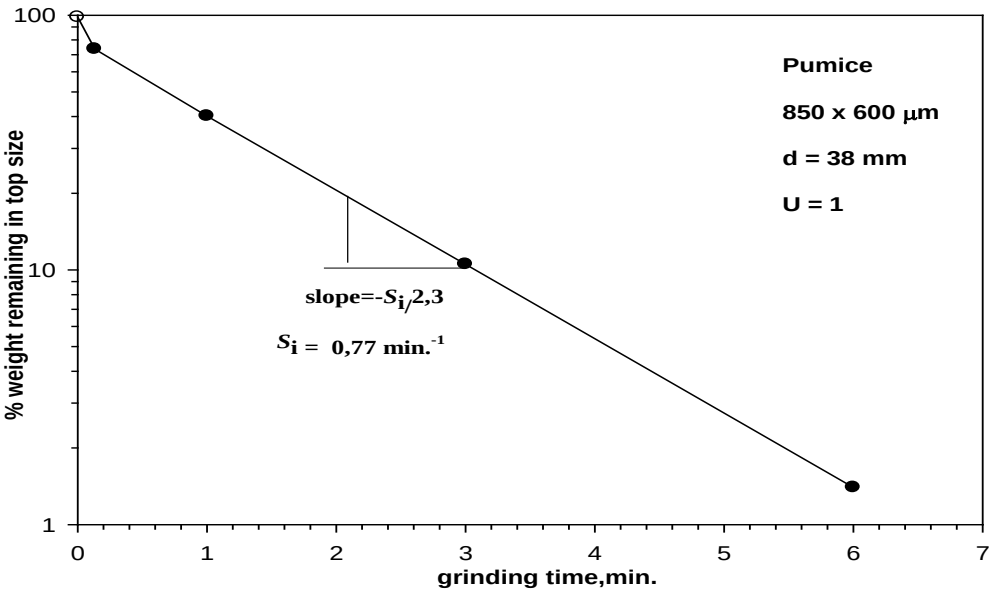

Figure C.20 First-order plot of breakage of - 850 + 600 µm feed of pumice ground with d = 38 mm ball diameter and U = 1.

425 x 300 micron

Table C.14 Determined B values of pumice for – 425 + 300 µm size interval ground with d = 38 mm ball diameter and U = 1.

INTERVAL NO,İ	SİZE (mesh)	Size (µm)	Xi/Xmax	B i,1	B VALUES
1	40x50	425x300	1,00	B1,1	1,0000
2	50x70	300x212	0,7	B2,1	1,0000
3	70x100	212x150	0,49	B3,1	0,1873
4	100x140	150x106	0,35	B4,1	0,1311
5	140x200	106x75	0,24	B5,1	0,0878
6	200x270	75x53	0,17	B6,1	0,0610
7	270x400	53x38	0,12	B7,1	0,0410
8	-400	-38	0,08	B8,1	0,0276

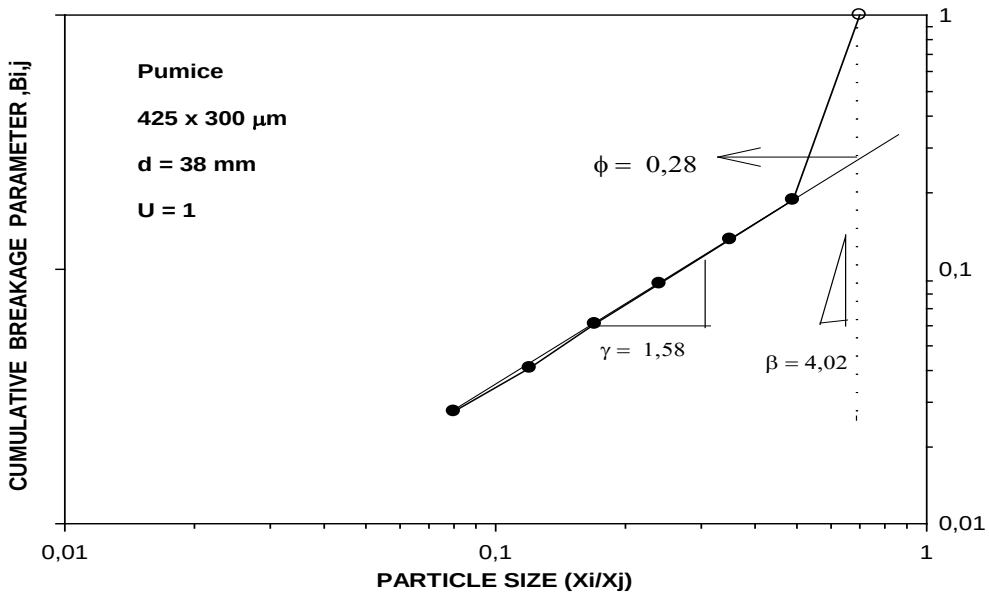

Figure C.21 Primary breakage distribution function of pumice for -425 + 300 µm feed size fraction ground with d = 38 mm ball diameter and U = 1.

Table C.15 Cumulative weight percent less than size values of pumice for - 425 + 300 µm size interval ground with d = 38 mm ball diameter and U = 1.

SIZE	0 min.	0,133 min	1 min	3 min	6 min
425	100,00	100,00	100,00	100,00	100,00
300	0,28	10,24	32,78	61,93	84,50
212	0,09	2,04	10,76	47,29	81,37
150	0,01	1,38	4,06	23,14	54,18
106	0,00	0,92	2,58	10,88	32,27
75	0,00	0,64	1,83	6,47	19,34
53	0,00	0,43	1,21	3,71	10,58
38	0,00	0,29	0,83	2,14	6,17
%w.r.top size	99,72	89,76	67,22	38,07	15,50

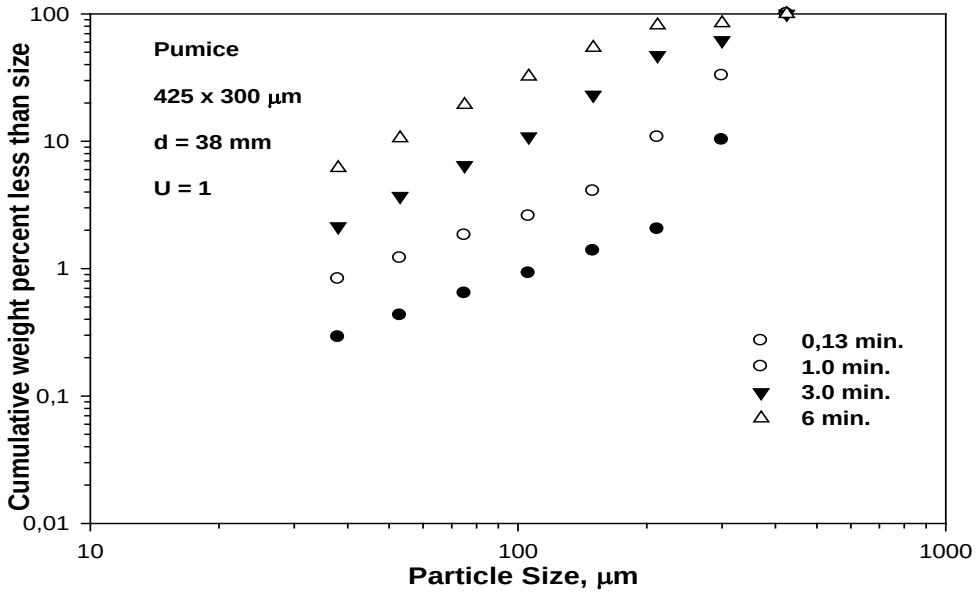

Figure C.22 Particle size distribution of pumice for -425 + 300 μm feed size fraction ground with d = 38 mm ball diameter and U = 1.

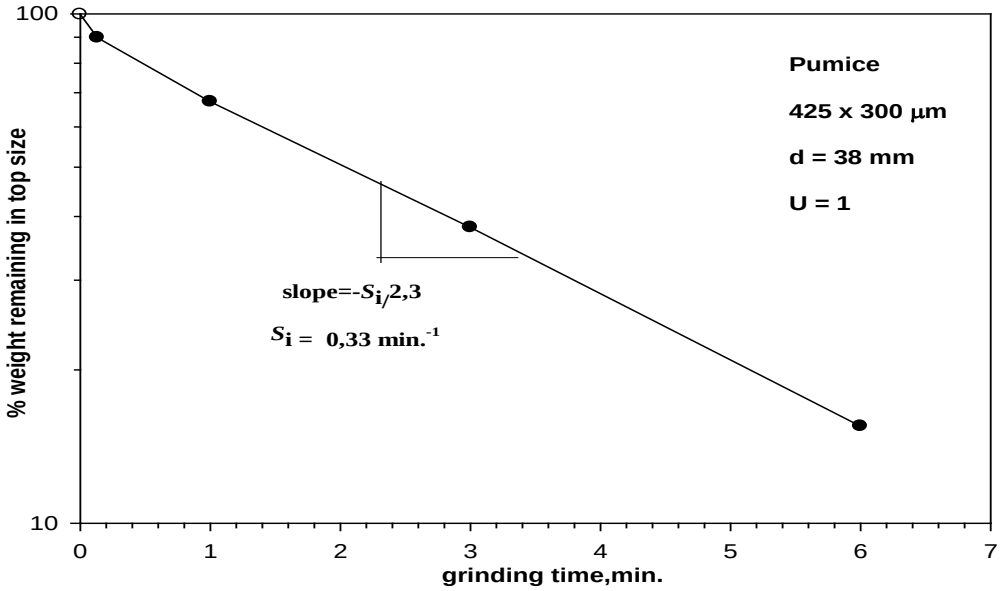

Figure C.23 First-order plot of breakage of - 425 + 300 μm feed of pumice ground with d = 38 mm ball diameter and U = 1.

212 x 150 micron

Table C.16 Determined B values of pumice for – 212 + 150 µm size interval ground with d = 38 mm ball diameter and U = 1.

INTERVAL NO,İ	SİZE (mesh)	Size (µm)	Xi/Xmax	B i,1	B VALUES
1	70x100	212x150	1,00	B1,1	1,0000
2	100x140	150x106	0,7	B2,1	1,0000
3	140x200	106x75	0,5	B3,1	0,1857
4	200x270	75x53	0,35	B4,1	0,1284
5	270x400	53x38	0,25	B5,1	0,0909
6	-400	-38	0,17	B6,1	0,0633

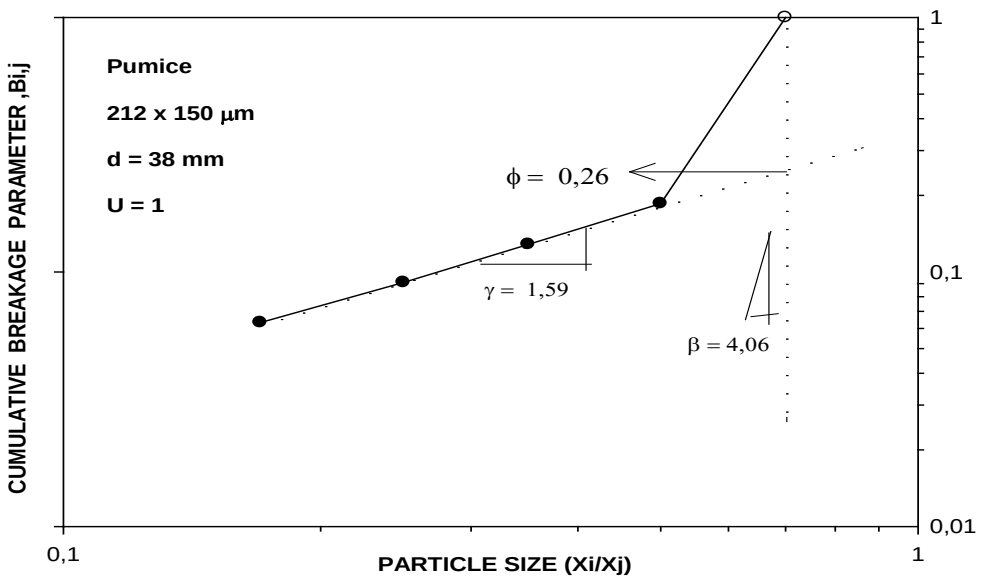

Figure C.24 Primary breakage distribution function of pumice for - 212 + 150 µm feed size fraction ground with d = 38 mm ball diameter and U = 1.

Table C.17 Cumulative weight percent less than size values of pumice for - 212 + 150 µm size interval ground with d = 38 mm ball diameter and U = 1.

SIZE	0 min.	0,133 min	1 min	3 min	6 min
212	100,00	100,00	100,00	100,00	100,00
150	0,16	6,14	18,84	37,93	58,49
106	0,04	1,18	4,28	13,39	27,74
75	0,00	0,79	1,97	5,16	13,22
53	0,00	0,56	1,18	2,74	6,48
38	0,00	0,39	0,84	1,53	3,76
%w.r.top size	99,84	93,86	81,16	62,07	41,51

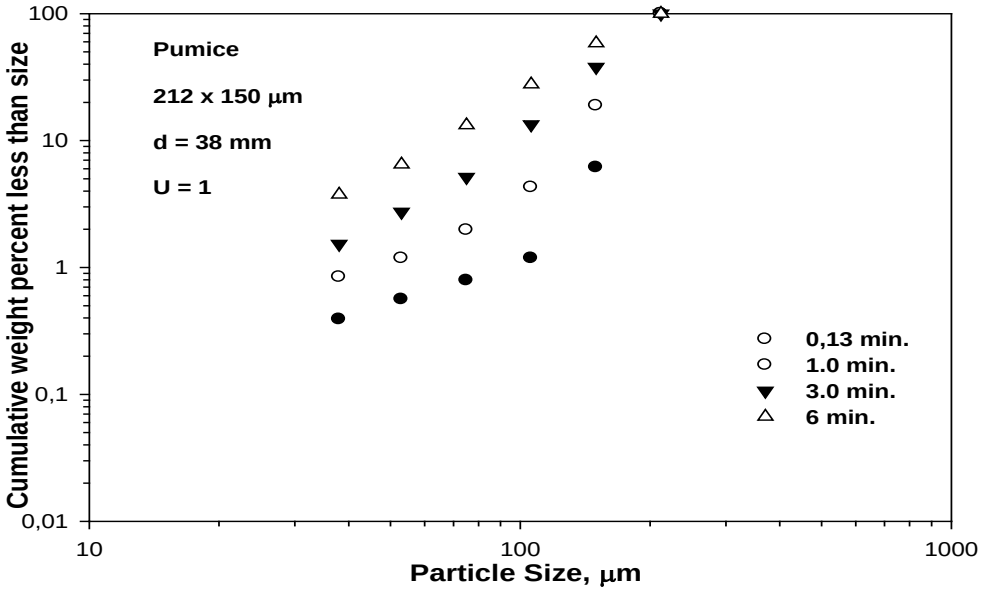

Figure C.25 Particle size distribution of pumice for -212 + 150 µm feed size fraction ground with d = 38 mm ball diameter and U = 1.

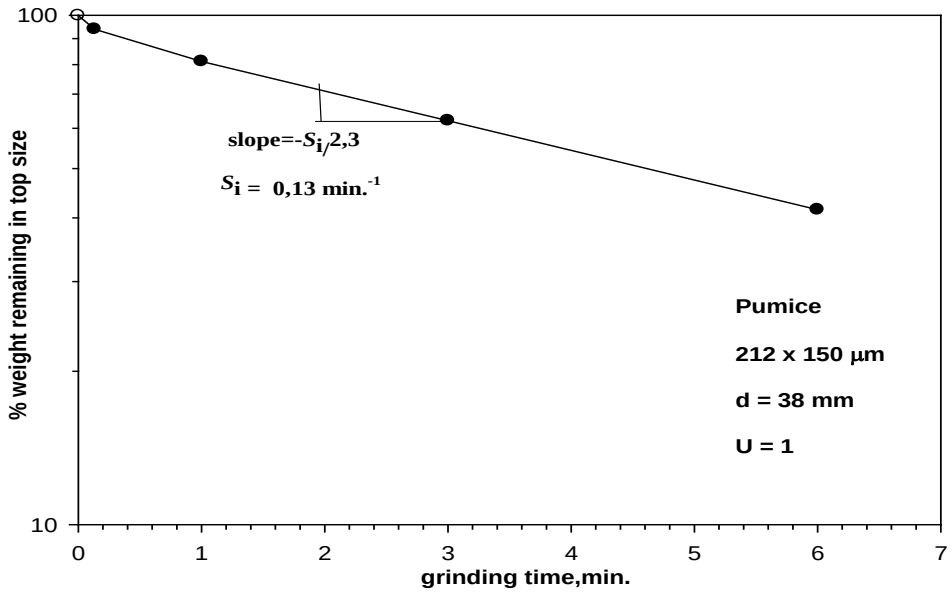

Figure C.26 First-order plot of breakage of - 212 + 150 µm feed of pumice ground with d = 38 mm ball diameter and U = 1.

Determination of aT value

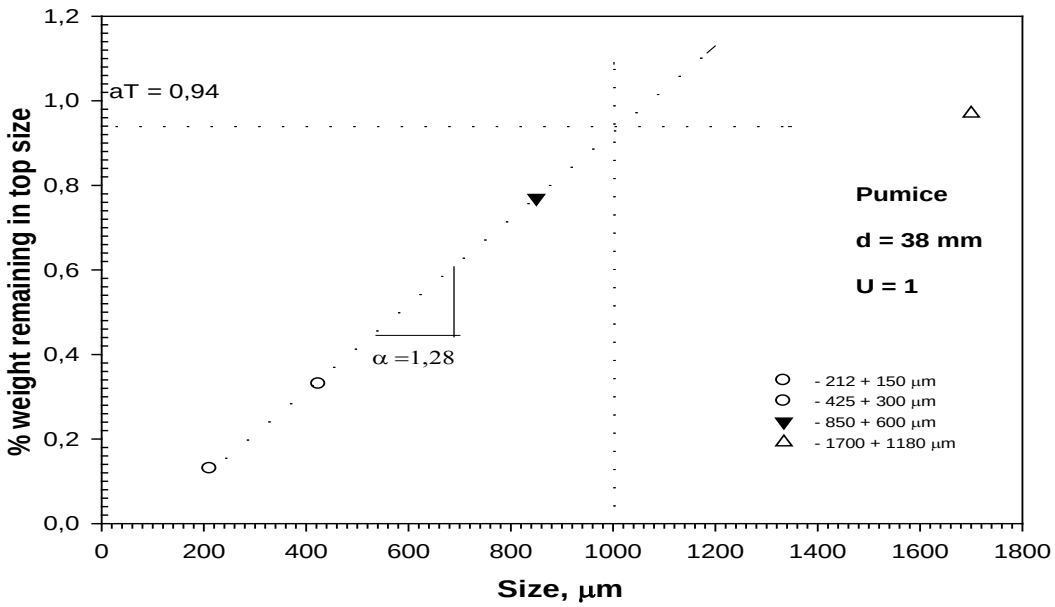

Figure C.27 Variation of first-order specific rates of breakage of pumice ground with d = 38 mm ball diameter and particle size: √2 intervals, plotted at upper size of interval at U=1.

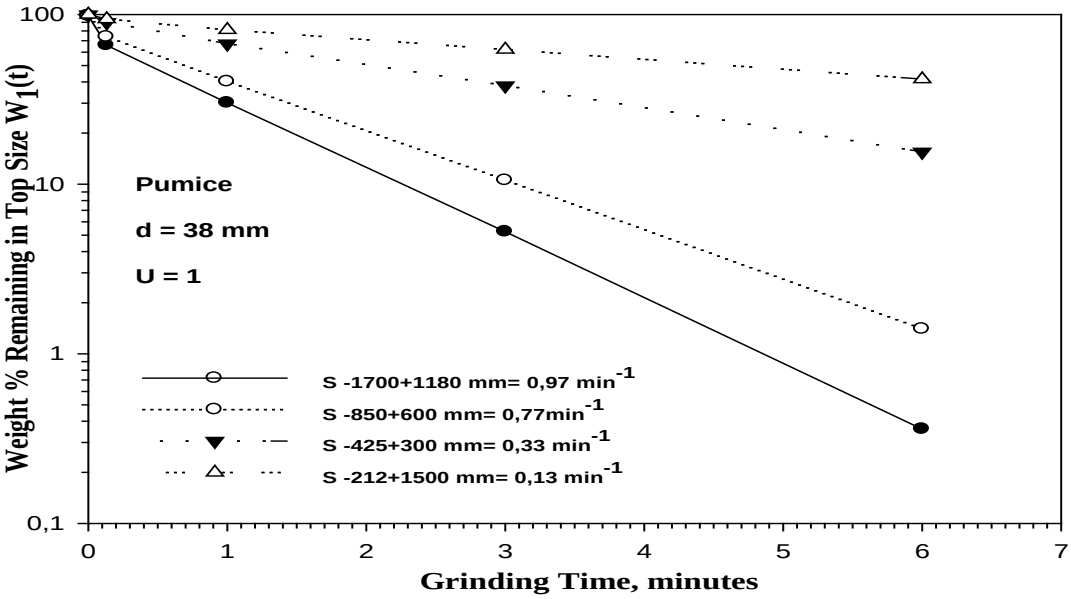

Figure C.28 First-order plots of breakage of -1700+1180, -850+600, -425+300, -212+150 µm feed size of pumice ground with d = 38 mm ball diameter and U=1.

Table C.18 Breakage parameters of pumice ground with d = 38 mm ball diameter at U=1.

1700x1180		**850x600**		**425x300**		**212x150**			
gama	1,25	**gama**	1,28	**gama**	1,33	**gama**	1,37		
beta	2,59	**beta**	2,61	**beta**	2,62	**beta**	2,63	**aT**	**α**
phi	0,47	**phi**	0,43	**phi**	0,43	**phi**	0,42	0,48	1,04
S value	0,470	**S value**	0,400	**S value**	0,210	**S value**	0,100		

30 mm ball size charge at U=0,6

1700 x 1180 micron

Table C.19 Determined B values of pumice for - 1700 + 1180 µm size interval ground with d = 30 mm ball diameter and U = 0,6.

INTERVAL NO,İ	SİZE (mesh)	Size (µm)	Xi/Xmax	B i,1	B VALUES
1	12x16	1700x1180	1,00	B1,1	1,0000
2	16x20	1180x850	0,69	B2,1	1,0000
3	20x30	850x600	0,50	B3,1	0,4543
4	30x40	600x425	0,35	B4,1	0,2772
5	40x50	425x300	0,25	B5,1	0,1766
6	50x70	300x212	0,17	B6,1	0,1139
7	70x100	212x150	0,12	B7,1	0,0721
8	100x140	150x106	0,088	B8,1	0,0456
9	140x200	106x75	0,062	B9,1	0,0282
10	200x270	75x53	0,044	B10,1	0,0176
11	270x400	53x38	0,031	B11,1	0,0112
12	-400	-38	0,022	B12,1	0,0071

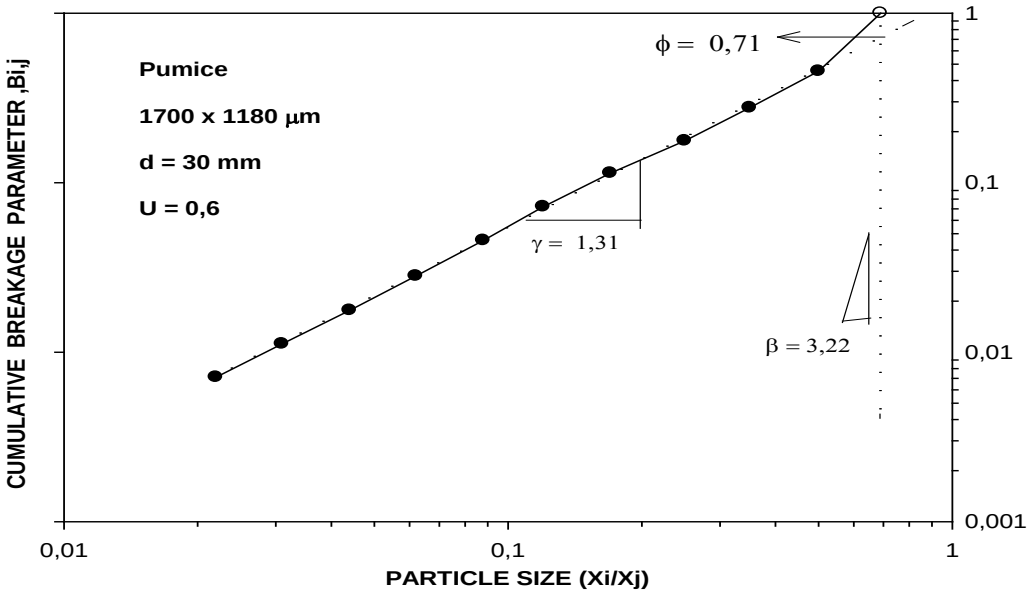

Figure C.29 Primary breakage distribution function of pumice for -1700 + 1180 µm feed size fraction ground with d = 30 mm ball diameter and U = 0,6.

Table C.20 Cumulative weight percent less than size values of pumice for 1700 x 1180 µm size interval ground with d = 30 mm ball diameter and U = 0,6.

SIZE	0 min.	0,133 min	1 min	3 min	6 min
1700	100,00	100,00	100,00	100,00	100,00
1180	1,16	26,45	80,64	99,58	100,00
850	0,40	12,92	69,13	99,52	99,98
600	0,08	7,94	47,44	98,25	99,97
425	0,00	5,09	32,20	90,17	99,94
300	0,00	3,31	22,42	70,47	99,27
212	0,00	2,11	15,18	47,71	91,98
150	0,00	1,34	9,59	28,71	65,92
106	0,00	0,83	5,83	16,45	42,32
75	0,00	0,52	3,34	8,86	28,88
53	0,00	0,33	1,87	5,32	17,08
38	0,00	0,21	0,98	2,78	11,00
%w.r.top size	98,84	73,55	19,36	0,42	0,00

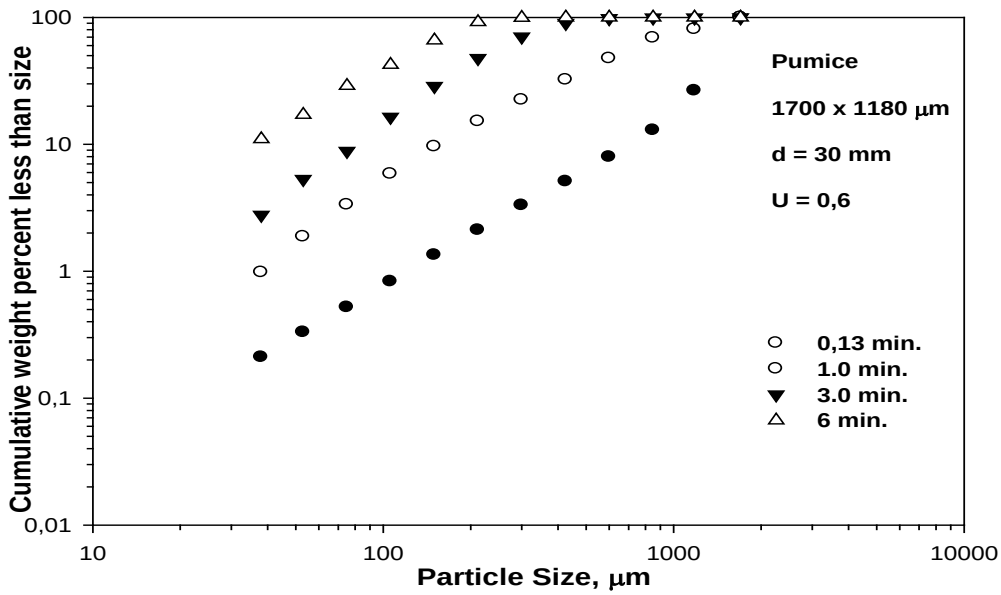

Figure C.30 Particle size distribution of pumice for -1700 + 1180 µm feed size fraction ground with d = 30 mm ball diameter and U = 0,6.

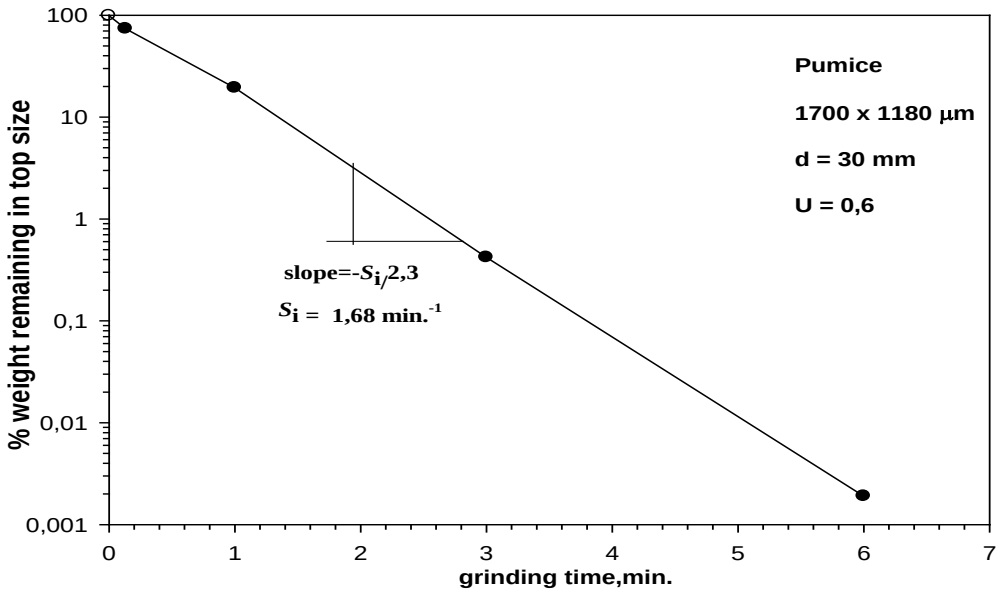

Figure C.31 First-order plot of breakage of - 1700 + 1180 µm feed of pumice ground with d = 30 mm ball diameter and U = 0,6.

850 x 600 micron

Table C.21 Determined B values of pumice for - 850 + 600 µm size interval ground with d = 30 mm ball diameter and U = 0,6.

INTERVAL NO,İ	SİZE (mesh)	Size (µm)	Xi/Xmax	B i,1	B VALUES
1	20x30	850x600	1,00	B3,1	1,0000
2	30x40	600x425	0,7	B4,1	1,0000
3	40x50	425x300	0,5	B5,1	0,4549
4	50x70	300x212	0,35	B6,1	0,2762
5	70x100	212x150	0,24	B7,1	0,1754
6	100x140	150x106	0,17	B8,1	0,1135
7	140x200	106x75	0,12	B9,1	0,0690
8	200x270	75x53	0,08	B10,1	0,0414
9	270x400	53x38	0,06	B11,1	0,0274
10	-400	-38	0,04	B12,1	0,0163

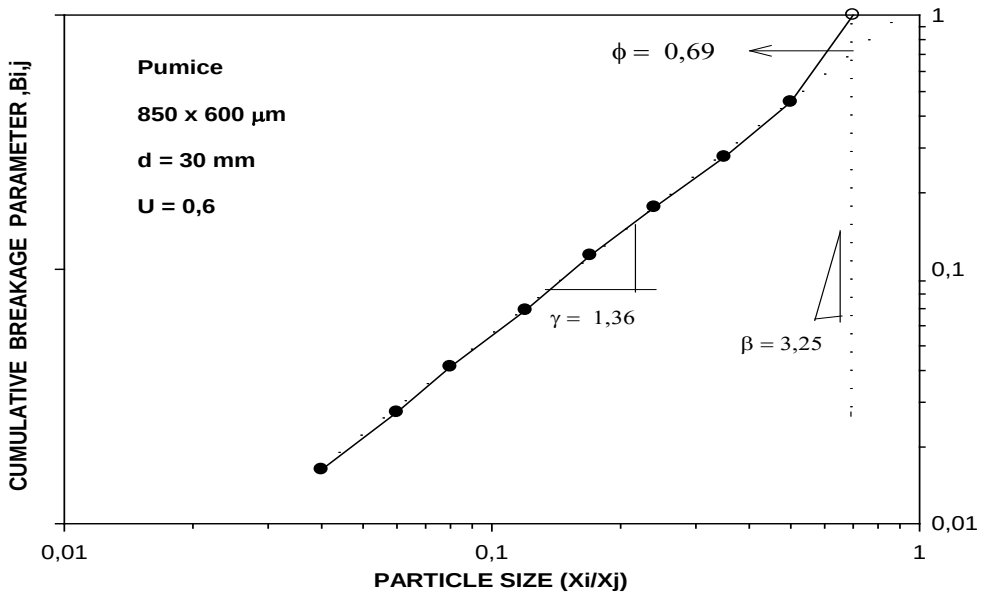

Figure C.32 Primary breakage distribution function of pumice for -850 + 600 µm feed size fraction ground with d = 30 mm ball diameter and U = 0,6.

Table C.22 Cumulative weight percent less than size values of pumice for - 850 + 600 µm size interval ground with d = 30 mm ball diameter and U = 0,6.

SIZE	0 min.	0,133 min	1 min	3 min	6 min
850	100,00	100,00	100,00	100,00	100,00
600	4,00	22,08	70,70	96,94	99,95
425	2,04	10,91	41,02	95,12	98,91
300	0,56	6,13	25,08	78,03	98,12
212	0,01	3,60	15,51	52,21	91,23
150	0,00	2,34	9,31	30,42	62,48
106	0,00	1,43	5,71	19,93	39,17
75	0,00	0,86	3,51	12,47	26,19
53	0,00	0,57	1,90	8,53	15,03
38	0,00	0,34	0,86	4,89	8,36
%w.r.top size	96,00	77,92	29,30	3,06	0,05

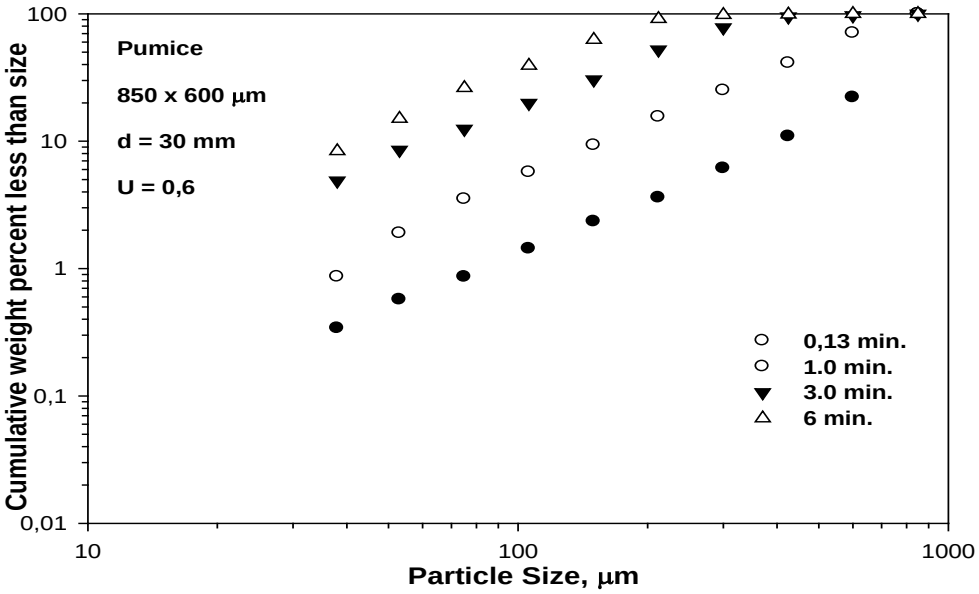

Figure C.33 Particle size distribution of pumice for -850 + 600 µm feed size fraction ground with d = 30 mm ball diameter and U = 0,6.

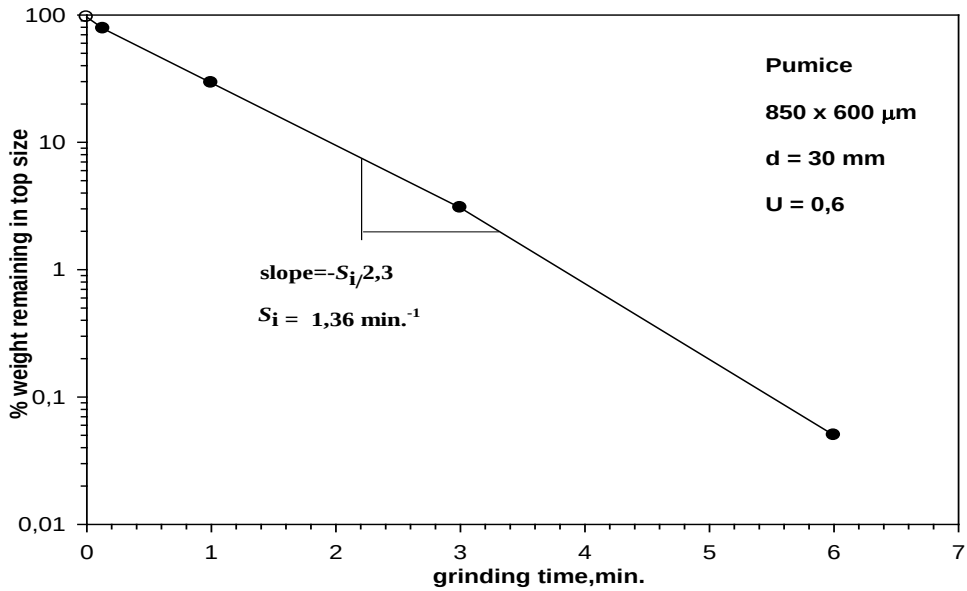

Figure C.34 First-order plot of breakage of - 850 + 600 µm feed of pumice ground with d = 30 mm ball diameter and U = 0,6.

425 x 300 micron

Table C.23 Determined B values of pumice for – 425 + 300 µm size interval ground with d = 30 mm ball diameter and U = 0,6.

INTERVAL NO,İ	SİZE (mesh)	Size (µm)	Xi/Xmax	B i,1	B VALUES
1	40x50	425x300	1,00	B1,1	1,0000
2	50x70	300x212	0,7	B2,1	1,0000
3	70x100	212x150	0,49	B3,1	0,4201
4	100x140	150x106	0,35	B4,1	0,2592
5	140x200	106x75	0,24	B5,1	0,1712
6	200x270	75x53	0,17	B6,1	0,1039
7	270x400	53x38	0,12	B7,1	0,0720
8	-400	-38	0,08	B8,1	0,0413

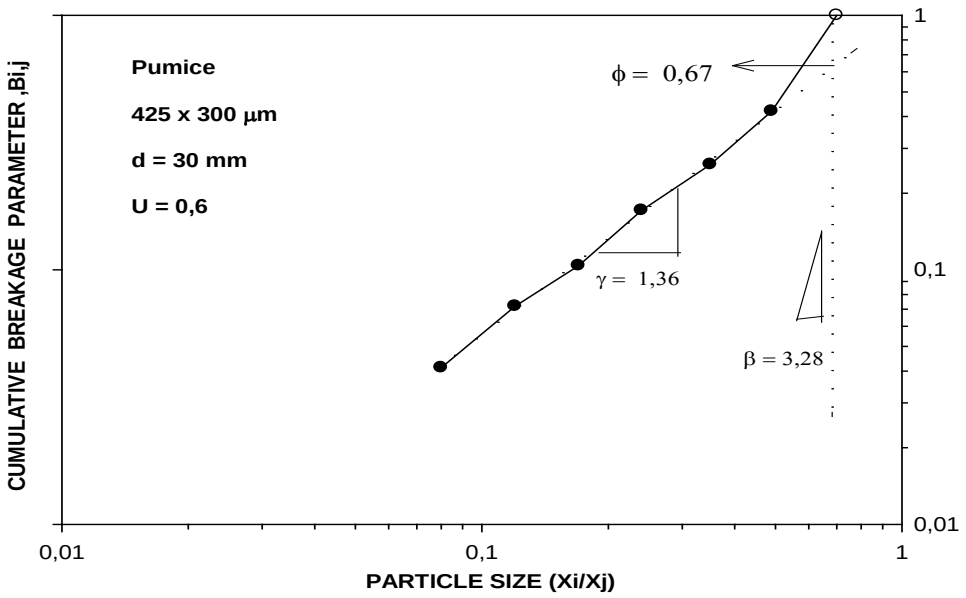

Figure C.35 Primary breakage distribution function of pumice for -425 + 300 µm feed size fraction ground with d = 30 mm ball diameter and U = 0,6.

Table C.24 Cumulative weight percent less than size values of pumice for - 425 + 300 µm size interval ground with d = 30 mm ball diameter and U = 0,6.

SIZE	0 min.	0,133 min	1 min	3 min	6 min
425	100,00	100,00	100,00	100,00	100,00
300	0,23	19,47	57,88	87,16	97,58
212	0,01	8,61	31,17	68,44	95,43
150	0,00	5,40	16,87	37,03	68,82
106	0,00	3,60	10,11	22,01	41,94
75	0,00	2,20	6,52	13,07	28,06
53	0,00	1,53	4,15	8,84	16,74
38	0,00	0,88	2,69	5,12	10,26
%w.r.top size	99,77	80,53	42,12	12,84	2,42

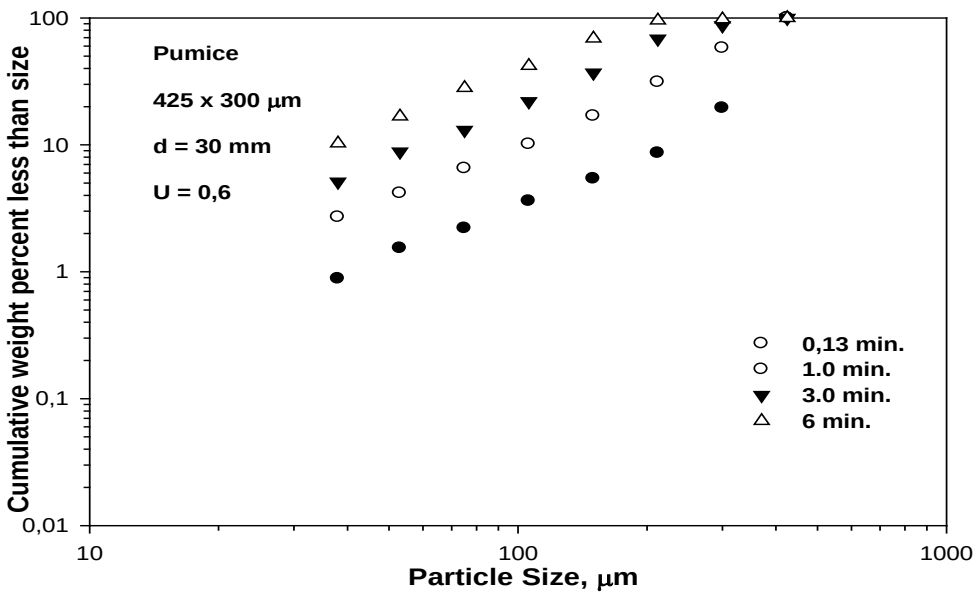

Figure C.36 Particle size distribution of pumice for -425 + 300 µm feed size fraction ground with d = 30 mm ball diameter and U = 0,6.

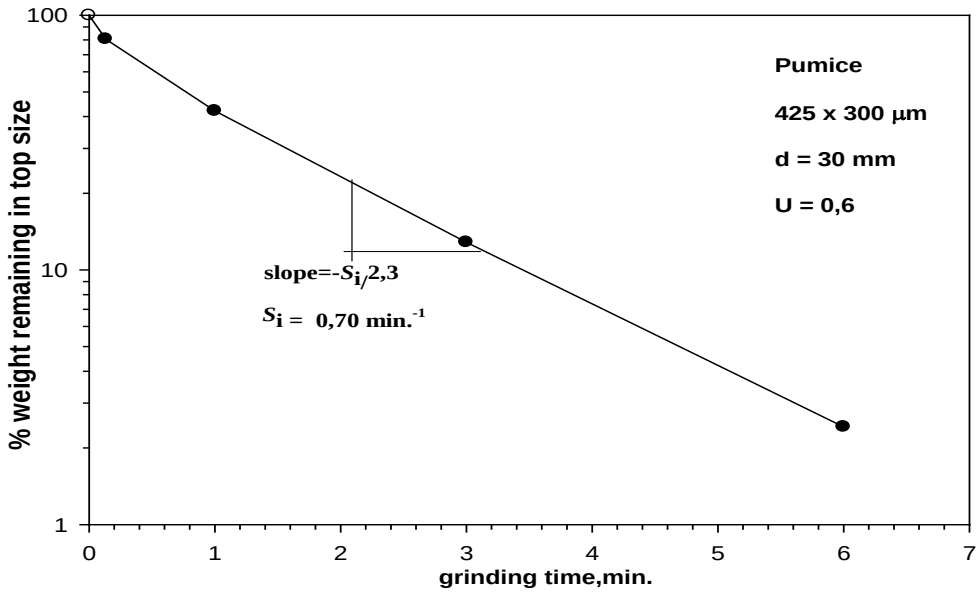

Figure C.37 First-order plot of breakage of - 425 + 300 µm feed of pumice ground with d = 30 mm ball diameter and U = 0,6.

212 x 150 micron

Table C.25 Determined B values of pumice for – 212 + 150 µm size interval ground with d = 30 mm ball diameter and U = 0,6.

INTERVAL NO,İ	SİZE (mesh)	Size (µm)	Xi/Xmax	B i,1	B VALUES
1	70x100	212x150	1,00	B1,1	1,0000
2	100x140	150x106	0,7	B2,1	1,0000
3	140x200	106x75	0,5	B3,1	0,4218
4	200x270	75x53	0,35	B4,1	0,2695
5	270x400	53x38	0,25	B5,1	0,1706
6	-400	-38	0,17	B6,1	0,1004

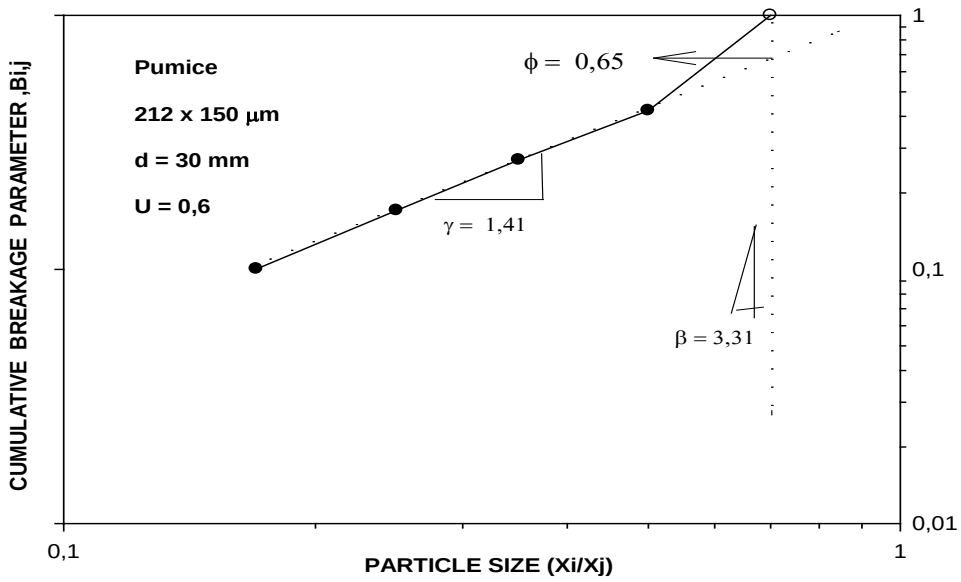

Figure C.38 Primary breakage distribution function of pumice for - 212 + 150 µm feed size fraction ground with d = 30 mm ball diameter and U = 0,6.

Table C.26 Cumulative weight percent less than size values of pumice for - 212 + 150 µm size interval ground with d = 30 mm ball diameter and U = 0,6.

SIZE	0 min.	0,133 min	1 min	3 min	6 min
212	100,00	100,00	100,00	100,00	100,00
150	5,20	14,06	41,03	64,76	84,09
106	0,10	4,15	18,16	30,11	48,72
75	0,00	2,61	10,94	17,84	28,64
53	0,00	1,66	6,81	10,52	17,25
38	0,00	0,98	4,06	6,31	9,41
%w.r.top size	94,80	85,94	58,97	35,24	15,91

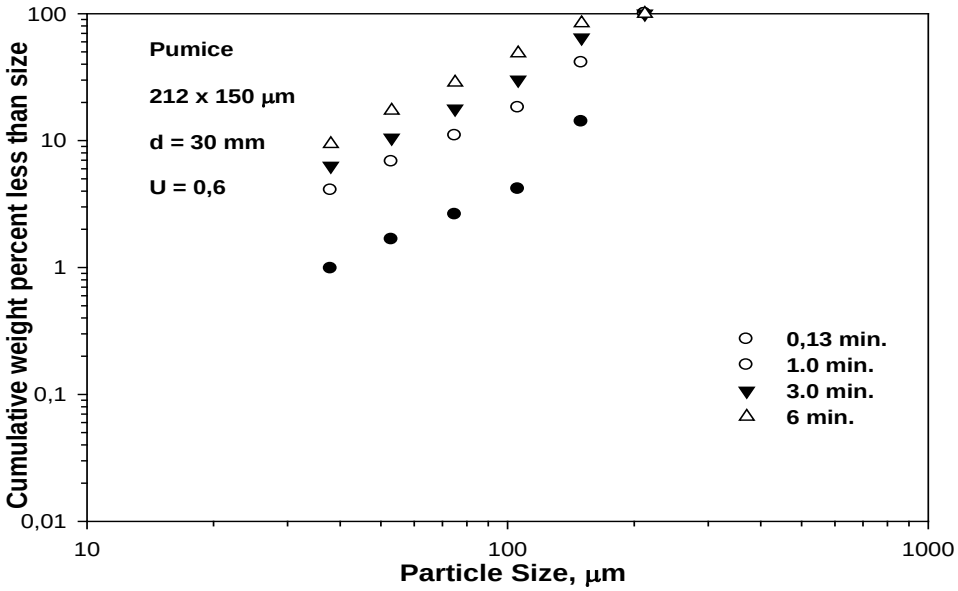

Figure C.39 Particle size distribution of pumice for -212 + 150 µm feed size fraction ground with d = 30 mm ball diameter and U = 0,6.

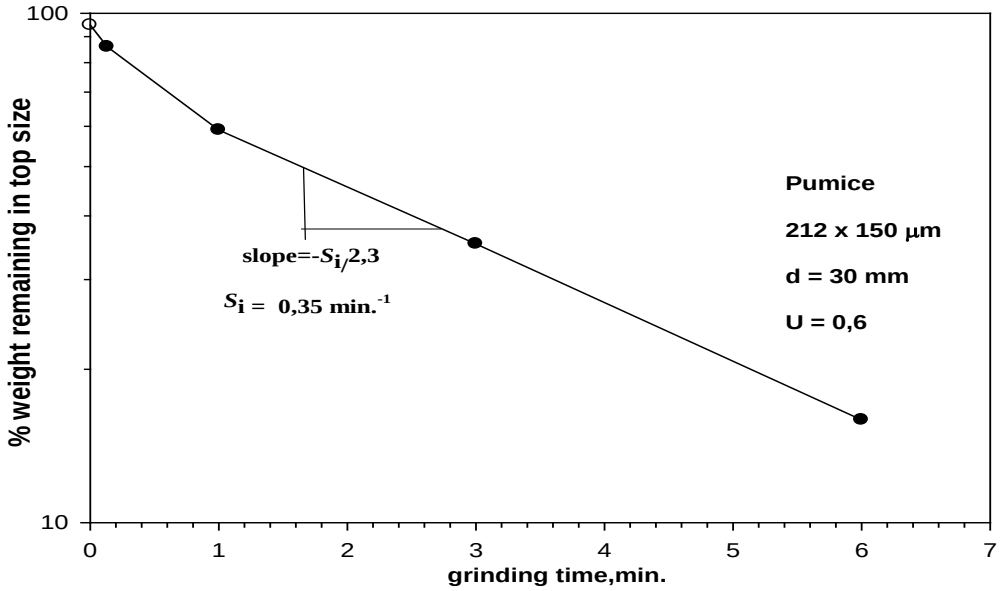

Figure C.40 First-order plot of breakage of - 212 + 150 µm feed of pumice ground with d = 30 mm ball diameter and U = 0,6.

Determination of aT value

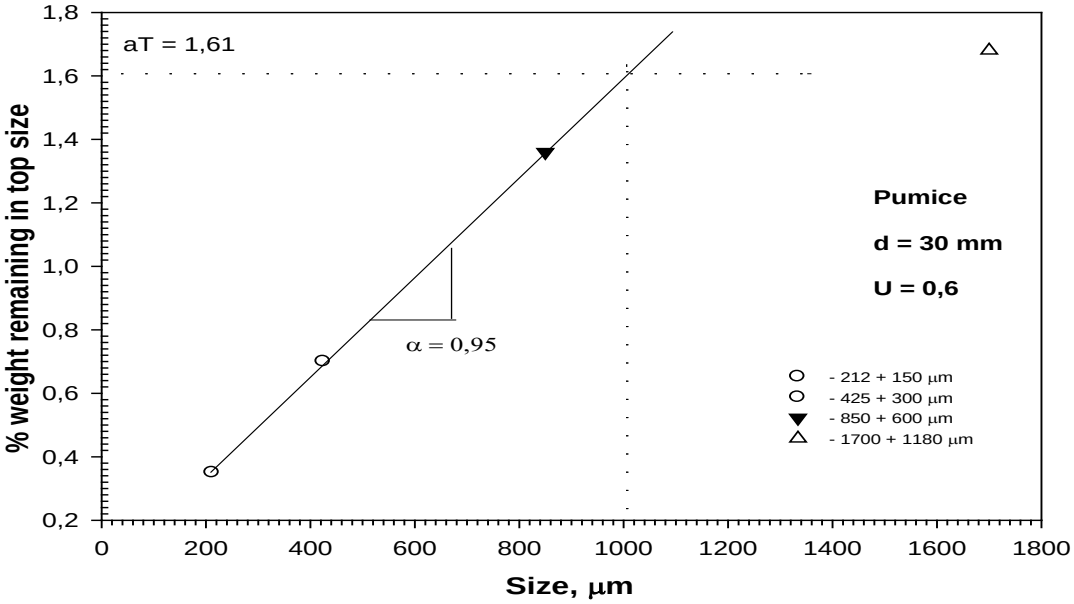

Figure C.41 Variation of first-order specific rates of breakage of pumice ground with d = 30 mm ball diameter and particle size: √2 intervals, plotted at upper size of interval at U=0,6.

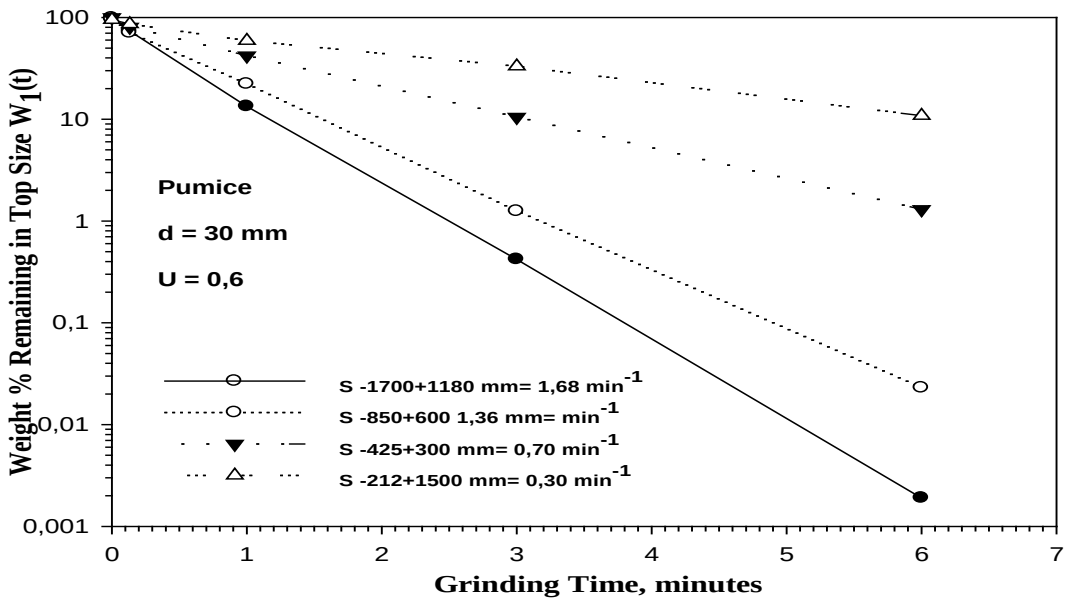

Figure C.42 First-order plots of breakage of -1700+1180, -850+600, -425+300, -212+150 μm feed size of pumice ground with d = 30 mm ball diameter and U=0,6.

Table C.27 Breakage parameters of pumice ground with d = 30 mm ball diameter at U=0,6.

1700x1180		**850x600**		**425x300**		**212x150**			
gama	1,08	**gama**	1,09	**gama**	1,10	**gama**	1,13		
beta	3,81	**beta**	3,84	**beta**	3,87	**beta**	3,90	**aT**	**α**
phi	0,61	**phi**	0,58	**phi**	0,54	**phi**	0,52	0,95	0,91
S value	0,920	**S value**	0,780	**S value**	0,410	**S value**	0,220		

30 mm ball size charge at U= 1

1700 x 1180 micron

Table C.28 Determined B values of pumice for - 1700 + 1180 µm size interval ground with d = 30 mm ball diameter and U = 1.

INTERVAL NO,İ	SİZE (mesh)	Size (µm)	Xi/Xmax	B i,1	B VALUES
1	12x16	1700x1180	1,00	B1,1	1,0000
2	16x20	1180x850	0,69	B2,1	1,0000
3	20x30	850x600	0,50	B3,1	0,2415
4	30x40	600x425	0,35	B4,1	0,1663
5	40x50	425x300	0,25	B5,1	0,1207
6	50x70	300x212	0,17	B6,1	0,0844
7	70x100	212x150	0,12	B7,1	0,0619
8	100x140	150x106	0,088	B8,1	0,0455
9	140x200	106x75	0,062	B9,1	0,0325
10	200x270	75x53	0,044	B10,1	0,0239
11	270x400	53x38	0,031	B11,1	0,0179
12	-400	-38	0,022	B12,1	0,0124

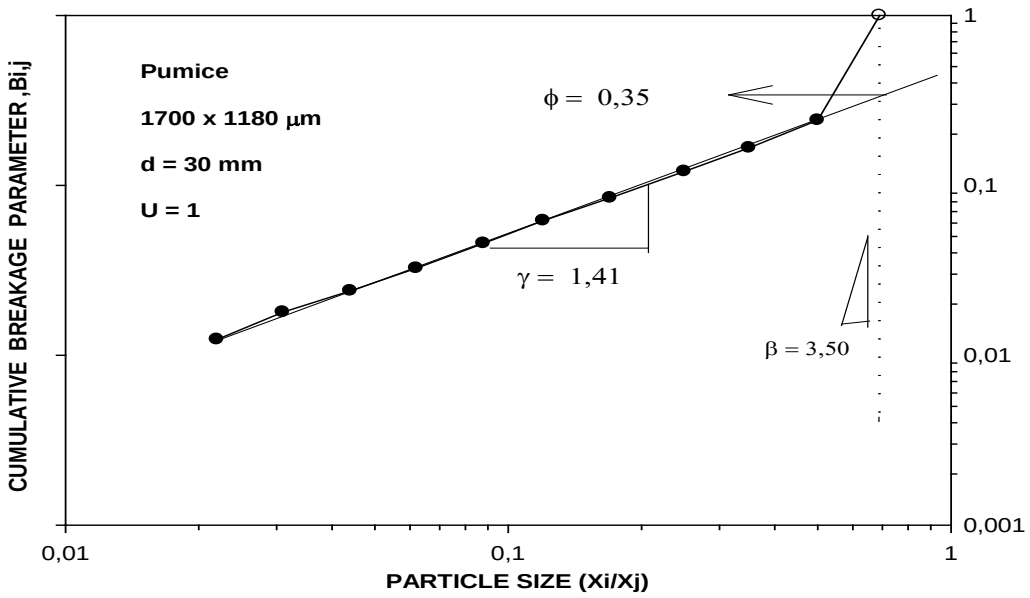

Figure C.43 Primary breakage distribution function of pumice for -1700 + 1180 µm feed size fraction ground with d = 30 mm ball diameter and U = 0,6.

Table C.29 Cumulative weight percent less than size values of pumice for 1700 x 1180 µm size interval ground with d = 30 mm ball diameter and U = 1.

SIZE	0 min.	0,133 min	1 min	3 min	6 min
1700	100,00	100,00	100,00	100,00	100,00
1180	1,68	36,49	74,86	96,47	99,84
850	0,06	10,07	62,71	97,56	97,94
600	0,01	7,02	42,58	94,91	96,52
425	0,00	5,14	24,13	83,47	95,23
300	0,00	3,62	14,36	66,76	95,06
212	0,00	2,67	8,25	47,13	88,14
150	0,00	1,97	5,34	29,14	62,71
106	0,00	1,41	3,02	18,78	37,58
75	0,00	1,04	1,99	11,03	24,18
53	0,00	0,78	1,26	6,44	13,97
38	0,00	0,54	0,86	3,92	8,54
%w.r.top size	98,32	63,51	25,14	3,53	0,16

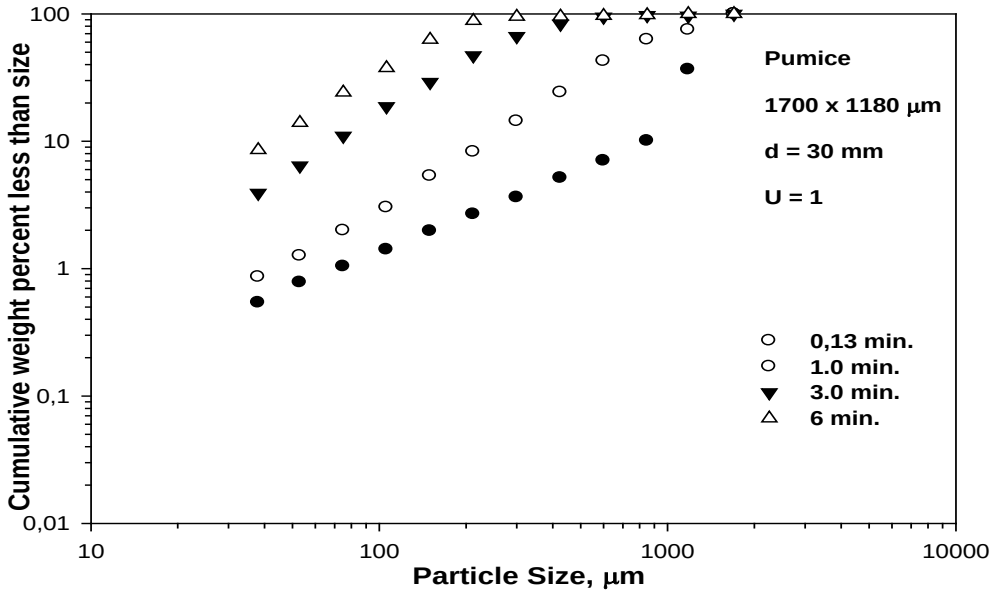

Figure C.44 Particle size distribution of pumice for -1700 + 1180 µm feed size fraction ground with d = 30 mm ball diameter and U = 1.

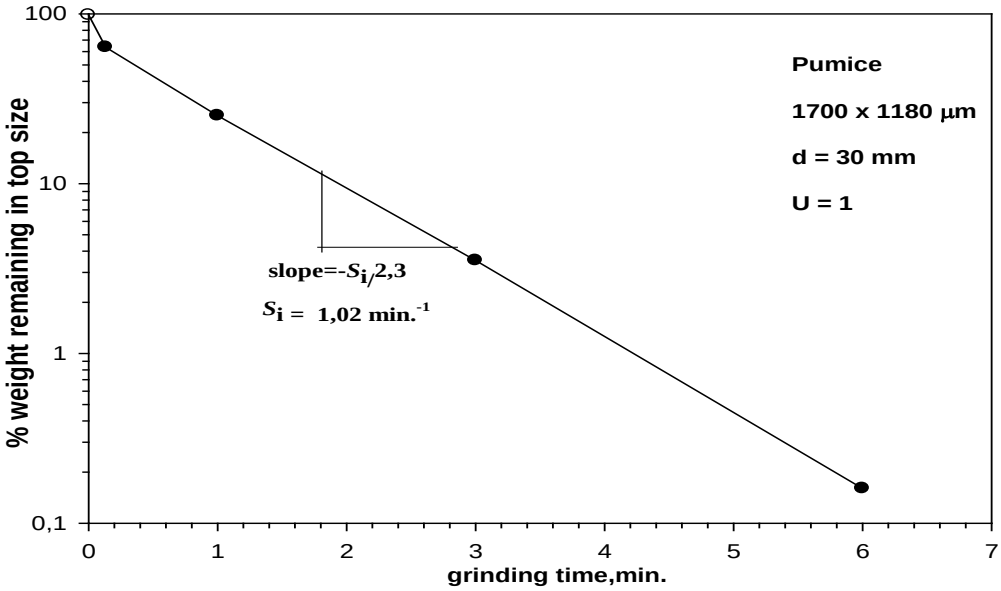

Figure C.45 First-order plot of breakage of - 1700 + 1180 µm feed of pumice ground with d = 30 mm ball diameter and U = 1.

850 x 600 micron

Table C.30 Determined B values of pumice for - 850 + 600 µm size interval ground with d = 30 mm ball diameter and U = 1.

INTERVAL NO,İ	SİZE (mesh)	Size (µm)	Xi/Xmax	B i,1	B VALUES
1	20x30	850x600	1,00	B3,1	1,0000
2	30x40	600x425	0,7	B4,1	1,0000
3	40x50	425x300	0,5	B5,1	0,2396
4	50x70	300x212	0,35	B6,1	0,1647
5	70x100	212x150	0,24	B7,1	0,1212
6	100x140	150x106	0,17	B8,1	0,0855
7	140x200	106x75	0,12	B9,1	0,0616
8	200x270	75x53	0,08	B10,1	0,0418
9	270x400	53x38	0,06	B11,1	0,0303
10	-400	-38	0,04	B12,1	0,0210

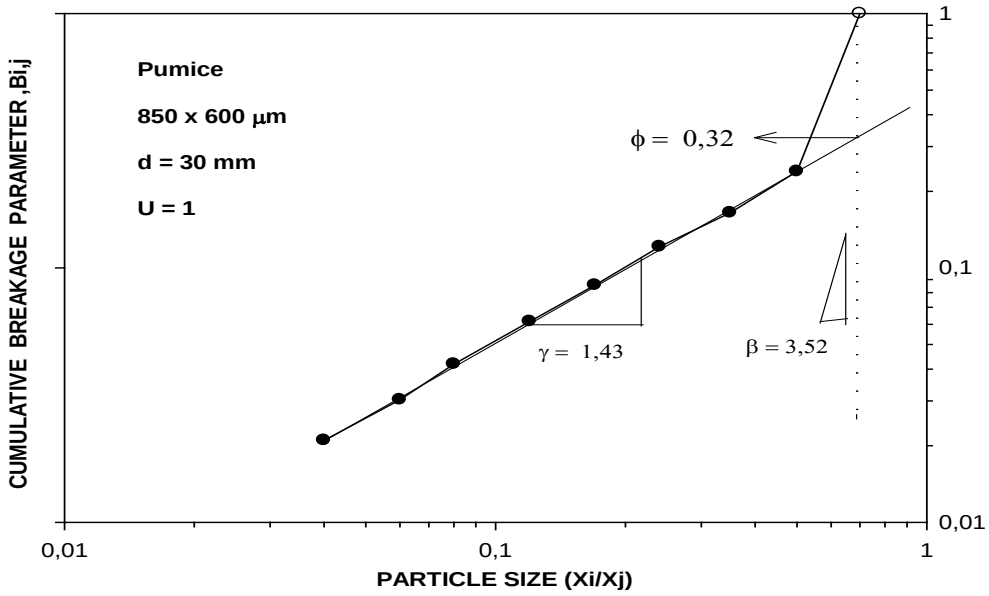

Figure C.46 Primary breakage distribution function of pumice for -850 + 600 µm feed size fraction ground with d = 30 mm ball diameter and U = 0,6.

Table C.31 Cumulative weight percent less than size values of pumice for - 850 + 600 µm size interval ground with d = 30 mm ball diameter and U = 1.

SIZE	0 min.	0,133 min	1 min	3 min	6 min
850	100,00	100,00	100,00	100,00	100,00
600	1,98	29,17	67,16	93,25	99,35
425	0,26	7,73	48,12	92,14	97,05
300	0,03	5,24	26,95	76,35	95,23
212	0,00	3,86	13,86	51,43	88,56
150	0,00	2,74	8,04	29,49	61,47
106	0,00	1,98	4,62	17,05	36,51
75	0,00	1,35	3,03	9,93	22,76
53	0,00	0,98	1,99	5,85	13,06
38	0,00	0,68	1,30	3,47	7,93
%w.r.top size	98,02	70,83	32,84	6,75	0,65

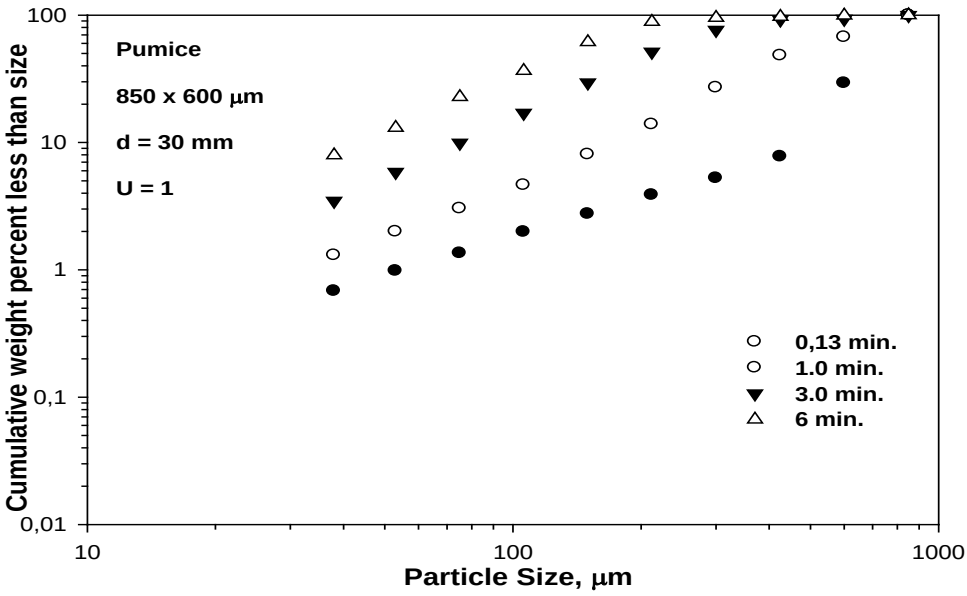

Figure C.47 Particle size distribution of pumice for -850 + 600 µm feed size fraction ground with d = 30 mm ball diameter and U = 1.

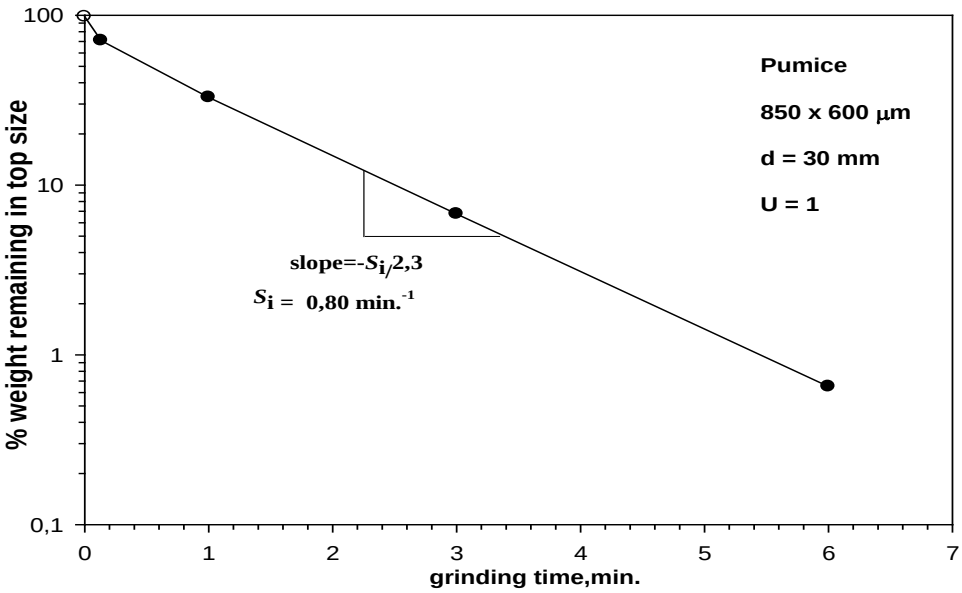

Figure C.48 First-order plot of breakage of - 850 + 600 µm feed of pumice ground with d = 30 mm ball diameter and U = 1.

425 x 300 micron

Table C.32 Determined B values of pumice for – 425 + 300 µm size interval ground with d = 30 mm ball diameter and U = 1.

INTERVAL NO,İ	SİZE (mesh)	Size (µm)	Xi/Xmax	B i,1	B VALUES
1	40x50	425x300	1,00	B1,1	1,0000
2	50x70	300x212	0,7	B2,1	1,0000
3	70x100	212x150	0,49	B3,1	0,2233
4	100x140	150x106	0,35	B4,1	0,1638
5	140x200	106x75	0,24	B5,1	0,1137
6	200x270	75x53	0,17	B6,1	0,0822
7	270x400	53x38	0,12	B7,1	0,0610
8	-400	-38	0,08	B8,1	0,0406

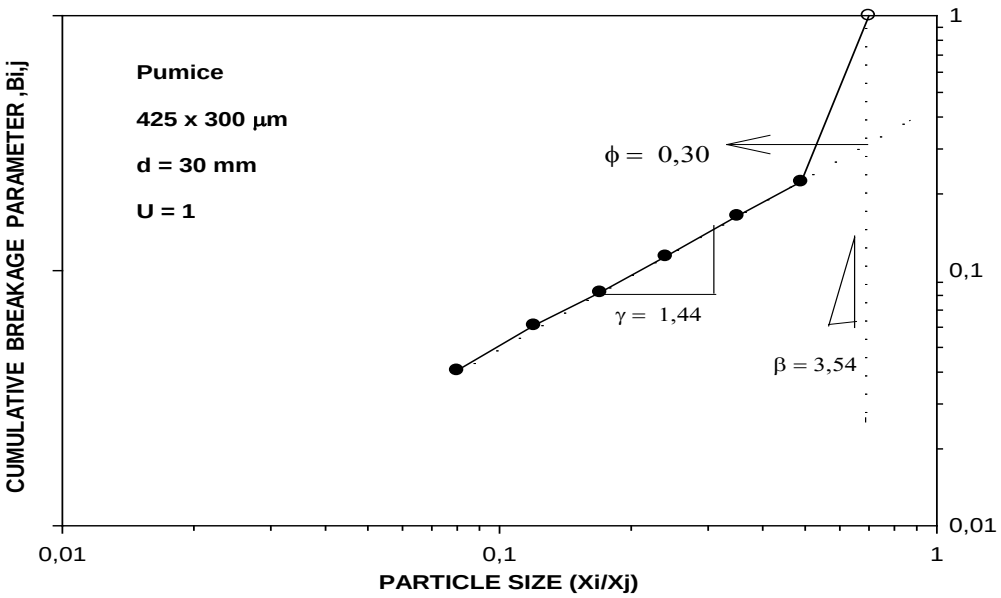

Figure C.49 Primary breakage distribution function of pumice for -425 + 300 µm feed size fraction ground with d = 30 mm ball diameter and U = 1.

Table C.33 Cumulative weight percent less than size values of pumice for - 425 + 300 µm size interval ground with d = 30 mm ball diameter and U = 1.

SIZE	0 min.	0,133 min	1 min	3 min	6 min
425	100,00	100,00	100,00	100,00	100,00
300	0,19	13,08	40,11	69,93	89,97
212	0,04	3,08	16,32	53,00	88,19
150	0,00	2,24	7,21	27,01	61,32
106	0,00	1,56	4,37	13,43	36,11
75	0,00	1,13	2,41	8,07	21,28
53	0,00	0,84	1,63	4,86	12,56
38	0,00	0,56	1,02	2,79	7,19
%w.r.top size	99,81	86,92	59,89	30,07	10,03

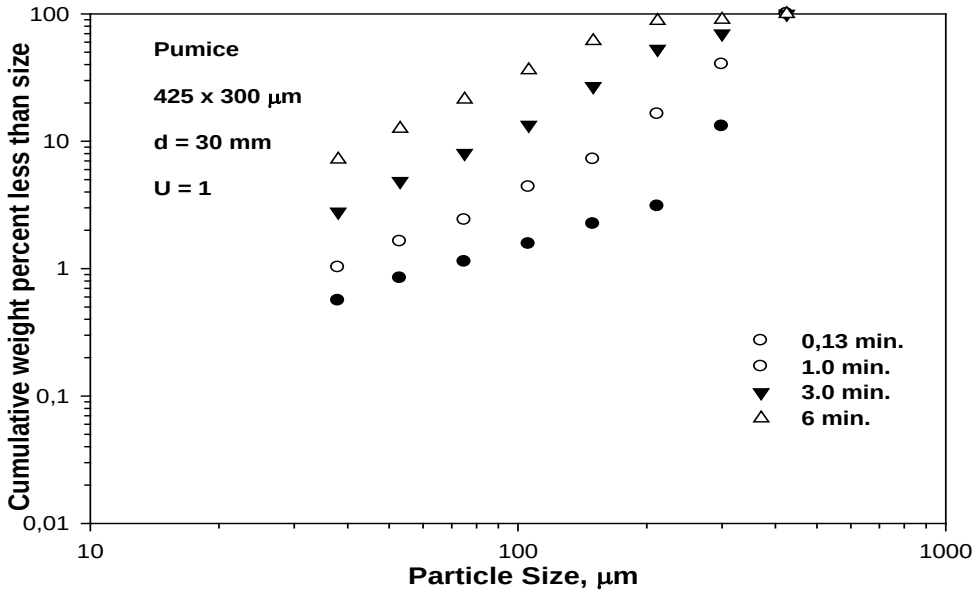

Figure C.50 Particle size distribution of pumice for -425 + 300 µm feed size fraction ground with d = 30 mm ball diameter and U = 1.

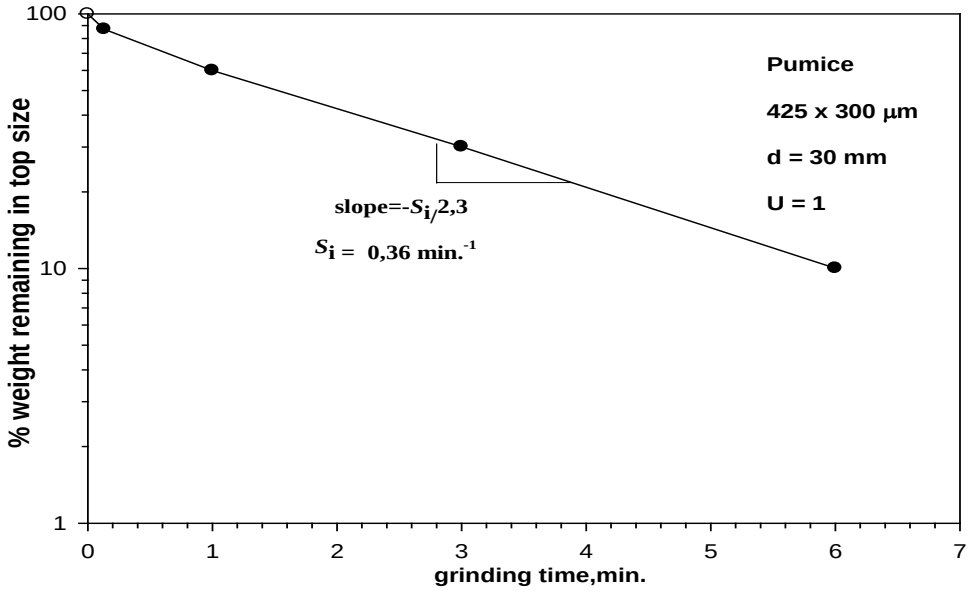

Figure C.51 First-order plot of breakage of - 425 + 300 µm feed of pumice ground with d = 30 mm ball diameter and U = 1.

212 x 150 micron

Table C.34 Determined B values of pumice for – 212 + 150 µm size interval ground with d = 30 mm ball diameter and U = 1.

INTERVAL NO,İ	SİZE (mesh)	Size (µm)	Xi/Xmax	B i,1	B VALUES
1	70x100	212x150	1,00	B1,1	1,0000
2	100x140	150x106	0,7	B2,1	1,0000
3	140x200	106x75	0,5	B3,1	0,2196
4	200x270	75x53	0,35	B4,1	0,1455
5	270x400	53x38	0,25	B5,1	0,1087
6	-400	-38	0,17	B6,1	0,0697

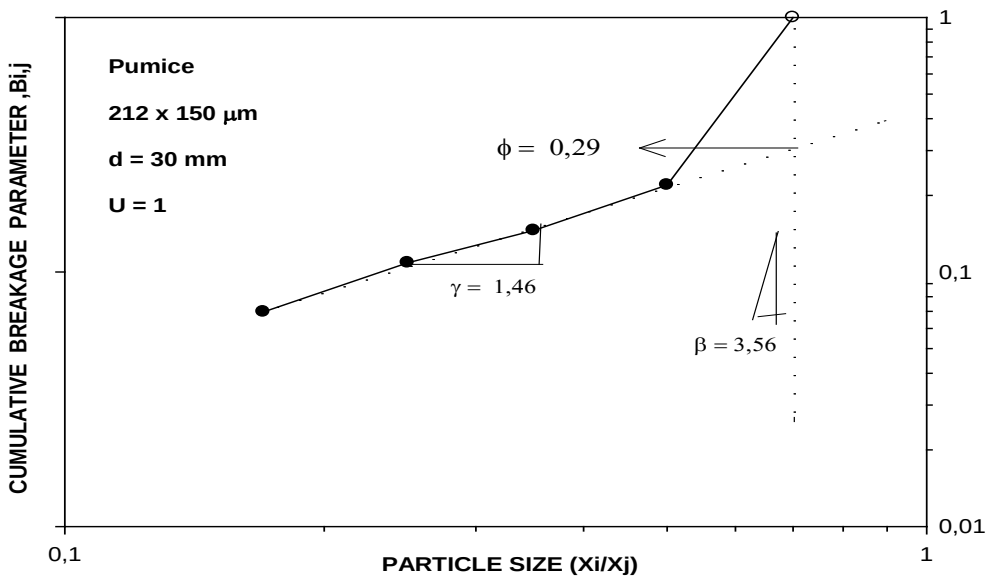

Figure C.52 Primary breakage distribution function of pumice for - 212 + 150 µm feed size fraction ground with d = 30 mm ball diameter and U = 1.

Table C.35 Cumulative weight percent less than size values of pumice for - 212 + 150 µm size interval ground with d = 30 mm ball diameter and U = 1.

SIZE	0 min.	0,133 min	1 min	3 min	6 min
212	100,00	100,00	100,00	100,00	100,00
150	0,11	8,51	25,12	46,82	69,08
106	0,03	1,94	6,92	19,45	34,78
75	0,00	1,27	2,81	8,66	18,16
53	0,00	0,95	1,74	4,07	9,65
38	0,00	0,61	1,13	2,26	5,28
%w.r.top size	99,89	91,49	74,88	53,18	30,92

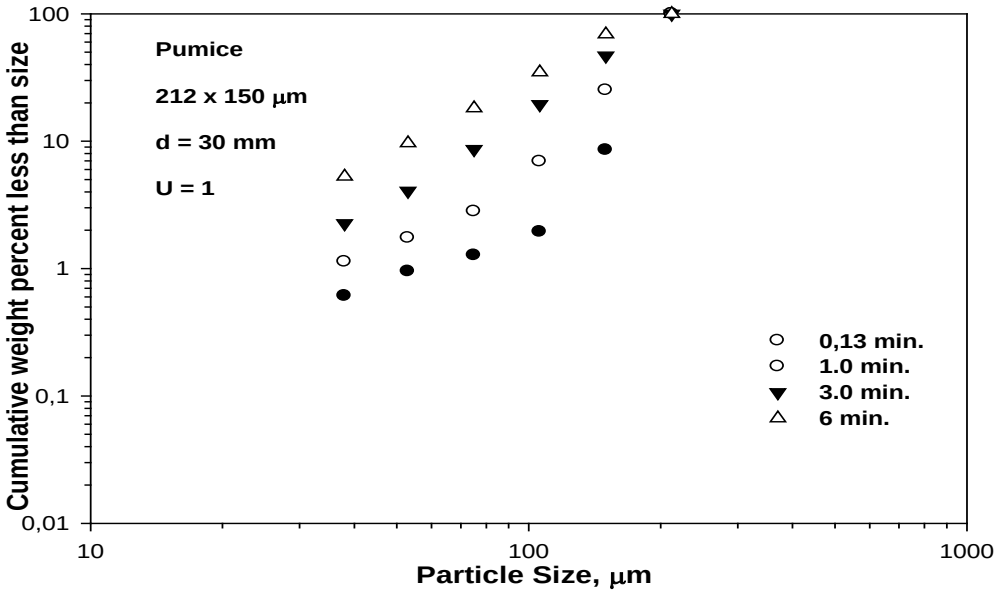

Figure C.53 Particle size distribution of pumice for -212 + 150 µm feed size fraction ground with d = 30 mm ball diameter and U = 1.

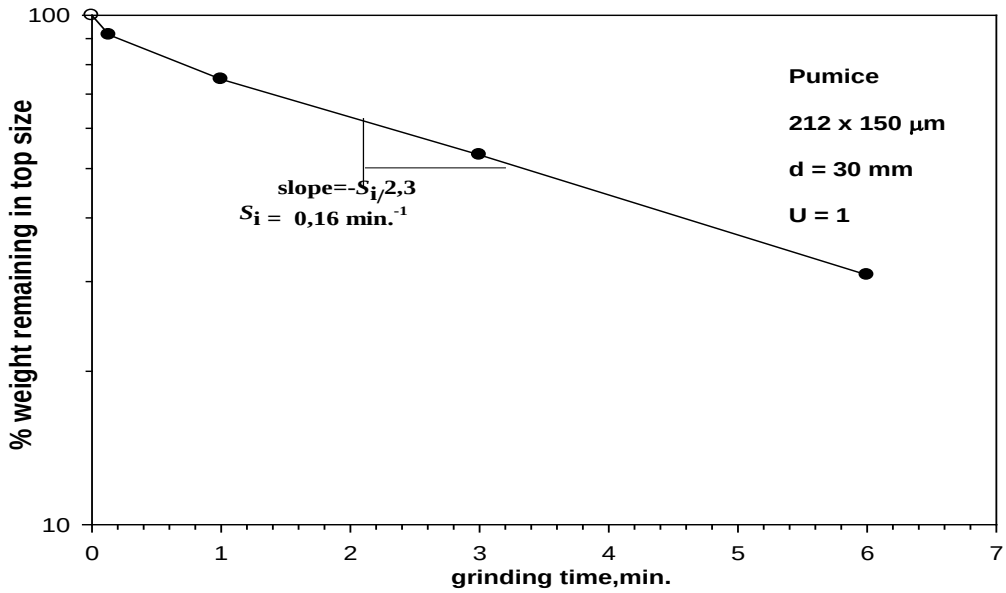

Figure C.54 First-order plot of breakage of - 212 + 150 µm feed of pumice ground with d = 30 mm ball diameter and U = 1.

Determination of aT value

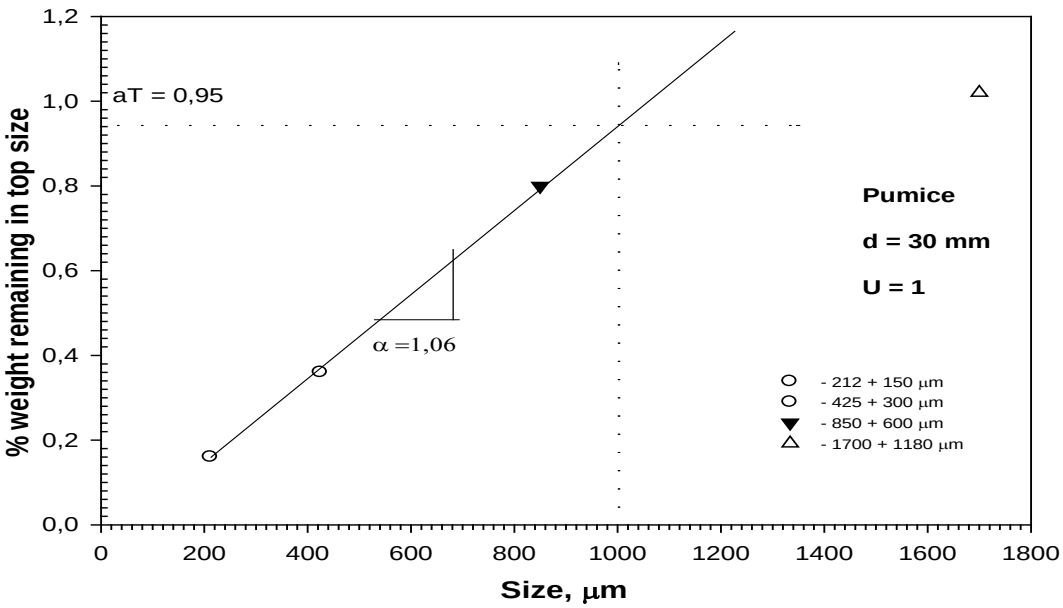

Figure C.55 Variation of first-order specific rates of breakage of pumice ground with d = 30 mm ball diameter and particle size: √2 intervals, plotted at upper size of interval at U=1.

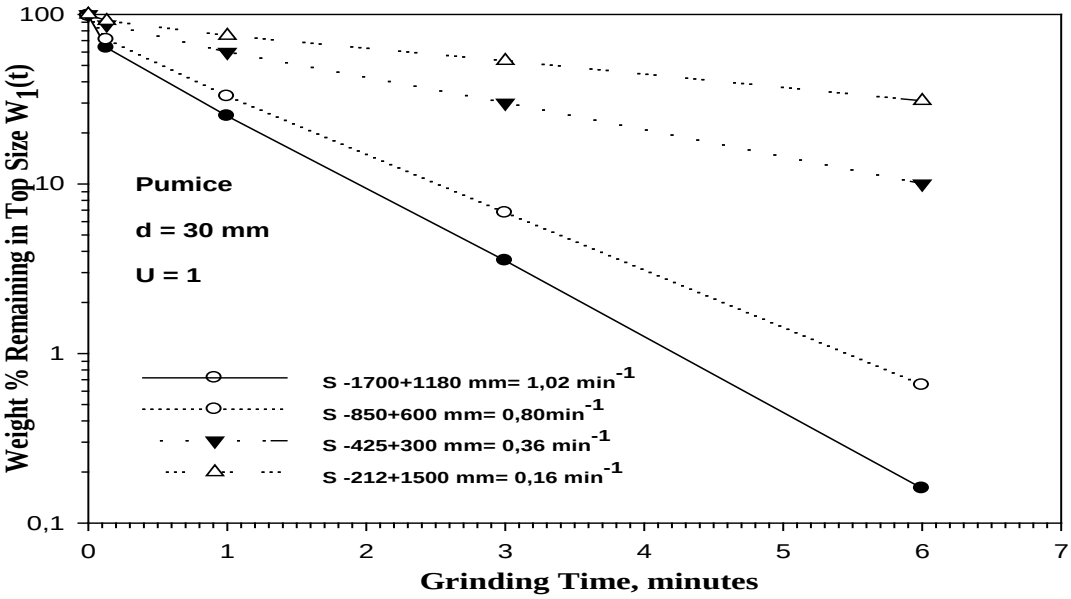

Figure C.56 First-order plots of breakage of -1700+1180, -850+600, -425+300, -212+150 μm feed size of pumice ground with d = 30 mm ball diameter and U=1.

Table C.36 Breakage parameters of pumice ground with d = 30 mm ball diameter at U=1.

1700x1180		**850x600**		**425x300**		**212x150**			
gama	1,16	**gama**	1,18	**gama**	1,19	**gama**	1,22		
beta	2,21	**beta**	2,23	**beta**	2,26	**beta**	2,29	**aT**	**α**
phi	0,51	**phi**	0,49	**phi**	0,47	**phi**	0,47	0,58	0,98
S value	0,56	**S value**	0,460	**S value**	0,240	**S value**	0,110		

30 – 25,4 – 19,05 mm ball size charge at U=0,6

1700 x 1180 micron

Table C.37 Determined B values of pumice for - 1700 + 1180 µm size interval ground with d = 30 – 25,4 – 19,05 mm ball diameter and U = 0,6.

INTERVAL NO,İ	SİZE (mesh)	Size (µm)	Xi/Xmax	B i,1	B VALUES
1	12x16	1700x1180	1,00	B1,1	1,0000
2	16x20	1180x850	0,69	B2,1	1,0000
3	20x30	850x600	0,50	B3,1	0,5423
4	30x40	600x425	0,35	B4,1	0,3434
5	40x50	425x300	0,25	B5,1	0,2064
6	50x70	300x212	0,17	B6,1	0,1266
7	70x100	212x150	0,12	B7,1	0,0802
8	100x140	150x106	0,088	B8,1	0,0512
9	140x200	106x75	0,062	B9,1	0,0297
10	200x270	75x53	0,044	B10,1	0,0191
11	270x400	53x38	0,031	B11,1	0,0113
12	-400	-38	0,022	B12,1	0,0072

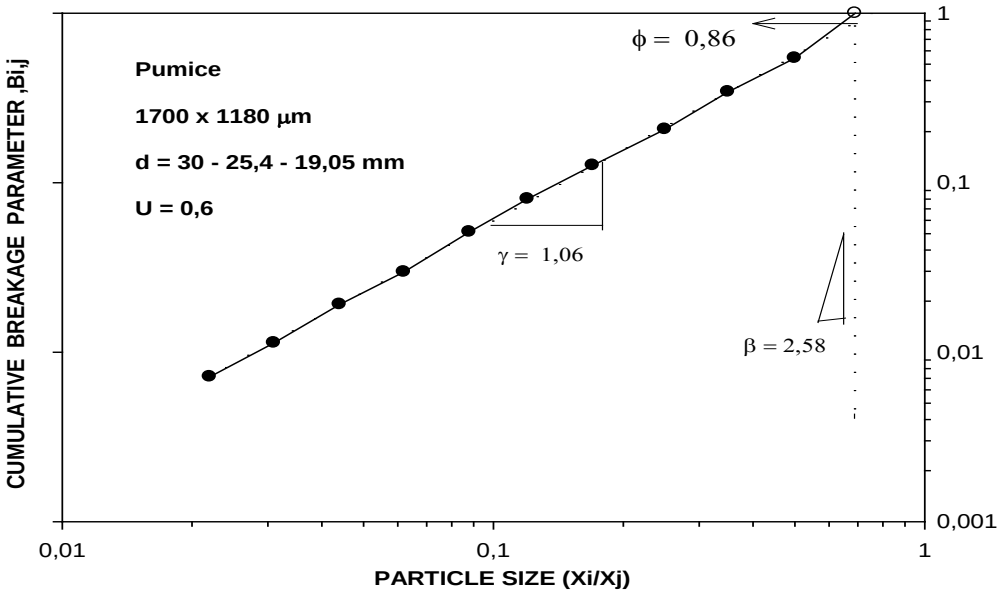

Figure C.57 Primary breakage distribution function of pumice for -1700 + 1180 µm feed size fraction ground with d = 30 – 25,4 – 19,05 mm ball diameter and U = 0,6.

Table C.38 Cumulative weight percent less than size values of pumice for 1700 x 1180 µm size interval ground with d = 30 – 25,4 – 19,05 mm ball diameter and U = 0,6.

SIZE	0 min.	0,133 min	1 min	3 min	6 min
1700	100,00	100,00	100,00	100,00	100,00
1180	2,12	70,73	92,00	99,71	100,00
850	0,16	48,12	67,17	99,08	100,00
600	0,04	33,96	48,59	96,77	99,95
425	0,00	22,05	35,19	88,31	99,89
300	0,00	14,17	26,03	71,37	99,13
212	0,00	9,23	18,85	52,38	92,04
150	0,00	5,99	12,99	35,46	67,41
106	0,00	3,52	8,79	23,09	43,72
75	0,00	2,28	6,16	16,01	30,52
53	0,00	1,36	4,23	11,49	20,82
38	0,00	0,86	2,73	7,91	13,94
%w.r.top size	97,88	29,27	8,00	0,29	0,00

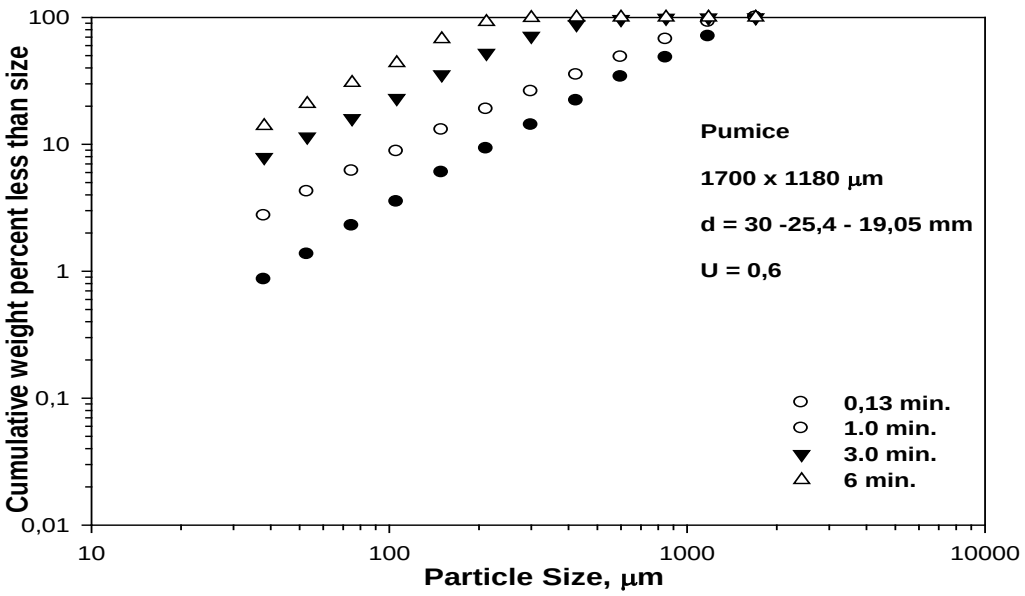

Figure C.58 Particle size distribution of pumice for -1700 + 1180 µm feed size fraction ground with d = 30 – 25,4 – 19,05 mm ball diameter and U = 0,6.

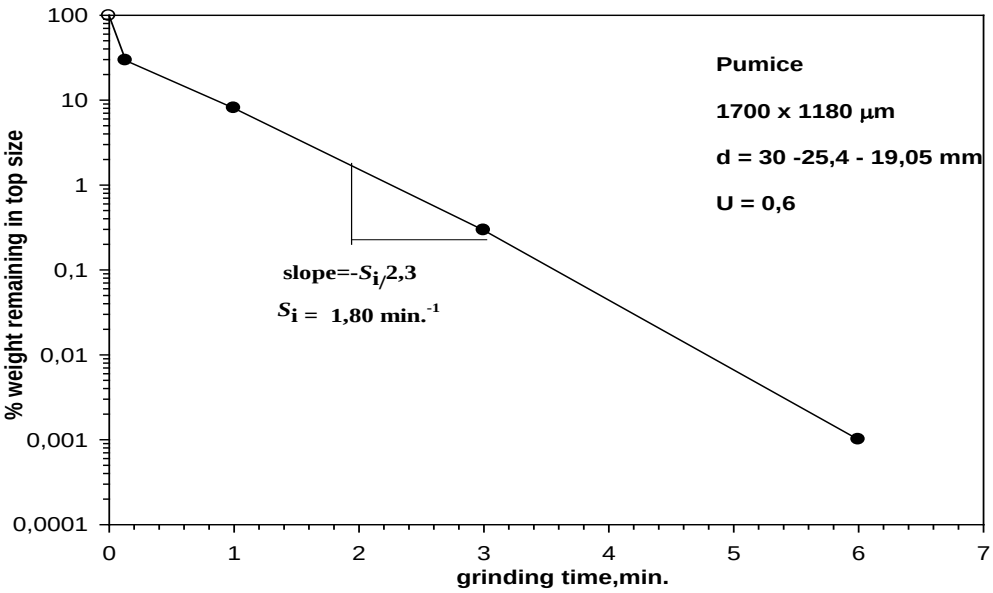

Figure C.59 First-order plot of breakage of - 1700 + 1180 µm feed of pumice ground with d = 30 – 25,4 – 19,05 mm ball diameter and U = 0,6.

850 x 600 micron

Table C.39 Determined B values of pumice for - 850 + 600 µm size interval ground with d = 30 – 25,4 – 19,05 mm ball diameter and U = 0,6.

INTERVAL NO,İ	SİZE (mesh)	Size (µm)	Xi/Xmax	B i,1	B VALUES
1	20x30	850x600	1,00	B3,1	1,0000
2	30x40	600x425	0,7	B4,1	1,0000
3	40x50	425x300	0,5	B5,1	0,5161
4	50x70	300x212	0,35	B6,1	0,3189
5	70x100	212x150	0,24	B7,1	0,2031
6	100x140	150x106	0,17	B8,1	0,1304
7	140x200	106x75	0,12	B9,1	0,0778
8	200x270	75x53	0,08	B10,1	0,0457
9	270x400	53x38	0,06	B11,1	0,0314
10	-400	-38	0,04	B12,1	0,0187

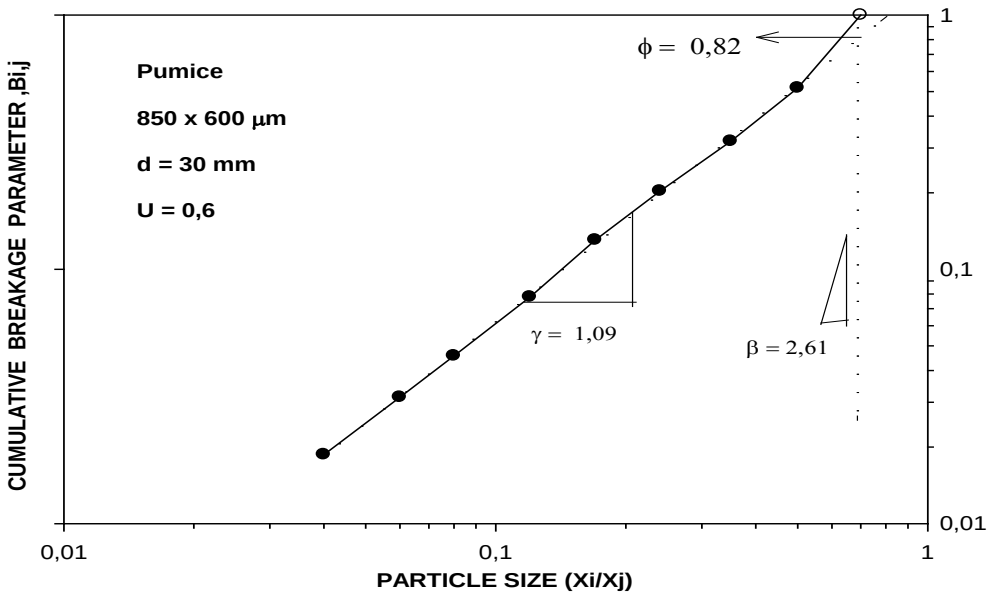

Figure C.60 Primary breakage distribution function of pumice for -850 + 600 µm feed size fraction ground with d = 30 – 25,4 – 19,05 mm ball diameter and U = 0,6.

Table C.40 Cumulative weight percent less than size values of pumice for - 850 + 600 µm size interval ground with d = 30 – 25,4 – 19,05 mm ball diameter and U = 0,6.

SIZE	0 min.	0,133 min	1 min	3 min	6 min
850	100,00	100,00	100,00	100,00	100,00
600	3,96	54,35	88,30	99,50	100,00
425	0,27	32,06	61,41	97,46	99,99
300	0,02	21,13	39,91	85,02	99,43
212	0,00	14,02	26,01	60,29	93,69
150	0,00	9,24	16,79	37,82	66,56
106	0,00	5,62	10,70	24,13	42,34
75	0,00	3,34	7,12	16,32	28,79
53	0,00	2,31	4,84	10,92	18,81
38	0,00	1,38	3,31	7,55	11,80
%w.r.top size	96,04	45,65	11,70	0,50	0,00

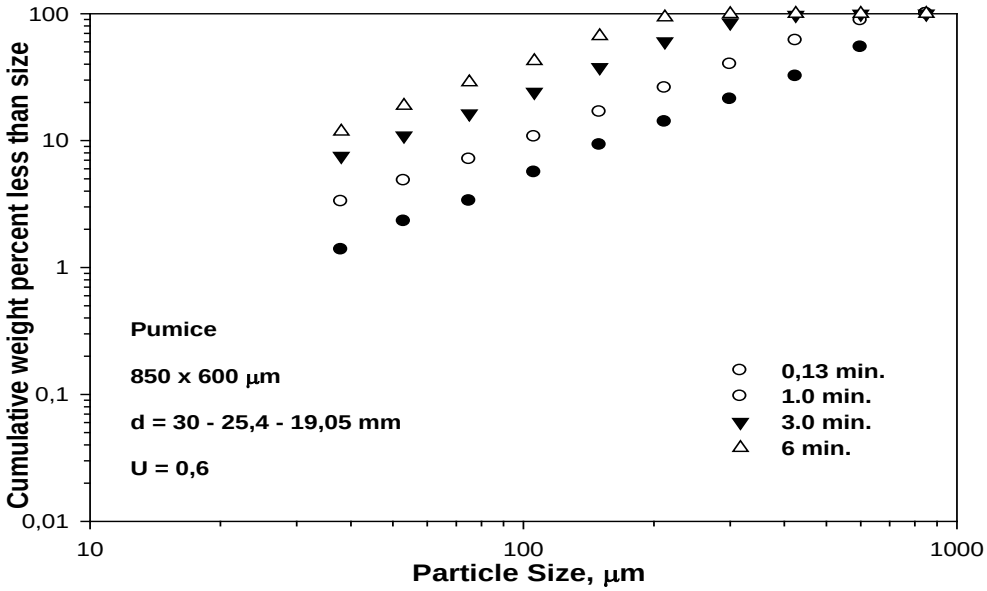

Figure C.61 Particle size distribution of pumice for -850 + 600 µm feed size fraction ground with d = 30 – 25,4 – 19,05 mm ball diameter and U = 0,6.

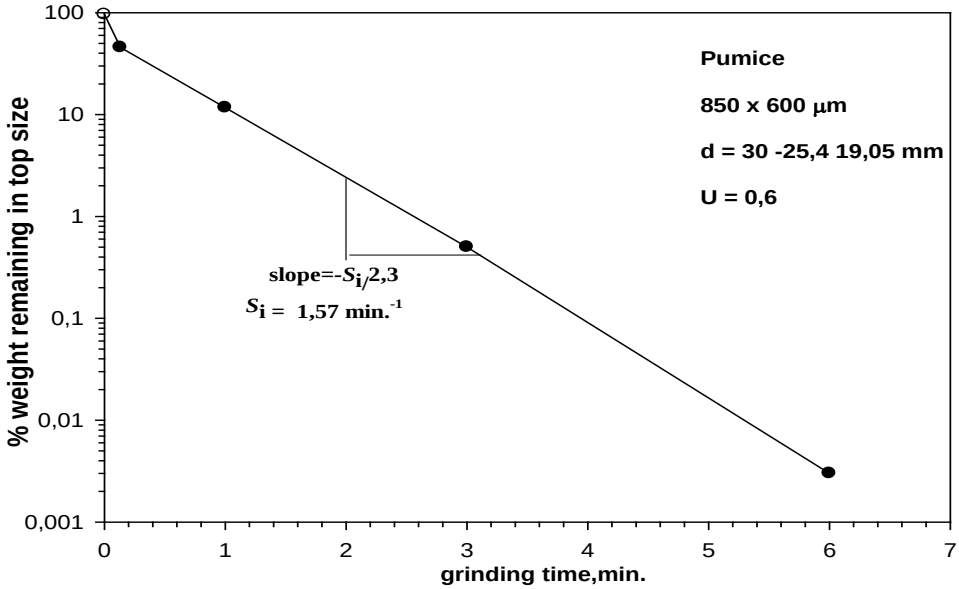

Figure C.62 First-order plot of breakage of - 850 + 600 µm feed of pumice ground with d = 30 – 25,4 – 19,05 mm ball diameter and U = 0,6.

425 x 300 micron

Table C.41 Determined B values of pumice for – 425 + 300 µm size interval ground with d = 30 – 25,4 – 19,05 mm ball diameter and U = 0,6.

INTERVAL NO,İ	SİZE (mesh)	Size (µm)	Xi/Xmax	B i,1	B VALUES
1	40x50	425x300	1,00	B1,1	1,0000
2	50x70	300x212	0,7	B2,1	1,0000
3	70x100	212x150	0,49	B3,1	0,4699
4	100x140	150x106	0,35	B4,1	0,2925
5	140x200	106x75	0,24	B5,1	0,1604
6	200x270	75x53	0,17	B6,1	0,0961
7	270x400	53x38	0,12	B7,1	0,0582
8	-400	-38	0,08	B8,1	0,0337

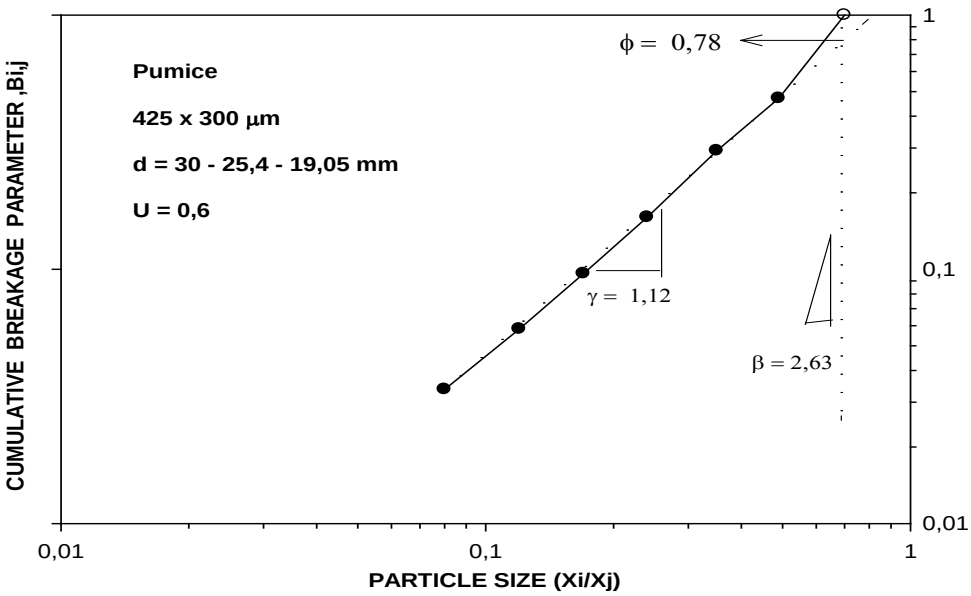

Figure C.63 Primary breakage distribution function of pumice for -425 + 300 µm feed size fraction ground with d = 30 – 25,4 – 19,05 mm ball diameter and U = 0,6.

Table C.42 Cumulative weight percent less than size values of pumice for - 425 + 300 µm size interval ground with d = 30 – 25,4 – 19,05 mm ball diameter and U = 0,6.

SIZE	0 min.	0,133 min	1 min	3 min	6 min
425	100	100,00	100,00	100,00	100,00
300	0,26	22,12	61,44	94,30	99,68
212	0,05	11,02	30,78	69,49	95,60
150	0,00	6,98	16,24	39,07	69,59
106	0,00	3,89	9,19	22,73	41,10
75	0,00	2,35	5,98	14,89	27,16
53	0,00	1,43	3,81	9,75	17,80
38	0,00	0,83	2,10	5,20	11,26
%w.r.top size	99,74	77,88	38,56	5,70	0,32

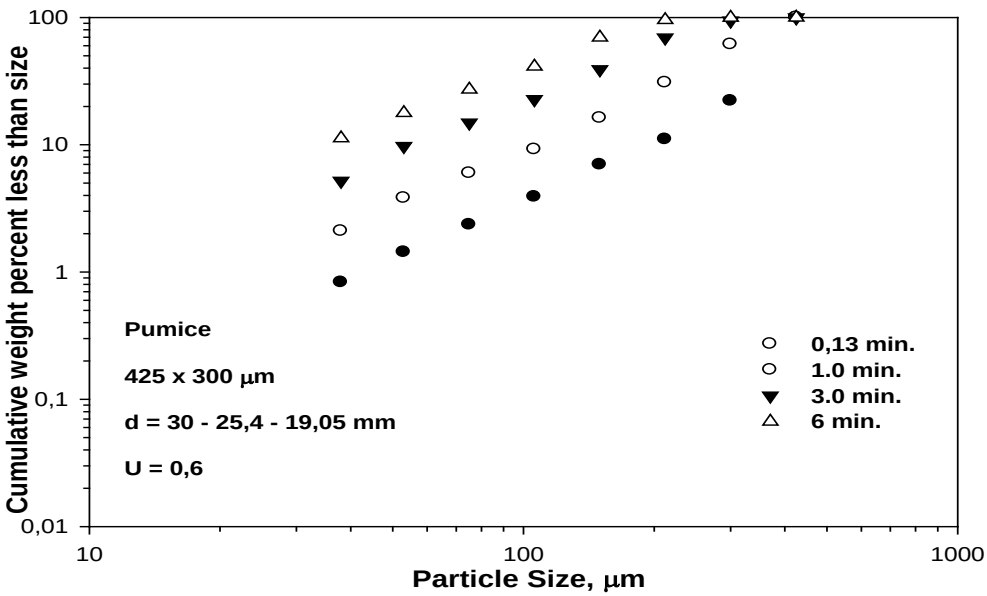

Figure C.64 Particle size distribution of pumice for -425 + 300 µm feed size fraction ground with d = 30 – 25,4 – 19,05 mm ball diameter and U = 0,6.

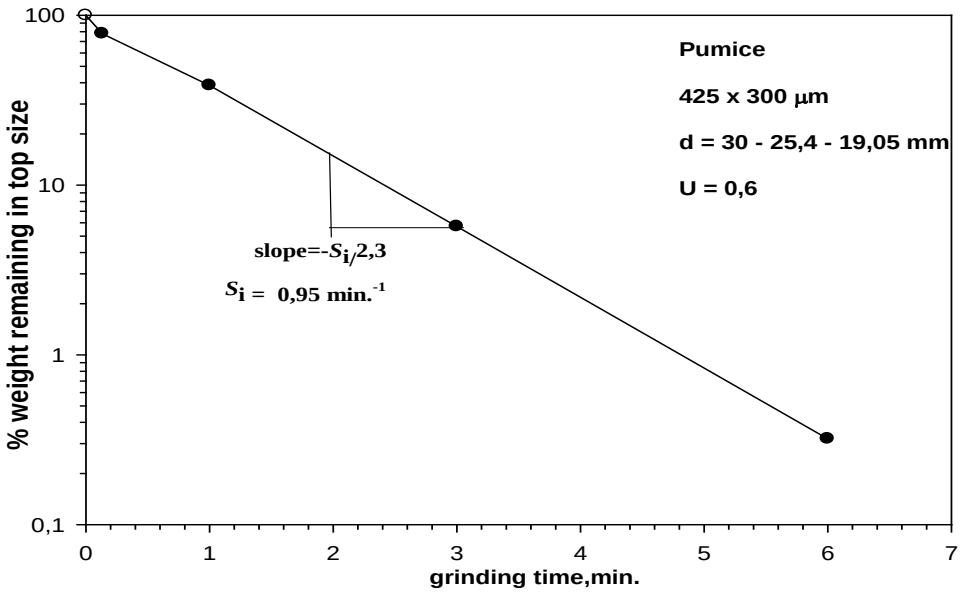

Figure C.65 First-order plot of breakage of - 425 + 300 µm feed of pumice ground with d = 30 – 25,4 – 19,05 mm ball diameter and U = 0,6.

212 x 150 micron

Table C.43 Determined B values of pumice for – 212 + 150 µm size interval ground with d = 30 – 25,4 – 19,05 mm ball diameter and U = 0,6.

INTERVAL NO,İ	SİZE (mesh)	Size (µm)	Xi/Xmax	B i,1	B VALUES
1	70x100	212x150	1,00	B1,1	1,0000
2	100x140	150x106	0,7	B2,1	1,0000
3	140x200	106x75	0,5	B3,1	0,4567
4	200x270	75x53	0,35	B4,1	0,2658
5	270x400	53x38	0,25	B5,1	0,1666
6	-400	-38	0,17	B6,1	0,0884

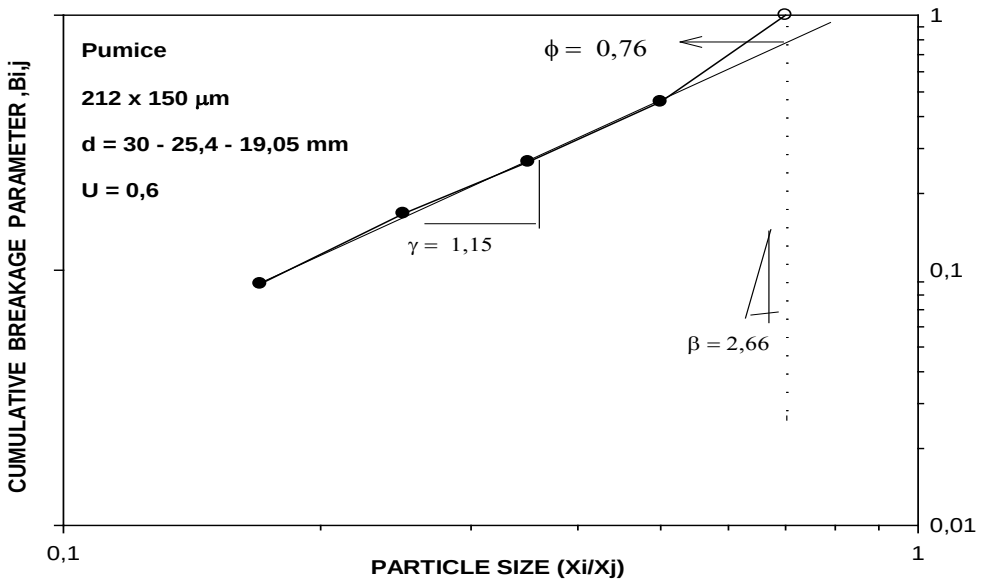

Figure C.66 Primary breakage distribution function of pumice for - 212 + 150 µm feed size fraction ground with d = 30 – 25,4 – 19,05 mm ball diameter and U = 0,6.

Table C.44 Cumulative weight percent less than size values of pumice for - 212 + 150 µm size interval ground with d = 30 – 25,4 – 19,05 mm ball diameter and U = 0,6.

SIZE	0 min.	0,133 min	1 min	3 min	6 min
212	100	100,00	100,00	100,00	100,00
150	0,26	15,06	47,64	81,97	96,20
106	0,04	7,11	12,74	30,06	50,74
75	0,00	4,18	7,48	18,22	31,76
53	0,00	2,64	4,43	11,20	20,83
38	0,00	1,41	2,84	6,27	12,09
%w.r.top size	99,74	84,94	52,36	18,03	3,80

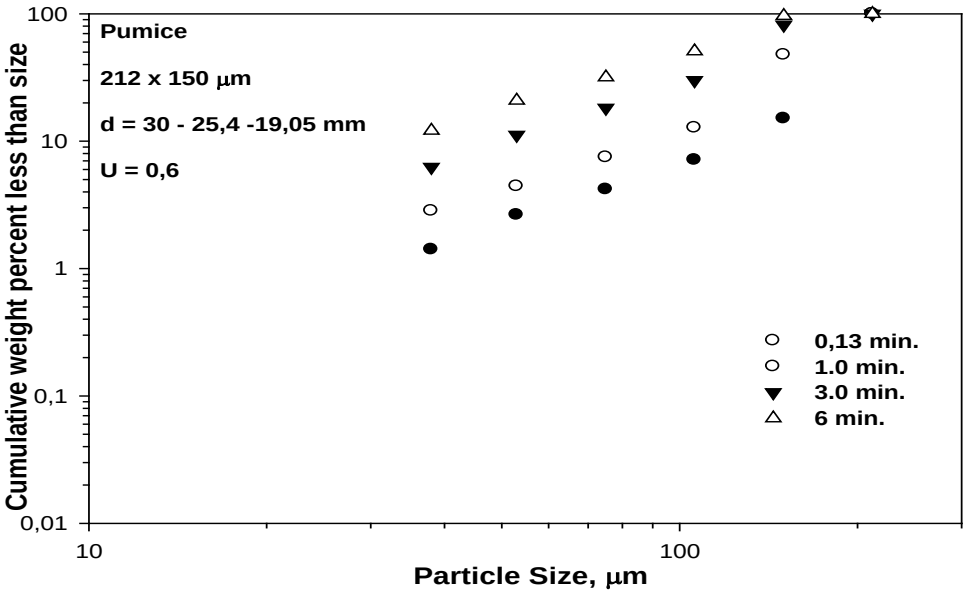

Figure C.67 Particle size distribution of pumice for -212 + 150 µm feed size fraction ground with d = 30 – 25,4 – 19,05 mm ball diameter and U = 0,6.

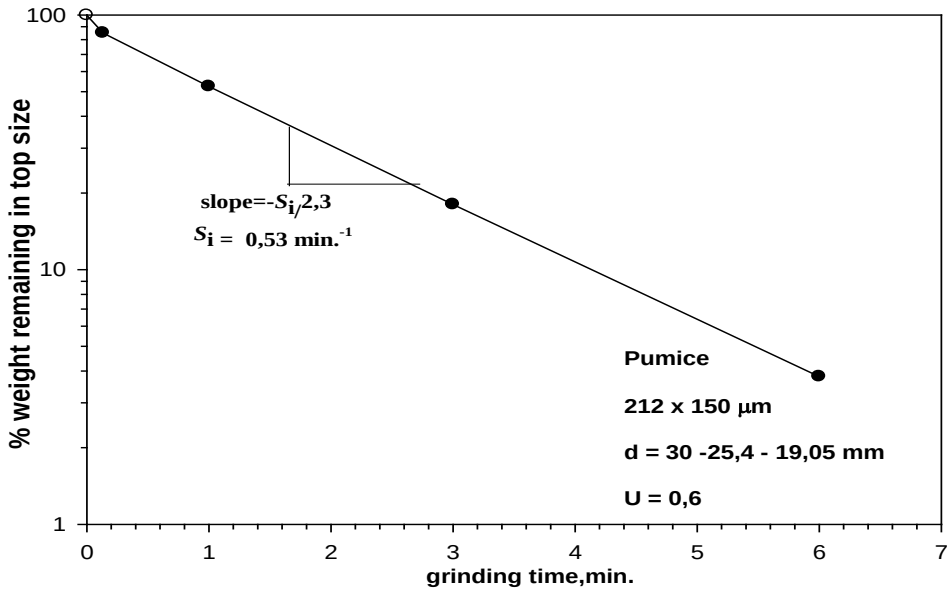

Figure C.68 First-order plot of breakage of - 212 + 150 µm feed of pumice ground with d = 30 – 25,4 – 19,05 mm ball diameter and U = 0,6.

Determination of aT value

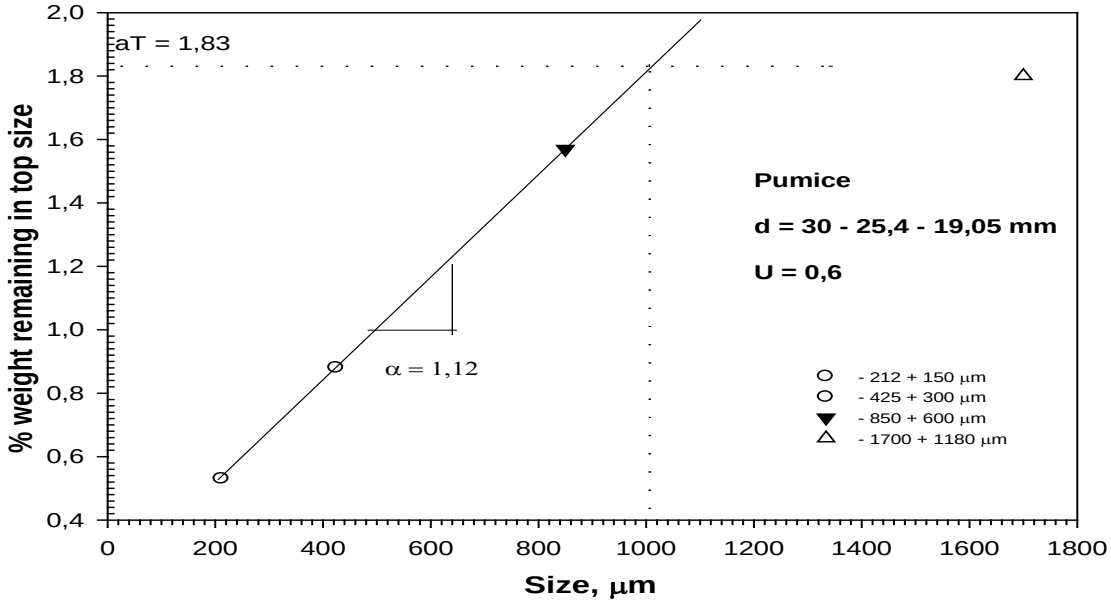

Figure C.69 Variation of first-order specific rates of breakage of pumice ground with d = 30 – 25,4 - 19,05 mm ball diameter and particle size: √2 intervals, plotted at upper size of interval at U=0,6.

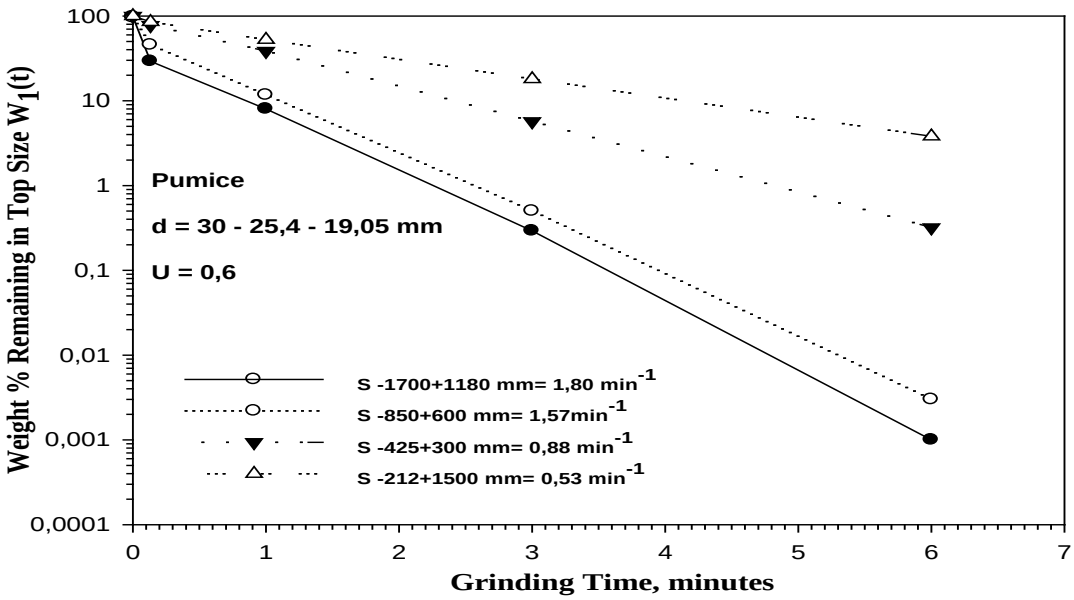

Figure C.70 First-order plots of breakage of -1700+1180, -850+600, -425+300, -212+150 μm feed size of pumice ground with d = 30 – 25,4 – 19,05 mm ball diameter and U=0,6.

Table C.45 Breakage parameters of pumice ground with d = 30 – 25,4 – 19,05 mm ball diameter at U=0,6.

1700x1180		**850x600**		**425x300**		**212x150**			
gama	0,92	**gama**	0,95	**gama**	0,96	**gama**	0,98		
beta	3,11	**beta**	3,14	**beta**	3,17	**beta**	3,19	**aT**	**α**
phi	0,64	**phi**	0,62	**phi**	0,60	**phi**	0,58	1,07	0,89
S value	1,060	**S value**	0,920	**S value**	0,490	**S value**	0,280		

30 -25,4 – 19,05 mm ball size charge at U= 1

1700 x 1180 micron

Table C.46 Determined B values of pumice for - 1700 + 1180 µm size interval ground with d = 30 – 25,4 – 19,05 mm ball diameter and U = 1.

INTERVAL NO,İ	**SİZE (mesh)**	**Size (µm)**	**Xi/Xmax**	**B i,1**	**B VALUES**
1	12x16	1700x1180	1,00	B1,1	1,0000
2	16x20	1180x850	0,69	B2,1	1,0000
3	20x30	850x600	0,50	B3,1	0,2783
4	30x40	600x425	0,35	B4,1	0,2049
5	40x50	425x300	0,25	B5,1	0,1493
6	50x70	300x212	0,17	B6,1	0,1003
7	70x100	212x150	0,12	B7,1	0,0735
8	100x140	150x106	0,088	B8,1	0,0535
9	140x200	106x75	0,062	B9,1	0,0391
10	200x270	75x53	0,044	B10,1	0,0283
11	270x400	53x38	0,031	B11,1	0,0212
12	-400	-38	0,022	B12,1	0,0158

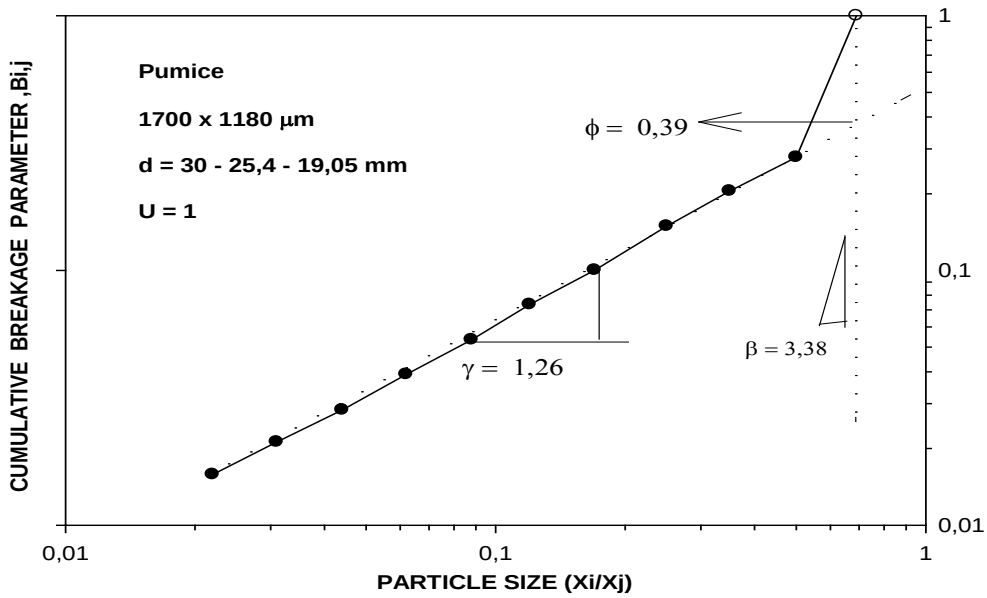

Figure C.71 Primary breakage distribution function of pumice for -1700 + 1180 µm feed size fraction ground with d = 30 – 25,4 – 19,05 mm ball diameter and U = 1.

Table C.47 Cumulative weight percent less than size values of pumice for 1700 x 1180 µm size interval ground with d = 30 – 25,4 – 19,05 mm ball diameter and U = 1.

SIZE	0 min.	0,133 min	1 min	3 min	6 min
1700	100,00	100,00	100,00	100,00	100,00
1180	1,96	42,51	83,13	99,09	99,99
850	0,08	13,87	65,26	98,26	98,92
600	0,00	10,36	45,41	95,13	98,16
425	0,00	7,66	29,53	86,03	97,23
300	0,00	5,21	18,61	69,41	96,19
212	0,00	3,85	11,66	50,06	90,16
150	0,00	2,81	6,70	32,29	65,02
106	0,00	2,06	4,00	21,02	40,93
75	0,00	1,50	2,50	14,06	27,91
53	0,00	1,13	1,60	9,87	18,06
38	0,00	0,84	1,20	6,31	11,42
%w.r.top size	98,04	57,49	16,87	0,91	0,01

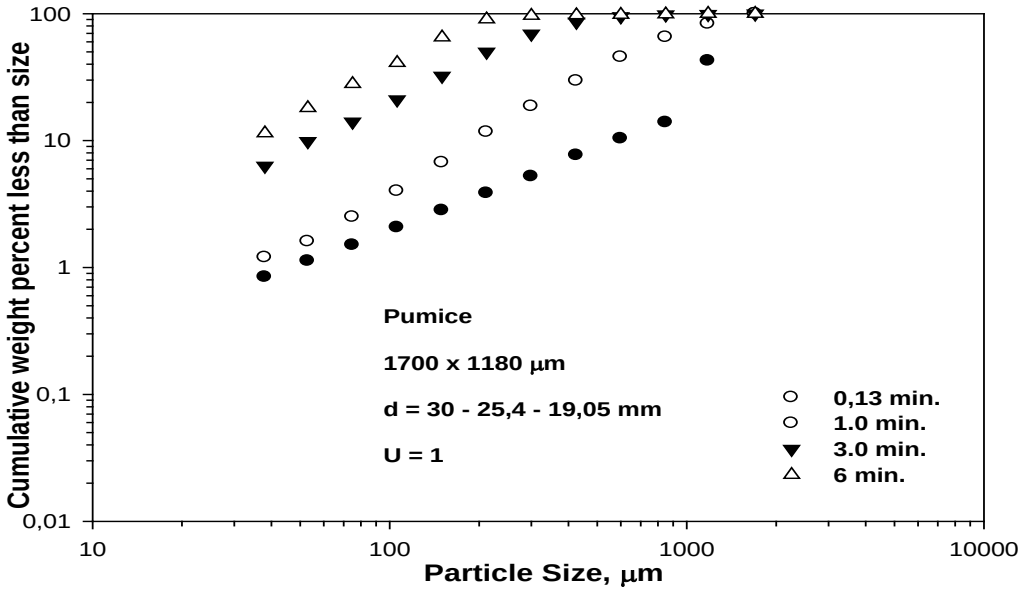

Figure C.72 Particle size distribution of pumice for -1700 + 1180 µm feed size fraction ground with d = 30 – 25,4 – 19,05 mm ball diameter and U = 1.

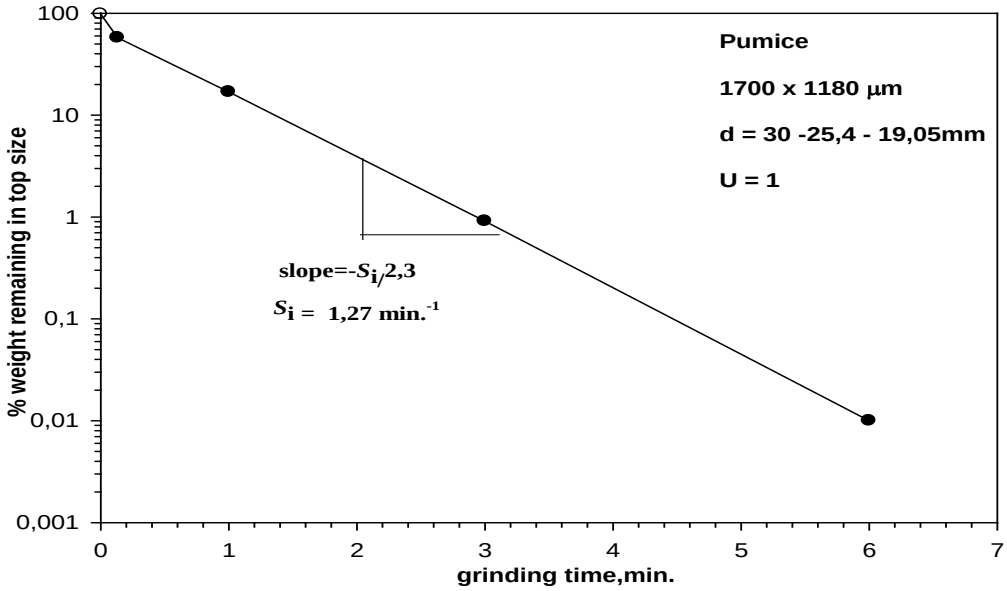

Figure C.73 First-order plot of breakage of - 1700 + 1180 µm feed of pumice ground with d = 30 – 25,4 – 19,05 mm ball diameter and U = 1.

850 x 600 micron

Table C.48 Determined B values of pumice for - 850 + 600 µm size interval ground with d = 30 – 25,4 – 19,05 mm ball diameter and U = 1.

INTERVAL NO,İ	SİZE (mesh)	Size (µm)	Xi/Xmax	B i,1	B VALUES
1	20x30	850x600	1,00	B3,1	1,0000
2	30x40	600x425	0,7	B4,1	1,0000
3	40x50	425x300	0,5	B5,1	0,2786
4	50x70	300x212	0,35	B6,1	0,2051
5	70x100	212x150	0,24	B7,1	0,1473
6	100x140	150x106	0,17	B8,1	0,1017
7	140x200	106x75	0,12	B9,1	0,0730
8	200x270	75x53	0,08	B10,1	0,0522
9	270x400	53x38	0,06	B11,1	0,0391
10	-400	-38	0,04	B12,1	0,0287

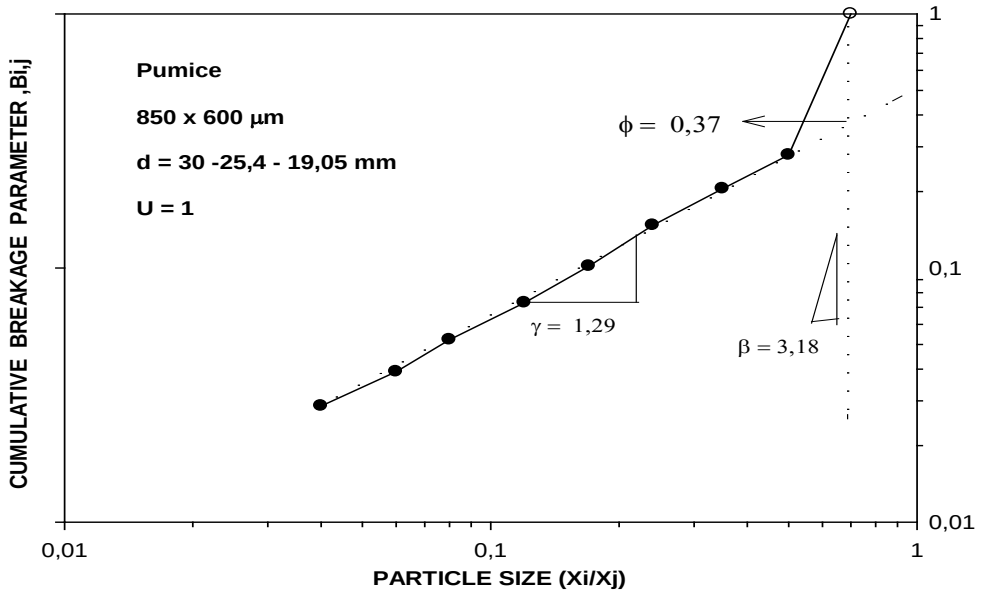

Figure C.74 Primary breakage distribution function of pumice for -850 + 600 µm feed size fraction ground with d = 30 – 25,4 – 19,05 mm ball diameter and U = 1.

Table C.49 Cumulative weight percent less than size values of pumice for - 850 + 600 µm size interval ground with d = 30 – 25,4 – 19,05 mm ball diameter and U = 1.

SIZE	0 min.	0,133 min	1 min	3 min	6 min
850	100,00	100,00	100,00	100,00	100,00
600	2,16	33,02	76,02	97,63	99,92
425	0,11	10,12	55,46	95,08	98,12
300	0,00	7,48	34,24	81,36	97,36
212	0,00	5,43	21,66	57,02	91,42
150	0,00	3,78	12,18	34,41	65,13
106	0,00	2,73	6,76	22,09	41,06
75	0,00	1,96	3,56	13,07	27,12
53	0,00	1,47	2,20	7,94	17,44
38	0,00	1,08	1,42	4,81	10,61
%w.r.top size	97,84	66,98	23,98	2,37	0,08

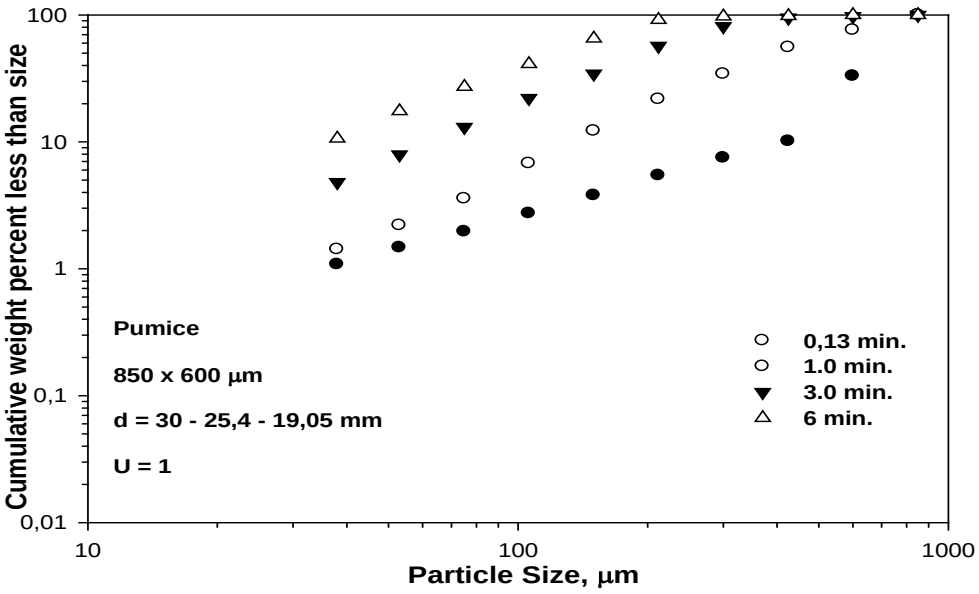

Figure C.75 Particle size distribution of pumice for -850 + 600 µm feed size fraction ground with d = 30 – 25,4 – 19,05 mm ball diameter and U = 1.

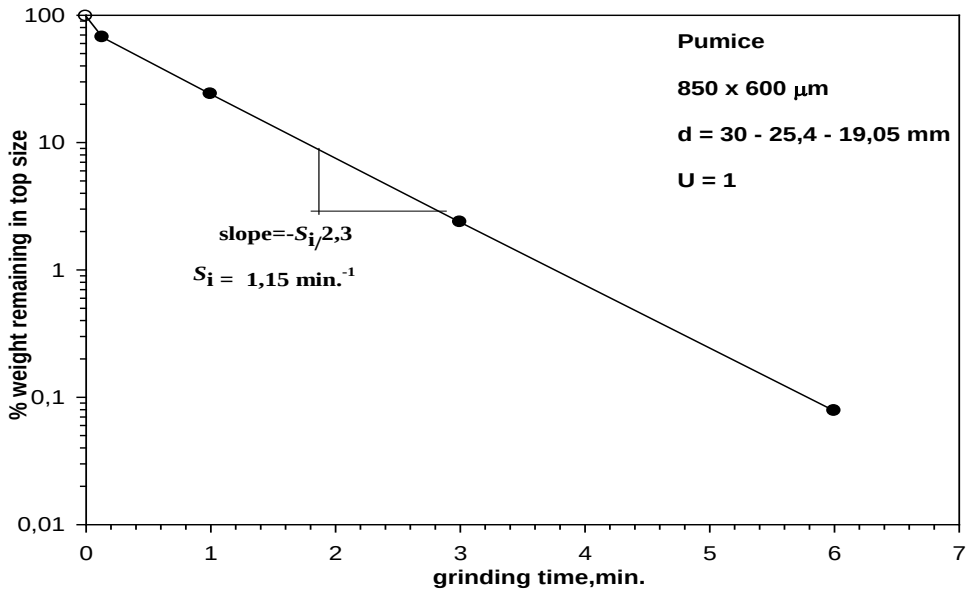

Figure C.76 First-order plot of breakage of - 850 + 600 µm feed of pumice ground with d = 30 – 25,4 – 19,05 mm ball diameter and U = 1.

425 x 300 micron

Table C.50 Determined B values of pumice for – 425 + 300 µm size interval ground with d = 30 – 25,4 – 19,05 mm ball diameter and U = 1.

INTERVAL NO,İ	SİZE (mesh)	Size (µm)	Xi/Xmax	B i,1	B VALUES
1	40x50	425x300	1,00	B1,1	1,0000
2	50x70	300x212	0,7	B2,1	1,0000
3	70x100	212x150	0,49	B3,1	0,2763
4	100x140	150x106	0,35	B4,1	0,2028
5	140x200	106x75	0,24	B5,1	0,1485
6	200x270	75x53	0,17	B6,1	0,1007
7	270x400	53x38	0,12	B7,1	0,0724
8	-400	-38	0,08	B8,1	0,0528

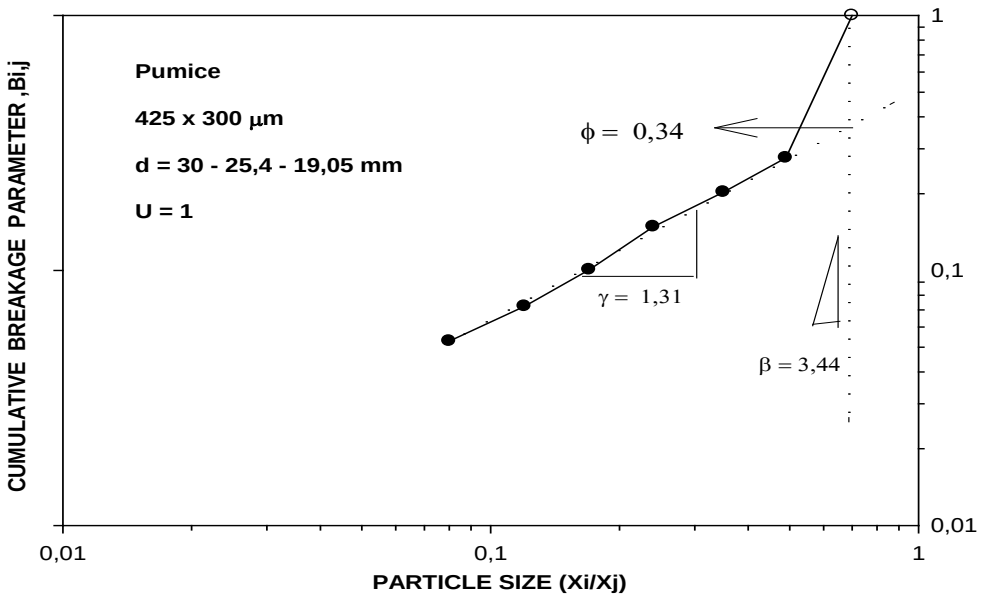

Figure C.77 Primary breakage distribution function of pumice for -425 + 300 µm feed size fraction ground with d = 30 – 25,4 – 19,05 mm ball diameter and U = 1.

Table C.51 Cumulative weight percent less than size values of pumice for - 425 + 300 µm size interval ground with d = 30 – 25,4 – 19,05 mm ball diameter and U = 1.

SIZE	0 min.	0,133 min	1 min	3 min	6 min
425	100,00	100,00	100,00	100,00	100,00
300	0,12	17,11	58,13	88,04	98,47
212	0,01	5,03	29,43	68,02	94,12
150	0,00	3,71	16,27	37,91	66,83
106	0,00	2,73	9,57	21,06	40,02
75	0,00	1,86	5,26	13,02	26,06
53	0,00	1,34	2,87	8,12	15,82
38	0,00	0,98	1,62	4,39	10,33
%w.r.top size	99,88	82,89	41,87	11,96	1,53

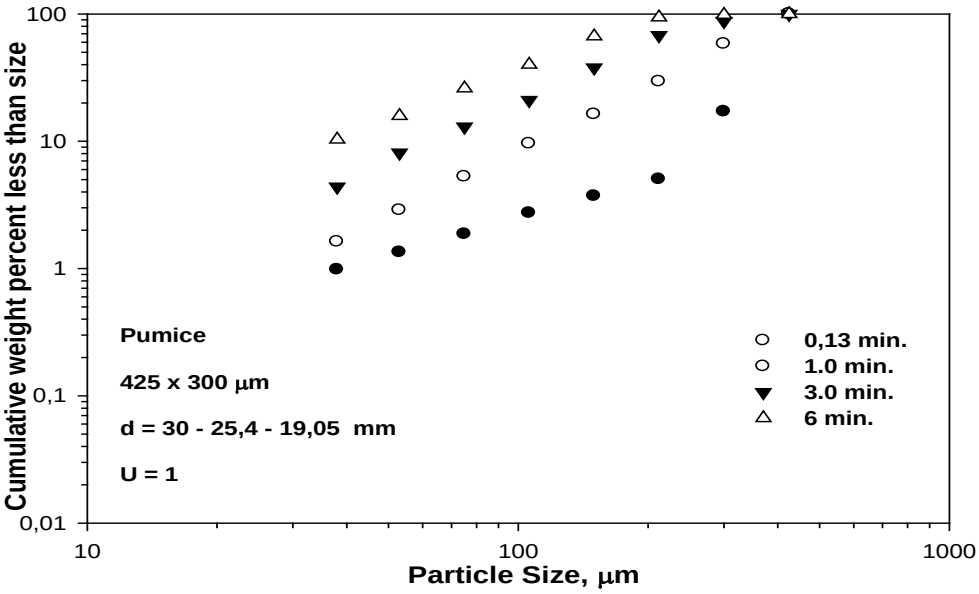

Figure C.78 Particle size distribution of pumice for -425 + 300 µm feed size fraction ground with d = 30 – 25,4 – 19,05 mm ball diameter and U = 1.

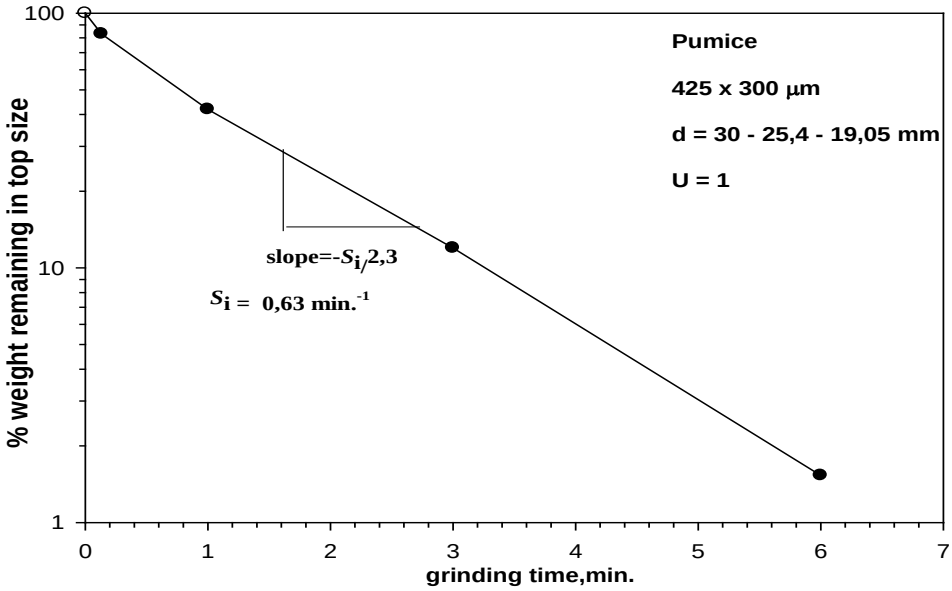

Figure C.79 First-order plot of breakage of - 425 + 300 µm feed of pumice ground with d = 30 – 25,4 – 19,05 mm ball diameter and U = 1.

212 x 150 micron

Table C.52 Determined B values of pumice for – 212 + 150 µm size interval ground with d = 30 – 25,4 – 19,05 mm ball diameter and U = 1.

INTERVAL NO,İ	SİZE (mesh)	Size (µm)	Xi/Xmax	B i,1	B VALUES
1	70x100	212x150	1,00	B1,1	1,0000
2	100x140	150x106	0,7	B2,1	1,0000
3	140x200	106x75	0,5	B3,1	0,2733
4	200x270	75x53	0,35	B4,1	0,1852
5	270x400	53x38	0,25	B5,1	0,1373
6	-400	-38	0,17	B6,1	0,0904

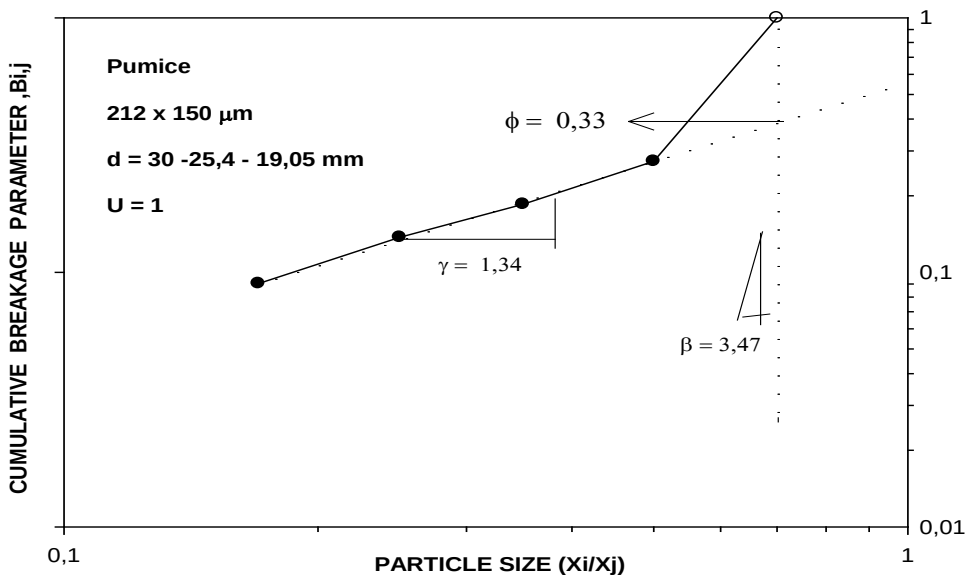

Figure C.80 Primary breakage distribution function of pumice for - 212 + 150 µm feed size fraction ground with d = 30 – 25,4 – 19,05 mm ball diameter and U = 1.

Table C.53 Cumulative weight percent less than size values of pumice for - 212 + 150 µm size interval ground with d = 30 – 25,4 – 19,05 mm ball diameter and U = 1.

SIZE	0 min.	0,133 min	1 min	3 min	6 min
212	100,00	100,00	100,00	100,00	100,00
150	0,16	11,36	38,43	69,91	90,04
106	0,00	3,20	9,32	27,38	47,68
75	0,00	2,38	5,21	15,21	28,03
53	0,00	1,72	2,88	9,06	18,12
38	0,00	1,17	1,61	5,02	10,09
%w.r.top size	99,84	88,64	61,57	30,09	9,96

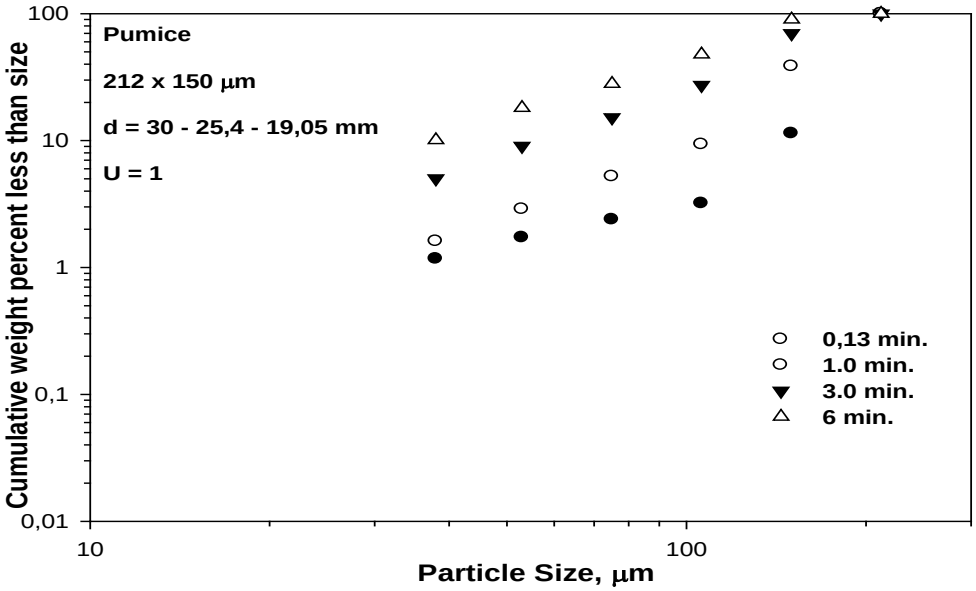

Figure C.81 Particle size distribution of pumice for -212 + 150 µm feed size fraction ground with d = 30 – 25,4 – 19,05 mm ball diameter and U = 1.

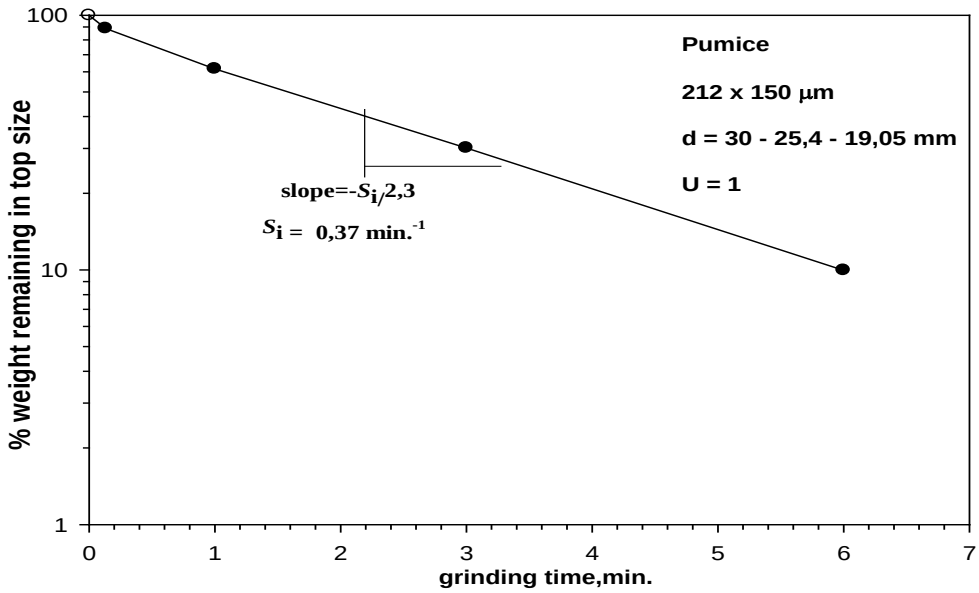

Figure C.82 First-order plot of breakage of - 212 + 150 μm feed of pumice ground with d = 30 – 25,4 – 19,05 mm ball diameter and U = 1.

Determination of aT value

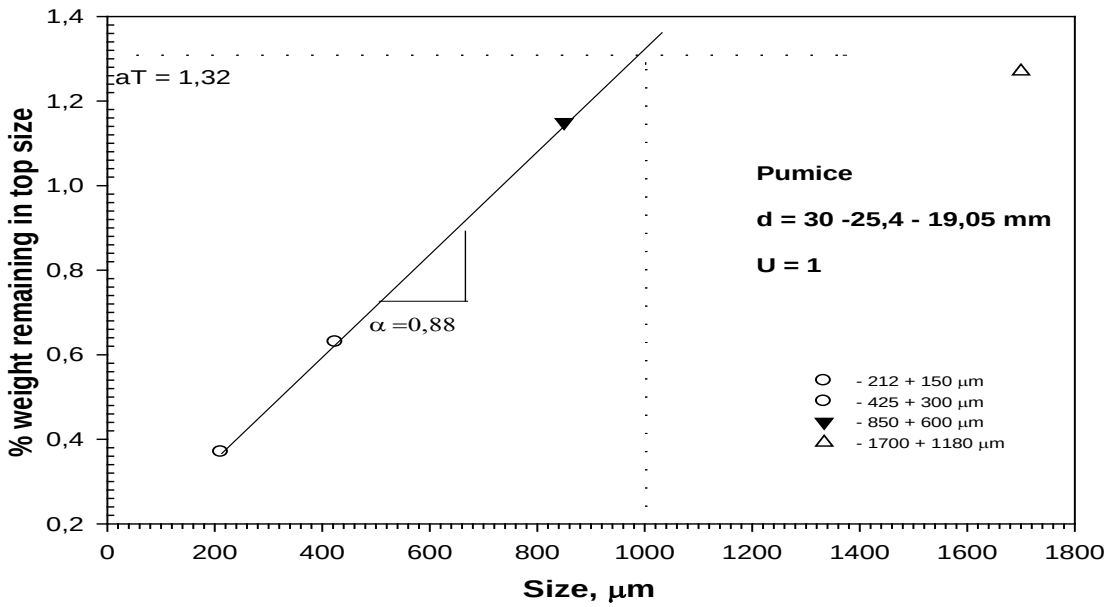

Figure C.83 Variation of first-order specific rates of breakage of pumice ground with d = 30 – 25,4 – 19,05 mm ball diameter and particle size: √2 intervals, plotted at upper size of interval at U=1.

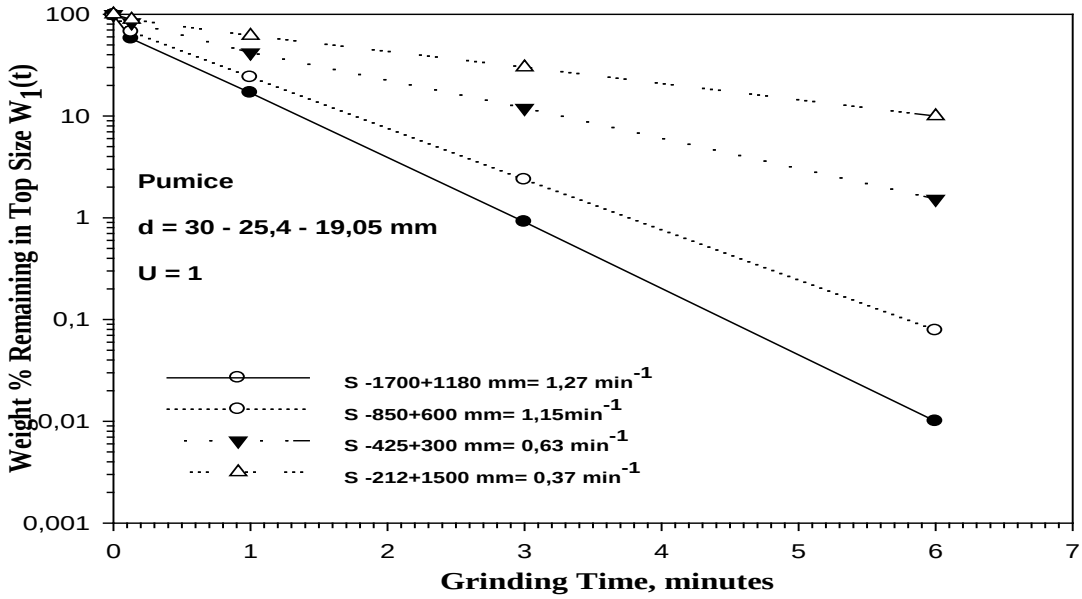

Figure C.84 First-order plots of breakage of -1700+1180, -850+600, -425+300, -212+150 µm feed size of pumice ground with d = 30 – 25,4 – 19,05 mm ball diameter and U=1.

Table C.54 Breakage parameters of pumice ground with d = 30 – 25,4 – 19,05 mm ball diameter at U=1.

gama	0,99	**gama**	1,02	**gama**	1,05	**gama**	1,06		
beta	2,04	**beta**	2,06	**beta**	2,09	**beta**	2,11	**aT**	**α**
phi	0,58	**phi**	0,55	**phi**	0,54	**phi**	0,52	0,77	0,93
S value	0,790	**S value**	0,680	**S value**	0,360	**S value**	0,190		

APPENDIX D
TABLES AND FIGURES FOR DETERMINATION BREAKAGE PARAMETERS OF ZEOLITE

38 mm ball size charge at U=0,6

1700 x 1180 micron

Table D.1 Determined B values of zeolite for - 1700 + 1180 µm size interval ground with d = 38 mm ball diameter and U = 0,6.

INTERVAL NO,İ	SİZE (mesh)	Size (µm)	Xi/Xmax	B i,1	B VALUES
1	12x16	1700x1180	1,00	B1,1	1
2	16x20	1180x850	0,69	B2,1	1
3	20x30	850x600	0,50	B3,1	0,456957227
4	30x40	600x425	0,35	B4,1	0,328634432
5	40x50	425x300	0,25	B5,1	0,239005113
6	50x70	300x212	0,17	B6,1	0,169635939
7	70x100	212x150	0,12	B7,1	0,12292607
8	100x140	150x106	0,088	B8,1	0,0927946
9	140x200	106x75	0,062	B9,1	0,067344096
10	200x270	75x53	0,044	B10,1	0,049344938
11	270x400	53x38	0,031	B11,1	0,035775917
12	-400	-38	0,022	B12,1	0,024565456

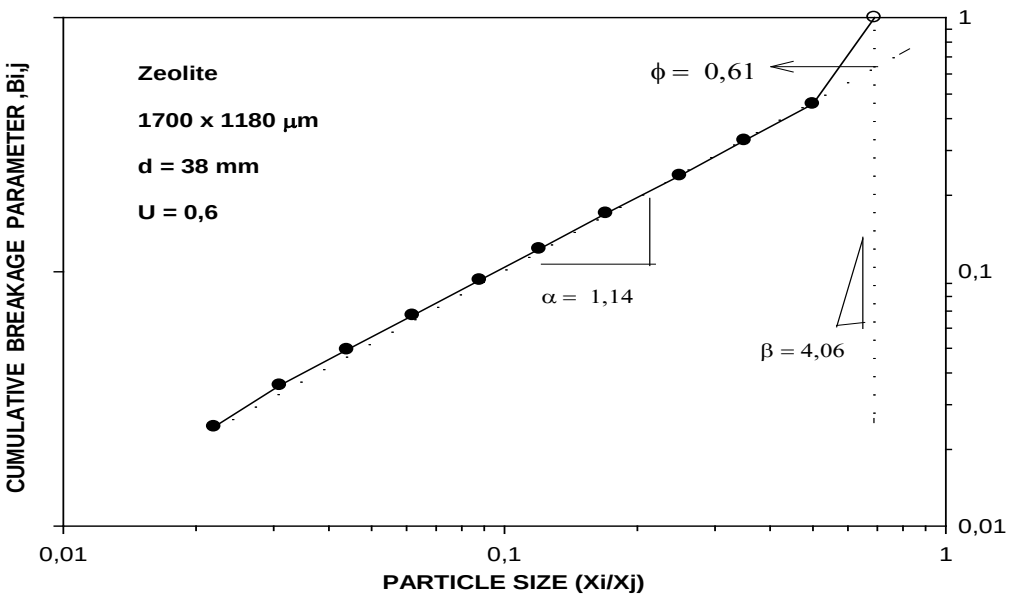

Figure D.1 Primary breakage distribution function of zeolite for -1700 + 1180 µm feed size fraction ground with d = 38 mm ball diameter and U = 0,6.

Table D.2 Cumulative weight percent less than size values of zeolite for 1700 x 1180 µm size interval ground with d = 38 mm ball diameter and U = 0,6.

SIZE	0 min.	0,133 min	1 min	3 min	6 min
1700	100,00	100,00	100,00	100,00	100,00
1180	0,62	30,08	60,03	88,14	98,01
850	0,01	14,85	40,54	83,64	94,58
600	0,02	10,93	27,18	68,42	85,67
425	0,00	8,06	20,33	49,26	67,45
300	0,00	5,79	16,48	38,17	53,16
212	0,00	4,23	12,16	28,53	41,84
150	0,00	3,21	9,25	19,45	31,16
106	0,00	2,34	7,51	13,76	22,47
75	0,00	1,72	5,44	10,05	15,63
53	0,00	1,25	3,92	7,21	11,36
38	0,00	0,86	2,76	5,37	8,01
%w.r.top size	99,38	69,92	39,97	11,86	1,99

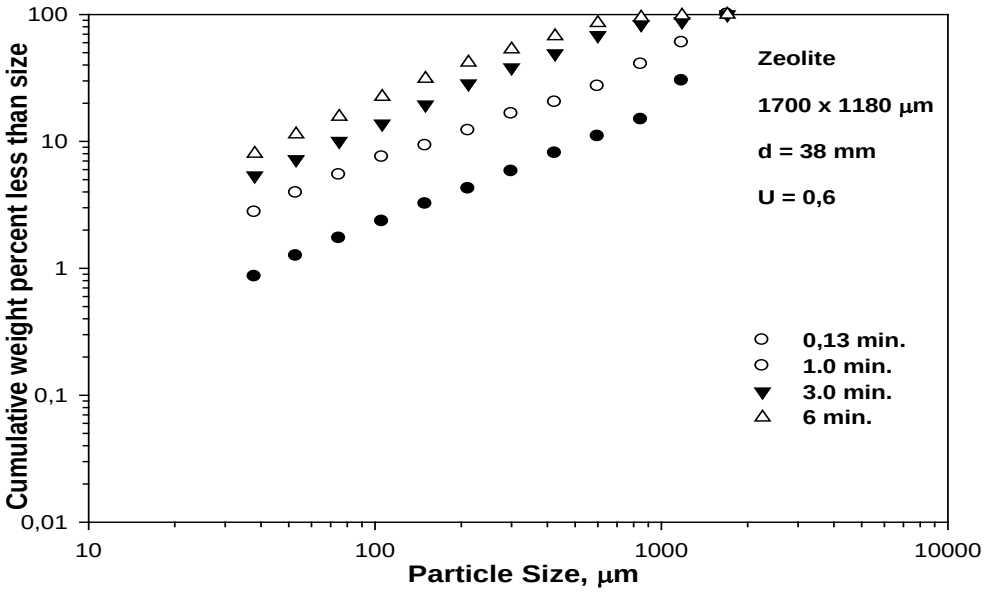

Figure D.2 Particle size distribution of zeolite for -1700 + 1180 µm feed size fraction ground with d = 38 mm ball diameter and U = 0,6.

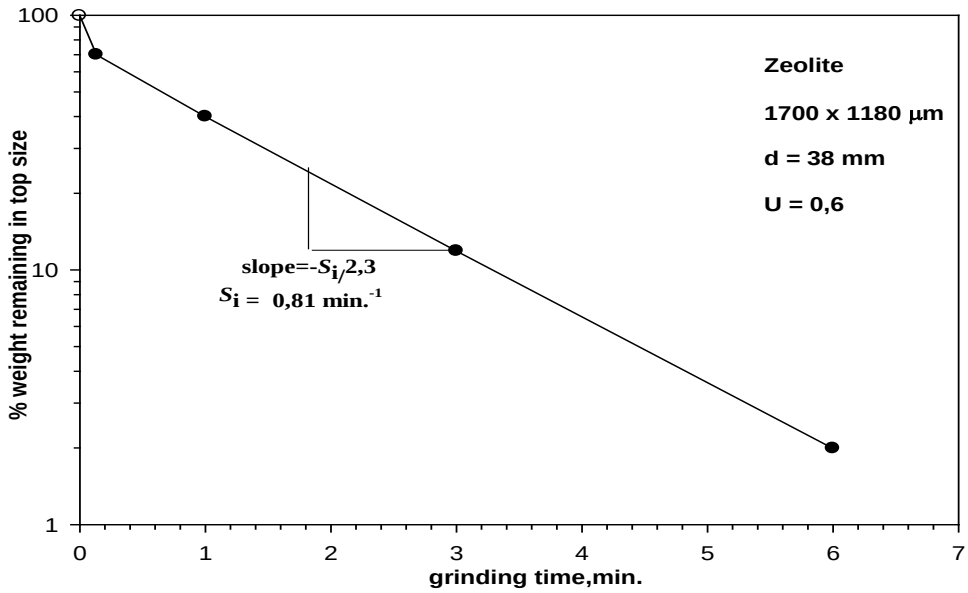

Figure D.3 First-order plot of breakage of - 1700 + 1180 µm feed of zeolite ground with d = 38 mm ball diameter and U = 0,6.

850 x 600 micron

Table D.3 Determined B values of zeolite for - 850 + 600 µm size interval ground with d = 38 mm ball diameter and U = 0,6.

INTERVAL NO,İ	SİZE (mesh)	Size (µm)	Xi/Xmax	B i,1	B VALUES
1	20x30	850x600	1,00	B3,1	1,000
2	30x40	600x425	0,7	B4,1	1,000
3	40x50	425x300	0,5	B5,1	0,458
4	50x70	300x212	0,35	B6,1	0,327
5	70x100	212x150	0,24	B7,1	0,235
6	100x140	150x106	0,17	B8,1	0,171
7	140x200	106x75	0,12	B9,1	0,125
8	200x270	75x53	0,08	B10,1	0,091
9	270x400	53x38	0,06	B11,1	0,068
10	-400	-38	0,04	B12,1	0,046

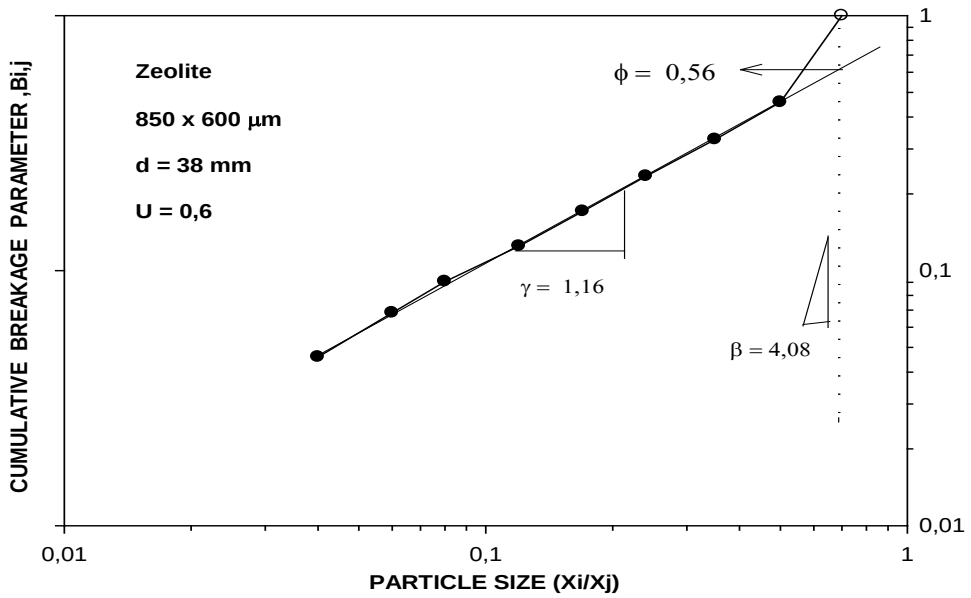

Figure D.4 Primary breakage distribution function of zeolite for -850 + 600 µm feed size fraction ground with d = 38 mm ball diameter and U = 0,6.

Table D.4 Cumulative weight percent less than size values of zeolite for - 850 + 600 µm size interval ground with d = 38 mm ball diameter and U = 0,6.

SIZE	0 min.	0,133 min	1 min	3 min	6 min
850	100,00	100,00	100,00	100,00	100,00
600	0,63	25,63	51,08	79,14	95,03
425	0,16	12,56	22,14	61,34	90,11
300	0,01	9,04	16,00	40,02	80,04
212	0,00	6,57	12,26	29,93	53,17
150	0,00	4,83	9,54	20,56	36,08
106	0,00	3,55	7,32	14,02	22,54
75	0,00	2,59	5,54	9,95	15,81
53	0,00	1,96	4,17	6,64	10,36
38	0,00	1,32	3,18	4,62	7,02
%w.r.top size	99,37	74,37	48,92	20,86	4,97

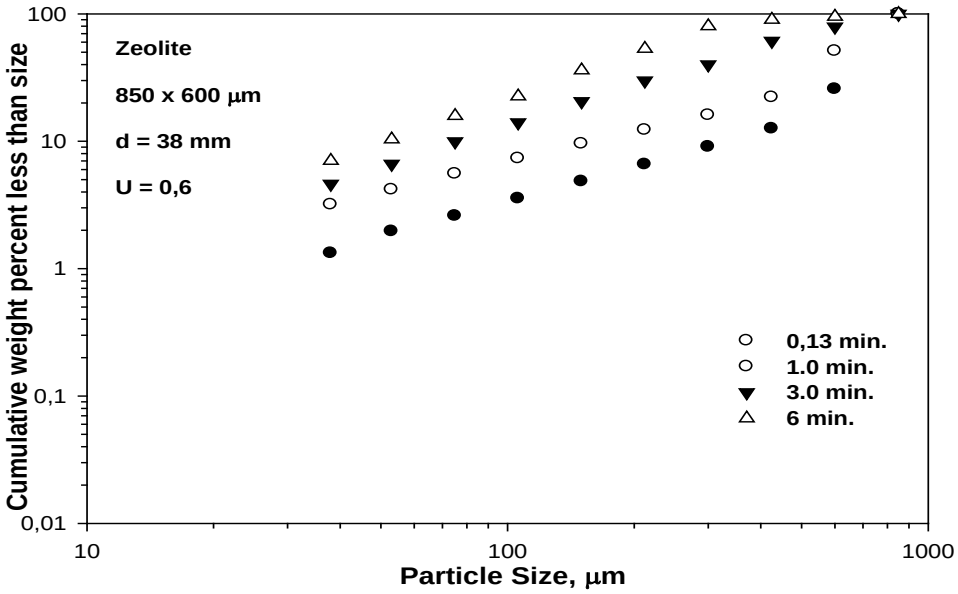

Figure D.5 Particle size distribution of zeolite for -850 + 600 µm feed size fraction ground with d = 38 mm ball diameter and U = 0,6.

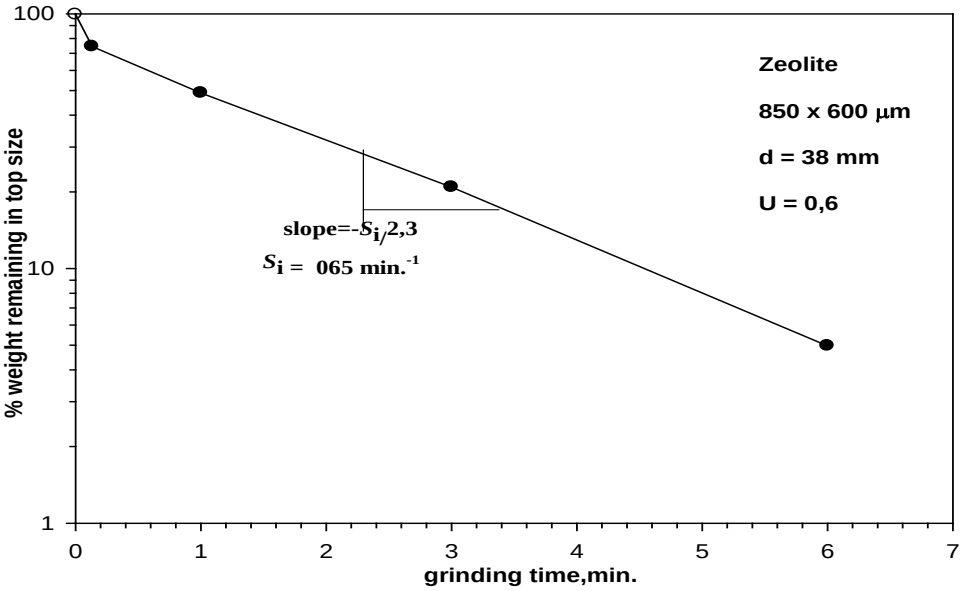

Figure D.6 First-order plot of breakage of - 850 + 600 µm feed of zeolite ground with d = 38 mm ball diameter and U = 0,6.

425 x 300 micron

Table D.5 Determined B values of zeolite for – 425 + 300 µm size interval ground with d = 38 mm ball diameter and U = 0,6.

INTERVAL NO,İ	SİZE (mesh)	Size (µm)	Xi/Xmax	B i,1	B VALUES
1	40x50	425x300	1,00	B1,1	1,0000
2	50x70	300x212	0,7	B2,1	1,0000
3	70x100	212x150	0,49	B3,1	0,4459
4	100x140	150x106	0,35	B4,1	0,3236
5	140x200	106x75	0,24	B5,1	0,2273
6	200x270	75x53	0,17	B6,1	0,1646
7	270x400	53x38	0,12	B7,1	0,1138
8	-400	-38	0,08	B8,1	0,0768

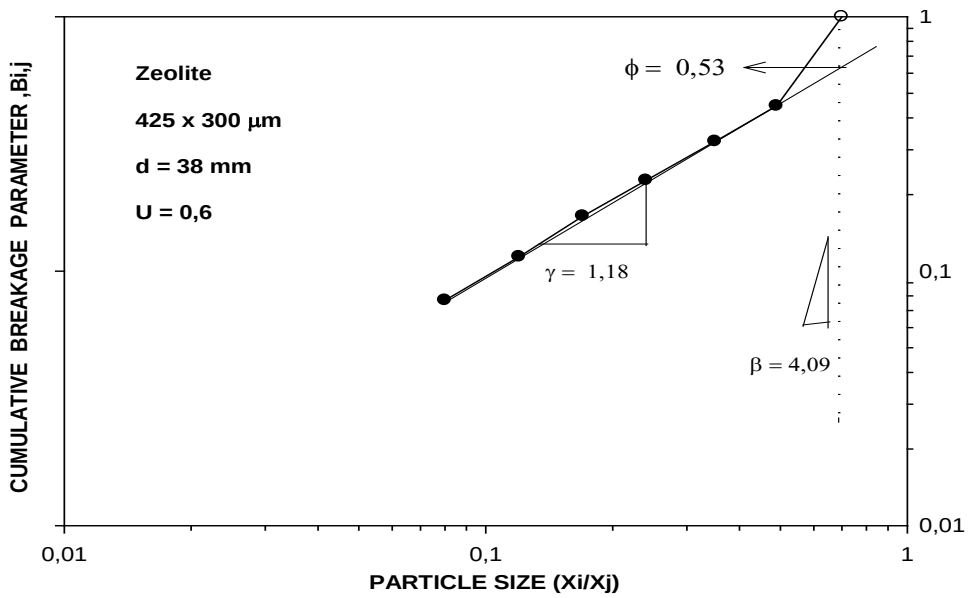

Figure D.7 Primary breakage distribution function of zeolite for -425 + 300 µm feed size fraction ground with d = 38 mm ball diameter and U = 0,6.

Table D.6 Cumulative weight percent less than size values of zeolite for - 425 + 300 µm size interval ground with d = 38 mm ball diameter and U = 0,6.

SIZE	0 min.	0,133 min	1 min	3 min	6 min
425	100,00	100,00	100,00	100,00	100,00
300	0,16	13,43	34,92	60,04	80,12
212	0,02	6,18	18,06	29,19	42,26
150	0,00	4,51	11,15	18,73	25,53
106	0,00	3,19	7,93	12,08	16,02
75	0,00	2,32	5,26	7,63	10,43
53	0,00	1,61	3,47	4,72	6,08
38	0,00	1,09	2,05	3,04	3,77
%w.r.top size	99,84	86,57	65,08	39,96	19,88

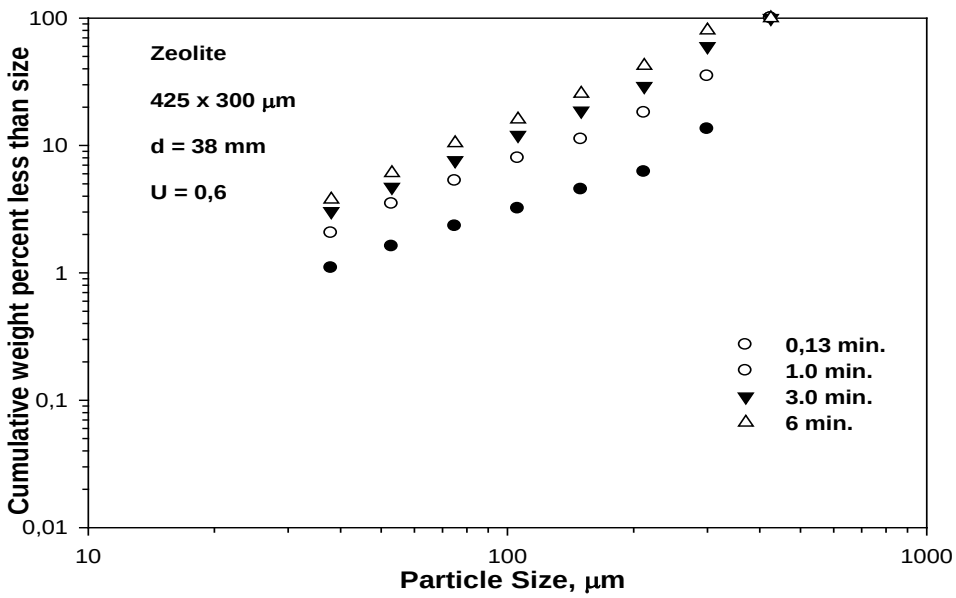

Figure D.8 Particle size distribution of zeolite for -425 + 300 µm feed size fraction ground with d = 38 mm ball diameter and U = 0,6.

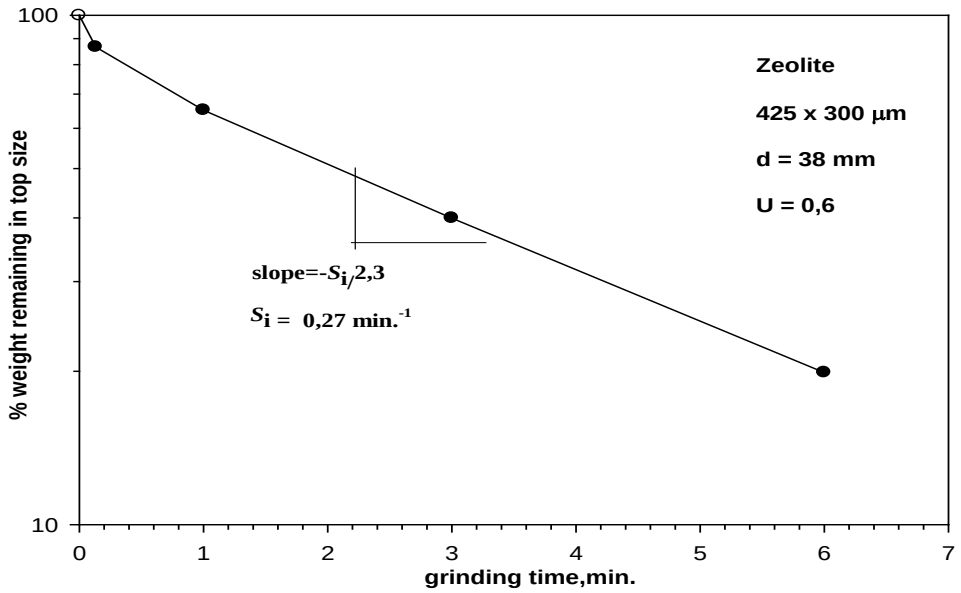

Figure D.9 First-order plot of breakage of - 425 + 300 µm feed of zeolite ground with d = 38 mm ball diameter and U = 0,6.

212 x 150 micron

Table D.7 Determined B values of zeolite for – 212 + 150 µm size interval ground with d = 38 mm ball diameter and U = 0,6.

INTERVAL NO,İ	SİZE (mesh)	Size (µm)	Xi/Xmax	B i,1	B VALUES
1	70x100	212x150	1,00	B1,1	1,0000
2	100x140	150x106	0,7	B2,1	1,0000
3	140x200	106x75	0,5	B3,1	0,3984
4	200x270	75x53	0,35	B4,1	0,2877
5	270x400	53x38	0,25	B5,1	0,2041
6	-400	-38	0,17	B6,1	0,1408

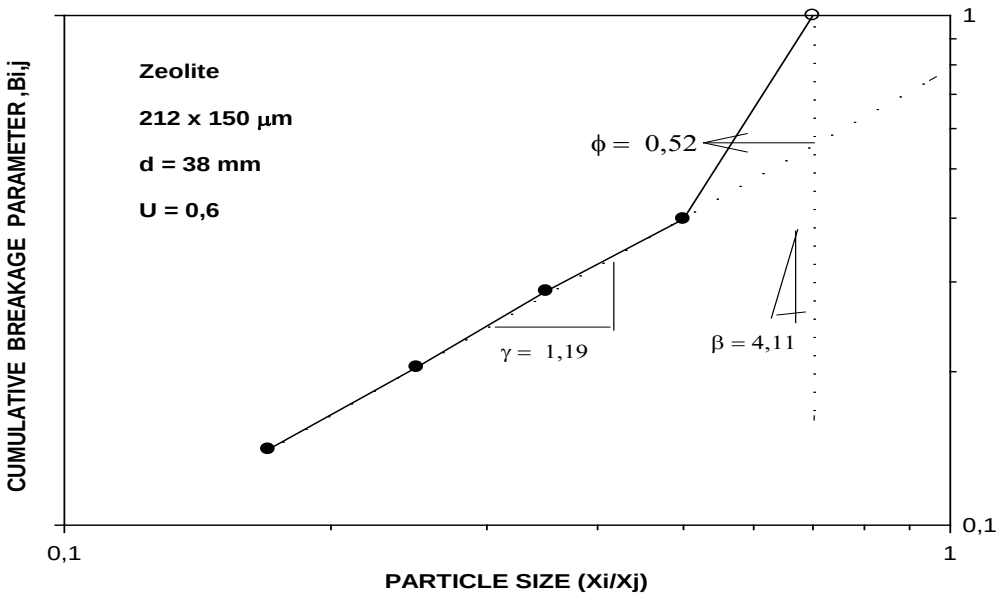

Figure D.10 Primary breakage distribution function of zeolite for - 212 + 150 µm feed size fraction ground with d = 38 mm ball diameter and U = 0,6.

Table D.8 Cumulative weight percent less than size values of zeolite for - 212 + 150 µm size interval ground with d = 38 mm ball diameter and U = 0,6.

SIZE	0 min.	0,133 min	1 min	3 min	6 min
212	100,00	100,00	100,00	100,00	100,00
150	0,17	9,94	24,07	40,98	57,60
106	0,01	4,42	11,93	19,23	29,86
75	0,00	3,18	5,76	9,42	12,73
53	0,00	2,31	3,61	4,93	7,09
38	0,00	1,62	2,46	3,11	4,47
%w.r.top size	99,83	90,06	75,93	59,02	42,40

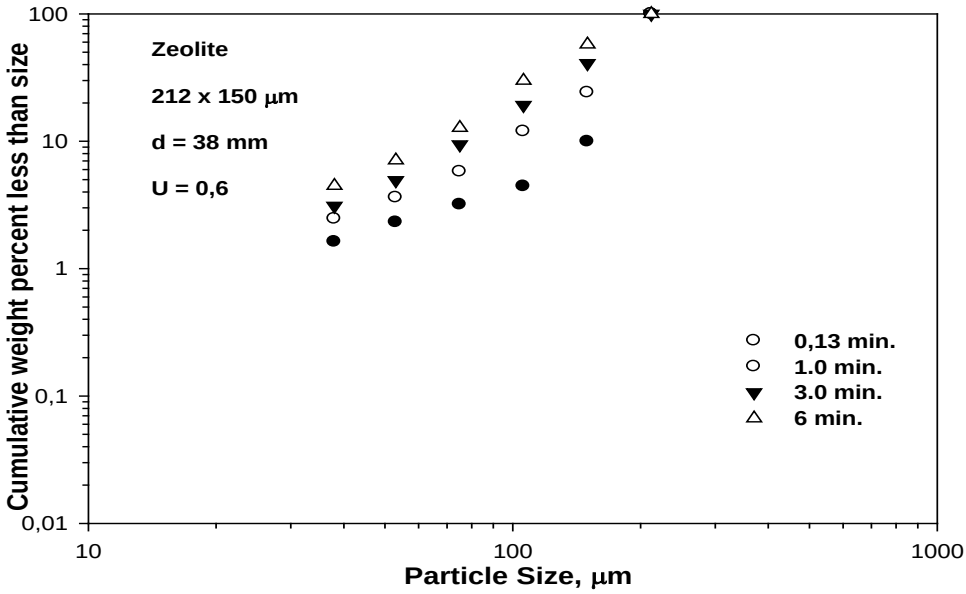

Figure D.11 Particle size distribution of zeolite for -212 + 150 μm feed size fraction ground with d = 38 mm ball diameter and U = 0,6.

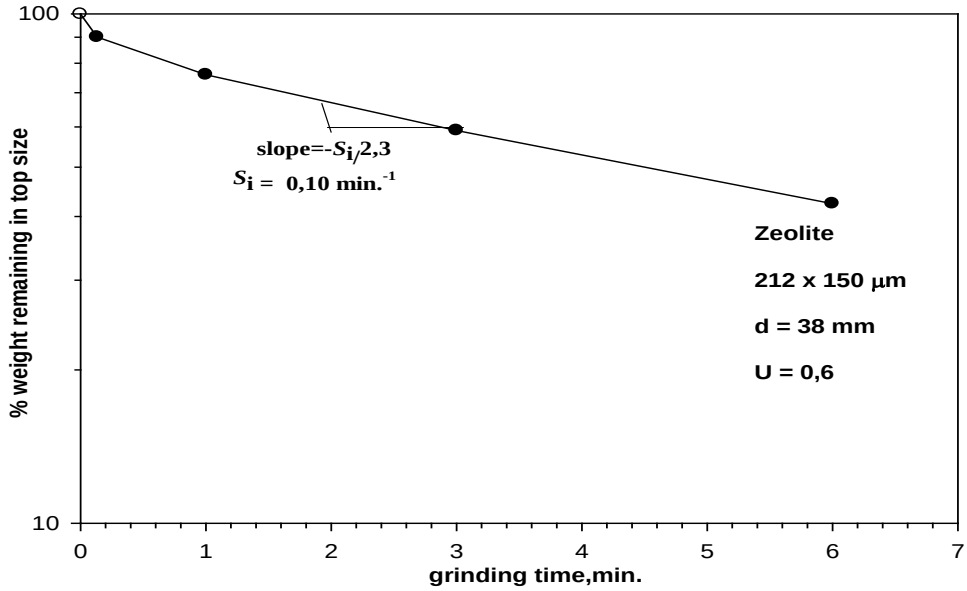

Figure D.12 First-order plot of breakage of - 212 + 150 μm feed of zeolite ground with d = 38 mm ball diameter and U = 0,6.

Determination of aT value

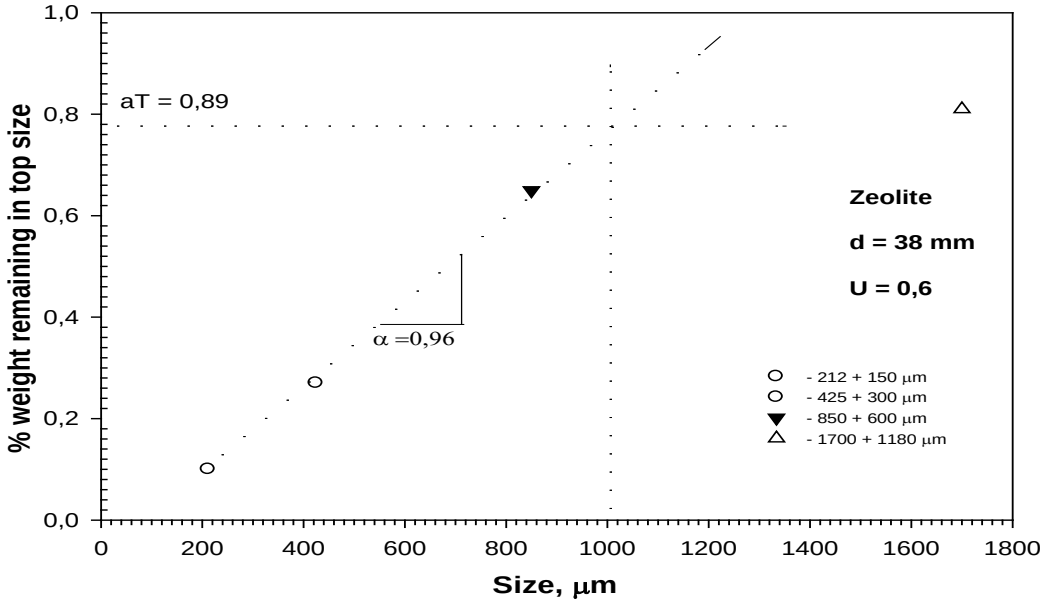

Figure D.13 Variation of first-order specific rates of breakage of zeolite ground with d = 38 mm ball diameter and particle size: √2 intervals, plotted at upper size of interval at U=0,6.

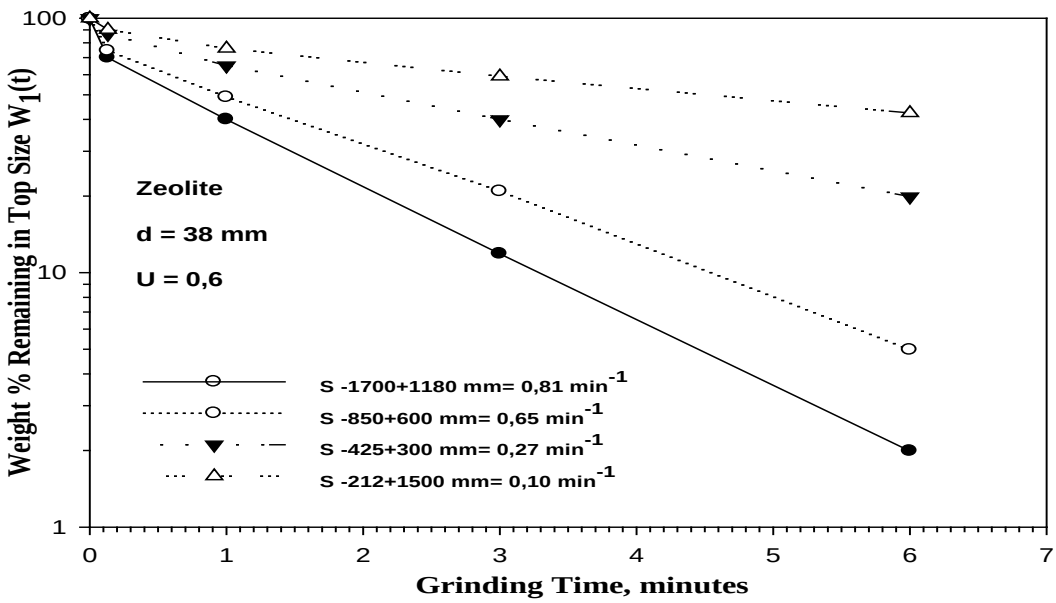

Figure D.14 First-order plots of breakage of -1700+1180, -850+600, -425+300, -212+150 μm feed size of zeolite ground with d = 38 mm ball diameter and U=0,6.

Table D.9 Breakage parameters of zeolite ground with d = 38 mm ball diameter at U=0,6.

1700x1180		**850x600**		**425x300**		**212x150**			
gama	1,14	**gama**	1,16	**gama**	1,18	**gama**	1,19		
beta	4,06	**beta**	4,08	**beta**	4,09	**beta**	4,11	**aT**	**α**
phi	0,81	**phi**	0,56	**phi**	0,53	**phi**	0,52	0,89	0,96
S value	0,810	**S value**	0,650	**S value**	0,27	**S value**	0,100		

38 mm ball size charge at U= 1

1700 x 1180 micron

Table D.10 Determined B values of zeolite for - 1700 + 1180 µm size interval ground with d = 38 mm ball diameter and U = 1.

INTERVAL NO,İ	**SİZE (mesh)**	**Size (µm)**	**Xi/Xmax**	**B i,1**	**B VALUES**
1	12x16	1700x1180	1,00	B1,1	1,0000
2	16x20	1180x850	0,69	B2,1	1,0000
3	20x30	850x600	0,50	B3,1	0,3343
4	30x40	600x425	0,35	B4,1	0,2313
5	40x50	425x300	0,25	B5,1	0,1596
6	50x70	300x212	0,17	B6,1	0,1050
7	70x100	212x150	0,12	B7,1	0,0732
8	100x140	150x106	0,088	B8,1	0,0519
9	140x200	106x75	0,062	B9,1	0,0364
10	200x270	75x53	0,044	B10,1	0,0247
11	270x400	53x38	0,031	B11,1	0,0176
12	-400	-38	0,022	B12,1	0,0120

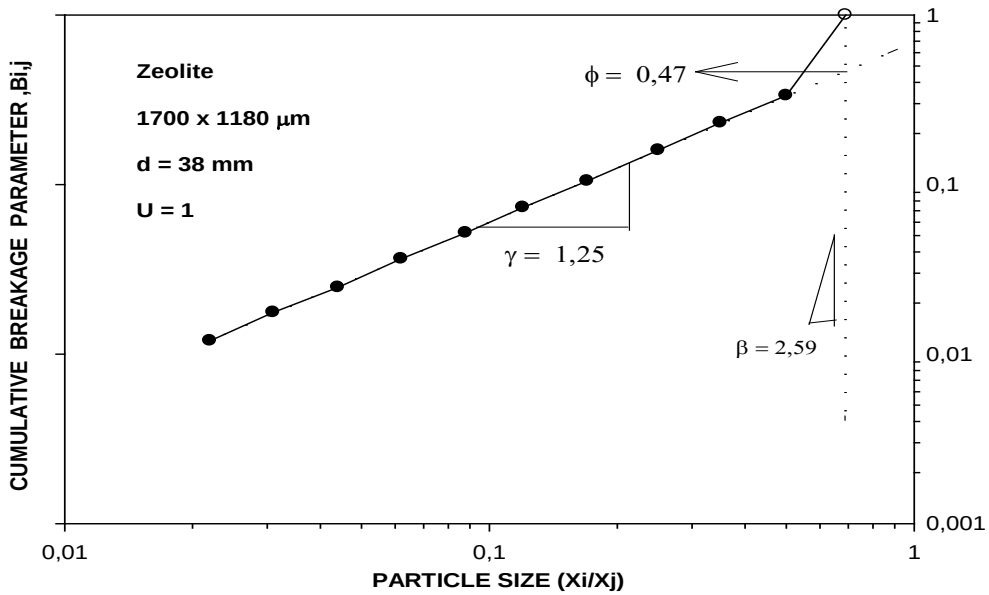

Figure D.15 Primary breakage distribution function of zeolite for -1700 + 1180 μm feed size fraction ground with d = 38 mm ball diameter and U = 0,6.

Table D.11 Cumulative weight percent less than size values of zeolite for 1700 x 1180 μm size interval ground with d = 38 mm ball diameter and U = 1.

SIZE	0 min.	0,133 min	1 min	3 min	6 min
1700	100,00	100,00	100,00	100,00	100,00
1180	0,84	24,12	55,21	86,03	97,59
850	0,09	8,64	28,56	77,21	91,25
600	0,02	6,02	18,92	61,48	76,11
425	0,00	4,18	12,06	43,18	57,46
300	0,00	2,77	8,97	29,36	45,82
212	0,00	1,94	6,02	20,47	33,08
150	0,00	1,38	3,78	13,58	23,41
106	0,00	0,97	2,41	8,79	16,96
75	0,00	0,66	1,36	5,87	11,03
53	0,00	0,47	0,92	3,74	7,21
38	0,00	0,32	0,62	2,26	4,73
%w.r.top size	99,16	75,88	44,79	13,97	2,41

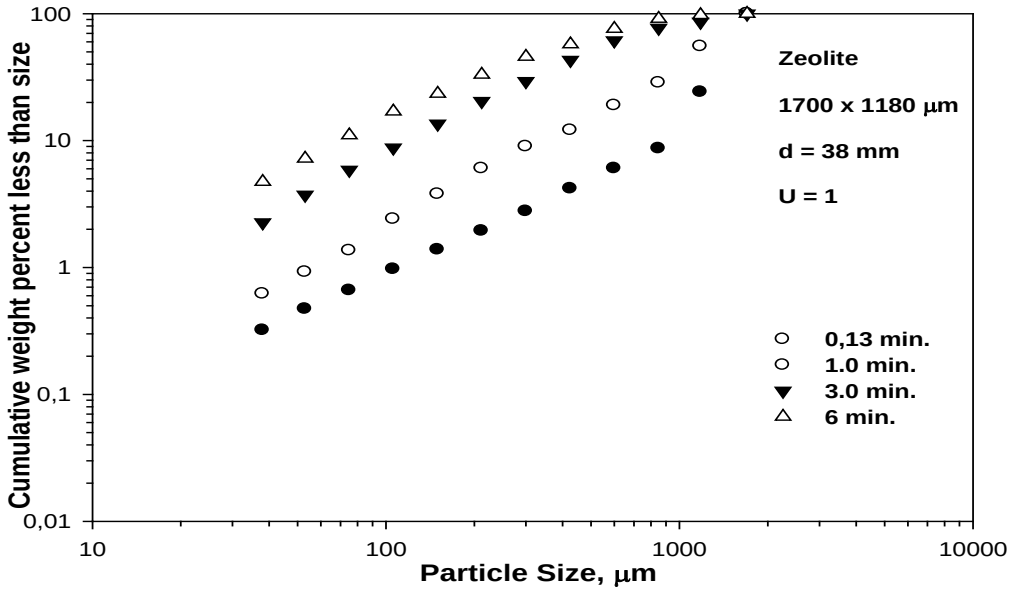

Figure D.16 Particle size distribution of zeolite for -1700 + 1180 μm feed size fraction ground with d = 38 mm ball diameter and U = 1.

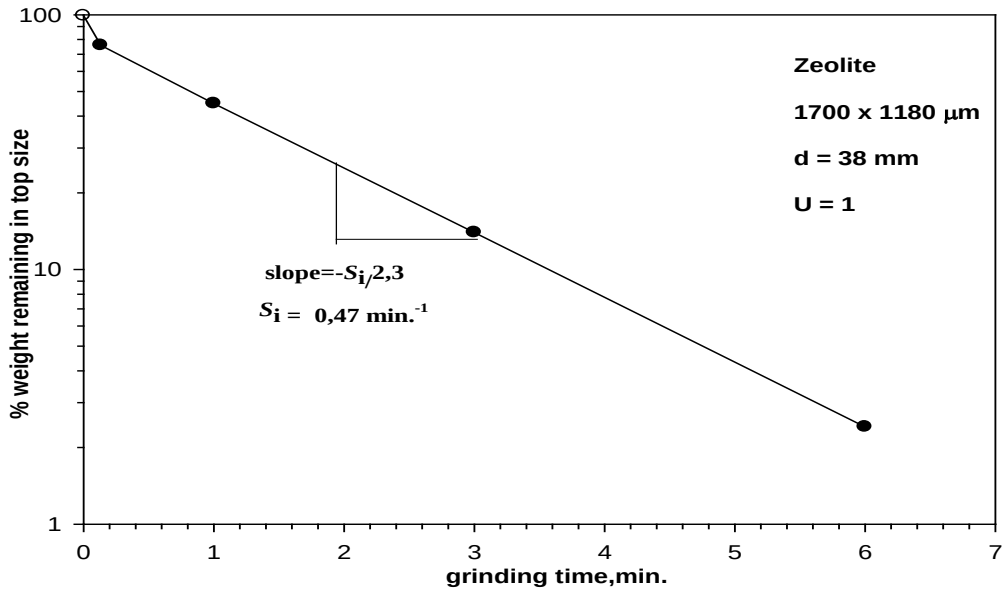

Figure D.17 First-order plot of breakage of - 1700 + 1180 μm feed of zeolite ground with d = 38 mm ball diameter and U = 1.

850 x 600 micron

Table D.12 Determined B values of zeolite for - 850 + 600 µm size interval ground with d = 38 mm ball diameter and U = 1.

INTERVAL NO,İ	SİZE (mesh)	Size (µm)	Xi/Xmax	B i,1	B VALUES
1	20x30	850x600	1,00	B3,1	1,000
2	30x40	600x425	0,7	B4,1	1,000
3	40x50	425x300	0,5	B5,1	0,335
4	50x70	300x212	0,35	B6,1	0,230
5	70x100	212x150	0,24	B7,1	0,159
6	100x140	150x106	0,17	B8,1	0,107
7	140x200	106x75	0,12	B9,1	0,073
8	200x270	75x53	0,08	B10,1	0,050
9	270x400	53x38	0,06	B11,1	0,036
10	-400	-38	0,04	B12,1	0,023

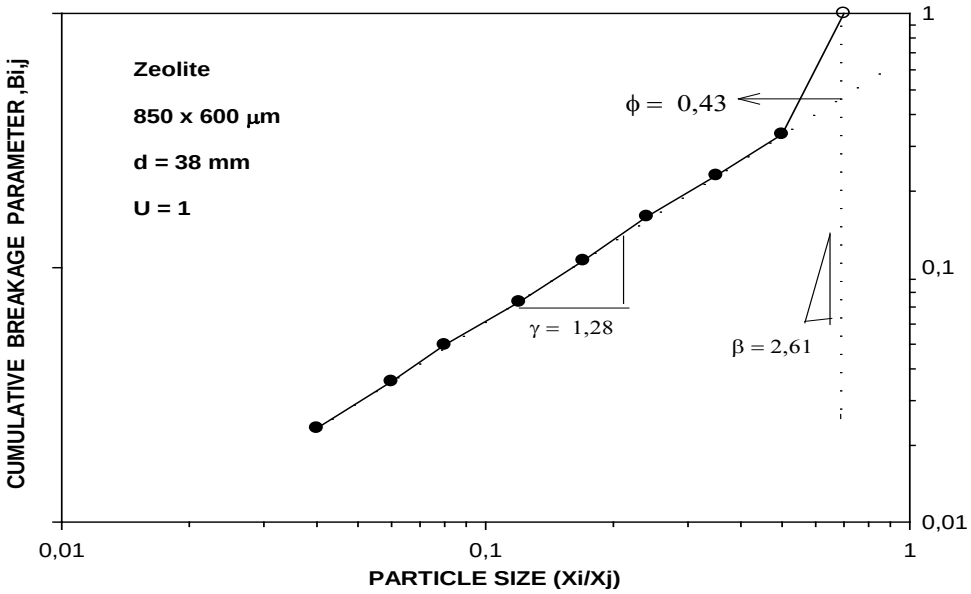

Figure D.18 Primary breakage distribution function of zeolite for -850 + 600 µm feed size fraction ground with d = 38 mm ball diameter and U = 0,6.

Table D.13 Cumulative weight percent less than size values of zeolite for - 850 + 600 µm size interval ground with d = 38 mm ball diameter and U = 1.

SIZE	0 min.	0,133 min	1 min	3 min	6 min
850	100,00	100,00	100,00	100,00	100,00
600	0,31	16,73	42,81	74,88	92,19
425	0,05	5,89	15,74	50,29	87,66
300	0,01	4,07	8,62	32,07	73,97
212	0,00	2,82	5,92	19,92	47,02
150	0,00	1,90	3,91	11,38	30,25
106	0,00	1,31	2,48	7,61	17,42
75	0,00	0,89	1,65	4,85	9,98
53	0,00	0,64	1,12	2,94	6,14
38	0,00	0,42	0,73	1,82	3,78
%w.r.top size	99,69	83,27	57,19	25,12	7,81

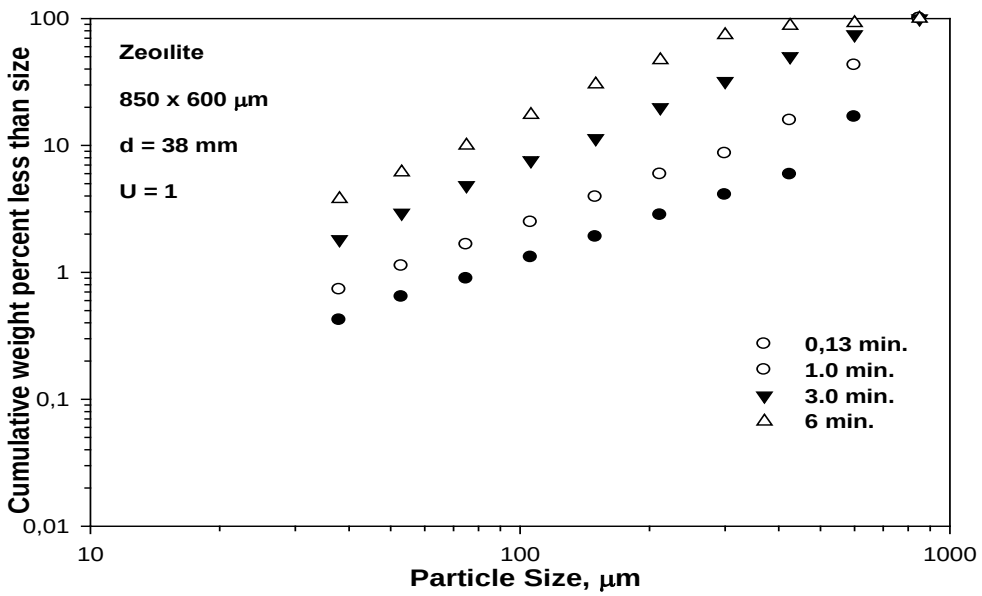

Figure D.19 Particle size distribution of zeolite for -850 + 600 µm feed size fraction ground with d = 38 mm ball diameter and U = 1.

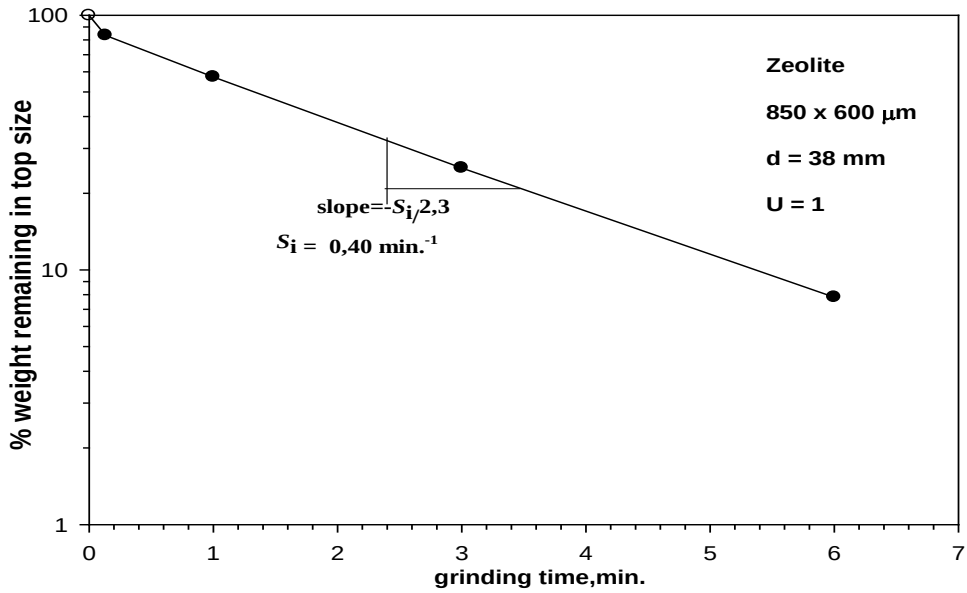

Figure D.20 First-order plot of breakage of - 850 + 600 µm feed of zeolite ground with d = 38 mm ball diameter and U = 1.

425 x 300 micron

Table D.14 Determined B values of zeolite for – 425 + 300 µm size interval ground with d = 38 mm ball diameter and U = 1.

INTERVAL NO,İ	SİZE (mesh)	Size (µm)	Xi/Xmax	B i,1	B VALUES
1	40x50	425x300	1,00	B1,1	1,0000
2	50x70	300x212	0,7	B2,1	1,0000
3	70x100	212x150	0,49	B3,1	0,3301
4	100x140	150x106	0,35	B4,1	0,2297
5	140x200	106x75	0,24	B5,1	0,1511
6	200x270	75x53	0,17	B6,1	0,1038
7	270x400	53x38	0,12	B7,1	0,0729
8	-400	-38	0,08	B8,1	0,0470

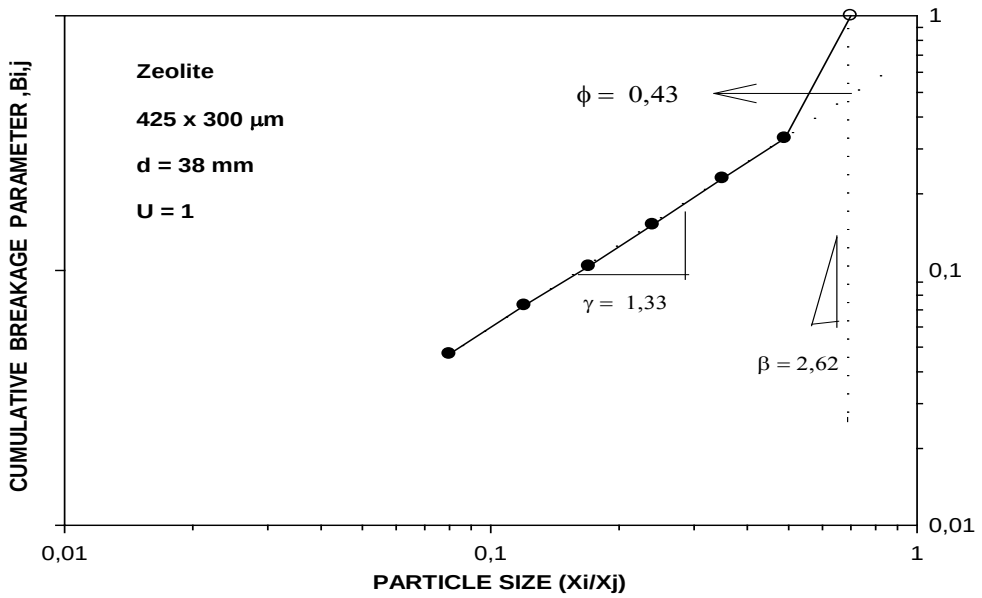

Figure D.21 Primary breakage distribution function of zeolite for -425 + 300 µm feed size fraction ground with d = 38 mm ball diameter and U = 1.

Table D.15 Cumulative weight percent less than size values of zeolite for - 425 + 300 µm size interval ground with d = 38 mm ball diameter and U = 1.

SIZE	0 min.	0,133 min	1 min	3 min	6 min
425	100,00	100,00	100,00	100,00	100,00
300	0,09	6,08	24,87	50,93	74,02
212	0,01	2,03	8,03	16,71	30,26
150	0,00	1,41	3,25	6,91	13,46
106	0,00	0,93	1,97	3,64	6,37
75	0,00	0,64	1,21	2,11	3,42
53	0,00	0,45	0,76	1,42	2,16
38	0,00	0,29	0,52	0,98	1,43
%w.r.top size	99,91	93,92	75,13	49,07	25,98

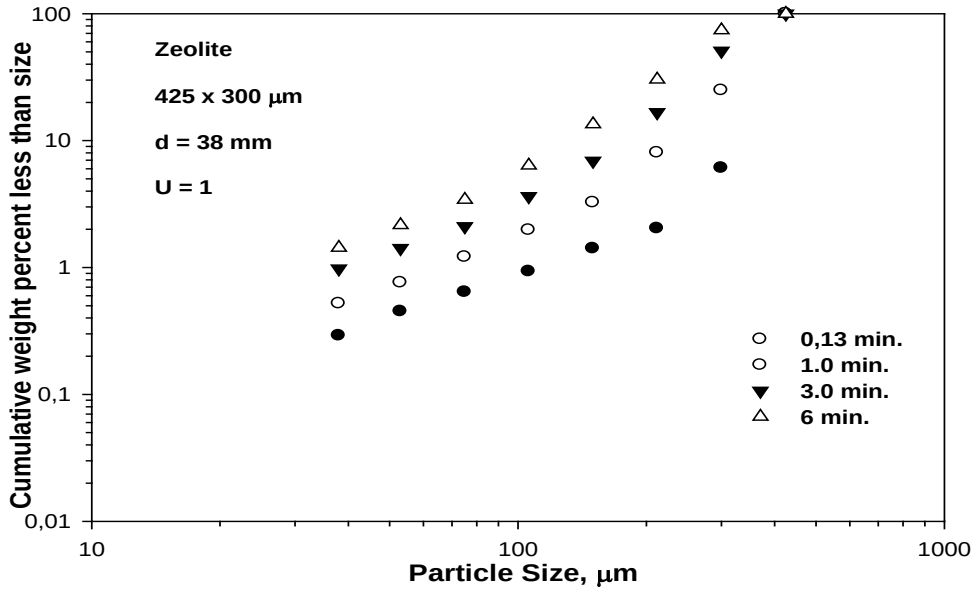

Figure D.22 Particle size distribution of zeolite for -425 + 300 µm feed size fraction ground with d = 38 mm ball diameter and U = 1.

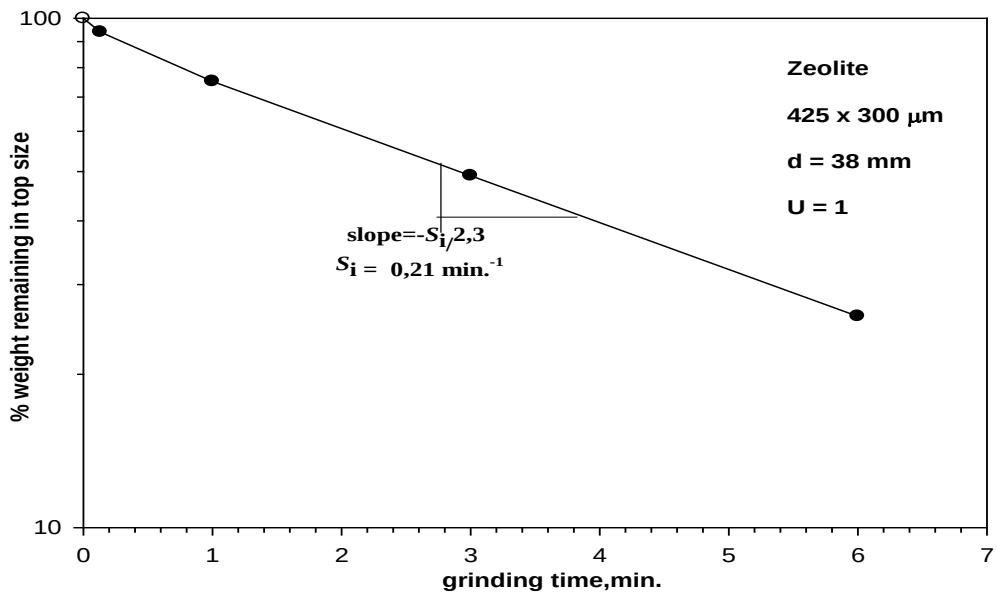

Figure D.23 First-order plot of breakage of - 425 + 300 µm feed of zeolite ground with d = 38 mm ball diameter and U = 1.

212 x 150 micron

Table D.16 Determined B values of zeolite for – 212 + 150 µm size interval ground with d = 38 mm ball diameter and U = 1.

INTERVAL NO,İ	SİZE (mesh)	Size (µm)	Xi/Xmax	B i,1	B VALUES
1	70x100	212x150	1,00	B1,1	1,0000
2	100x140	150x106	0,7	B2,1	1,0000
3	140x200	106x75	0,5	B3,1	0,3268
4	200x270	75x53	0,35	B4,1	0,2258
5	270x400	53x38	0,25	B5,1	0,1556
6	-400	-38	0,17	B6,1	0,1016

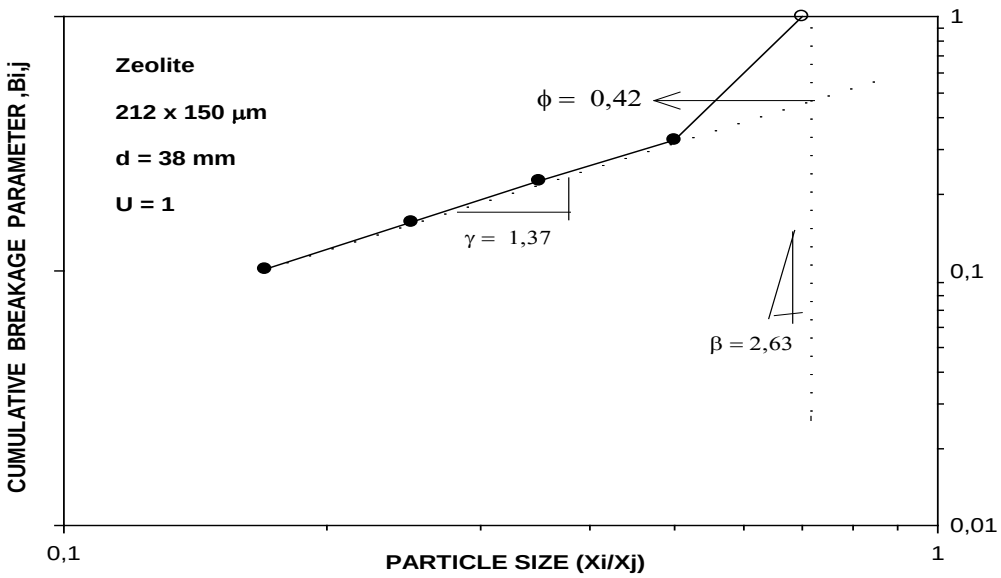

Figure D.24 Primary breakage distribution function of zeolite for - 212 + 150 µm feed size fraction ground with d = 38 mm ball diameter and U = 1.

Table D.17 Cumulative weight percent less than size values of zeolite for - 212 + 150 µm size interval ground with d = 38 mm ball diameter and U = 1.

SIZE	0 min.	0,133 min	1 min	3 min	6 min
212	100,00	100,00	100,00	100,00	100,00
150	0,17	5,07	14,59	31,93	49,98
106	0,08	1,71	11,16	16,38	24,71
75	0,01	1,14	7,23	11,08	15,32
53	0,00	0,78	4,82	7,79	10,38
38	0,00	0,51	3,04	5,12	7,13
%w.r.top size	99,83	94,93	85,41	68,07	50,02

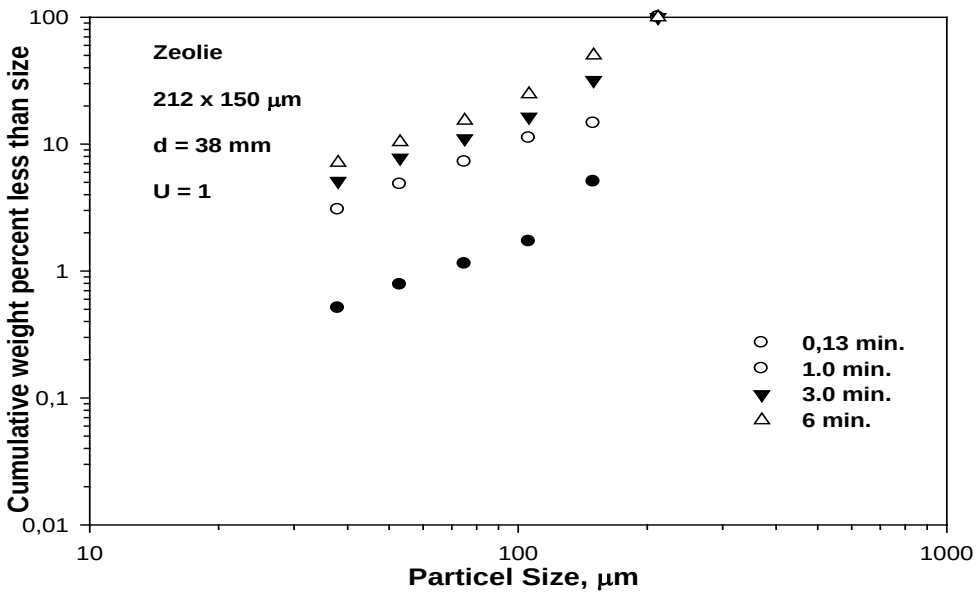

Figure D.25 Particle size distribution of zeolite for -212 + 150 µm feed size fraction ground with d = 38 mm ball diameter and U = 1.

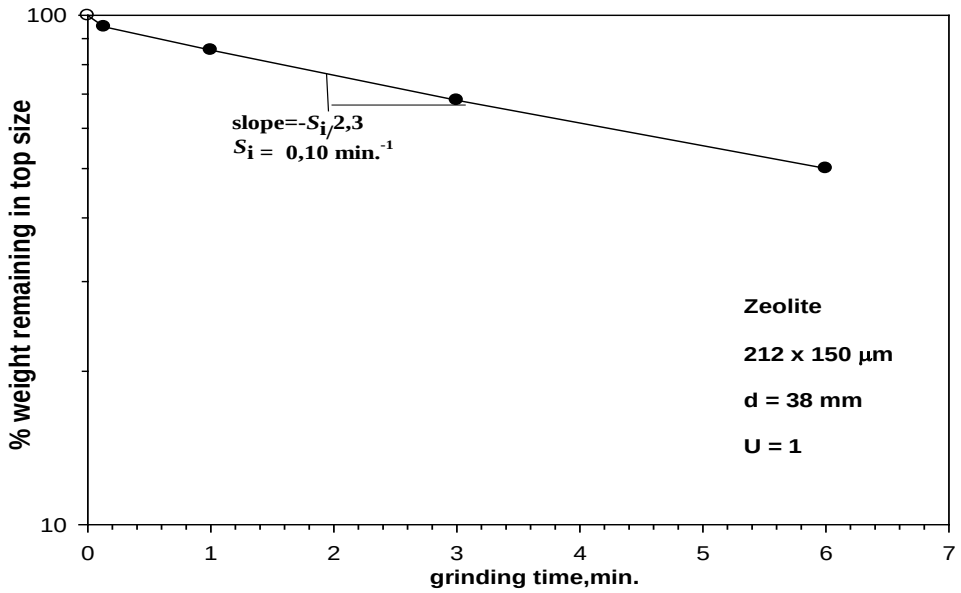

Figure D.26 First-order plot of breakage of - 212 + 150 μm feed of zeolite ground with d = 38 mm ball diameter and U = 1.

Determination of aT value

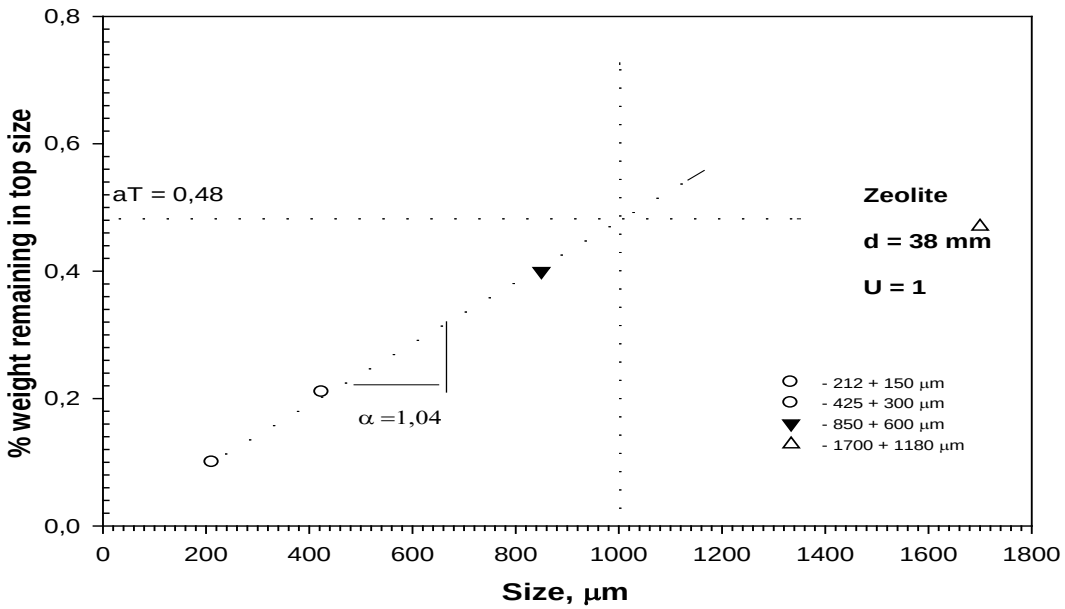

Figure D.27 Variation of first-order specific rates of breakage of zeolite ground with d = 38 mm ball diameter and particle size: √2 intervals, plotted at upper size of interval at U=1.

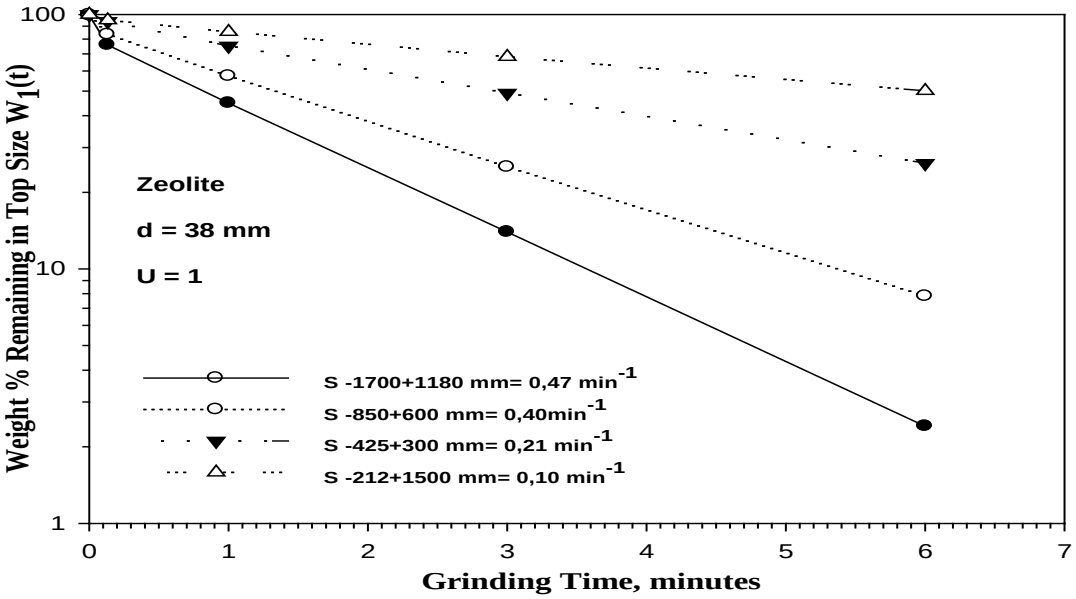

Figure D.28 First-order plots of breakage of -1700+1180, -850+600, -425+300, -212+150 μm feed size of zeolite ground with d = 38 mm ball diameter and U=1.

Table D.18 Breakage parameters of zeolite ground with d = 38 mm ball diameter at U=1.

1700x1180		**850x600**		**425x300**		**212x150**			
gama	1,25	**gama**	1,28	**gama**	1,33	**gama**	1,37		
beta	2,59	**beta**	2,61	**beta**	2,62	**beta**	2,63	**aT**	**α**
phi	0,47	**phi**	0,43	**phi**	0,43	**phi**	0,42	0,48	1,04
S value	0,470	**S value**	0,400	**S value**	0,210	**S value**	0,100		

30 mm ball size charge at U=0,6

1700 x 1180 micron

Table D19 Determined B values of zeolite for - 1700 + 1180 µm size interval ground with d = 30 mm ball diameter and U = 0,6.

INTERVAL NO,İ	SİZE (mesh)	Size (µm)	Xi/Xmax	B i,1	B VALUES
1	12x16	1700x1180	1,00	B1,1	1
2	16x20	1180x850	0,69	B2,1	1
3	20x30	850x600	0,50	B3,1	0,428235222
4	30x40	600x425	0,35	B4,1	0,302849104
5	40x50	425x300	0,25	B5,1	0,224978139
6	50x70	300x212	0,17	B6,1	0,157384353
7	70x100	212x150	0,12	B7,1	0,112055363
8	100x140	150x106	0,088	B8,1	0,080396697
9	140x200	106x75	0,062	B9,1	0,061365797
10	200x270	75x53	0,044	B10,1	0,044651798
11	270x400	53x38	0,031	B11,1	0,030844158
12	-400	-38	0,022	B12,1	0,021777177

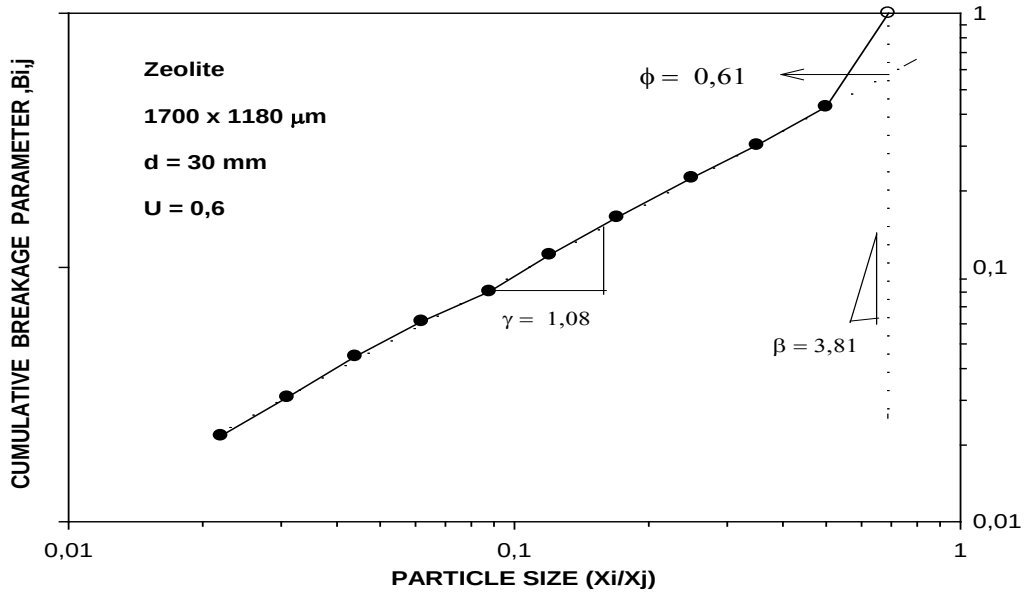

Figure D.29 Primary breakage distribution function of zeolite for -1700 + 1180 µm feed size fraction ground with d = 30 mm ball diameter and U = 0,6.

Table D.20 Cumulative weight percent less than size values of zeolite for 1700 x 1180 µm size interval ground with d = 30 mm ball diameter and U = 0,6.

SIZE	0 min.	0,133 min	1 min	3 min	6 min
1700	100,00	100,00	100,00	100,00	100,00
1180	0,75	28,11	59,92	86,43	97,91
850	0,12	13,01	39,39	80,54	91,49
600	0,06	9,36	26,75	65,43	80,39
425	0,00	7,00	19,72	46,86	63,06
300	0,00	4,95	15,13	35,06	49,92
212	0,00	3,55	11,71	25,15	38,02
150	0,00	2,56	8,88	17,19	27,11
106	0,00	1,96	6,55	12,49	18,95
75	0,00	1,43	4,53	8,56	12,87
53	0,00	0,99	3,06	6,15	9,04
38	0,00	0,70	2,01	4,02	6,12
%w.r.top size	99,25	71,89	40,08	13,57	2,09

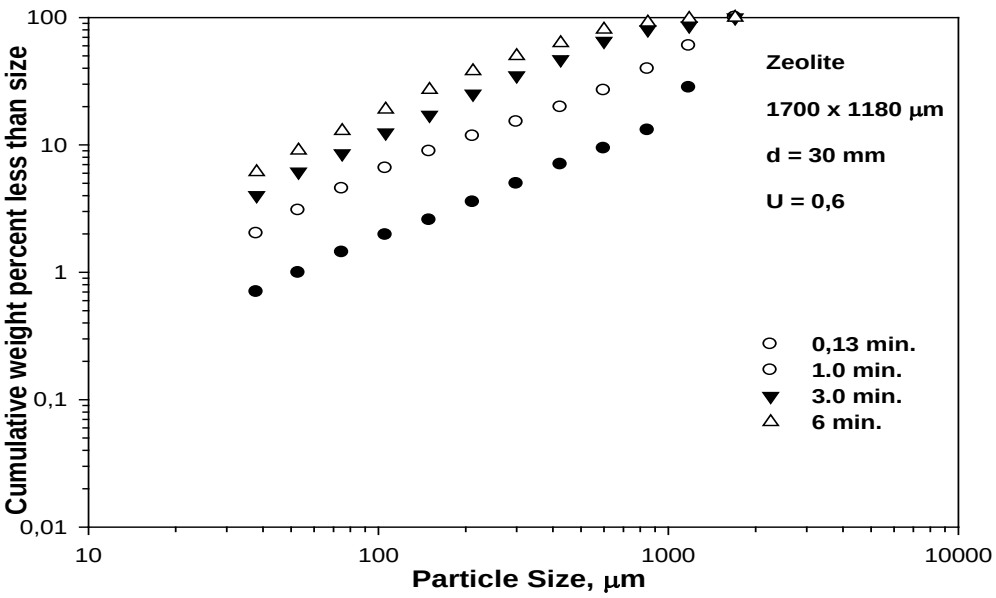

Figure D.30 Particle size distribution of zeolite for -1700 + 1180 µm feed size fraction ground with d = 30 mm ball diameter and U = 0,6.

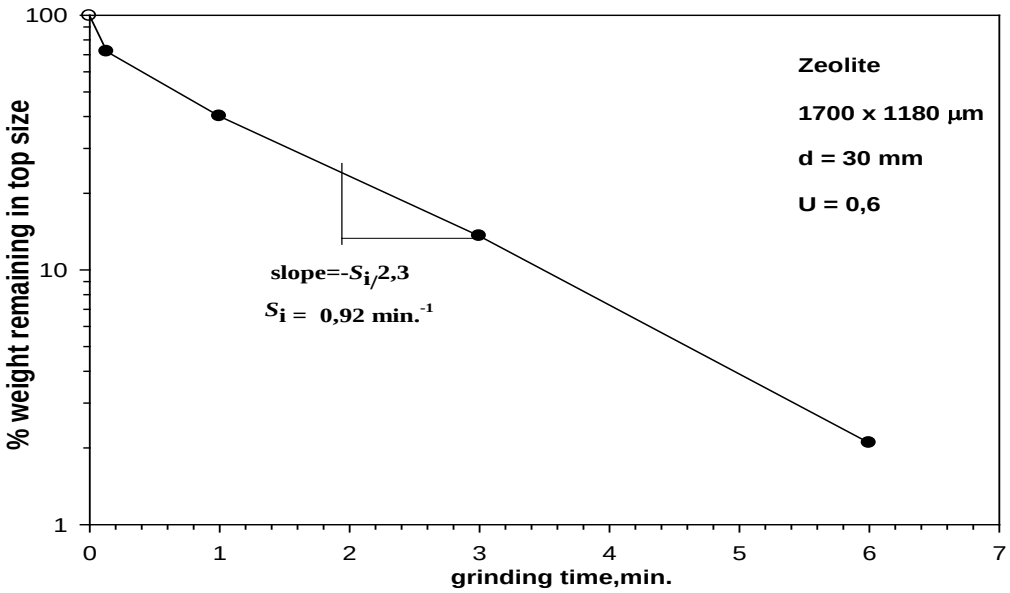

Figure D.31 First-order plot of breakage of - 1700 + 1180 µm feed of zeolite ground with d = 30 mm ball diameter and U = 0,6.

850 x 600 micron

Table D.21 Determined B values of zeolite for - 850 + 600 µm size interval ground with d = 30 mm ball diameter and U = 0,6.

INTERVAL NO,İ	SİZE (mesh)	Size (µm)	Xi/Xmax	B i,1	B VALUES
1	20x30	850x600	1,00	B3,1	1,000
2	30x40	600x425	0,7	B4,1	1,000
3	40x50	425x300	0,5	B5,1	0,424
4	50x70	300x212	0,35	B6,1	0,308
5	70x100	212x150	0,24	B7,1	0,221
6	100x140	150x106	0,17	B8,1	0,151
7	140x200	106x75	0,12	B9,1	0,112
8	200x270	75x53	0,08	B10,1	0,080
9	270x400	53x38	0,06	B11,1	0,062
10	-400	-38	0,04	B12,1	0,043

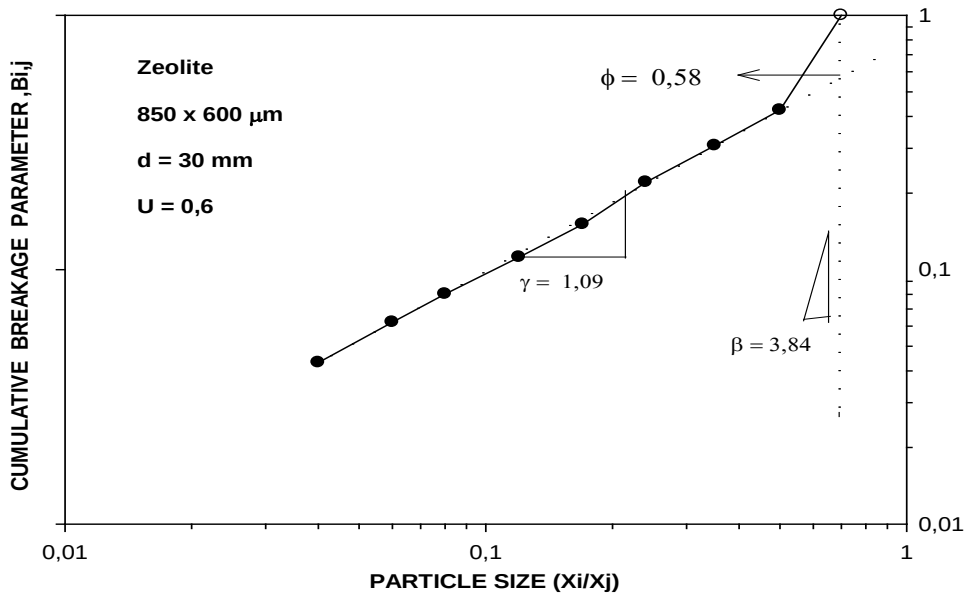

Figure D.32 Primary breakage distribution function of zeolite for -850 + 600 µm feed size fraction ground with d = 30 mm ball diameter and U = 0,6.

Table D.22 Cumulative weight percent less than size values of zeolite for - 850 + 600 µm size interval ground with d = 30 mm ball diameter and U = 0,6.

SIZE	0 min.	0,133 min	1 min	3 min	6 min
850	100,00	100,00	100,00	100,00	100,00
600	0,39	24,53	49,28	78,12	94,16
425	0,11	11,20	20,42	60,12	89,93
300	0,03	8,21	13,53	38,91	78,43
212	0,00	5,94	10,00	28,14	52,69
150	0,00	4,10	7,61	19,42	35,33
106	0,00	3,06	5,88	13,08	22,10
75	0,00	2,20	4,33	9,32	15,31
53	0,00	1,71	3,30	6,61	10,02
38	0,00	1,19	2,46	4,48	6,72
%w.r.top size	99,61	75,47	50,72	21,88	5,84

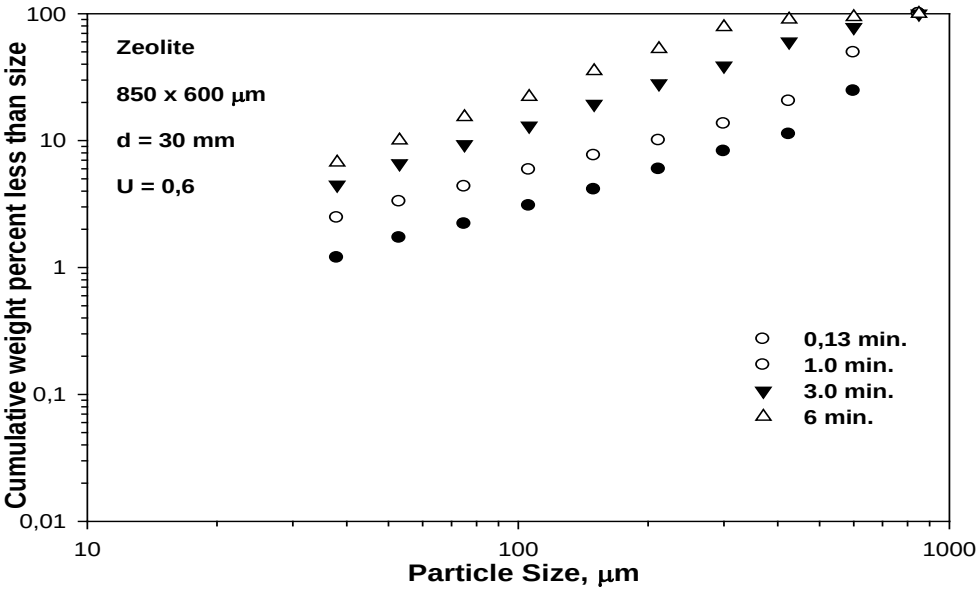

Figure D.33 Particle size distribution of zeolite for -850 + 600 µm feed size fraction ground with d = 30 mm ball diameter and U = 0,6.

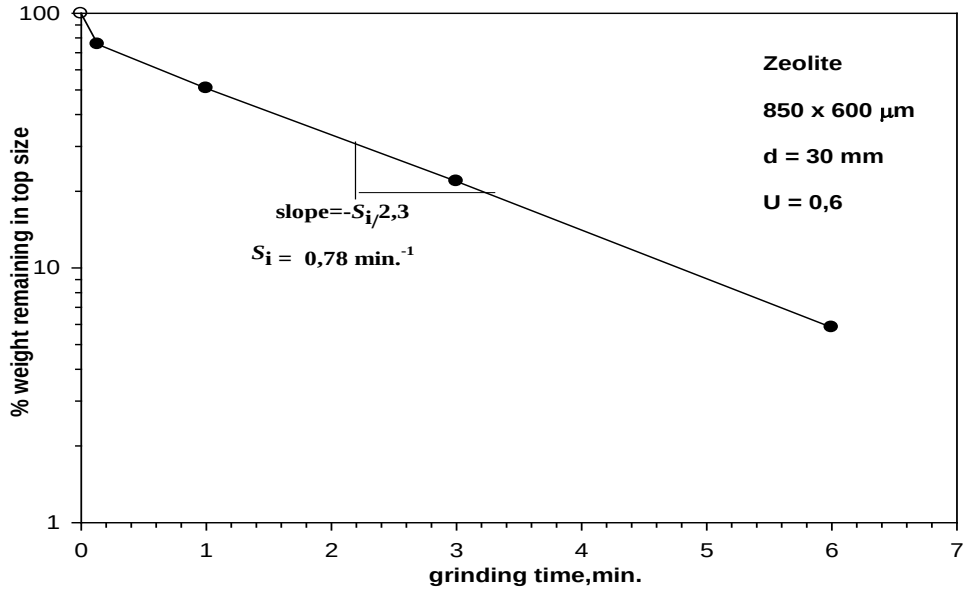

Figure D.34 First-order plot of breakage of - 850 + 600 µm feed of zeolite ground with d = 30 mm ball diameter and U = 0,6.

425 x 300 micron

Table D.23 Determined B values of zeolite for – 425 + 300 µm size interval ground with d = 30 mm ball diameter and U = 0,6.

INTERVAL NO,İ	SİZE (mesh)	Size (µm)	Xi/Xmax	B i,1	B VALUES
1	40x50	425x300	1,00	B1,1	1,0000
2	50x70	300x212	0,7	B2,1	1,0000
3	70x100	212x150	0,49	B3,1	0,4246
4	100x140	150x106	0,35	B4,1	0,3011
5	140x200	106x75	0,24	B5,1	0,2158
6	200x270	75x53	0,17	B6,1	0,1507
7	270x400	53x38	0,12	B7,1	0,1100
8	-400	-38	0,08	B8,1	0,0774

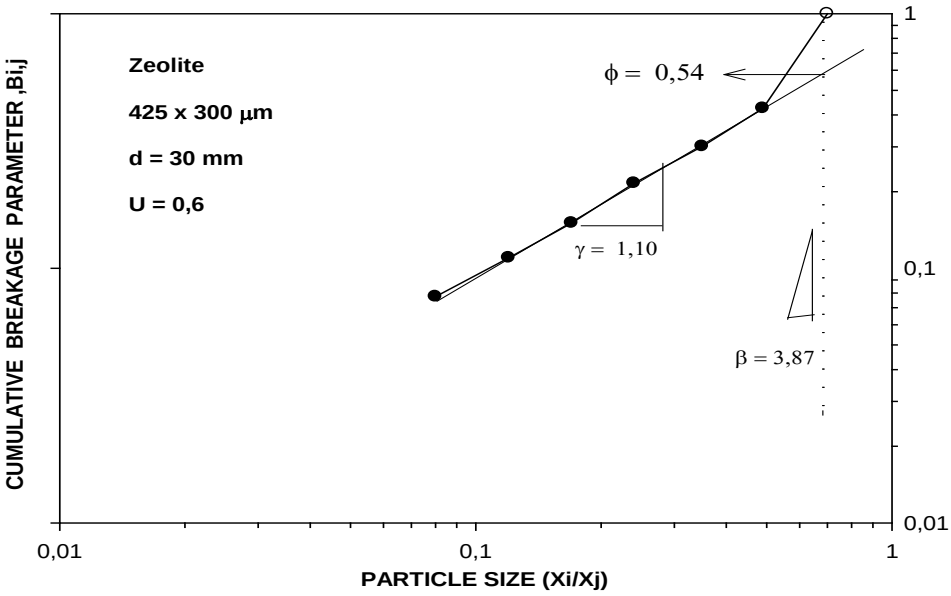

Figure D.35 Primary breakage distribution function of zeolite for -425 + 300 µm feed size fraction ground with d = 30 mm ball diameter and U = 0,6.

Table D.24 Cumulative weight percent less than size values of zeolite for - 425 + 300 µm size interval ground with d = 30 mm ball diameter and U = 0,6.

SIZE	0 min.	0,133 min	1 min	3 min	6 min
425	100,00	100,00	100,00	100,00	100,00
300	0,22	12,15	33,42	65,09	88,15
212	0,04	5,30	17,37	31,26	46,89
150	0,00	3,76	10,92	19,63	29,44
106	0,00	2,71	7,51	13,51	20,26
75	0,00	1,90	5,10	9,18	13,77
53	0,00	1,39	3,08	5,54	8,31
38	0,00	0,98	1,88	3,38	5,07
%w.r.top size	99,78	87,85	66,58	34,91	11,85

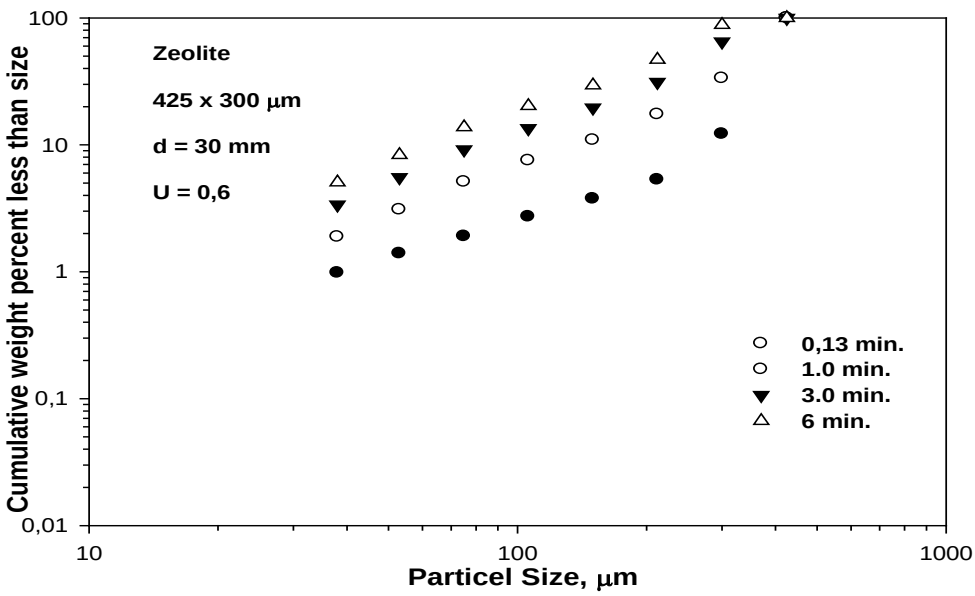

Figure D.36 Particle size distribution of zeolite for -425 + 300 µm feed size fraction ground with d = 30 mm ball diameter and U = 0,6.

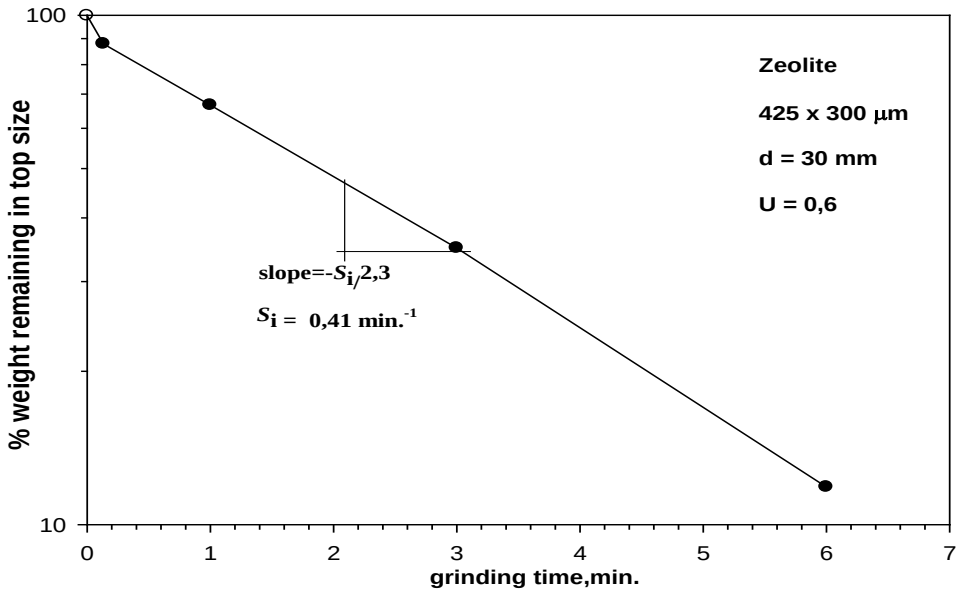

Figure D.37 First-order plot of breakage of - 425 + 300 µm feed of zeolite ground with d = 30 mm ball diameter and U = 0,6.

212 x 150 micron

Table D.25 Determined B values of zeolite for – 212 + 150 µm size interval ground with d = 30 mm ball diameter and U = 0,6.

INTERVAL NO,İ	SİZE (mesh)	Size (µm)	Xi/Xmax	B i,1	B VALUES
1	70x100	212x150	1,00	B1,1	1,0000
2	100x140	150x106	0,7	B2,1	1,0000
3	140x200	106x75	0,5	B3,1	0,4116
4	200x270	75x53	0,35	B4,1	0,2985
5	270x400	53x38	0,25	B5,1	0,2135
6	-400	-38	0,17	B6,1	0,1456

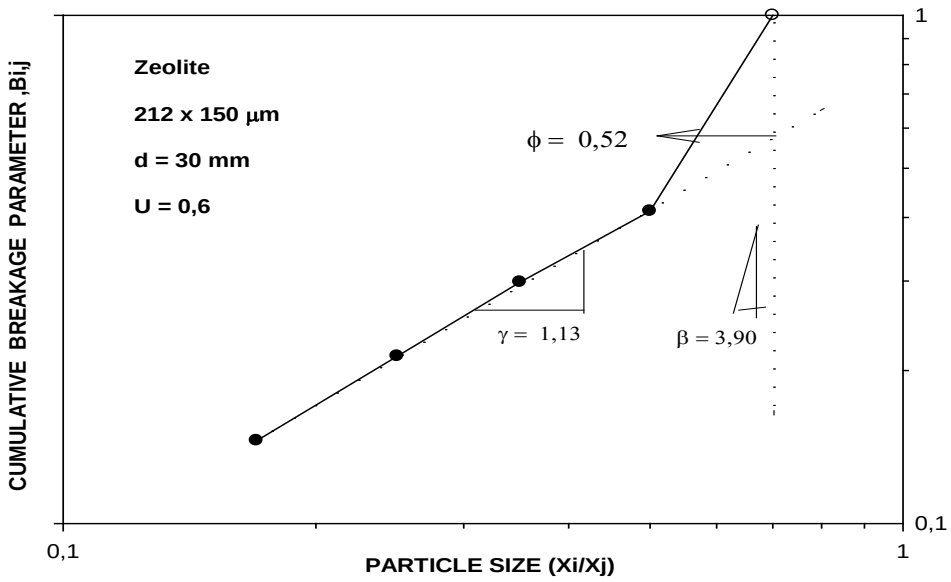

Figure D.38 Primary breakage distribution function of zeolite for - 212 + 150 µm feed size fraction ground with d = 30 mm ball diameter and U = 0,6.

Table D.26 Cumulative weight percent less than size values of zeolite for - 212 + 150 µm size interval ground with d = 30 mm ball diameter and U = 0,6.

SIZE	0 min.	0,133 min	1 min	3 min	6 min
212	100,00	100,00	100,00	100,00	100,00
150	0,11	9,52	29,92	60,08	82,11
106	0,02	4,01	16,33	29,39	44,08
75	0,00	2,91	9,82	17,67	26,50
53	0,00	2,09	6,01	10,81	16,21
38	0,00	1,43	3,82	6,87	10,30
%w.r.top size	99,89	90,48	70,08	39,92	17,89

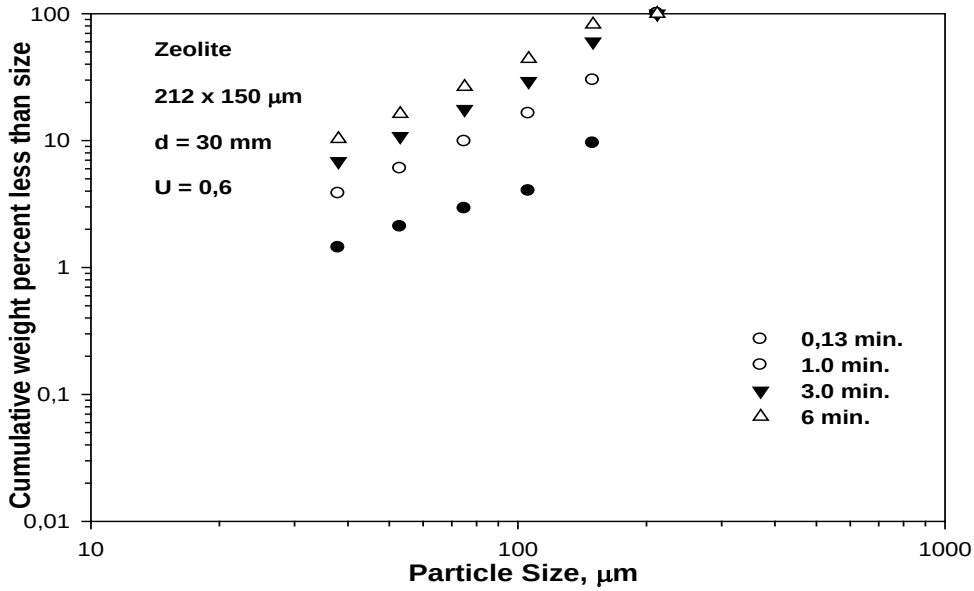

Figure D.39 Particle size distribution of zeolite for -212 + 150 µm feed size fraction ground with d = 30 mm ball diameter and U = 0,6.

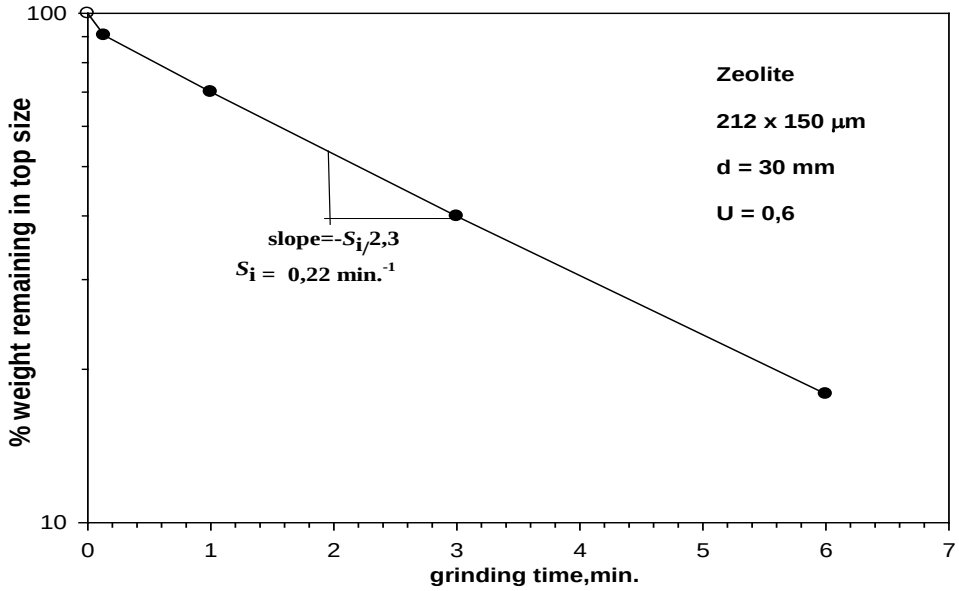

Figure D.40 First-order plot of breakage of - 212 + 150 µm feed of zeolite ground with d = 30 mm ball diameter and U = 0,6.

Determination of aT value

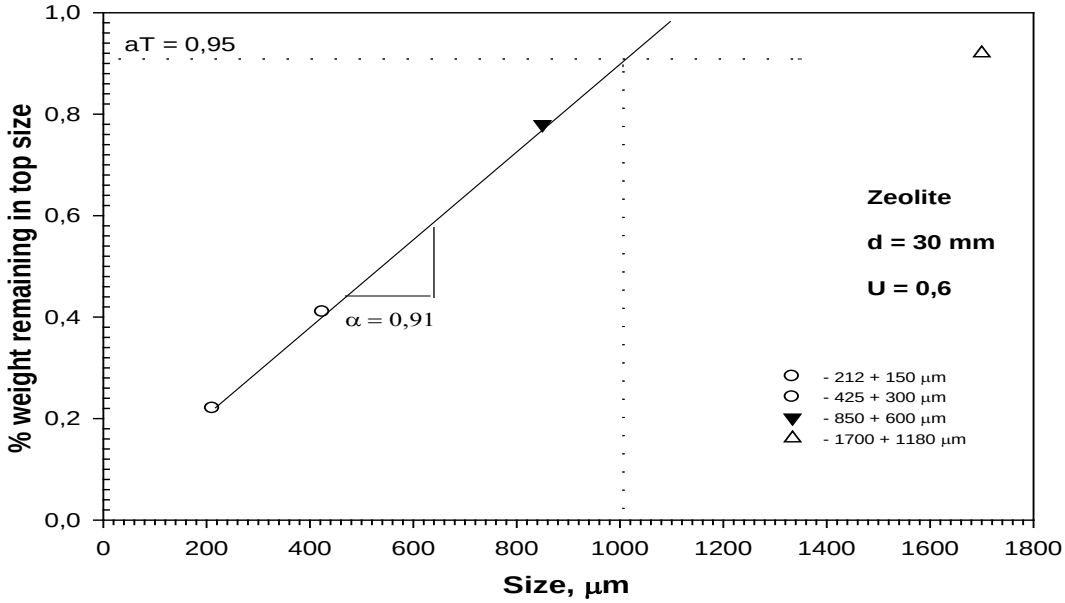

Figure D.41 Variation of first-order specific rates of breakage of zeolite ground with d = 30 mm ball diameter and particle size: √2 intervals, plotted at upper size of interval at U=0,6.

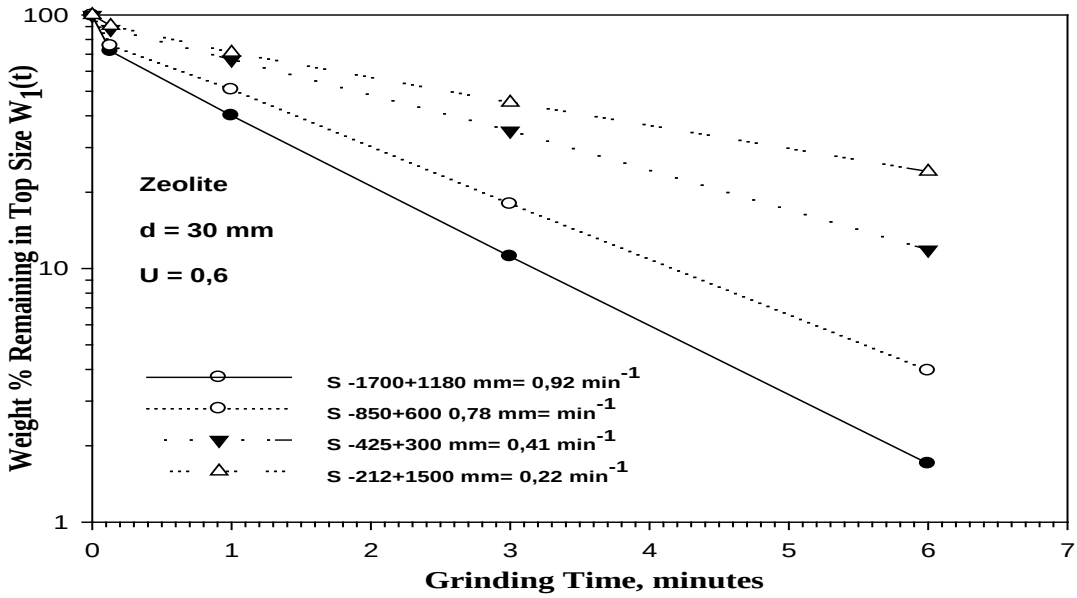

Figure D.42 First-order plots of breakage of -1700+1180, -850+600, -425+300, -212+150 μm feed size of zeolite ground with d = 30 mm ball diameter and U=0,6.

Table D.27 Breakage parameters of zeolite ground with d = 30 mm ball diameter at U=0,6.

1700x1180		**850x600**		**425x300**		**212x150**			
gama	1,08	**gama**	1,09	**gama**	1,10	**gama**	1,13		
beta	3,81	**beta**	3,84	**beta**	3,87	**beta**	3,90	**aT**	**α**
phi	0,61	**phi**	0,58	**phi**	0,54	**phi**	0,52	0,95	0,91
S value	0,920	**S value**	0,780	**S value**	0,410	**S value**	0,220		

30 mm ball size charge at U= 1

1700 x 1180 micron

Table D.28 Determined B values of zeolite for - 1700 + 1180 µm size interval ground with d = 30 mm ball diameter and U = 1.

INTERVAL NO,İ	**SİZE (mesh)**	**Size (µm)**	**Xi/Xmax**	**B i,1**	**B VALUES**
1	12x16	1700x1180	1,00	B1,1	1,0000
2	16x20	1180x850	0,69	B2,1	1,0000
3	20x30	850x600	0,50	B3,1	0,3659
4	30x40	600x425	0,35	B4,1	0,2489
5	40x50	425x300	0,25	B5,1	0,1804
6	50x70	300x212	0,17	B6,1	0,1292
7	70x100	212x150	0,12	B7,1	0,0924
8	100x140	150x106	0,088	B8,1	0,0679
9	140x200	106x75	0,062	B9,1	0,0476
10	200x270	75x53	0,044	B10,1	0,0331
11	270x400	53x38	0,031	B11,1	0,0237
12	-400	-38	0,022	B12,1	0,0167

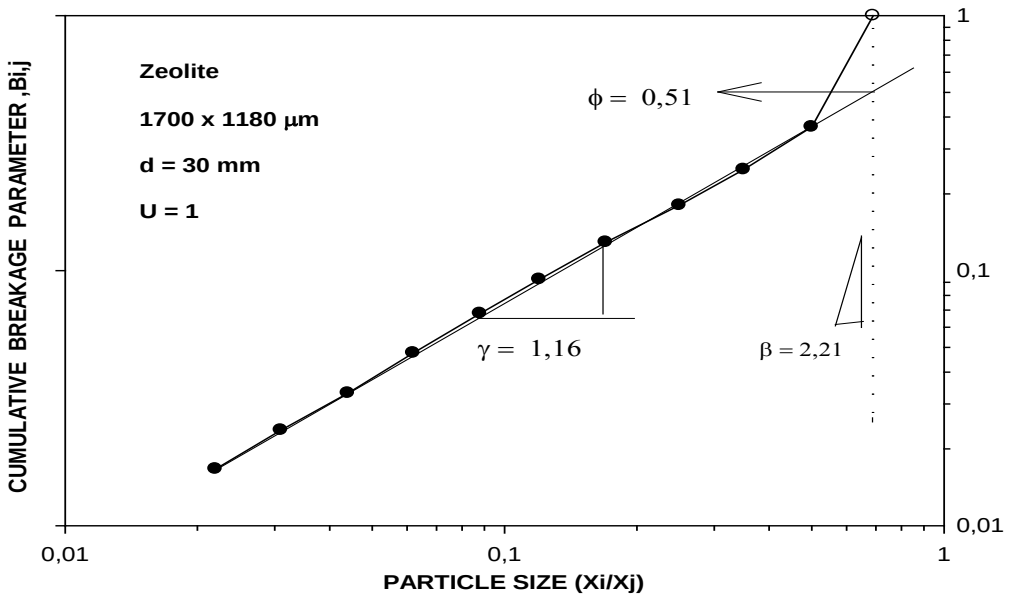

Figure D.43 Primary breakage distribution function of zeolite for -1700 + 1180 µm feed size fraction ground with d = 30 mm ball diameter and U = 0,6.

Table D.29 Cumulative weight percent less than size values of zeolite for 1700 x 1180 µm size interval ground with d = 30 mm ball diameter and U = 1.

SIZE	0 min.	0,133 min	1 min	3 min	6 min
1700	100,00	100,00	100,00	100,00	100,00
1180	0,56	26,38	59,91	90,13	98,70
850	0,06	10,47	32,29	80,16	93,22
600	0,00	7,21	21,67	64,41	78,91
425	0,00	5,28	14,81	45,19	60,14
300	0,00	3,81	10,62	31,29	47,72
212	0,00	2,74	7,41	22,83	36,56
150	0,00	2,02	4,66	15,42	26,03
106	0,00	1,42	3,02	10,95	18,47
75	0,00	0,99	1,87	7,36	12,84
53	0,00	0,71	1,23	4,62	8,54
38	0,00	0,50	0,86	2,84	5,07
%w.r.top size	99,44	73,62	40,09	9,87	1,30

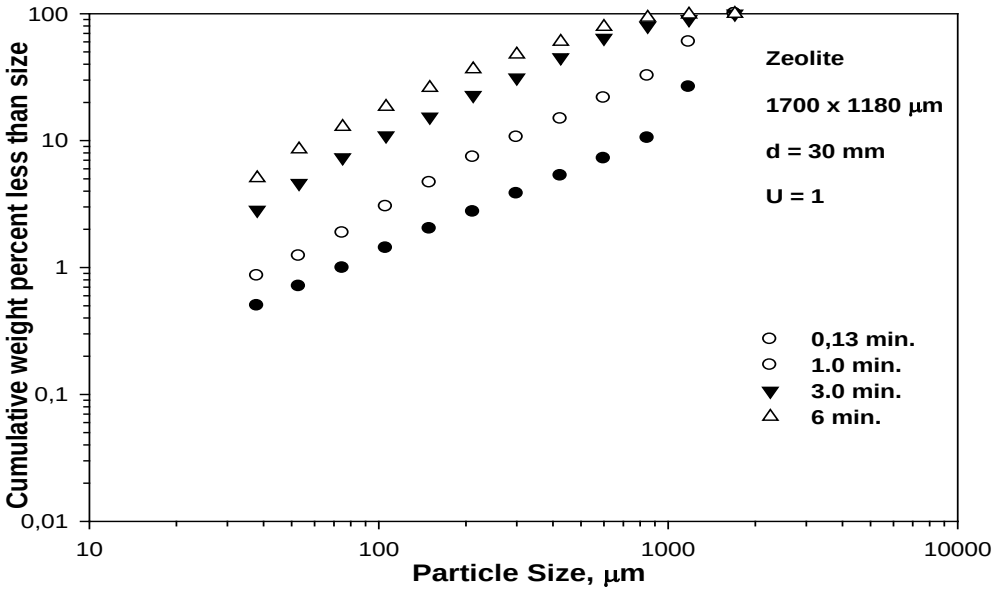

Figure D.44 Particle size distribution of zeolite for -1700 + 1180 μm feed size fraction ground with d = 30 mm ball diameter and U = 1.

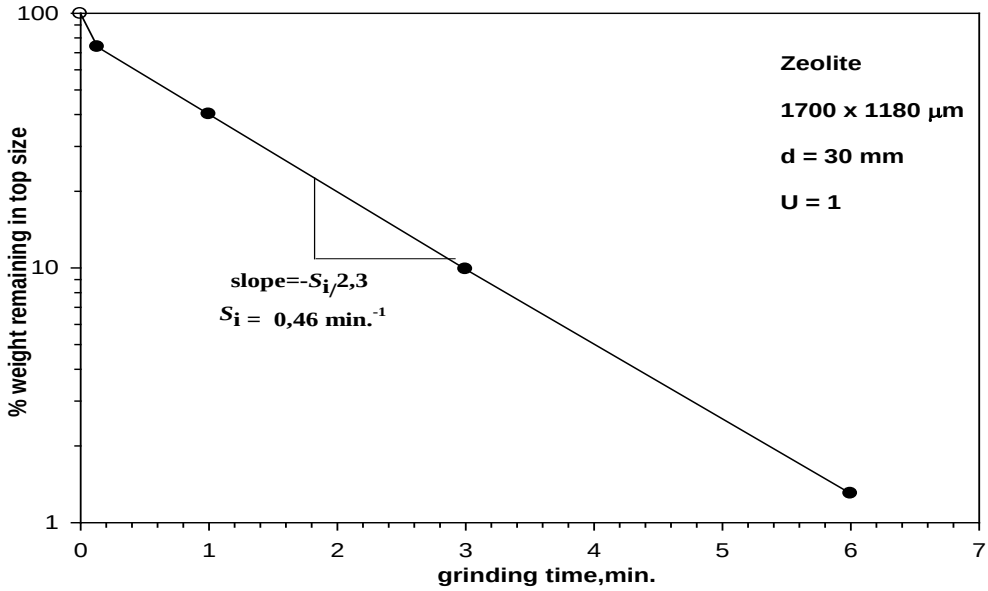

Figure D.45 First-order plot of breakage of - 1700 + 1180 μm feed of zeolite ground with d = 30 mm ball diameter and U = 1.

850 x 600 micron

Table D.30 Determined B values of zeolite for - 850 + 600 µm size interval ground with d = 30 mm ball diameter and U = 1.

INTERVAL NO,İ	SİZE (mesh)	Size (µm)	Xi/Xmax	B i,1	B VALUES
1	20x30	850x600	1,00	B3,1	1,000
2	30x40	600x425	0,7	B4,1	1,000
3	40x50	425x300	0,5	B5,1	0,363
4	50x70	300x212	0,35	B6,1	0,248
5	70x100	212x150	0,24	B7,1	0,180
6	100x140	150x106	0,17	B8,1	0,126
7	140x200	106x75	0,12	B9,1	0,089
8	200x270	75x53	0,08	B10,1	0,058
9	270x400	53x38	0,06	B11,1	0,042
10	-400	-38	0,04	B12,1	0,028

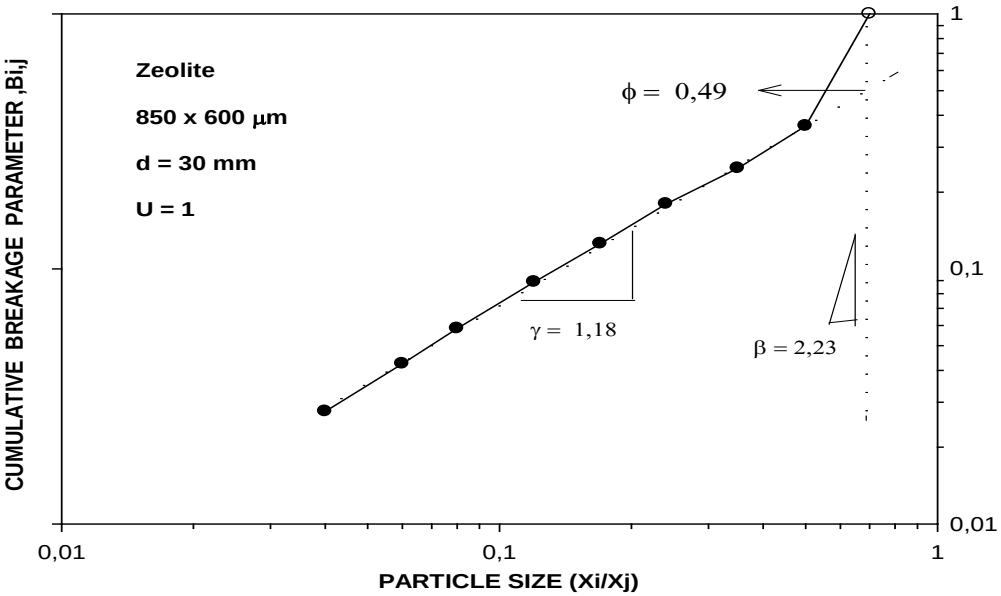

Figure D.46 Primary breakage distribution function of zeolite for -850 + 600 µm feed size fraction ground with d = 30 mm ball diameter and U = 0,6.

Table D.31 Cumulative weight percent less than size values of zeolite for - 850 + 600 µm size interval ground with d = 30 mm ball diameter and U = 1.

SIZE	0 min.	0,133 min	1 min	3 min	6 min
850	100,00	100,00	100,00	100,00	100,00
600	0,21	18,57	44,92	78,04	93,88
425	0,04	7,16	18,41	53,96	88,16
300	0,00	4,92	10,68	34,25	75,21
212	0,00	3,59	6,84	22,84	48,13
150	0,00	2,52	4,69	13,79	31,78
106	0,00	1,79	2,92	8,86	18,67
75	0,00	1,18	2,03	5,63	11,52
53	0,00	0,86	1,47	3,41	7,33
38	0,00	0,56	0,96	2,05	4,21
%w.r.top size	99,79	81,43	55,08	21,96	6,12

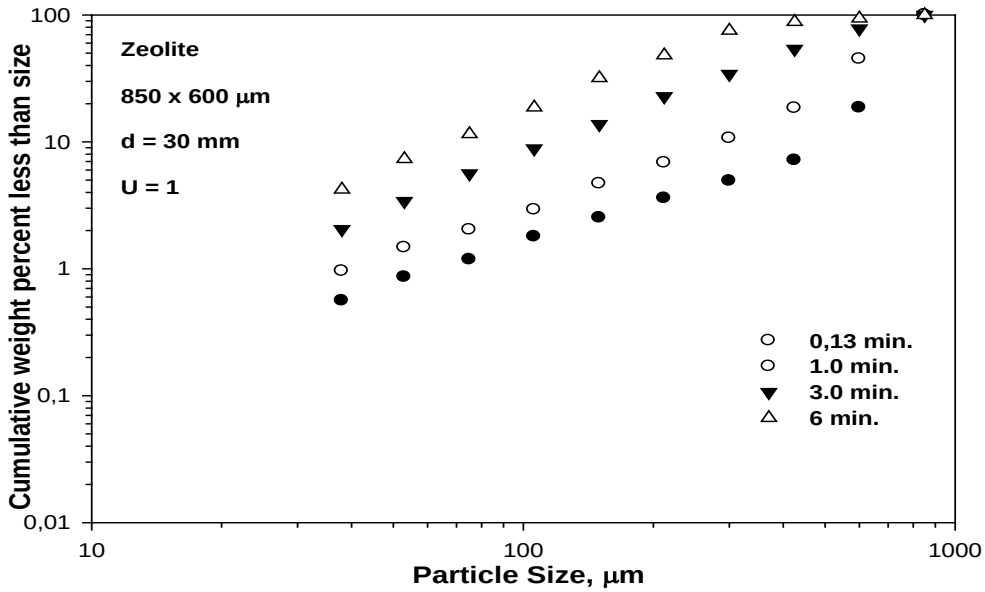

Figure D.47 Particle size distribution of zeolite for -850 + 600 µm feed size fraction ground with d = 30 mm ball diameter and U = 1.

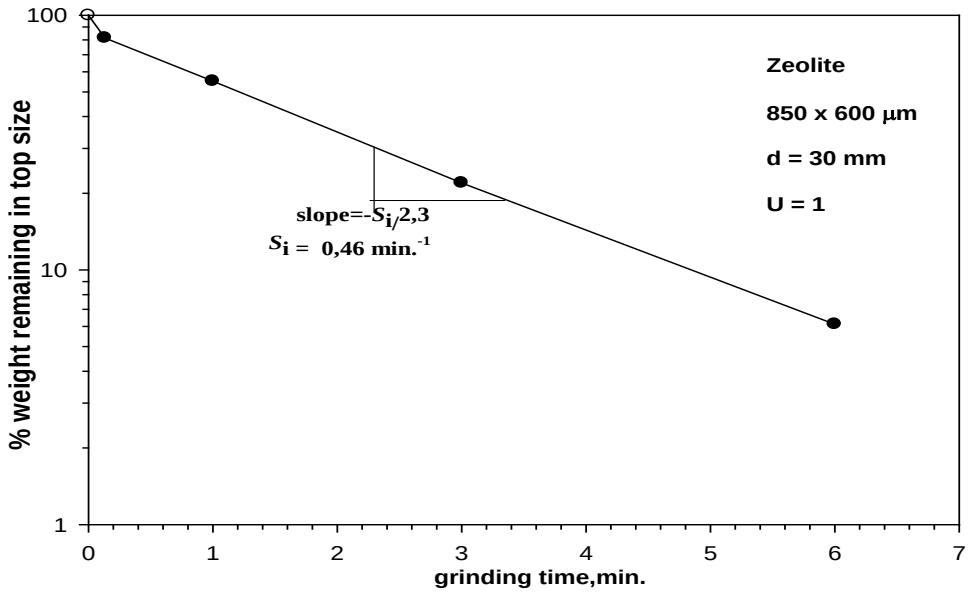

Figure D.48 First-order plot of breakage of - 850 + 600 µm feed of zeolite ground with d = 30 mm ball diameter and U = 1.

425 x 300 micron

Table D.32 Determined B values of zeolite for – 425 + 300 µm size interval ground with d = 30 mm ball diameter and U = 1.

INTERVAL NO,İ	SİZE (mesh)	Size (µm)	Xi/Xmax	B i,1	B VALUES
1	40x50	425x300	1,00	B1,1	1,0000
2	50x70	300x212	0,7	B2,1	1,0000
3	70x100	212x150	0,49	B3,1	0,3610
4	100x140	150x106	0,35	B4,1	0,2446
5	140x200	106x75	0,24	B5,1	0,1753
6	200x270	75x53	0,17	B6,1	0,1217
7	270x400	53x38	0,12	B7,1	0,0861
8	-400	-38	0,08	B8,1	0,0544

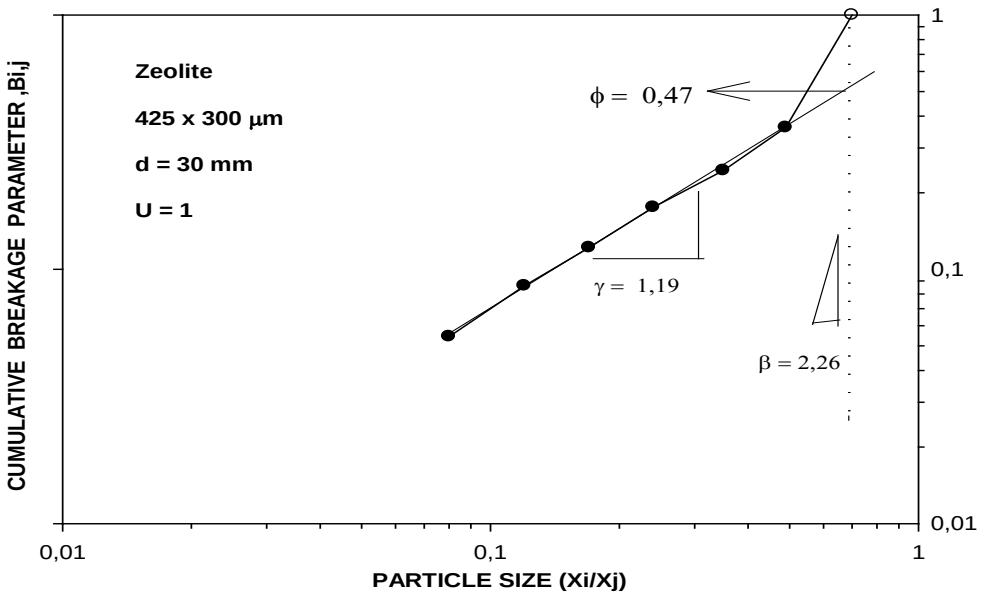

Figure D.49 Primary breakage distribution function of zeolite for -425 + 300 μm feed size fraction ground with d = 30 mm ball diameter and U = 1.

Table D.33 Cumulative weight percent less than size values of zeolite for - 425 + 300 μm size interval ground with d = 30 mm ball diameter and U = 1.

SIZE	0 min.	0,133 min	1 min	3 min	6 min
425	100,00	100,00	100,00	100,00	100,00
300	0,12	7,73	27,68	56,21	78,92
212	0,02	2,84	11,54	19,04	33,48
150	0,00	1,92	4,42	8,12	15,36
106	0,00	1,38	2,56	4,11	7,04
75	0,00	0,96	1,64	2,53	3,86
53	0,00	0,68	1,17	1,76	2,53
38	0,00	0,43	0,79	1,27	1,73
%w.r.top size	99,88	92,27	72,32	43,79	21,08

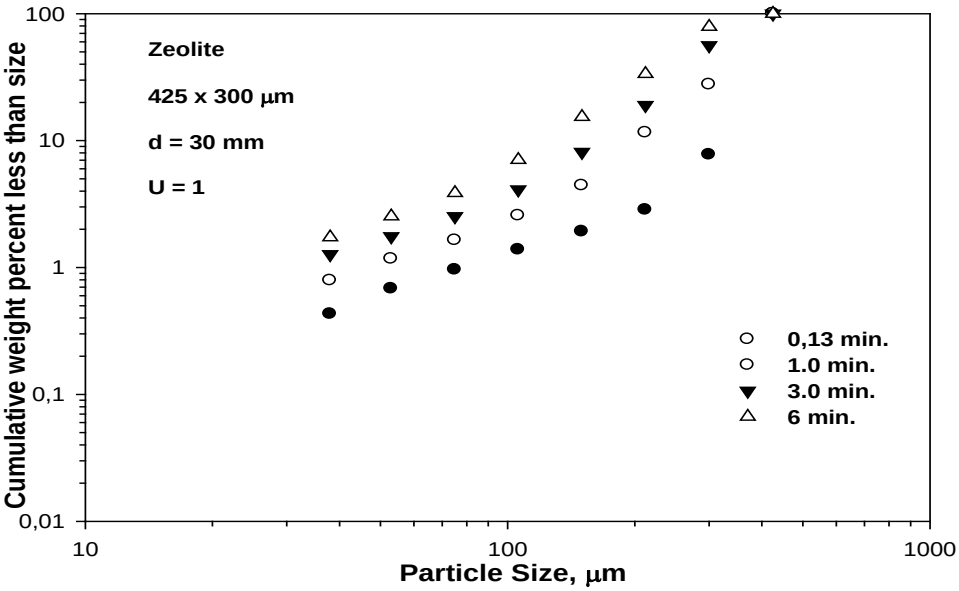

Figure D.50 Particle size distribution of zeolite for -425 + 300 µm feed size fraction ground with d = 30 mm ball diameter and U = 1.

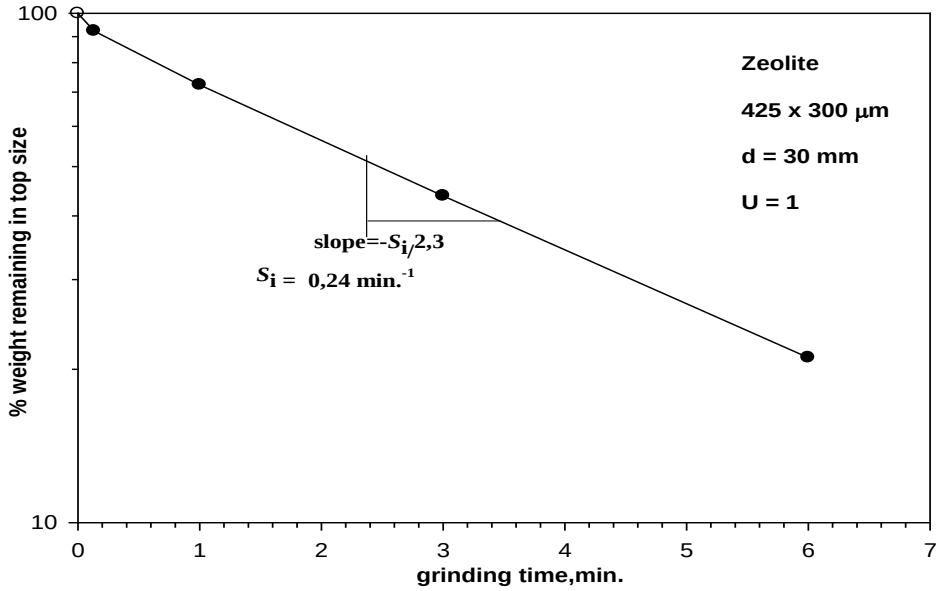

Figure D.51 First-order plot of breakage of - 425 + 300 µm feed of zeolite ground with d = 30 mm ball diameter and U = 1.

212 x 150 micron

Table D.34 Determined B values of zeolite for – 212 + 150 µm size interval ground with d = 30 mm ball diameter and U = 1.

INTERVAL NO,İ	SİZE (mesh)	Size (µm)	Xi/Xmax	B i,1	B VALUES
1	70x100	212x150	1,00	B1,1	1,0000
2	100x140	150x106	0,7	B2,1	1,0000
3	140x200	106x75	0,5	B3,1	0,3378
4	200x270	75x53	0,35	B4,1	0,2325
5	270x400	53x38	0,25	B5,1	0,1688
6	-400	-38	0,17	B6,1	0,1118

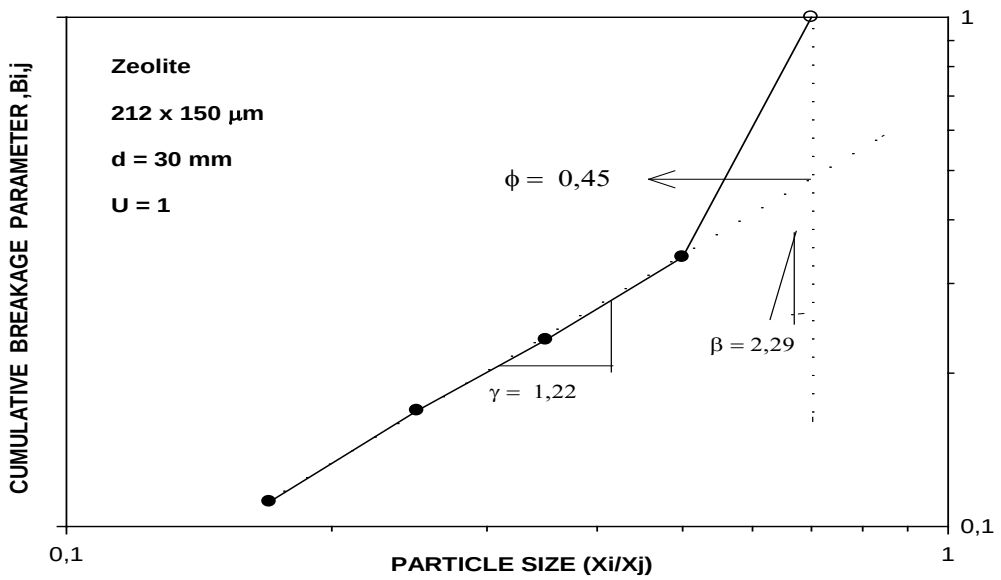

Figure D.52 Primary breakage distribution function of zeolite for - 212 + 150 µm feed size fraction ground with d = 30 mm ball diameter and U = 1.

Table D.35 Cumulative weight percent less than size values of zeolite for - 212 + 150 µm size interval ground with d = 30 mm ball diameter and U = 1.

SIZE	0 min.	0,133 min	1 min	3 min	6 min
212	100,00	100,00	100,00	100,00	100,00
150	0,11	6,11	19,91	52,67	78,37
106	0,04	2,11	14,06	22,10	36,41
75	0,00	1,43	9,61	15,03	26,32
53	0,00	1,04	6,12	10,60	18,43
38	0,00	0,69	3,43	6,91	12,78
%w.r.top size	99,89	93,89	80,09	47,33	21,63

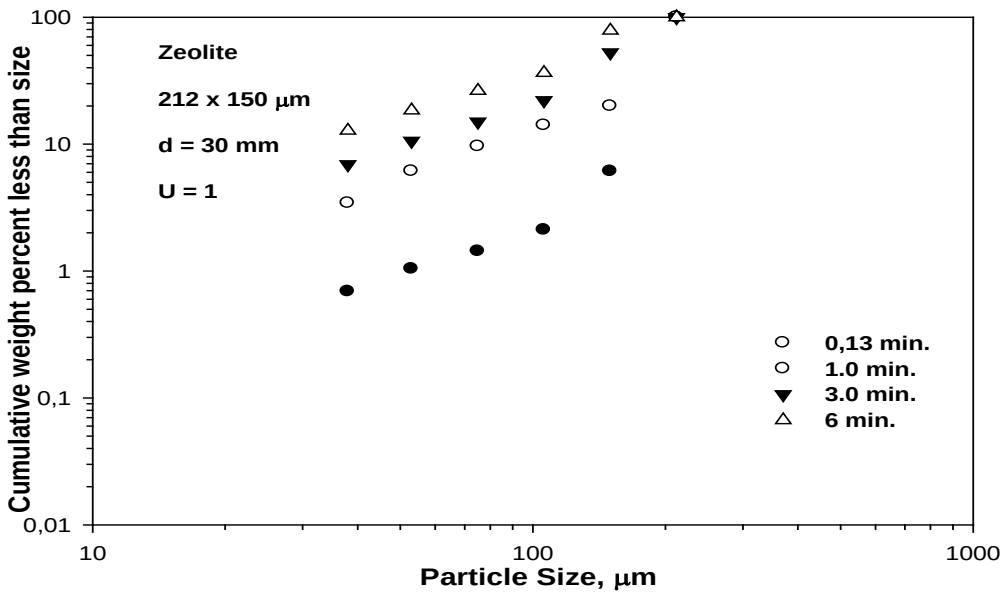

Figure D.53 Particle size distribution of zeolite for -212 + 150 µm feed size fraction ground with d = 30 mm ball diameter and U = 1.

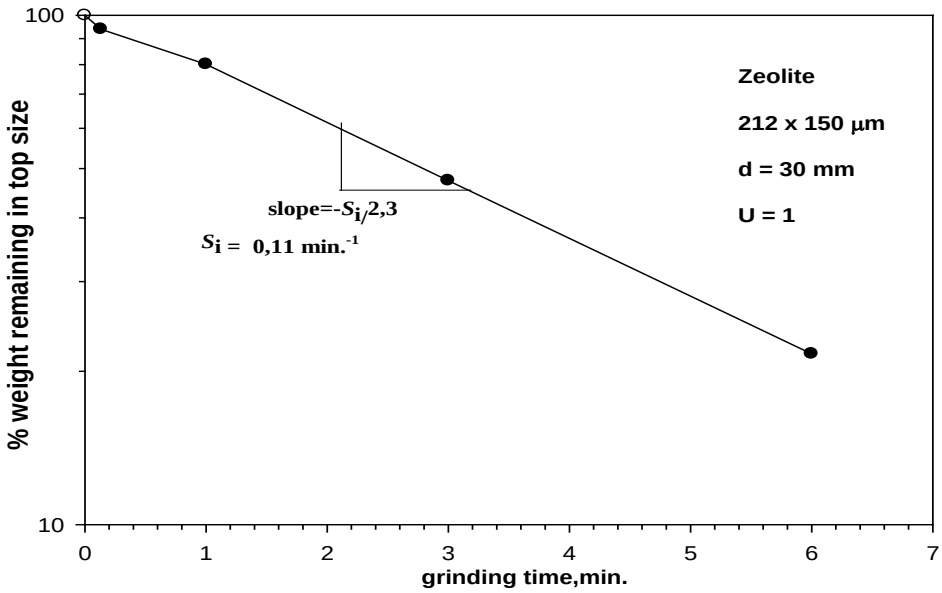

Figure D.54 First-order plot of breakage of - 212 + 150 μm feed of zeolite ground with d = 30 mm ball diameter and U = 1.

Determination of aT value

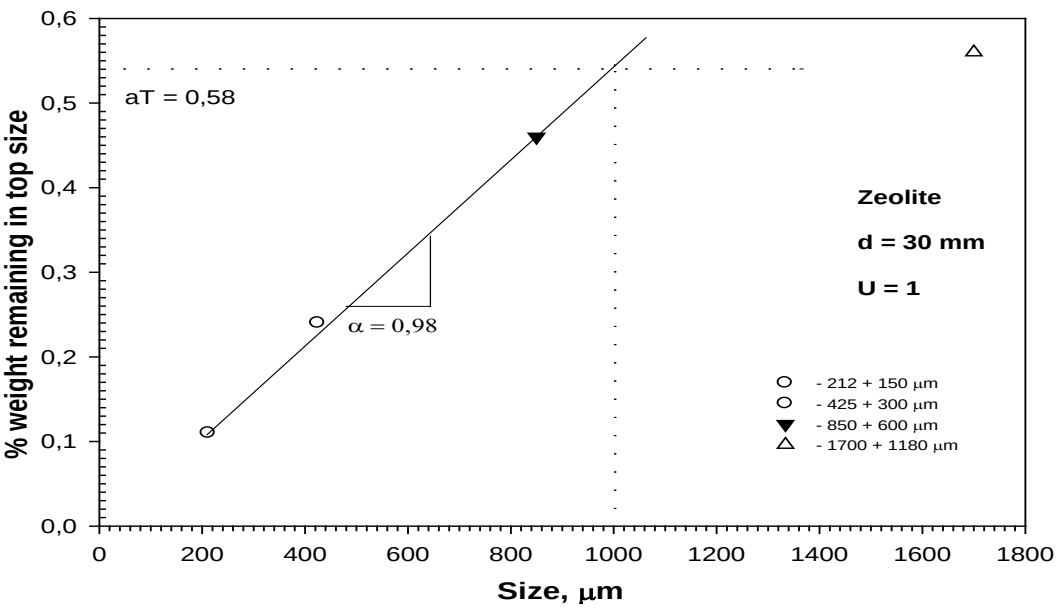

Figure D.55 Variation of first-order specific rates of breakage of zeolite ground with d = 30 mm ball diameter and particle size: √2 intervals, plotted at upper size of interval at U=1.

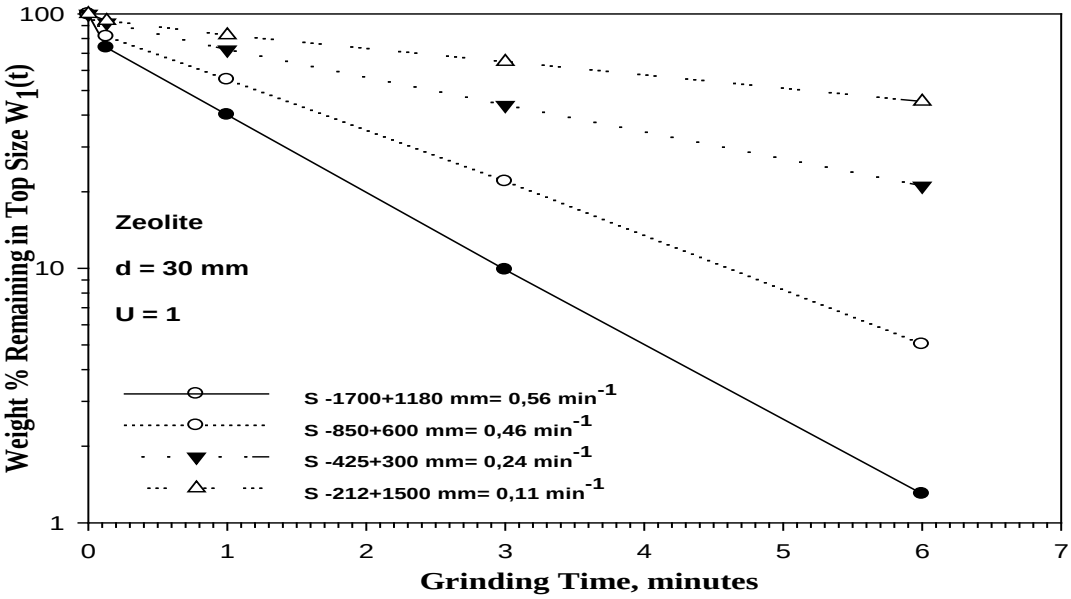

Figure D.56 First-order plots of breakage of -1700+1180, -850+600, -425+300, -212+150 μm feed size of zeolite ground with d = 30 mm ball diameter and U=1.

Table D.36 Breakage parameters of zeolite ground with d = 30 mm ball diameter at U=1.

1700x1180		**850x600**		**425x300**		**212x150**			
gama	1,16	**gama**	1,18	**gama**	1,19	**gama**	1,22		
beta	2,21	**beta**	2,23	**beta**	2,26	**beta**	2,29	**aT**	**α**
phi	0,51	**phi**	0,49	**phi**	0,47	**phi**	0,47	0,58	0,98
S value	0,56	**S value**	0,460	**S value**	0,240	**S value**	0,110		

30 – 25,4 – 19,05 mm ball size charge at U=0,6

1700 x 1180 micron

Table D.37 Determined B values of zeolite for - 1700 + 1180 µm size interval ground with d = 30 – 25,4 – 19,05 mm ball diameter and U = 0,6.

INTERVAL NO,İ	SİZE (mesh)	Size (µm)	Xi/Xmax	B i,1	B VALUES
1	12x16	1700x1180	1,00	B1,1	1
2	16x20	1180x850	0,69	B2,1	1
3	20x30	850x600	0,50	B3,1	0,417785993
4	30x40	600x425	0,35	B4,1	0,263047761
5	40x50	425x300	0,25	B5,1	0,178385538
6	50x70	300x212	0,17	B6,1	0,113823375
7	70x100	212x150	0,12	B7,1	0,071636902
8	100x140	150x106	0,088	B8,1	0,048655934
9	140x200	106x75	0,062	B9,1	0,033138209
10	200x270	75x53	0,044	B10,1	0,020670729
11	270x400	53x38	0,031	B11,1	0,013108418
12	-400	-38	0,022	B12,1	0,008620227

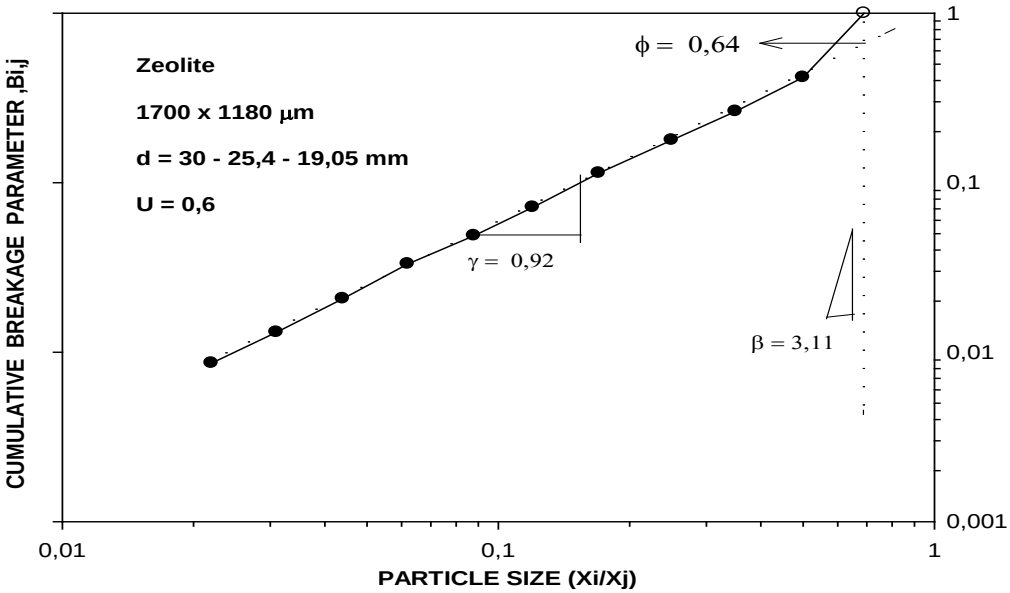

Figure D.57 Primary breakage distribution function of zeolite for -1700 + 1180 µm feed size fraction ground with d = 30 – 25,4 – 19,05 mm ball diameter and U = 0,6.

Table D.38 Cumulative weight percent less than size values of zeolite for 1700 x 1180 µm size interval ground with d = 30 – 25,4 – 19,05 mm ball diameter and U = 0,6.

SIZE	0 min.	0,133 min	1 min	3 min	6 min
1700	100,00	100,00	100,00	100,00	100,00
1180	0,56	46,94	79,89	97,07	99,81
850	0,18	23,22	33,14	69,56	92,64
600	0,00	15,23	20,42	50,11	81,54
425	0,00	10,60	15,05	37,58	66,36
300	0,00	6,90	10,41	28,63	54,39
212	0,00	4,40	7,32	22,19	42,33
150	0,00	3,01	5,12	16,50	29,96
106	0,00	2,06	3,49	12,33	20,10
75	0,00	1,29	2,33	8,90	14,02
53	0,00	0,82	1,48	6,12	9,00
38	0,00	0,54	1,07	3,91	6,20
%w.r.top size	99,44	53,06	20,11	2,93	0,19

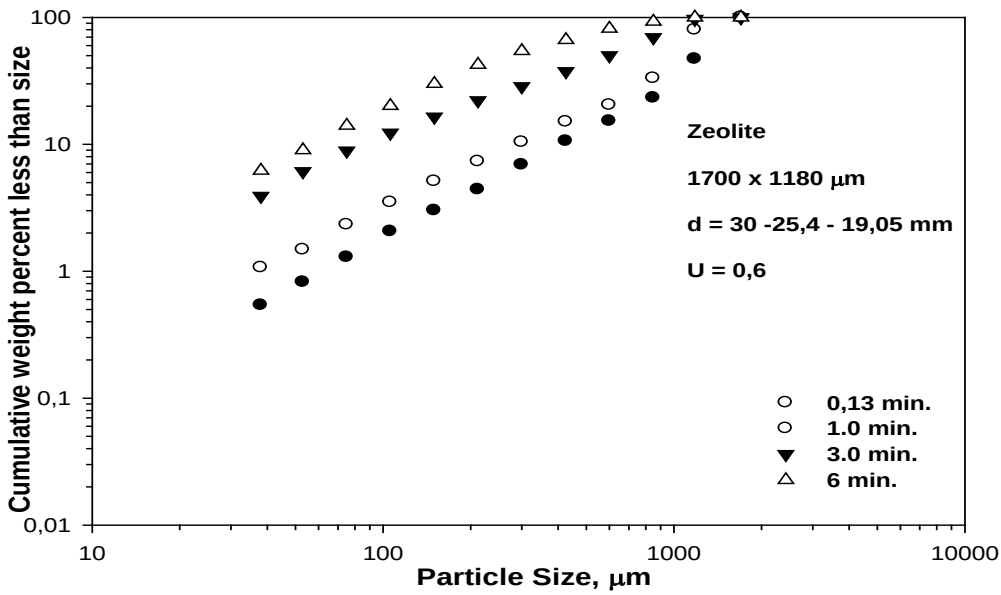

Figure D.58 Particle size distribution of zeolite for -1700 + 1180 µm feed size fraction ground with d = 30 – 25,4 – 19,05 mm ball diameter and U = 0,6.

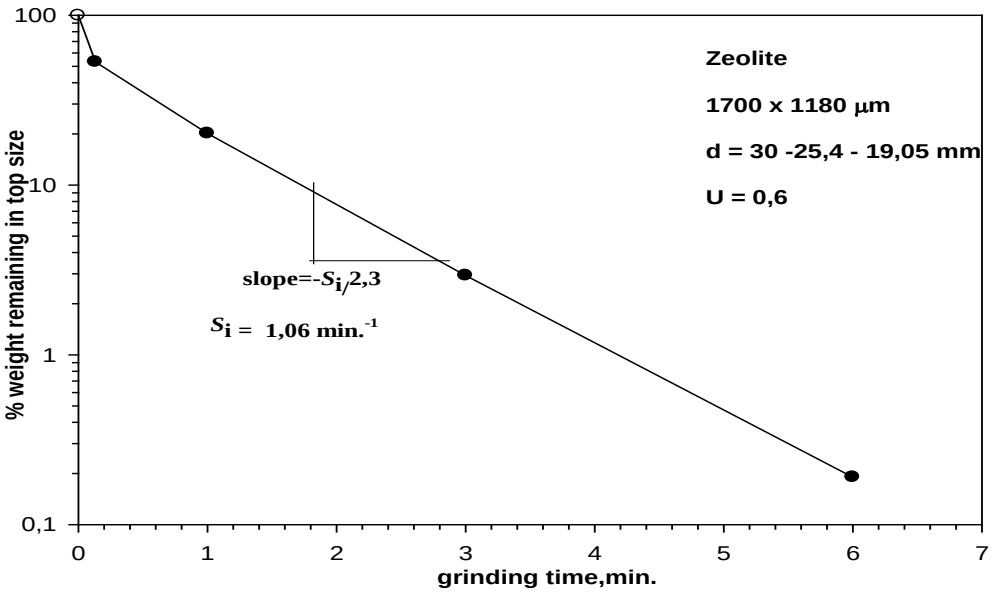

Figure D.59 First-order plot of breakage of - 1700 + 1180 µm feed of zeolite ground with d = 30 – 25,4 – 19,05 mm ball diameter and U = 0,6.

850 x 600 micron

Table D.39 Determined B values of zeolite for - 850 + 600 µm size interval ground with d = 30 – 25,4 – 19,05 mm ball diameter and U = 0,6.

INTERVAL NO,İ	SİZE (mesh)	Size (µm)	Xi/Xmax	B i,1	B VALUES
1	20x30	850x600	1,00	B3,1	1,000
2	30x40	600x425	0,7	B4,1	1,000
3	40x50	425x300	0,5	B5,1	0,417
4	50x70	300x212	0,35	B6,1	0,269
5	70x100	212x150	0,24	B7,1	0,171
6	100x140	150x106	0,17	B8,1	0,113
7	140x200	106x75	0,12	B9,1	0,076
8	200x270	75x53	0,08	B10,1	0,048
9	270x400	53x38	0,06	B11,1	0,034
10	-400	-38	0,04	B12,1	0,021

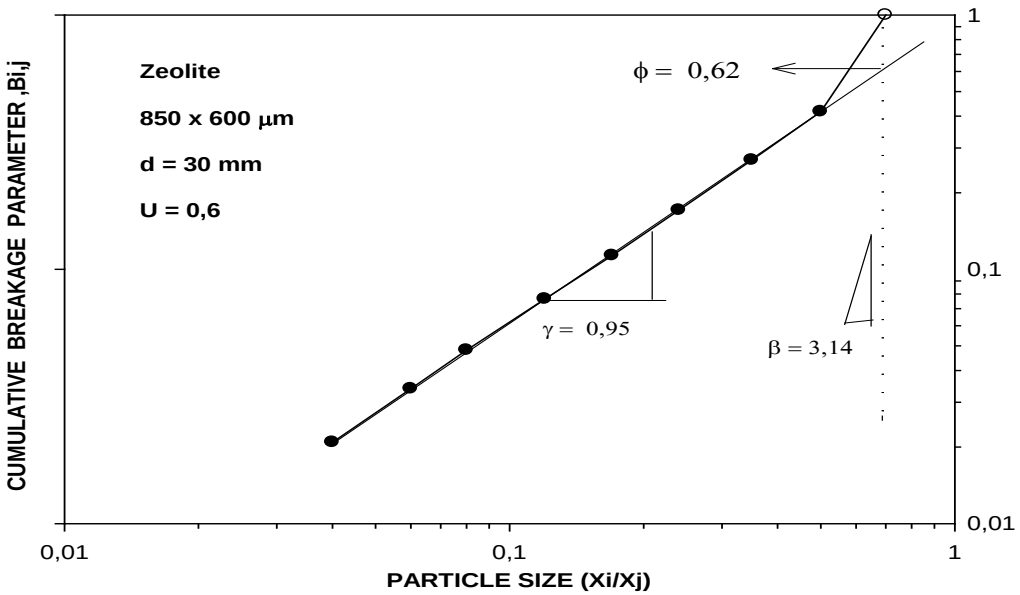

Figure D.60 Primary breakage distribution function of zeolite for -850 + 600 µm feed size fraction ground with d = 30 – 25,4 – 19,05 mm ball diameter and U = 0,6.

Table D.40 Cumulative weight percent less than size values of zeolite for - 850 + 600 µm size interval ground with d = 30 – 25,4 – 19,05 mm ball diameter and U = 0,6.

SIZE	0 min.	0,133 min	1 min	3 min	6 min
850	100,00	100,00	100,00	100,00	100,00
600	0,37	31,85	71,92	95,04	99,72
425	0,16	14,77	45,38	90,85	98,73
300	0,00	9,71	30,20	76,25	97,14
212	0,00	6,28	21,17	60,11	93,41
150	0,00	4,21	15,24	45,66	80,91
106	0,00	2,86	11,02	33,51	62,77
75	0,00	1,81	7,03	25,17	47,39
53	0,00	1,28	3,69	16,14	32,34
38	0,00	0,79	1,90	10,71	21,56
%w.r.top size	99,63	68,15	28,08	4,96	0,28

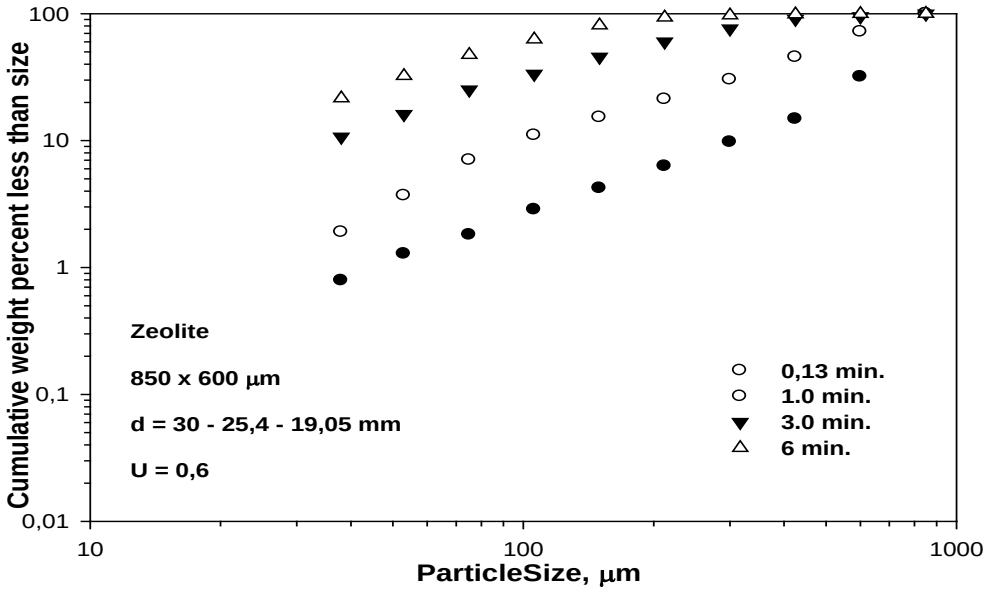

Figure D.61 Particle size distribution of zeolite for -850 + 600 µm feed size fraction ground with d = 30 – 25,4 – 19,05 mm ball diameter and U = 0,6.

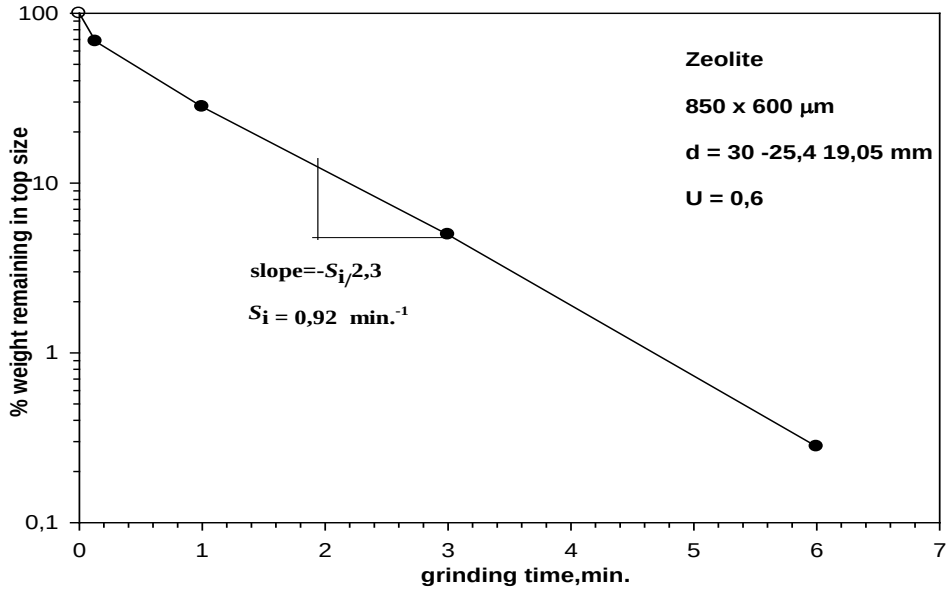

Figure D.62 First-order plot of breakage of - 850 + 600 µm feed of zeolite ground with d = 30 – 25,4 – 19,05 mm ball diameter and U = 0,6.

425 x 300 micron

Table D.41 Determined B values of zeolite for – 425 + 300 µm size interval ground with d = 30 – 25,4 – 19,05 mm ball diameter and U = 0,6.

INTERVAL NO,İ	SİZE (mesh)	Size (µm)	Xi/Xmax	B i,1	B VALUES
1	40x50	425x300	1,00	B1,1	1,0000
2	50x70	300x212	0,7	B2,1	1,0000
3	70x100	212x150	0,49	B3,1	0,4149
4	100x140	150x106	0,35	B4,1	0,2616
5	140x200	106x75	0,24	B5,1	0,1703
6	200x270	75x53	0,17	B6,1	0,1139
7	270x400	53x38	0,12	B7,1	0,0743
8	-400	-38	0,08	B8,1	0,0482

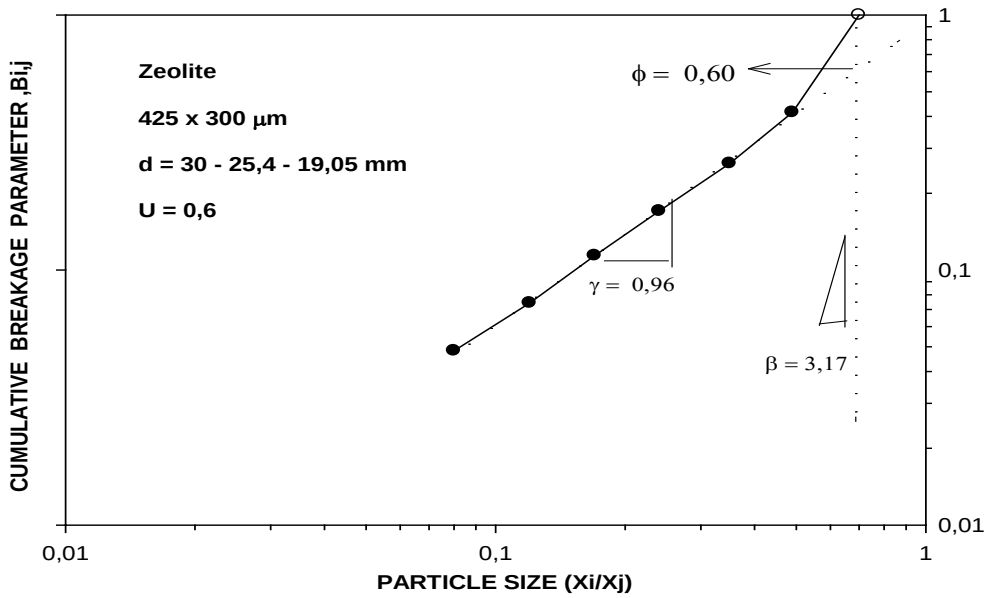

Figure D.63 Primary breakage distribution function of zeolite for -425 + 300 µm feed size fraction ground with d = 30 – 25,4 – 19,05 mm ball diameter and U = 0,6.

Table D.42 Cumulative weight percent less than size values of zeolite for - 425 + 300 µm size interval ground with d = 30 – 25,4 – 19,05 mm ball diameter and U = 0,6.

SIZE	0 min.	0,133 min	1 min	3 min	6 min
425	100,00	100,00	100,00	100,00	100,00
300	0,21	23,74	45,53	79,88	95,62
212	0,09	10,62	21,41	43,83	69,33
150	0,00	6,80	13,63	29,27	47,88
106	0,00	4,48	9,20	20,29	34,72
75	0,00	3,02	6,35	14,59	24,80
53	0,00	1,98	4,29	9,22	14,08
38	0,00	1,29	2,80	5,91	8,52
%w.r.top size	99,79	76,26	54,47	20,12	4,38

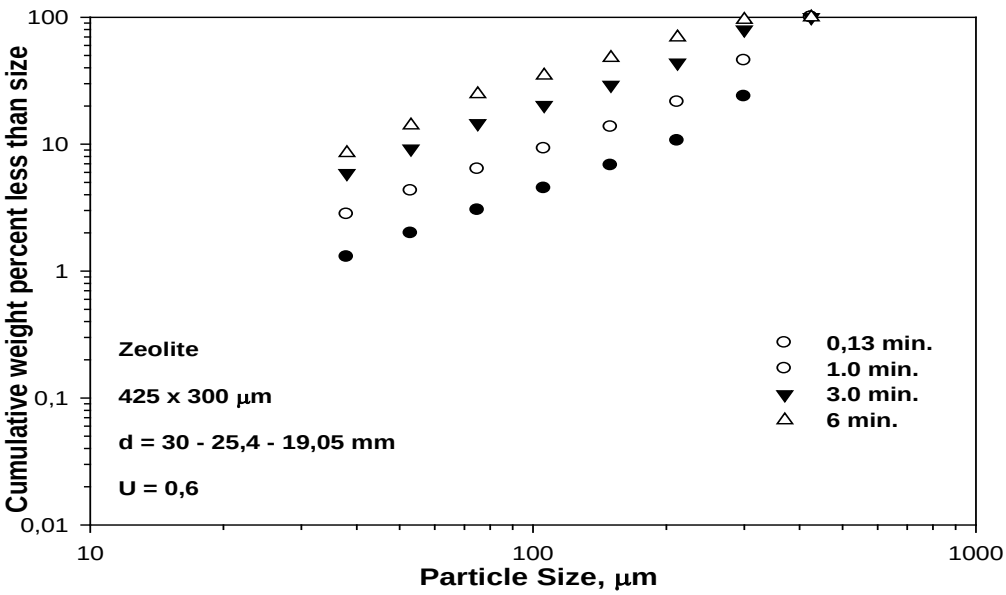

Figure D.43 Particle size distribution of zeolite for -425 + 300 µm feed size fraction ground with d = 30 – 25,4 – 19,05 mm ball diameter and U = 0,6.

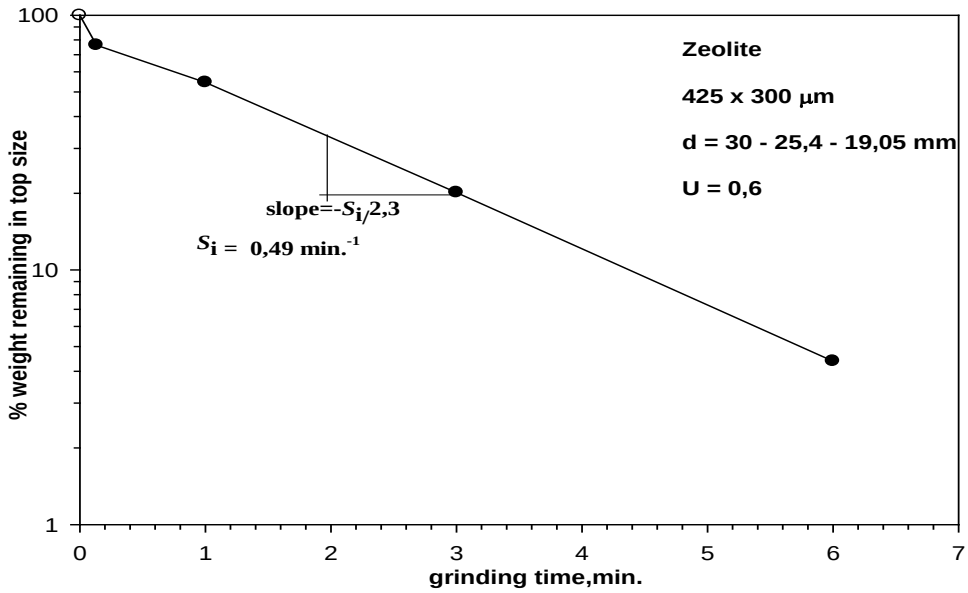

Figure D.65 First-order plot of breakage of - 425 + 300 µm feed of zeolite ground with d = 30 – 25,4 – 19,05 mm ball diameter and U = 0,6.

212 x 150 micron

Table D.43 Determined B values of zeolite for – 212 + 150 µm size interval ground with d = 30 – 25,4 – 19,05 mm ball diameter and U = 0,6.

INTERVAL NO,İ	SİZE (mesh)	Size (µm)	Xi/Xmax	B i,1	B VALUES
1	70x100	212x150	1,00	B1,1	1,0000
2	100x140	150x106	0,7	B2,1	1,0000
3	140x200	106x75	0,5	B3,1	0,3748
4	200x270	75x53	0,35	B4,1	0,2194
5	270x400	53x38	0,25	B5,1	0,1394
6	-400	-38	0,17	B6,1	0,0813

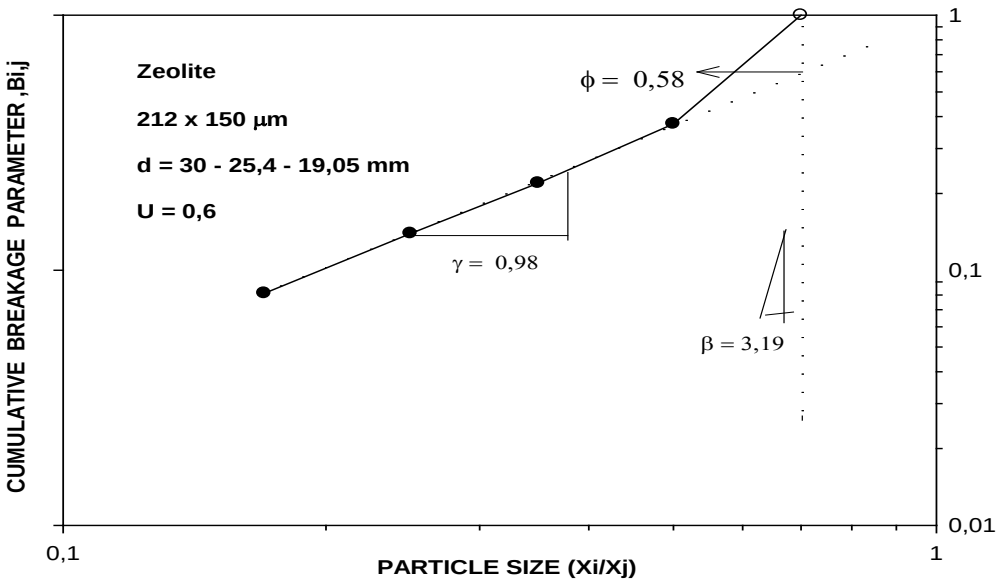

Figure D.66 Primary breakage distribution function of zeolite for - 212 + 150 µm feed size fraction ground with d = 30 – 25,4 – 19,05 mm ball diameter and U = 0,6.

Table D.44 Cumulative weight percent less than size values of zeolite for - 212 + 150 µm size interval ground with d = 30 – 25,4 – 19,05 mm ball diameter and U = 0,6.

SIZE	100,00	100,00	100,00	100,00	100,00
212	0,19	18,25	36,90	63,45	84,26
150	0,07	7,26	18,10	35,87	56,22
106	0,00	4,29	11,78	23,98	37,80
75	0,00	2,75	7,49	14,25	22,14
53	0,00	1,61	4,36	8,23	13,41
38	100,00	100,00	100,00	100,00	100,00
%w.r.top size	99,81	81,75	63,10	36,55	15,74

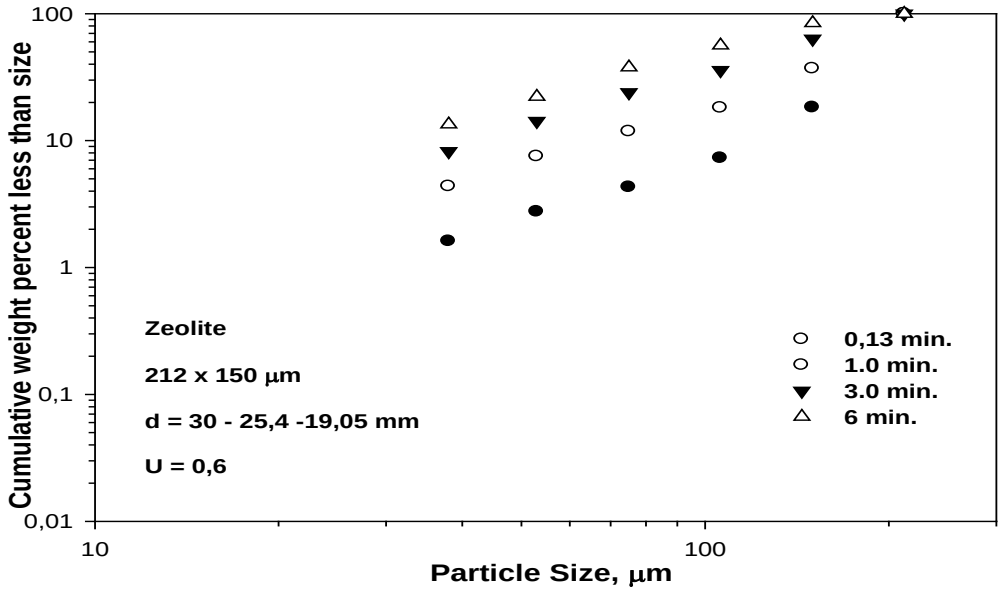

Figure D.67 Particle size distribution of zeolite for -212 + 150 µm feed size fraction ground with d = 30 – 25,4 – 19,05 mm ball diameter and U = 0,6.

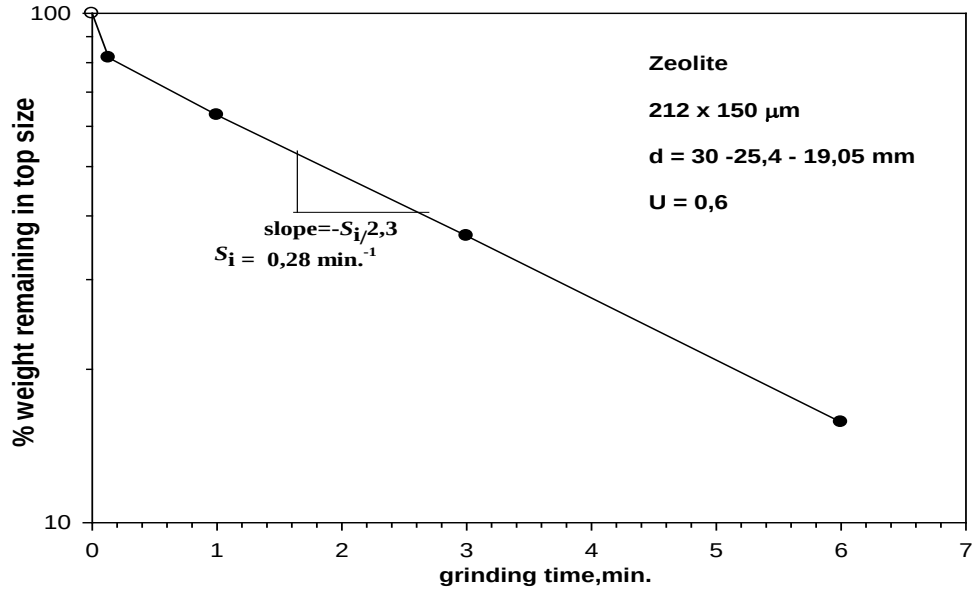

Figure D.68 First-order plot of breakage of - 212 + 150 µm feed of zeolite ground with d = 30 – 25,4 – 19,05 mm ball diameter and U = 0,6.

Determination of aT value

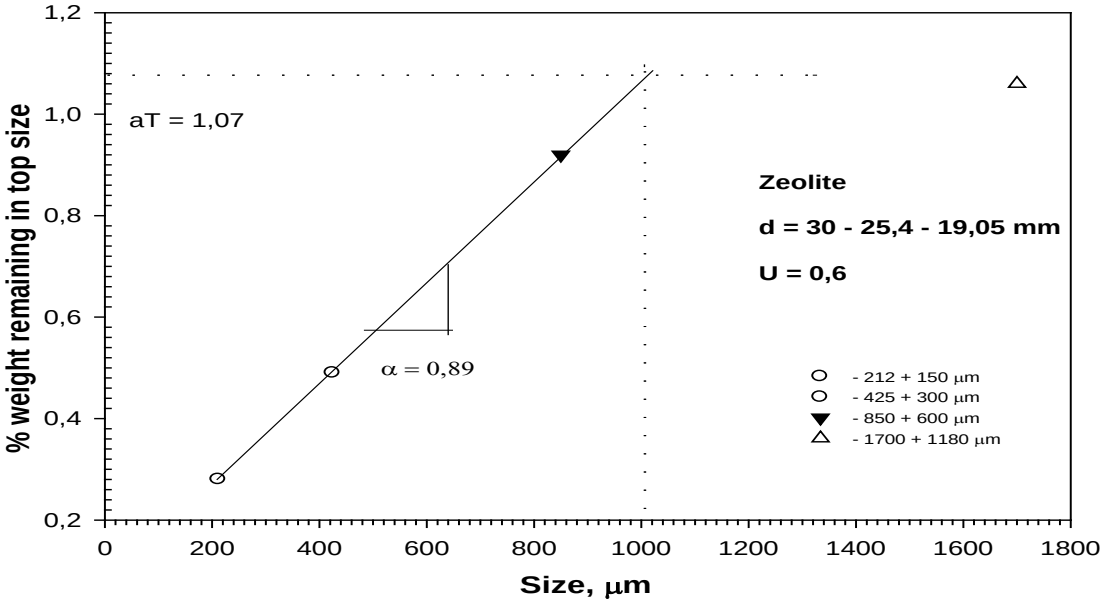

Figure D.69 Variation of first-order specific rates of breakage of zeolite ground with d = 30 – 25,4 - 19,05 mm ball diameter and particle size: √2 intervals, plotted at upper size of interval at U=0,6.

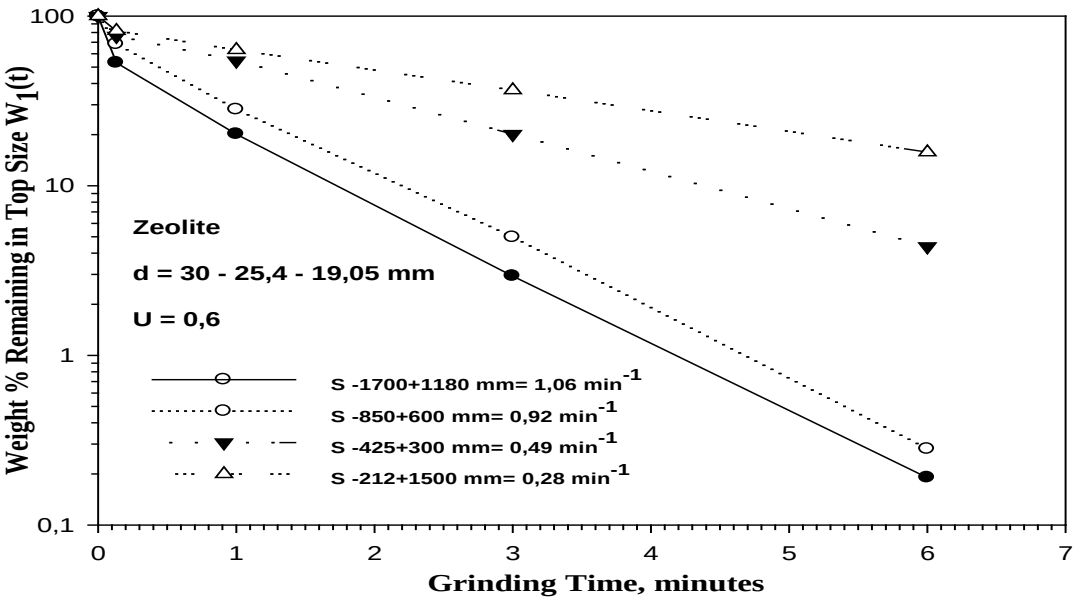

Figure D.70 First-order plots of breakage of -1700+1180, -850+600, -425+300, -212+150 μm feed size of zeolite ground with d = 30 – 25,4 – 19,05 mm ball diameter and U=0,6.

Table D.45 Breakage parameters of zeolite ground with d = 30 – 25,4 – 19,05 mm ball diameter at U=0,6.

1700x1180		**850x600**		**425x300**		**212x150**			
gama	0,92	**gama**	0,95	**gama**	0,96	**gama**	0,98		
beta	3,11	**beta**	3,14	**beta**	3,17	**beta**	3,19	**aT**	**α**
phi	0,64	**phi**	0,62	**phi**	0,60	**phi**	0,58	1,07	0,89
S value	1,060	**S value**	0,920	**S value**	0,490	**S value**	0,280		

30 -25,4 – 19,05 mm ball size charge at U= 1

1700 x 1180 micron

Table D.46 Determined B values of zeolite for - 1700 + 1180 µm size interval ground with d = 30 – 25,4 – 19,05 mm ball diameter and U = 1.

INTERVAL NO,İ	**SİZE (mesh)**	**Size (µm)**	**Xi/Xmax**	**B i,1**	**B VALUES**
1	12x16	1700x1180	1,00	B1,1	1,0000
2	16x20	1180x850	0,69	B2,1	1,0000
3	20x30	850x600	0,50	B3,1	0,4077
4	30x40	600x425	0,35	B4,1	0,2847
5	40x50	425x300	0,25	B5,1	0,1969
6	50x70	300x212	0,17	B6,1	0,1418
7	70x100	212x150	0,12	B7,1	0,0998
8	100x140	150x106	0,088	B8,1	0,0759
9	140x200	106x75	0,062	B9,1	0,0523
10	200x270	75x53	0,044	B10,1	0,0376
11	270x400	53x38	0,031	B11,1	0,0273
12	-400	-38	0,022	B12,1	0,0193

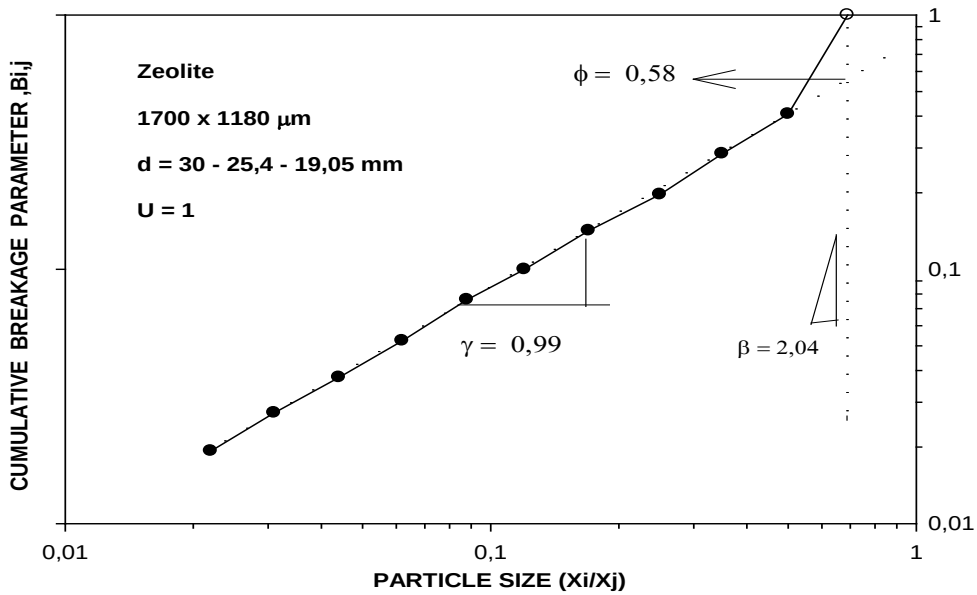

Figure D.71 Primary breakage distribution function of zeolite for -1700 + 1180 µm feed size fraction ground with d = 30 – 25,4 – 19,05 mm ball diameter and U = 1.

Table D.47 Cumulative weight percent less than size values of zeolite for 1700 x 1180 µm size interval ground with d = 30 – 25,4 – 19,05 mm ball diameter and U = 1.

SIZE	0 min.	0,133 min	1 min	3 min	6 min
1700	100,00	100,00	100,00	100,00	100,00
1180	0,68	30,28	63,35	92,46	99,10
850	0,09	13,51	36,85	82,11	94,12
600	0,00	9,58	24,60	66,16	81,36
425	0,00	6,73	17,63	48,22	63,42
300	0,00	4,89	13,55	37,24	51,19
212	0,00	3,47	10,66	27,85	40,00
150	0,00	2,65	8,17	19,11	29,69
106	0,00	1,83	6,27	13,10	22,00
75	0,00	1,32	4,48	9,18	14,32
53	0,00	0,96	2,95	6,21	9,85
38	0,00	0,68	1,91	4,33	6,87
%w.r.top size	99,32	69,72	36,65	7,54	0,90

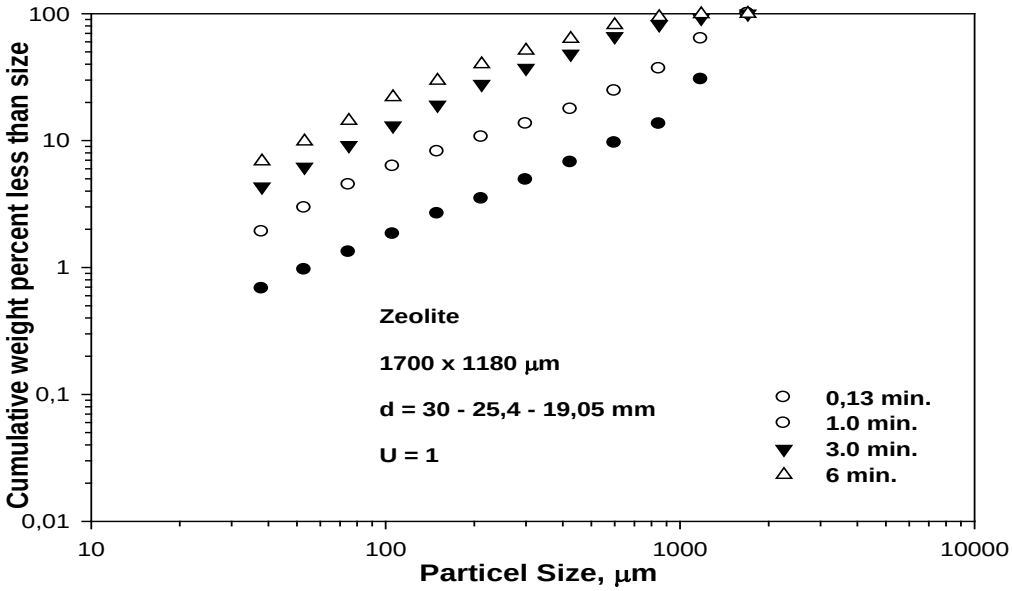

Figure D.72 Particle size distribution of zeolite for -1700 + 1180 µm feed size fraction ground with d = 30 – 25,4 – 19,05 mm ball diameter and U = 1.

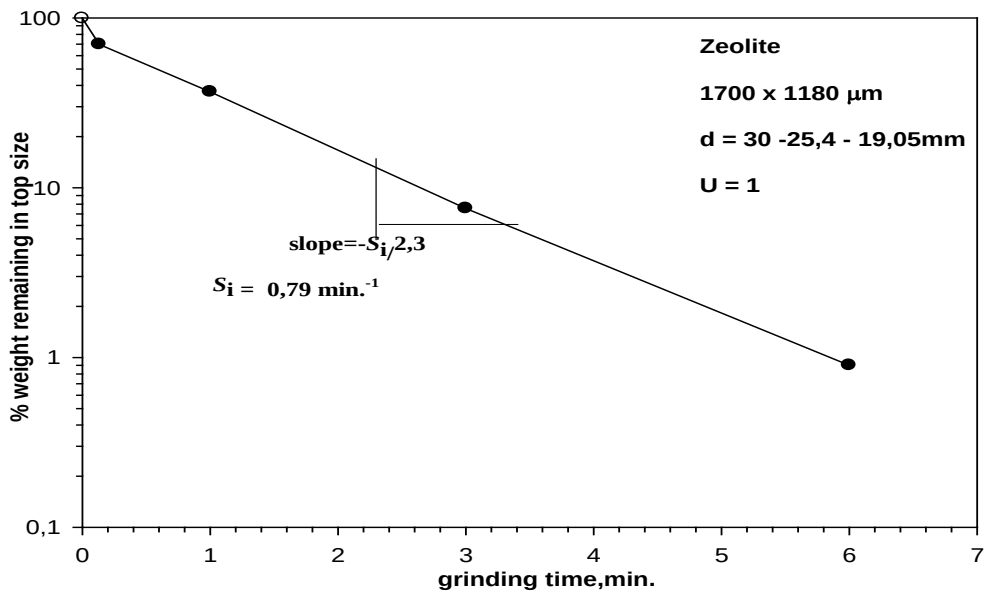

Figure D.73 First-order plot of breakage of - 1700 + 1180 µm feed of zeolite ground with d = 30 – 25,4 – 19,05 mm ball diameter and U = 1.

850 x 600 micron

Table D.48 Determined B values of zeolite for - 850 + 600 µm size interval ground with d = 30 – 25,4 – 19,05 mm ball diameter and U = 1.

INTERVAL NO,İ	SİZE (mesh)	Size (µm)	Xi/Xmax	B i,1	B VALUES
1	20x30	850x600	1,00	B3,1	1,000
2	30x40	600x425	0,7	B4,1	1,000
3	40x50	425x300	0,5	B5,1	0,400
4	50x70	300x212	0,35	B6,1	0,276
5	70x100	212x150	0,24	B7,1	0,187
6	100x140	150x106	0,17	B8,1	0,131
7	140x200	106x75	0,12	B9,1	0,093
8	200x270	75x53	0,08	B10,1	0,064
9	270x400	53x38	0,06	B11,1	0,045
10	-400	-38	0,04	B12,1	0,030

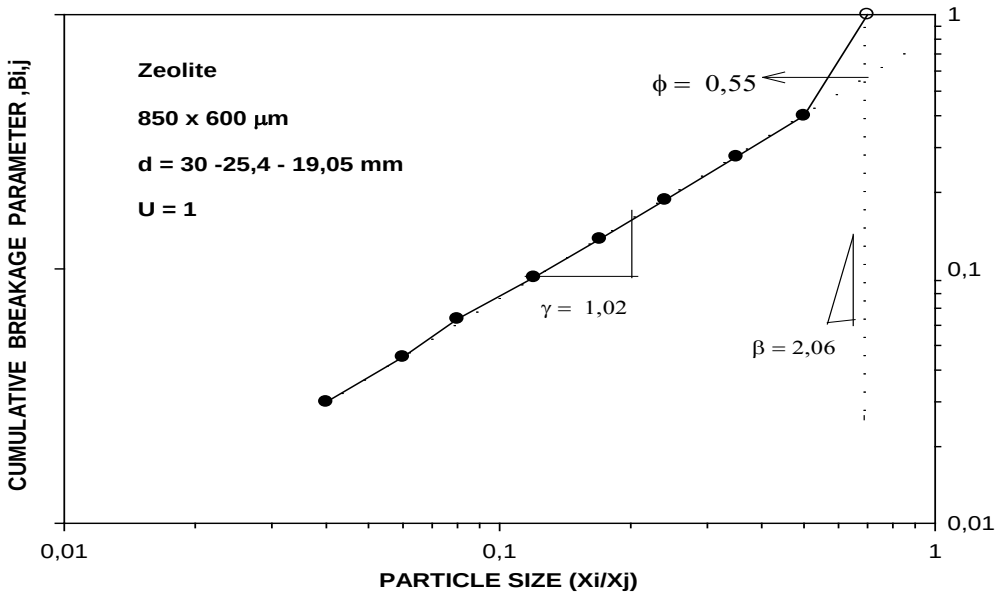

Figure D.74 Primary breakage distribution function of zeolite for -850 + 600 µm feed size fraction ground with d = 30 – 25,4 – 19,05 mm ball diameter and U = 1.

Table D.49 Cumulative weight percent less than size values of zeolite for - 850 + 600 µm size interval ground with d = 30 – 25,4 – 19,05 mm ball diameter and U = 1.

SIZE	0 min.	0,133 min	1 min	3 min	6 min
850	100,00	100,00	100,00	100,00	100,00
600	0,19	21,58	50,64	81,16	95,36
425	0,04	9,24	23,69	57,49	89,20
300	0,00	6,44	15,78	37,11	77,43
212	0,00	4,40	11,38	27,10	51,02
150	0,00	3,11	8,25	18,94	35,28
106	0,00	2,21	6,04	13,08	21,46
75	0,00	1,52	4,16	9,02	14,06
53	0,00	1,08	2,58	5,88	9,96
38	0,00	0,72	1,49	4,06	6,38
%w.r.top size	99,81	78,42	49,36	18,84	4,64

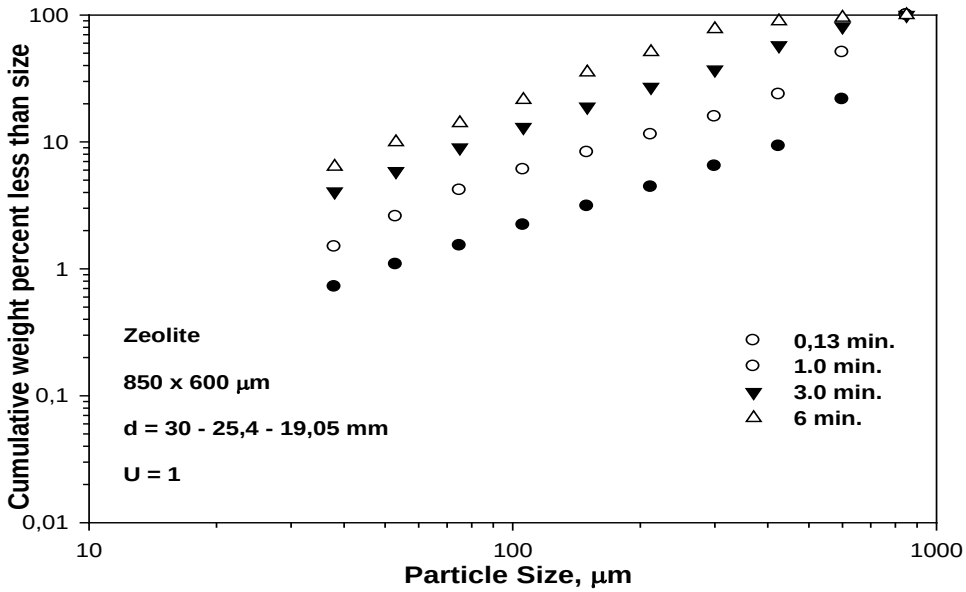

Figure D.75 Particle size distribution of zeolite for -850 + 600 µm feed size fraction ground with d = 30 – 25,4 – 19,05 mm ball diameter and U = 1.

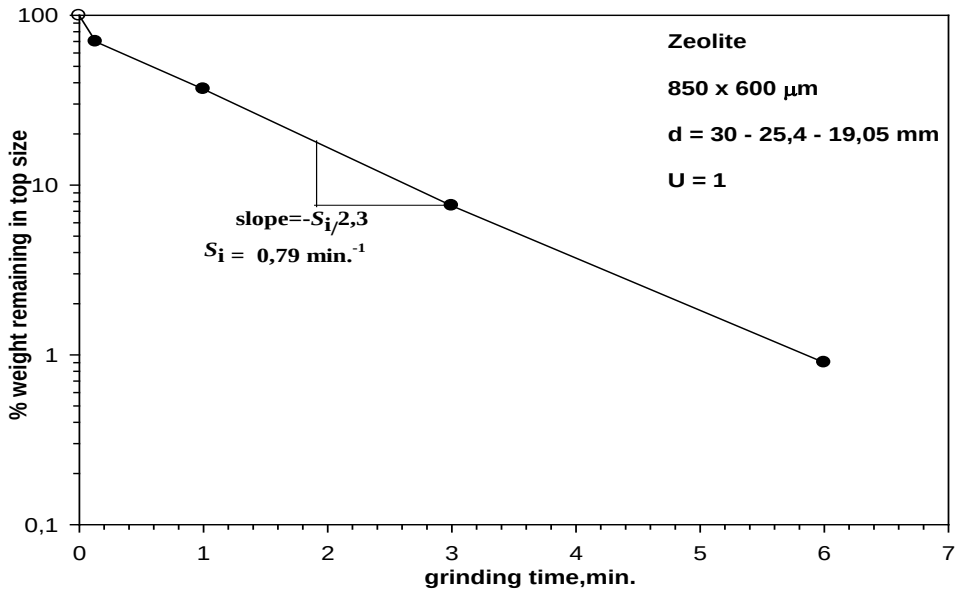

Figure D.76 First-order plot of breakage of - 850 + 600 µm feed of zeolite ground with d = 30 – 25,4 – 19,05 mm ball diameter and U = 1.

425 x 300 micron

Table D.50 Determined B values of zeolite for – 425 + 300 µm size interval ground with d = 30 – 25,4 – 19,05 mm ball diameter and U = 1.

INTERVAL NO,İ	SİZE (mesh)	Size (µm)	Xi/Xmax	B i,1	B VALUES
1	40x50	425x300	1,00	B1,1	1,0000
2	50x70	300x212	0,7	B2,1	1,0000
3	70x100	212x150	0,49	B3,1	0,3932
4	100x140	150x106	0,35	B4,1	0,2704
5	140x200	106x75	0,24	B5,1	0,1809
6	200x270	75x53	0,17	B6,1	0,1234
7	270x400	53x38	0,12	B7,1	0,0851
8	-400	-38	0,08	B8,1	0,0540

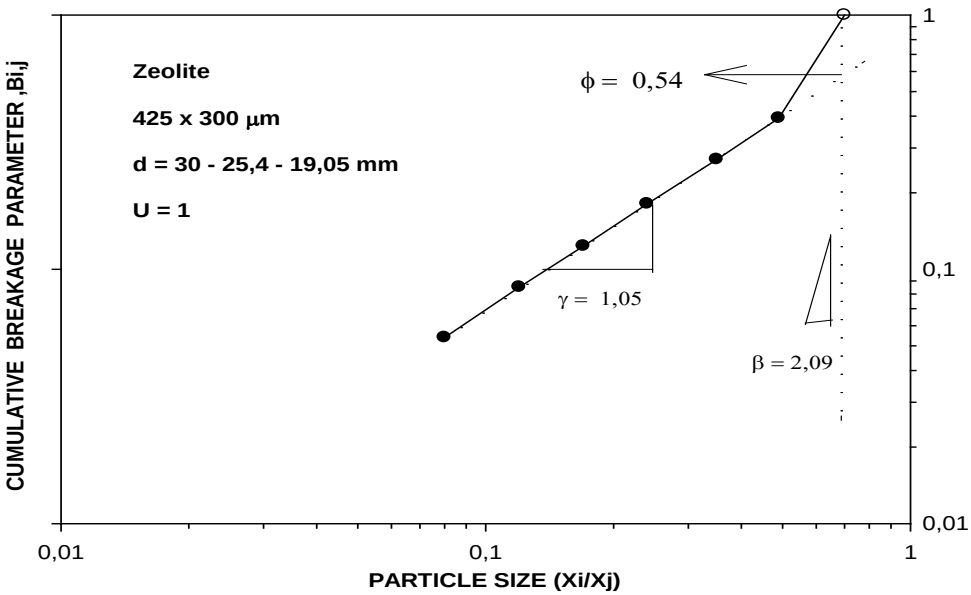

Figure D.77 Primary breakage distribution function of zeolite for -425 + 300 µm feed size fraction ground with d = 30 – 25,4 – 19,05 mm ball diameter and U = 1.

Table D.51 Cumulative weight percent less than size values of zeolite for - 425 + 300 µm size interval ground with d = 30 – 25,4 – 19,05 mm ball diameter and U = 1.

SIZE	0 min.	0,133 min	1 min	3 min	6 min
425	100,00	100,00	100,00	100,00	100,00
300	0,16	10,86	31,48	68,84	90,49
212	0,01	4,37	15,43	28,96	44,06
150	0,00	3,02	8,95	17,10	27,19
106	0,00	2,03	5,56	11,00	18,22
75	0,00	1,39	3,19	7,08	11,15
53	0,00	0,96	1,85	4,56	7,06
38	0,00	0,61	1,08	2,57	4,18
%w.r.top size	99,84	89,14	68,52	31,16	9,51

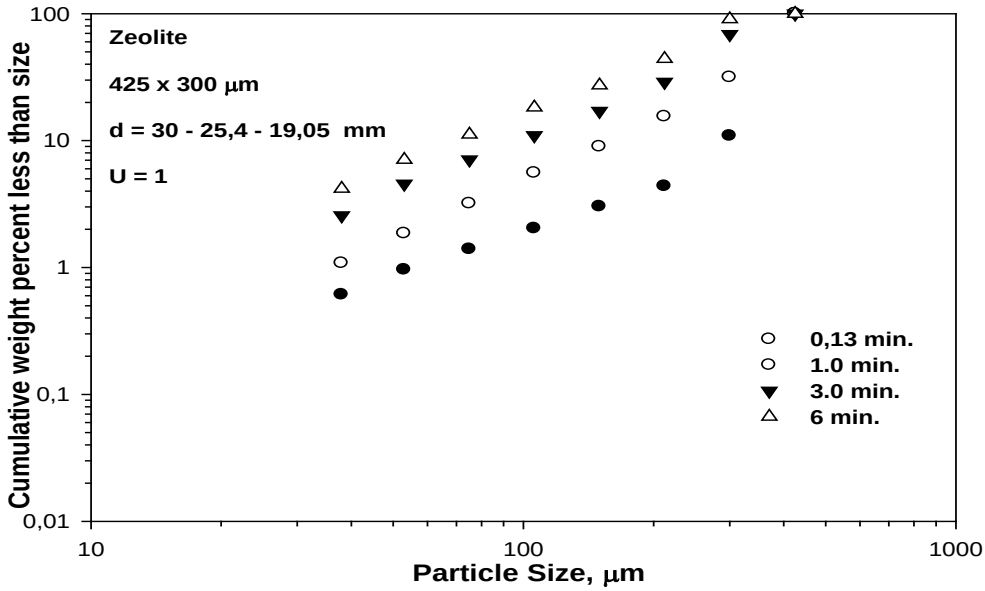

Figure D.78 Particle size distribution of zeolite for -425 + 300 µm feed size fraction ground with d = 30 – 25,4 – 19,05 mm ball diameter and U = 1.

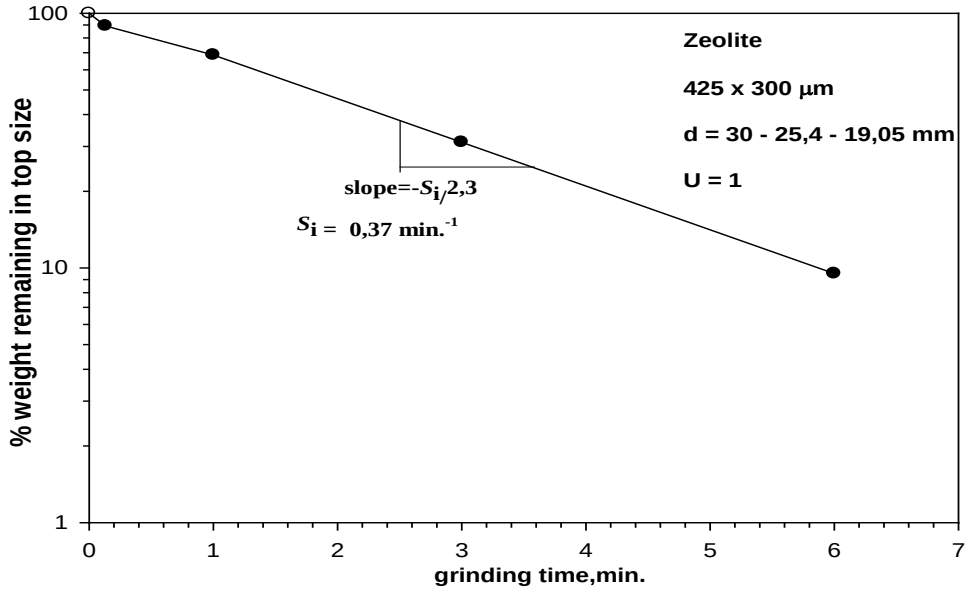

Figure D.79 First-order plot of breakage of - 425 + 300 µm feed of zeolite ground with d = 30 – 25,4 – 19,05 mm ball diameter and U = 1.

212 x 150 micron

Table D.52 Determined B values of zeolite for – 212 + 150 µm size interval ground with d = 30 – 25,4 – 19,05 mm ball diameter and U = 1.

INTERVAL NO,İ	SİZE (mesh)	Size (µm)	Xi/Xmax	B i,1	B VALUES
1	70x100	212x150	1,00	B1,1	1,0000
2	100x140	150x106	0,7	B2,1	1,0000
3	140x200	106x75	0,5	B3,1	0,3959
4	200x270	75x53	0,35	B4,1	0,2685
5	270x400	53x38	0,25	B5,1	0,1819
6	-400	-38	0,17	B6,1	0,1162

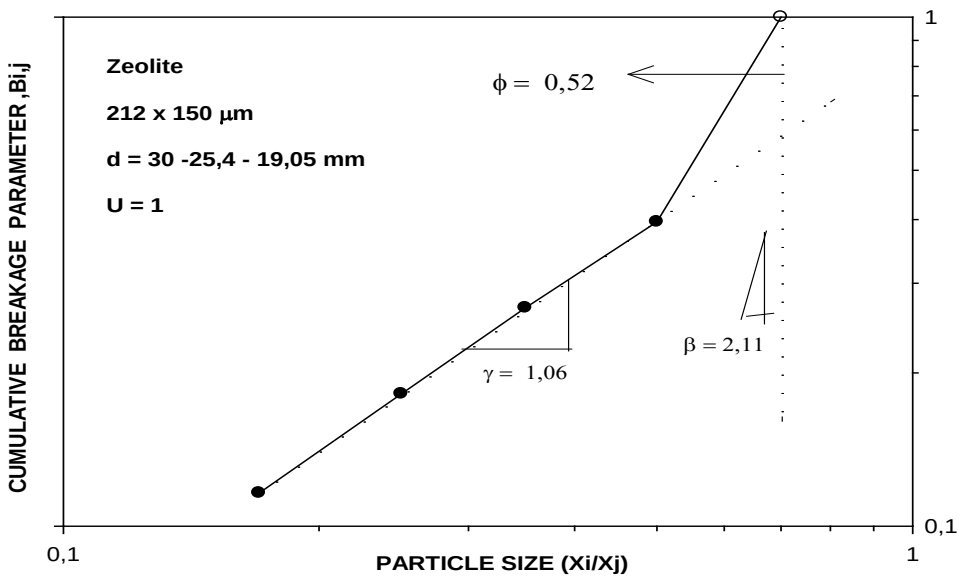

Figure D.80 Primary breakage distribution function of zeolite for - 212 + 150 µm feed size fraction ground with d = 30 – 25,4 – 19,05 mm ball diameter and U = 1.

Table D.53 Cumulative weight percent less than size values of zeolite for - 212 + 150 µm size interval ground with d = 30 – 25,4 – 19,05 mm ball diameter and U = 1.

SIZE	0 min.	0,133 min	1 min	3 min	6 min
212	100,00	100,00	100,00	100,00	100,00
150	0,09	8,21	19,91	52,67	78,37
106	0,01	3,31	14,06	22,10	36,41
75	0,00	2,25	9,61	15,03	26,32
53	0,00	1,53	6,12	10,60	18,43
38	0,00	0,98	3,43	6,91	12,78
%w.r.top size	99,91	91,79	80,09	47,33	21,63

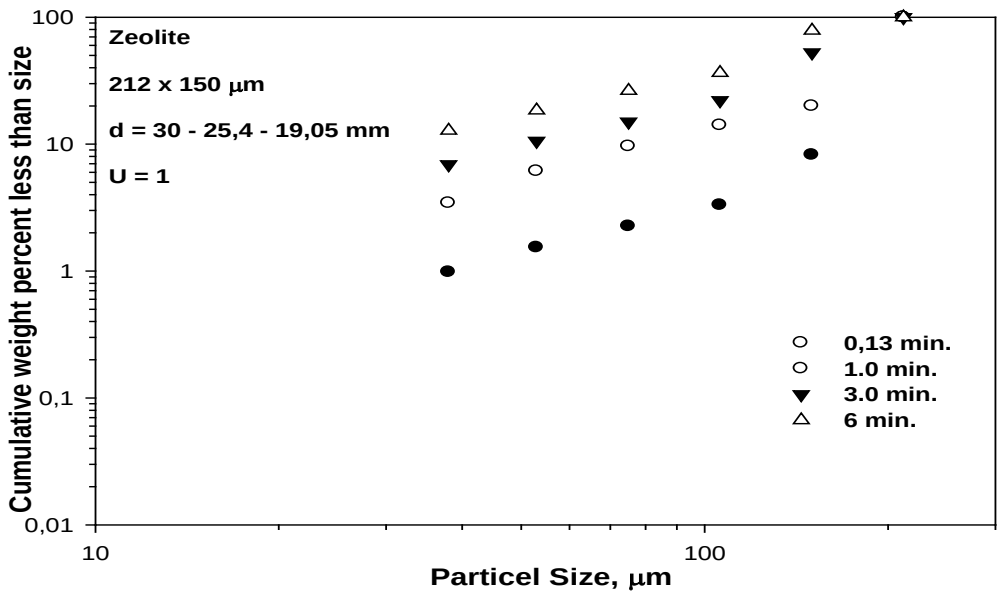

Figure D.81 Particle size distribution of zeolite for -212 + 150 µm feed size fraction ground with d = 30 – 25,4 – 19,05 mm ball diameter and U = 1.

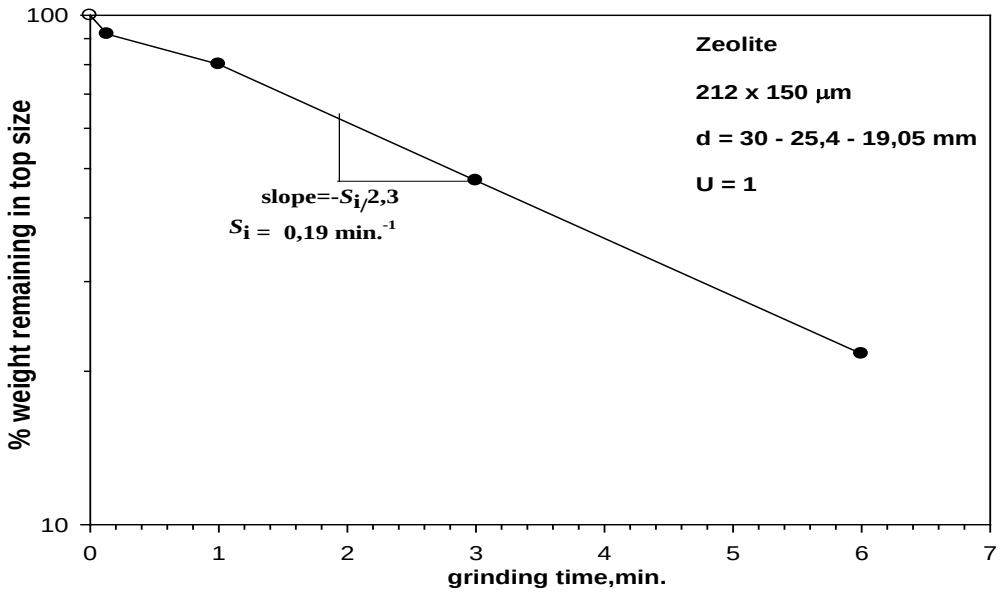

Figure D.82 First-order plot of breakage of - 212 + 150 μm feed of zeolite ground with d = 30 – 25,4 – 19,05 mm ball diameter and U = 1.

Determination of aT value

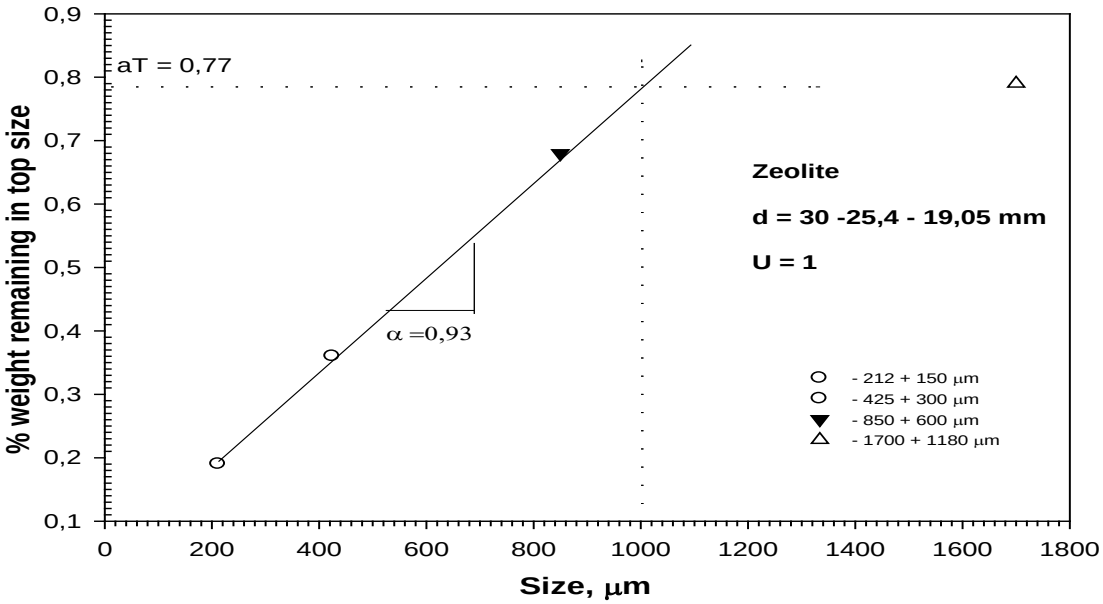

Figure D.83Variation of first-order specific rates of breakage of zeolite ground with d = 30 – 25,4 – 19,05 mm ball diameter and particle size: √2 intervals, plotted at upper size of interval at U=1.

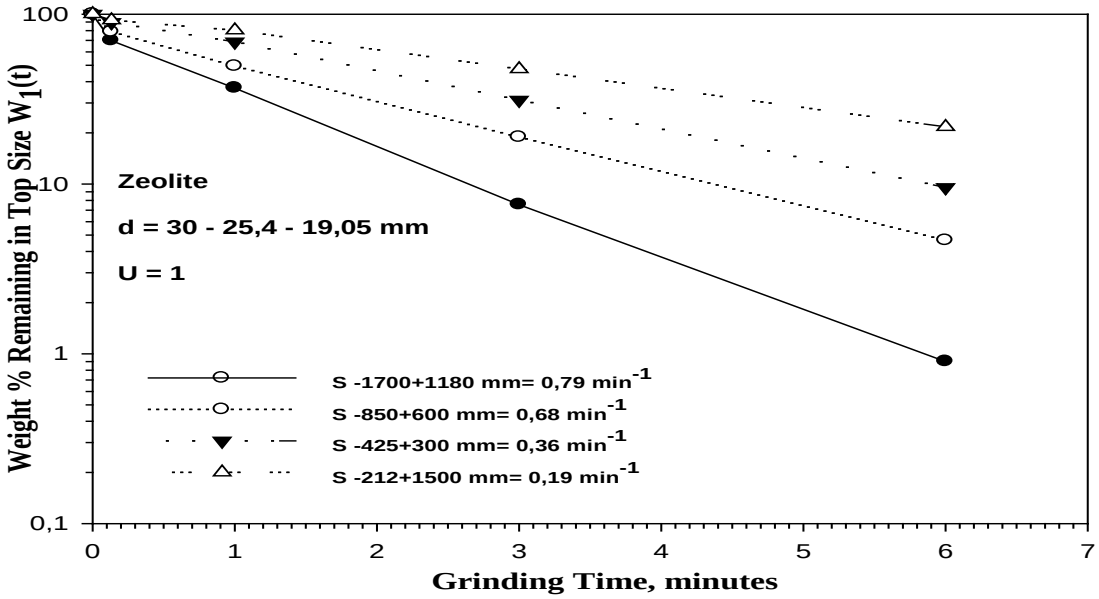

Figure D.84 First-order plots of breakage of -1700+1180, -850+600, -425+300, -212+150 µm feed size of zeolite ground with d = 30 – 25,4 – 19,05 mm ball diameter and U=1.

Table D.54 Breakage parameters of zeolite ground with d = 30 – 25,4 – 19,05 mm ball diameter at U=1.

1700x1180		**850x600**		**425x300**		**212x150**			
gama	0,99	**gama**	1,02	**gama**	1,05	**gama**	1,06		
beta	2,04	**beta**	2,06	**beta**	2,09	**beta**	2,11	**aT**	**α**
phi	0,58	**phi**	0,55	**phi**	0,54	**phi**	0,52	0,77	0,93
S value	0,790	**S value**	0,680	**S value**	0,360	**S value**	0,190		

APPENDIX E
VARIATIONS OF THE S_I VALUES OF PERLITE, PUMICE AND ZEOLITE WITH PARTICLE SIZE FOR DIFFERENT BALL DIAMETERS AT U=0,6 AND U= 1.

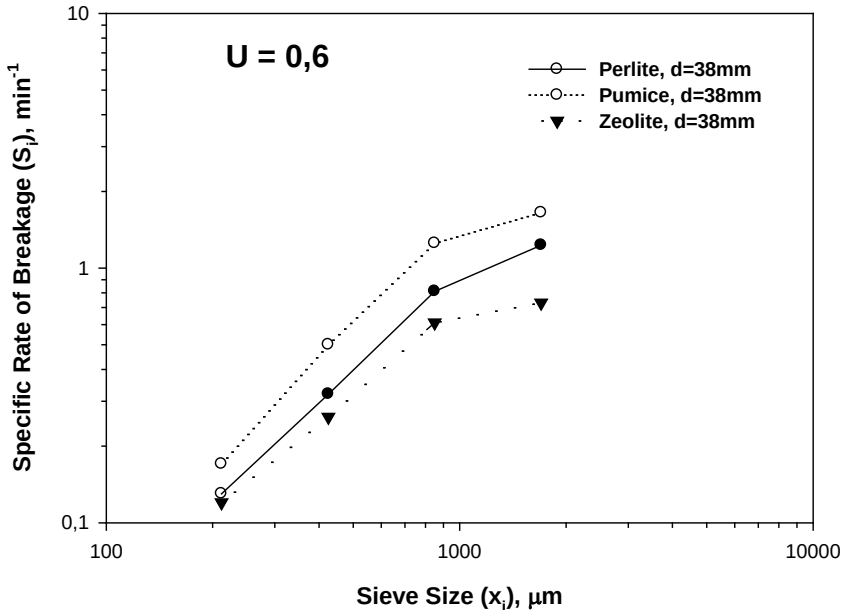

Fig. E.1 Variations of the s_i values of perlite, pumice and zeolite with particle size for d=38 mm ball size charge at U=0,6.

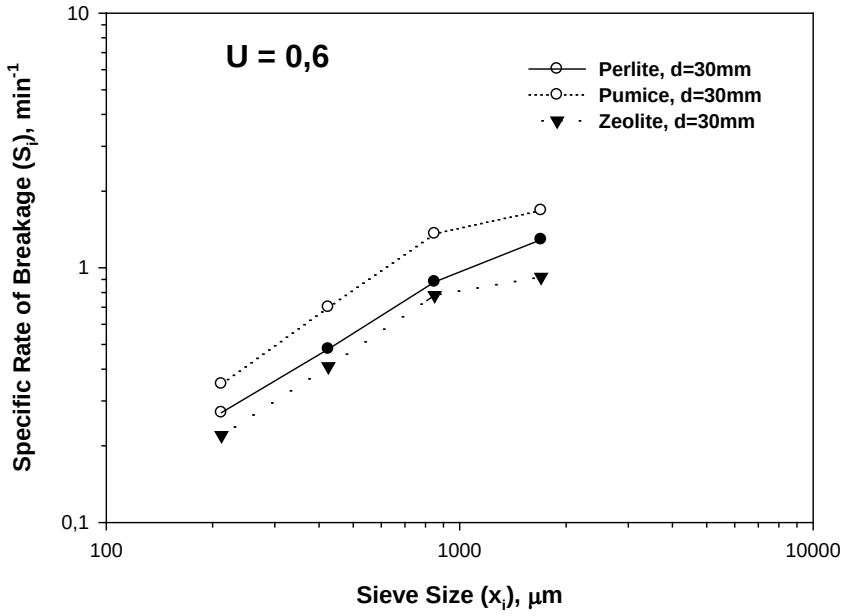

Fig. E.2 Variations of the s_i values of perlite, pumice and zeolite with particle size for d=30 mm ball size charge at U=0,6.

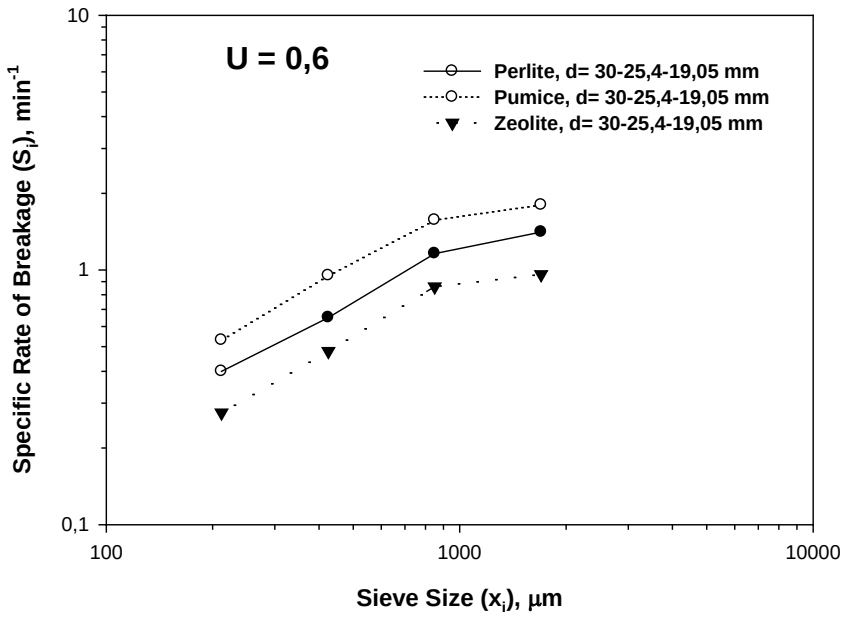

Fig. E.3 Variations of the s_i values of perlite, pumice and zeolite with particle size for d=30-25,4-19,05 mm ball size charge at U=0,6.

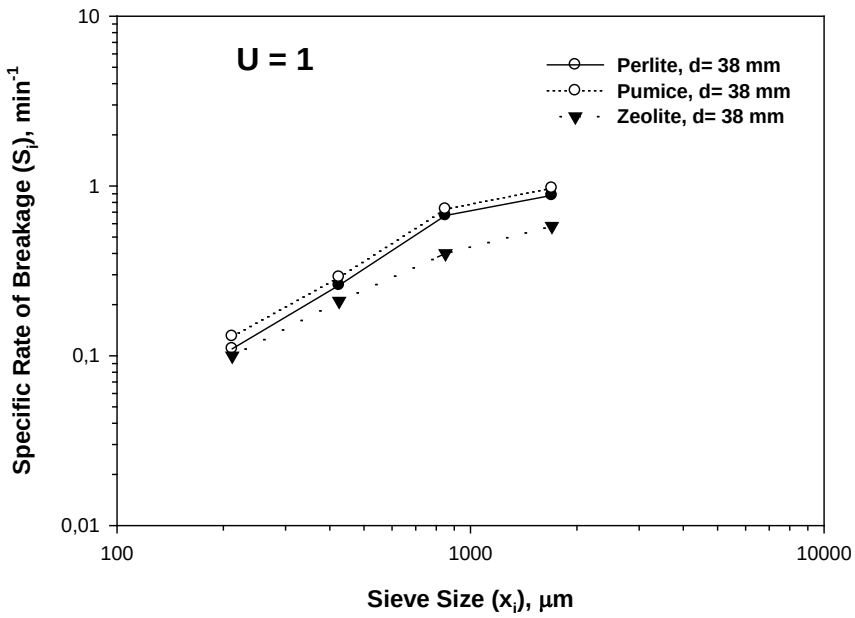

Fig. E.4 Variations of the s_i values of perlite, pumice and zeolite with particle size for d=38 mm ball size charge at U=1.

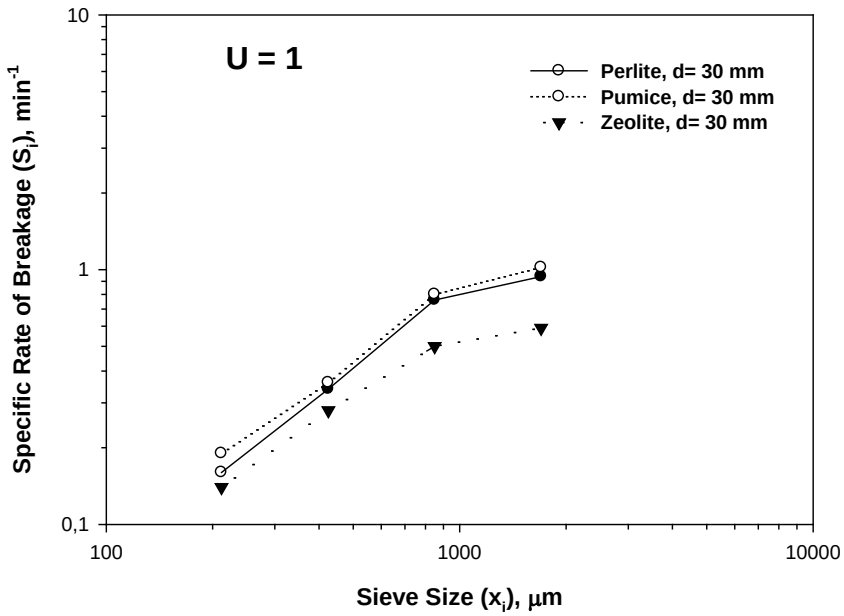

Fig. E.5 Variations of the s_i values of perlite, pumice and zeolite with particle size for d=30 mm ball size charge at U=1.

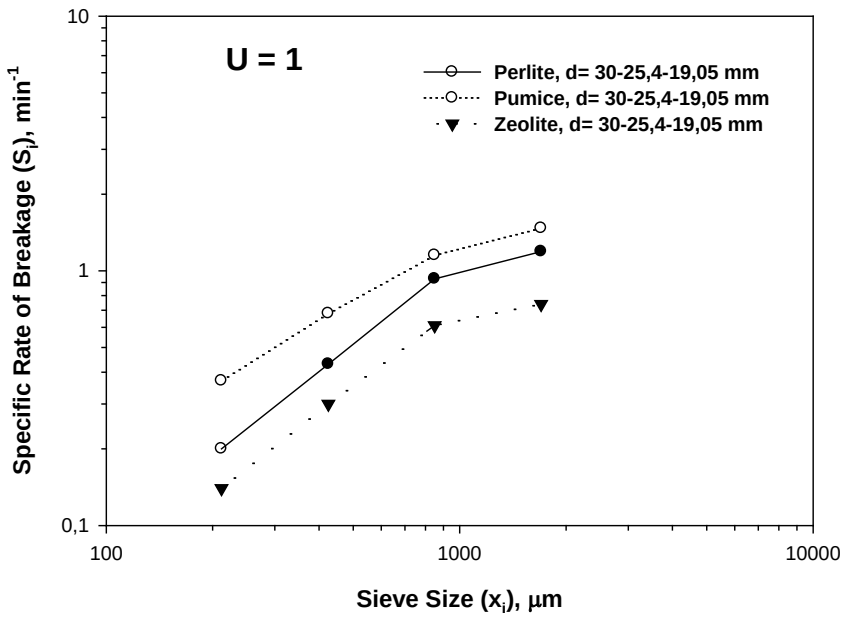

Fig. E.6 Variations of the s_i values of perlite, pumice and zeolite with particle size for d=30-25,4-19,05 mm ball size charge at U=1.

PERLITE

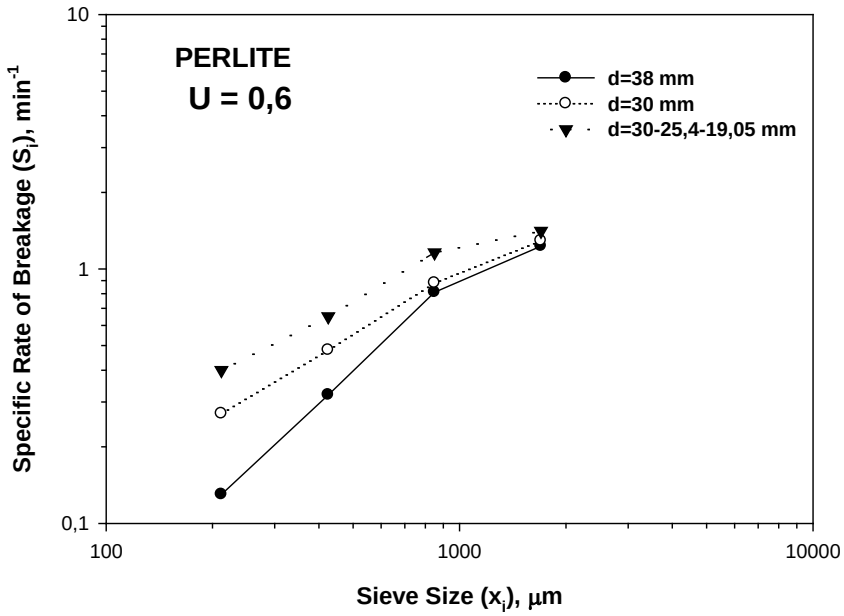

Fig. E.7 Variations of the s_i values of perlite with particle size for different ball diameters at U=0,6.

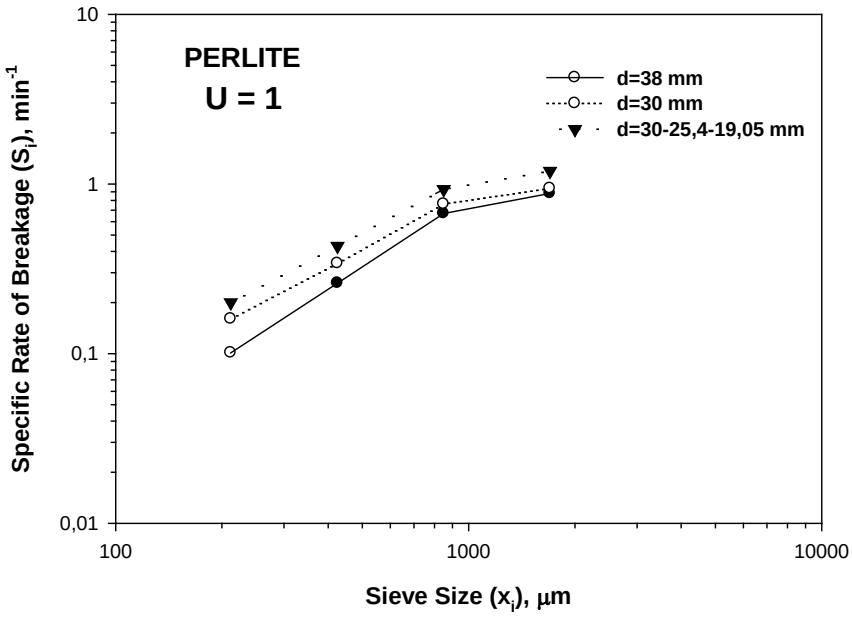

Fig. E.8 Variations of the s_i values of perlite with particle size for different ball diameters at U=1.

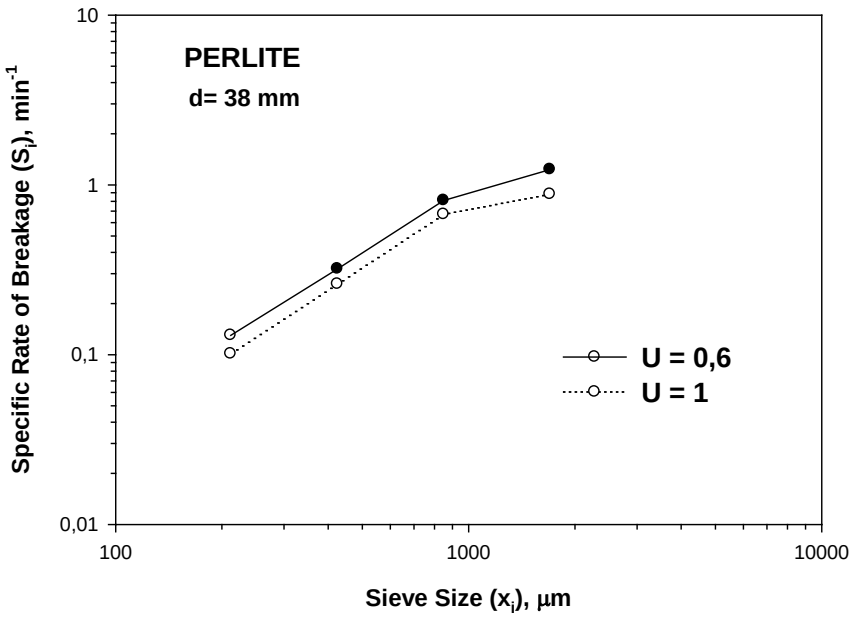

Fig. E.9 Variations of the s_i values of perlite with particle size for 38mm ball diameters at U=0,6 and U=1.

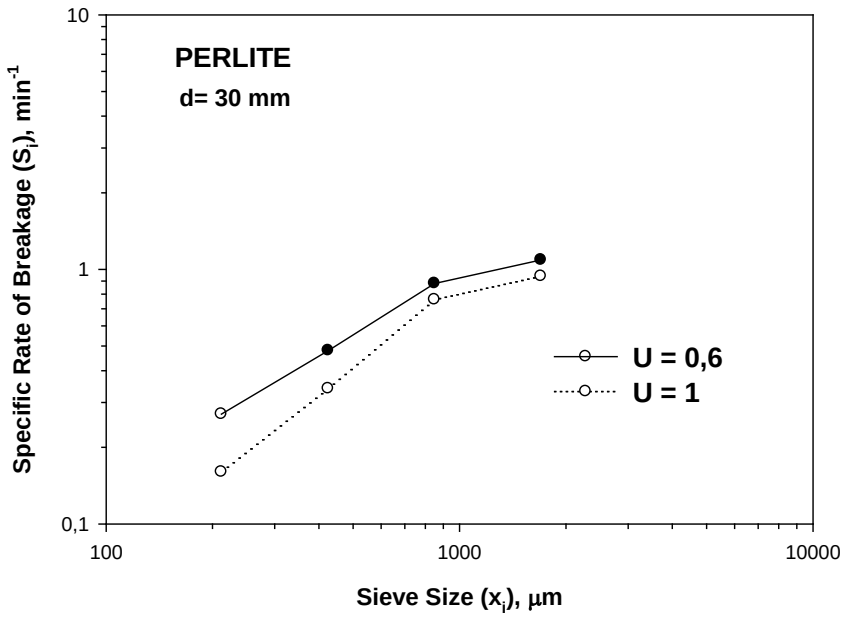

Fig. E.10 Variations of the s_i values of perlite with particle size for 30mm ball diameters at U=0,6 and U=1.

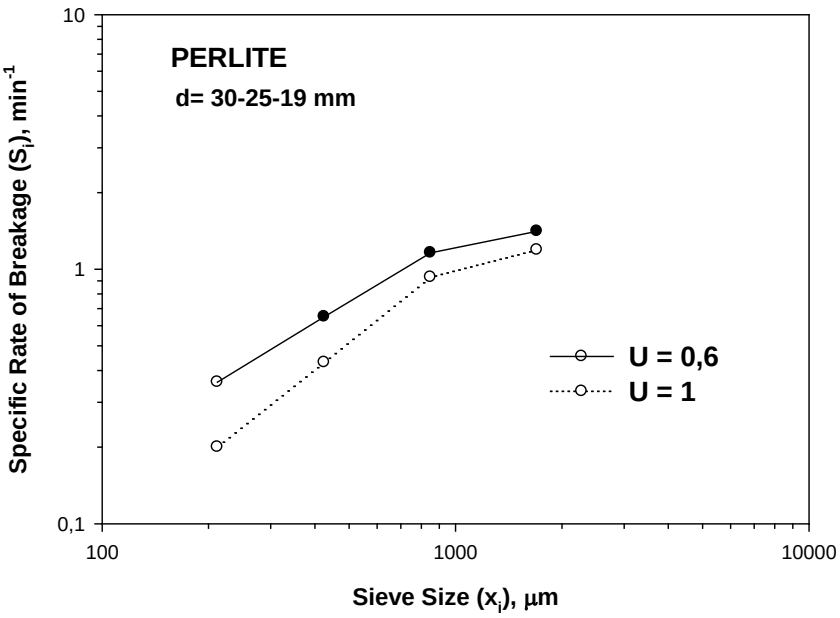

Fig. E.11 Variations of the s_i values of perlite with particle size for 30-25,4-19,05 mm ball diameters at U=0,6 and U=1.

PUMICE

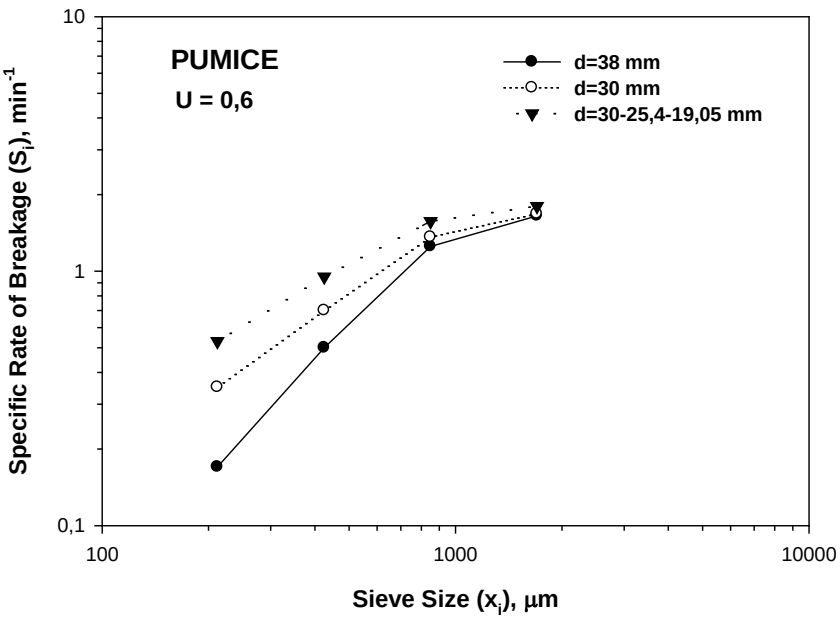

Fig. E.12 Variations of the s_i values of pumice with particle size for different ball diameters at U=0,6.

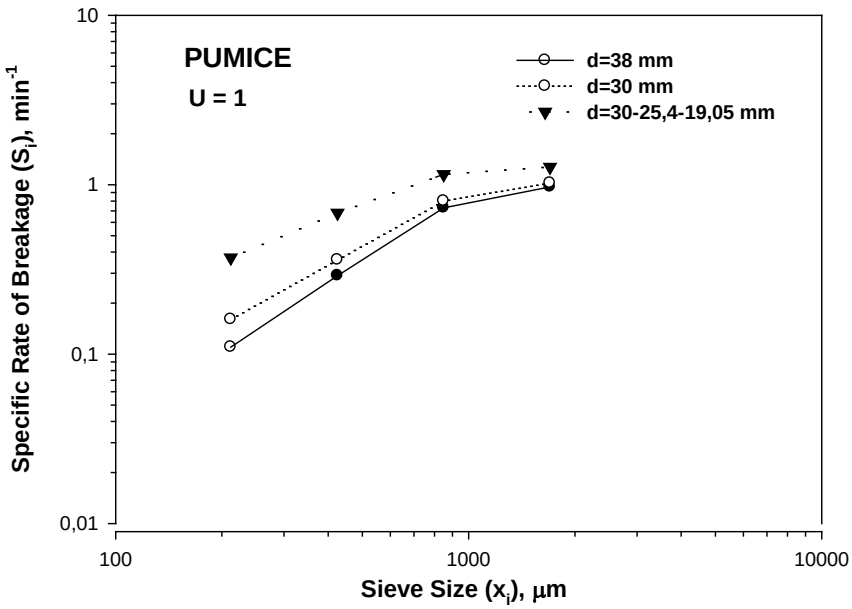

Fig. E.13 Variations of the s_i values of pumice with particle size for different ball diameters at U=1.

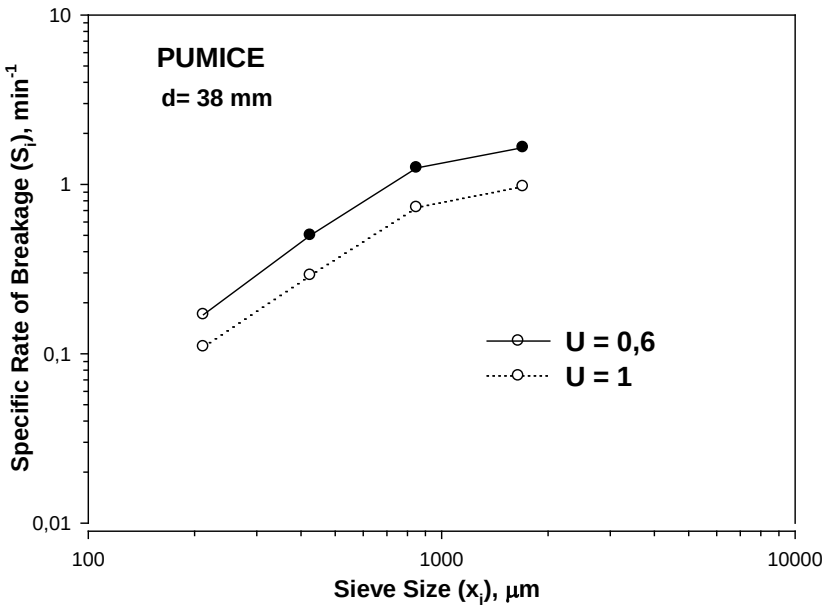

Fig. E.14 Variations of the s_i values of pumice with particle size for 38mm ball diameters at U=0,6 and U=1.

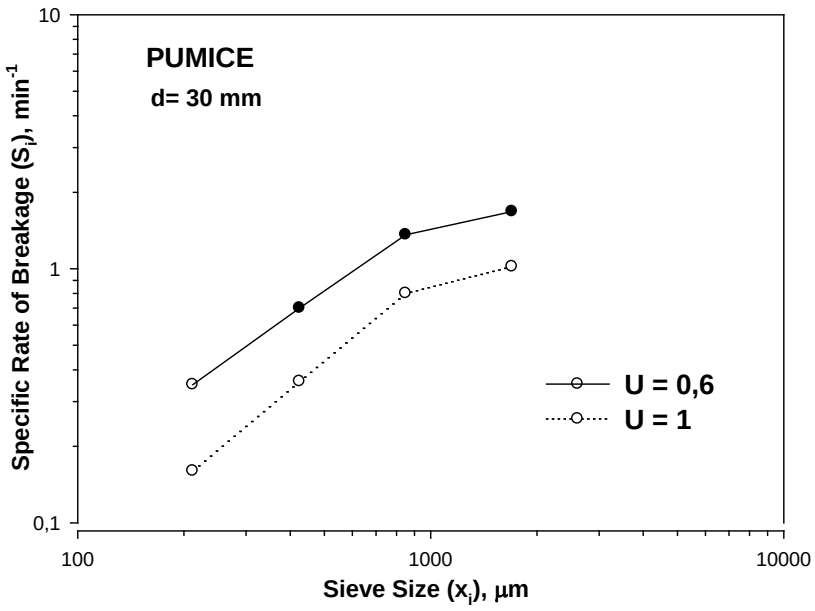

Fig. E.15 Variations of the s_i values of pumice with particle size for 30mm ball diameters at U=0,6 and U=1.

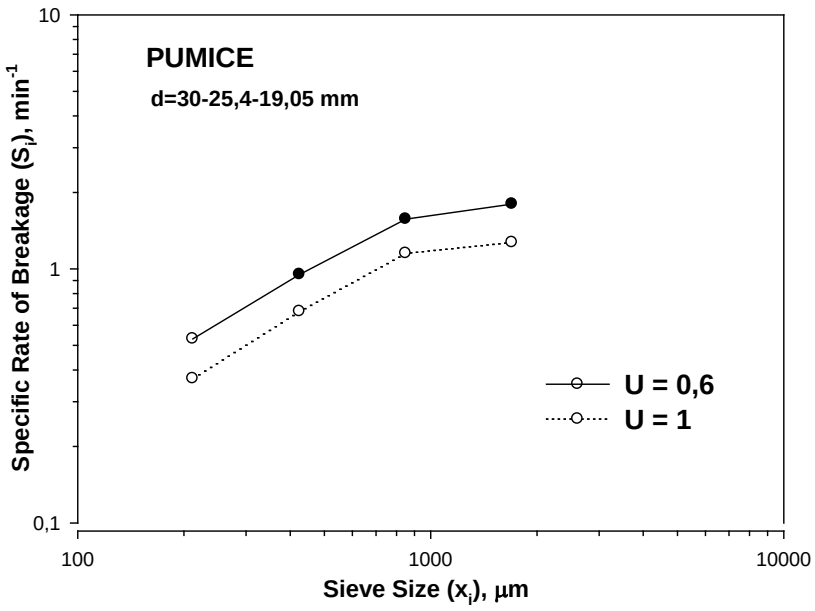

Fig. E.16 Variations of the s_i values of pumice with particle size for 30-25,4-19,05 mm ball diameters at U=0,6 and U=1.

ZEOLITE

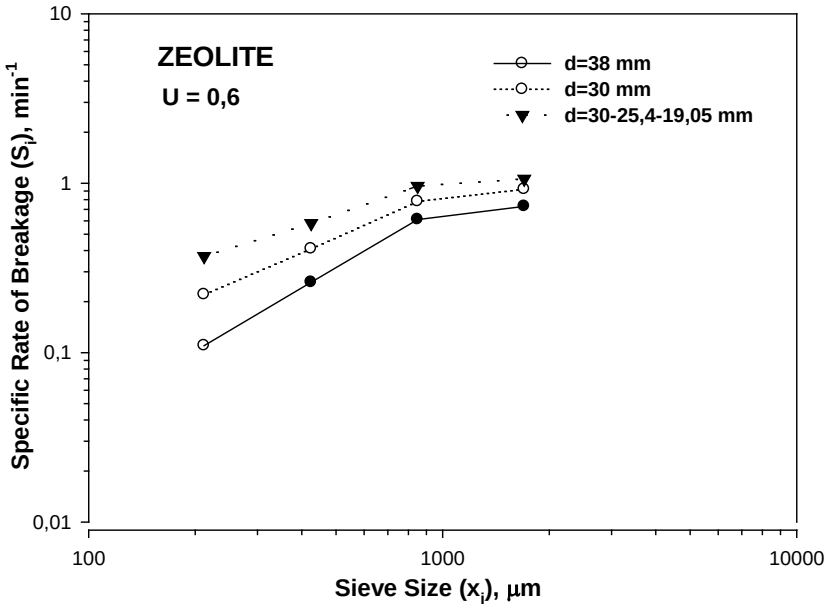

Fig. E.17 Variations of the s_i values of zeolite with particle size for different ball diameters at U=0,6.

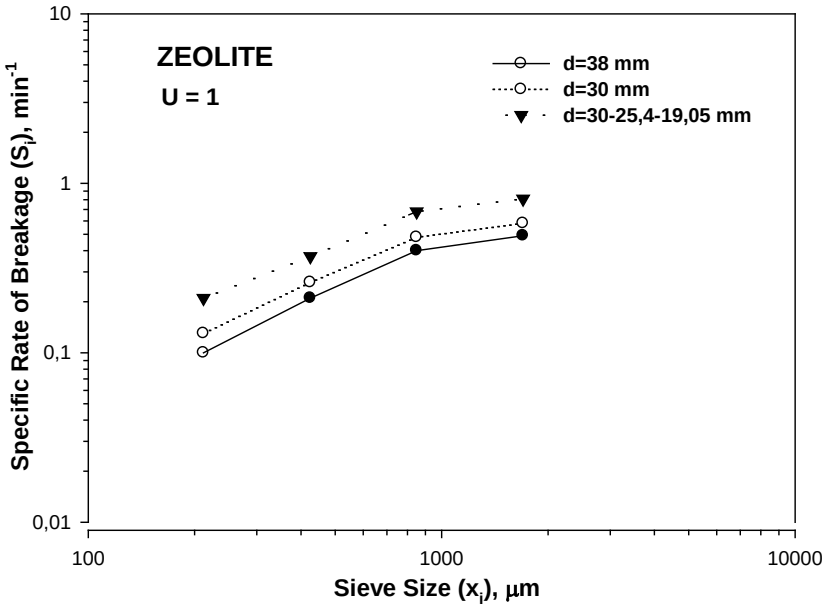

Fig. E.18 Variations of the s_i values of zeolite with particle size for different ball diameters at U=1.

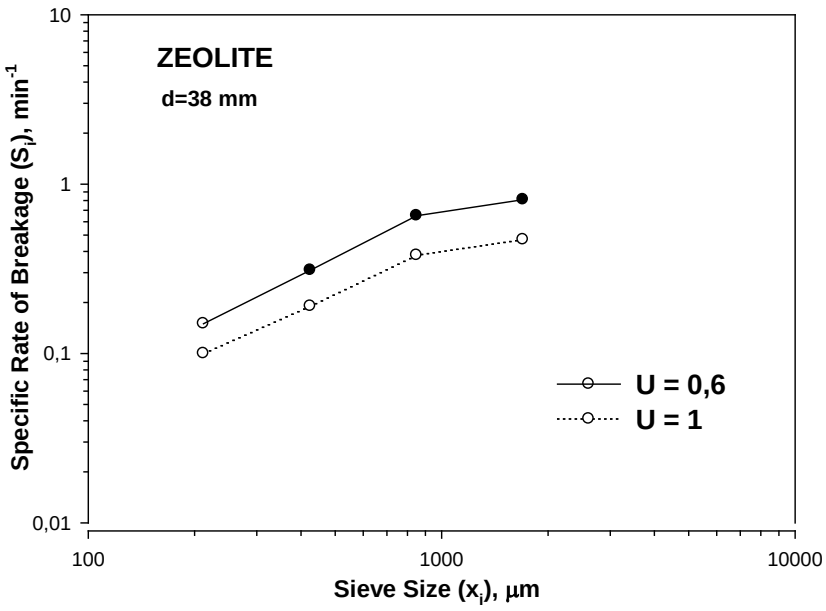

Fig. E.19 Variations of the s_i values of zeolite with particle size for 38mm ball diameters at U=0,6 and U=1

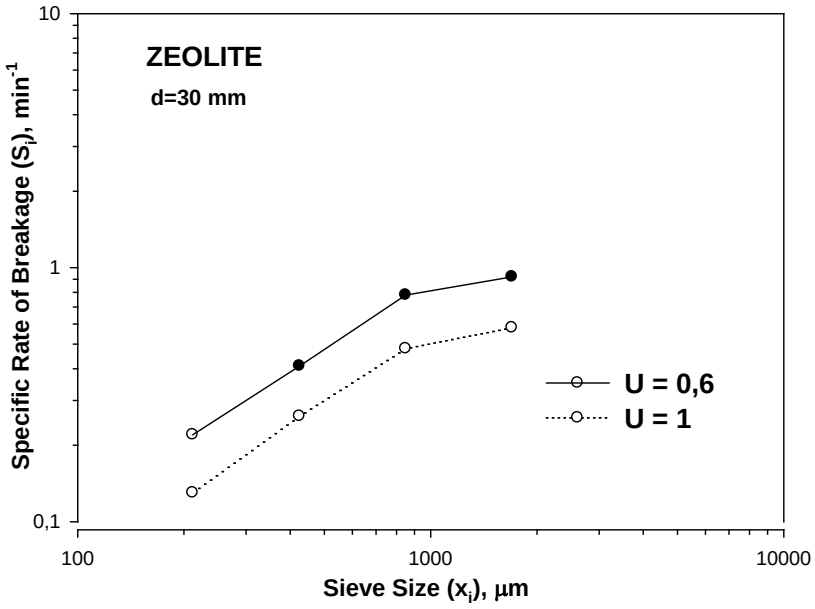

Fig. E.20 Variations of the s_i values of zeolite with particle size for 30mm ball diameters at U=0,6 and U=1

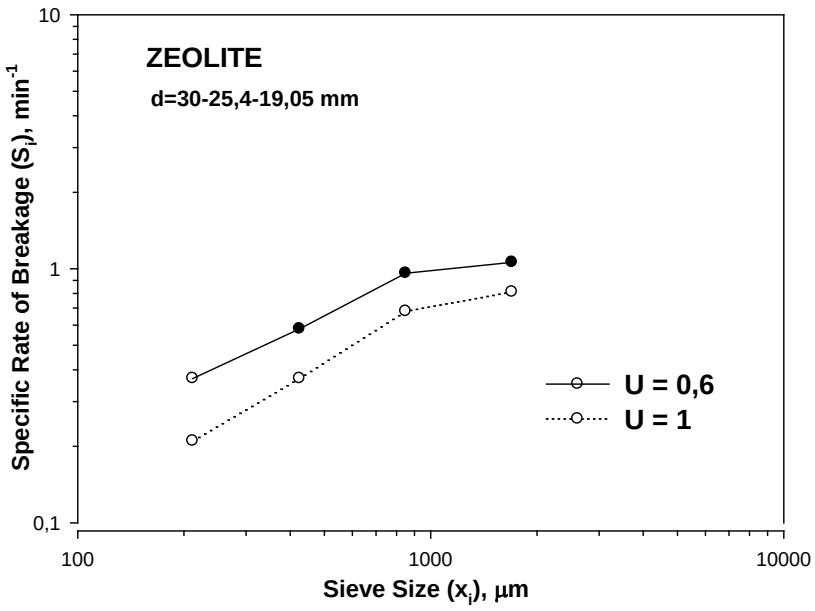

Fig. E.21 Variations of the s_i values of zeolite with particle size for 30-25,4-19,05 mm ball diameters at U=0,6 and U=1